SAPTHAGIRI COLLEGE OF ENGINEERING

Affiliated to VTU, Belagavi, Approved by AICTE, New Delhi
Accredited By NAAC with "A" Grade, Accredited by NBA for CSE,ISE,ECE,EEE & ME
ISO 9001-2015 & 14001-2015 Certified Institute

In Association With

International Conference on

"Global Convergence in Technology, Entrepreneurship, Computing and Value Engineering: Principles and Practices"

(ICGCP—2022)

24th - 26th June, 2022

Conference Proceedings

Jointly Organized by

Department of

Mechanical Engineering, Civil Engineering, Physics & Mathematics

Preface

Sapthagiri College of Engineering, Bengaluru was established in the year 2001 by Srinivasa Education and Charitable Trust with a vision to transform its students into competent, inspired and responsible professionals. It is one of the best Engineering Colleges in India.

It is our great honour and pleasure to publish the Proceedings of the **International Conference on Global Convergence in Technology and Entrepreneurship, Computing and Value Engineering, Principles and Practices - 2022 (ICGCP – 2022).** The conference was held on 24th and 26th June, 2022 in virtual mode. To encourage the young research minds and to bring all researchers, academics, scientists, industry experts, in common platform, the college organized this conference.

Present global scenario demands unprecedented actions and efforts across multiple convergences of social, economic and environment issues. Science, Technology and Innovations in the area of Internet of Things, Artificial Intelligence, Bio-Technology, Nano Materials and Renewable Energy must play a key role in achieving these goals. Also this is the era of start – ups, to achieve ambitious dream of Make in India concept. The conference covered all emerging areas of Science, Engineering and Technology.

The response to call for papers was excellent. More than 500 papers were received across the country, out of which 300 papers were selected for presentation and publication in the proceeding. These papers provided wide spectrum of research covering all the areas for which the conference was intended for.

We would like to express our gratitude and appreciation to the authors for their contributions. Many thanks go as well to all of the reviewers who helped us maintain the quality of the research papers included in the Proceedings. We also express our sincere thanks to the members of the organizing team for their hard work.

Conference Chair of ICGCP – 2022
Dr. Ramakrishna H
Principal,
Sapthagiri College of Engineering, Bengaluru.

Conference Co-Chair
Dr. Tulsidas.D
Prof. & Head, Department of Mechanical Engineering
Sapthagiri College of Engineering, Bengaluru

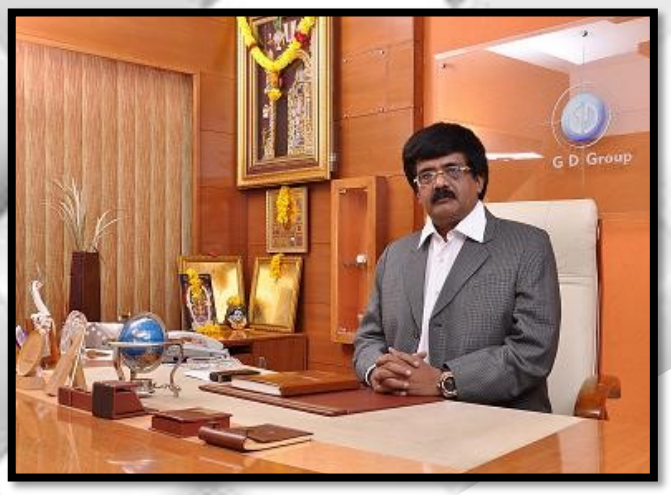

Message from Chairman

It gives me immense pleasure in congratulating the Chairman and team members of ICGCP- 2022, on successfully hosting the two days international conference at Sapthagiri college of Engineering. We are overwhelmed by the kind of response received by the research scholars across the country and I wish all of them a bright future and successful career. Also I would like to appreciate the contributions from the Principal, Heads of department, teaching and non-teaching faculties and other supporting staff of Sapthagiri college of Engineering for joining their hands in successful execution of the international conference.

Message from Managing Director

On this occasion, I express my heartiest congratulations to all the participants of ICGCP-2022 for publishing their research findings in the international conference. I hope that, the two days international conference has motivated faculties, research scholars and students to continue their research work. Also on behalf of management, I would like to extend my appreciation towards the sincere efforts of Principal, Heads of Department and Staff members of Sapthagiri College Engineering.

Message from Principal

At the outset I would like to congratulate the entire team of ICGCP-2022 for the successful conduction of international conference that witnessed an active participation of more than 350 research scholars across the state and also from outside Karnataka. On this occasion, I would like to thank our Chairman, Shri. G. Dayananda and executive director, Shri. G.D.Manoj for the magnanimous support extended in organizing the international conference. I would also like to congratulate all the faculties, research scholars and undergraduate students for publishing their research works in the conference and I hope that the two days interaction has motivated them to further pursue their research work and contribute to the society. Also I would like to appreciate the efforts of session chairs / reviewers / heads of department / technical support for their contributions in adding value to each session. Finally, I would like to congratulate the team ICGCP-2022 for bringing out the proceedings of international conference in a precise manner and for making it available for the researchers' community across the globe.

Editorial Board

Conference Chair of ICGCP – 2022
Dr. Ramakrishna H
Principal

Conference Co-Chair
Dr. Tulsidas.D
Prof. & Head, Department of Mechanical Engineering

Coordinators:
Dr. Ragavendra Deshpande
Associate Professor
Department of Mechanical Engineering

Dr. Devaraja.C
Assistant Professor
Department of Physics

Mr. Nagaraja B S
Assistant Professor
Department of Electrical and Electronics Engineering

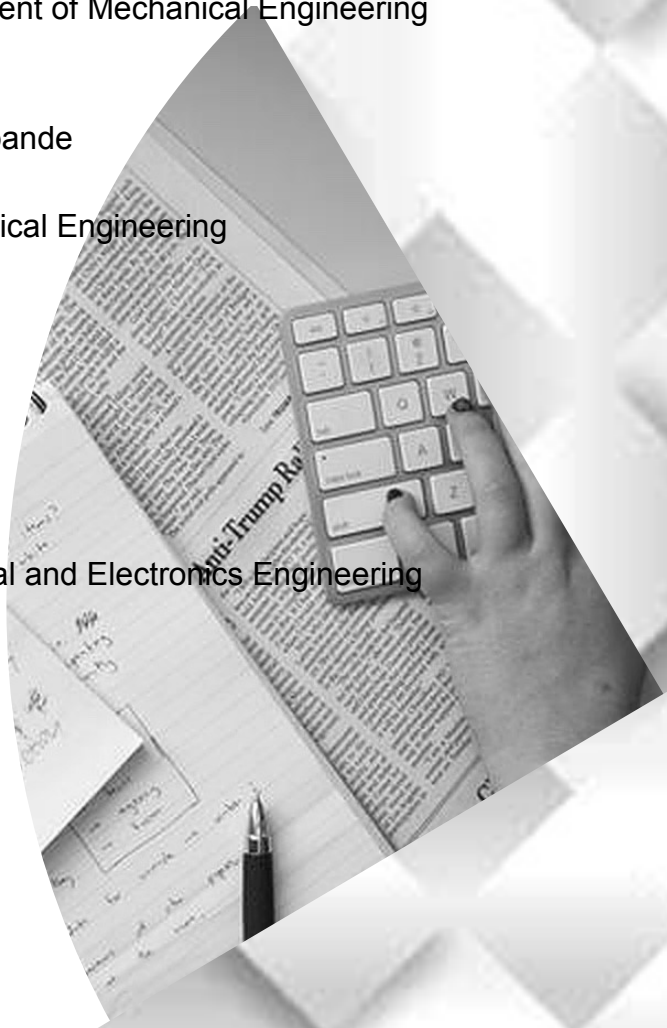

Glimpses of ICGCP - 2022

ICGCP-2022

SAPTHAGIRI
College of Engineering
Creating Tomorrow

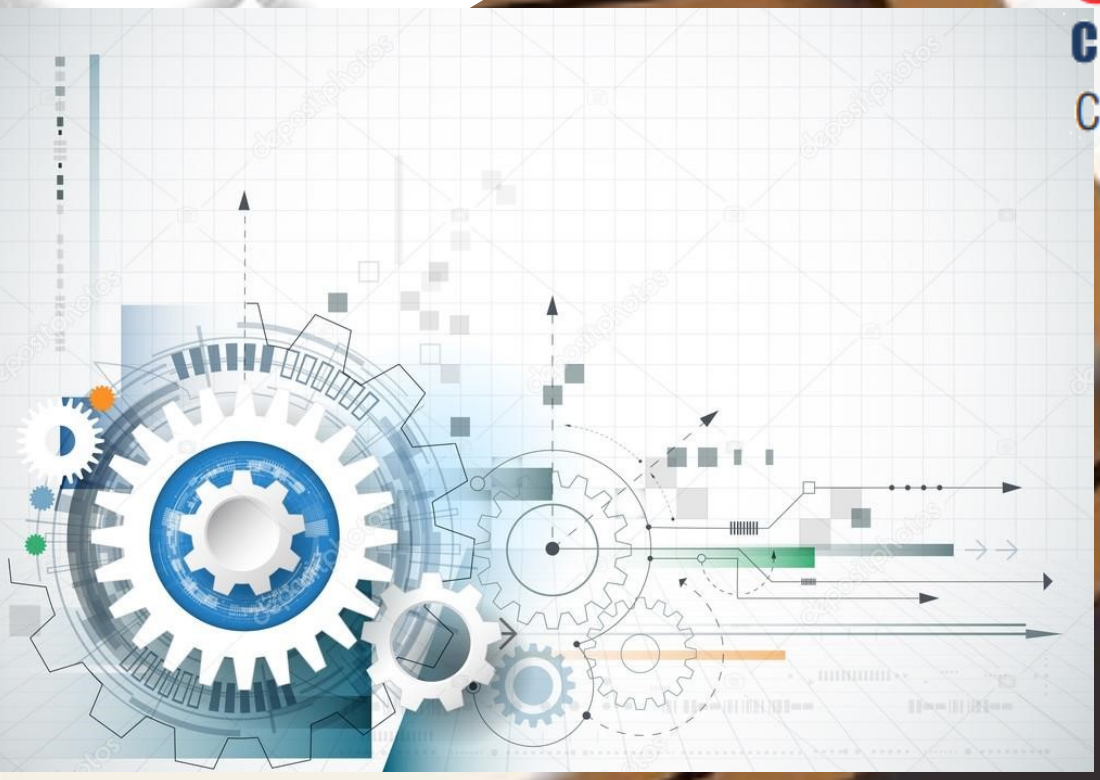

sapthagiri.edu.in

Google Map

Sapthagiri College of Engineering

Affiliated to VTU, Belagavi, Approved by AICTE, New Delhi
(Accredited by NAAC with "A" Grade) (Accredited by NBA for ECE, CSE, ISE, ME, EEE)
& ISO 9001:2015 and ISO 14001:2015 Certified Institution
#14/5, Chikkasandra, Hesaraghatta Main Road, Bengaluru-560057

INDEX

Mechanical Sciences Proceedings

Sapthagiri College of Engineering
Affiliated to VTU, Belagavi, Approved by AICTE, New Delhi
(Accredited by NAAC with "A" Grade) (Accredited by NBA for ECE, CSE, ISE, ME, EEE)
& ISO 9001:2015 and ISO 14001:2015 Certified Institution
#14/5, Chikkasandra, Hesaraghatta Main Road, Bengaluru-560057

45.	Ultrasonication Assisted Synthesis of Dy3 Activated caal2o4 Nanophosphor: Photoluminescent and Photometric Properties Prompted WLED's and Latent Fingerprints Development Applications	233

Automatic Bike Side Stand

Mr. Mohan AE
Asst. Professor
Dept. of Mechanical engineering
Sapthagiri college of engineering
Bangalore, India
mohan@sapthagiri.edu.in

Mr. Rohith A N
student
Dept. of Mechanical engineering
Sapthagiri college of engineering
Bangalore, India
rohithan2463@gmail.com

Mr. Moneeth Kumar B
Student
Dept. of Mechanical engineering
Sapthagiri college of engineering
Bangalore, India
moneethkumar@gmail.com

Mr. Praveen c
Student
Dept. of Mechanical engineering
Sapthagiri college of engineering
Bangalore, India
Yashpraveen1234@gmail.com

Mr. Thyagaraju B M
Student
Dept. of Mechanical engineering
Sapthagiri college of engineering
Bangalore, India
thyagarajubm25@gmail.com

Abstract— The side stand is used for supporting a parked motorcycle. If the rider may forget to retract the side stands before riding, then the undistracted stand hitting the ground and affected the riders control during the turn.
Now a day's sensor are used for ensure that the stand is in released condition. The motorcycle side stand consists of a metallic rod and helical spring which is offset from the centre. Some side stand retract automatically when the motorcycle is lifted up the support some other are fit with electrical interlocks , warning devices or special retracting mechanism. In this paper there is possibility to reduce the evident which is takes place by the side stand.
Side stand in two wheelers function the entire weight of the vehicle when it is parked. They are perfect on quick stop when one need to leave the vehicle for short while. They are provided with the spring that pulls it back into position to ensure extra safety. The presented mechanism consists of D.C. motor powered by motorcycles battery. Connected to the worm and worm gear mechanism for reduction of speed of motor and multiply the torque. The motor is actuated by the Rotation sensor which is mounted on the front of the wheel.
Keywords- D.C

I. INTRODUCTION

In all over world everywhere motorcycle are used. The side stand plays major roll while the vehicle is in rest position. But it has some disadvantages takes place as while the driver starting the motorcycle, there may be possibility of forget to release the side stand this will caused to unwanted troubles. This is a new type of side stand which is automatically retracting the side stand through some mechanical and electronic arrangement. In this system microcontroller, speed sensor, dc battery is used. Through the speed sensor, sensor sense the rotation of the wheel and sends the signal to the microcontroller which is actuate the dc motor which is caused the disengage the stand from the road.
A motorcycle side stand is nearly universal method of allowing a motorcycle rider to park his vehicle easily. If this stand is in the park position while the motorcycle is ridden through left turn a serious hazard exists. A new type stand side stand which is automatically retracting side stand is invented to prevent such type of accidents. Side stand mounted behind bottom bracket and can be bolted on either clamping the chain stays, or welded in to place as an integral part of the frame.
The motorcycle side stand consists of steel rod held in both park and stopped position by an over centered spring. It is to provide the stand stability and a support to the motorcycle. Many side stand designs, attachments, mechanisms and rider warning system. Some side stand retracts automatically when the motorcycle is lifted off the support. Some retract if they contact the ground when the motorcycle is moving. Many different concepts have been applied for this hazard.

ISBN: 979-88-35073-61-0

II. LITERATURE REVIEW: Rohith A N, Moneeth kumar B, Thyagaraju B M, Praveen C, has worked on automatic side stand. If the rider may have forgot to retract the side stand before riding, then undistracted stand hitting the ground and effected the rider control during the turn and this will have caused to unwanted troubles.
In this paper the presented mechanism consists of D.C. motor powered by motor cycle battery which is connected o the worm and worm gear mechanism for reduction of speed of motor and multiplying the torque then the motor is activated by micro controller circuit. We observe that from the design and analysis D.C. motor and other components like micro controller circuit, switch is occupying less space and this space is easily available into the mechanical frame of the motorcycle. After analysis of torque the required torque to rise the side stand is 6070 Nm and the power required to stand which is 19.078 W. has worked on sprocket side stand retrieve system it is based on the working principle of two wheelers. In motor bike power is transmitted from engines pinion to rear wheel, the linear motion of the chain is obsorbed b rear wheels spocket and converted into rotary motion. That rotary motion of the rear wheel makes the bie to move. This system could be used in all type of two wheelers for retrieving side stand and to control accident due to side stand problem and protected the careless rider. Rohith A N, Moneeth kumar B, Thyagaraju B M, Praveen C has worked on automatic side stand retrieve system, this system is based on working principle of two-wheeler. The power is generated in the engines and it transmit power to the pinion and it to rotate the pinion transmits power to the rear wheels Pinion and makes vehicle to move, the objectives of the system is to provide a device responsive to an operating condition of the engines of the motor cycle for moving the stand to its raised position when motor cycle is in its running position.

III. COMPONENT OF SYSTEM

1) Battery
2) Servo Motor
3) Push button
4) Micro controller (Arduino Controller)
5) Side stand
6) Buck convector

Dry cell Battery -
A dry cell uses a paste electrolyte, with only enough moisture to allow current to flow. Unlike a wet cell, a dry cell can operate in any orientation without spilling, as it contains no free liquid, making it suitable for portable equipment. By comparison, the first wet cells were typically fragile glass containers with lead rods hanging from the open top and needed careful handling to avoid spillage. Lead–acid batteries did not achieve the safety and portability of the dry cell until the development of the gel battery. A common dry cell is the zinc–carbon battery, sometimes called the dry Leclanché cell, with a nominal voltage of 1.5 volts, the same as the alkaline battery (since both use the same zinc–manganese dioxide combination). A standard dry cell comprises a zinc anode, usually in the form of a cylindrical pot, with a carbon cathode in the form of a central rod. The electrolyte is ammonium chloride in the form of a paste next

to the zinc anode. The remaining space between the electrolyte and carbon cathode is taken up by a second paste consisting of ammonium chloride and manganese dioxide, the latter acting as a depolarizer. In some designs, the ammonium chloride is replaced by zinc chloride.

Servo Motor -

Servo motor is designed for two speed operation. It consists of three brushes namely: common, low speed, high speed. Two of the brushes will be supplied for different made of operation. The DC motor does not oscillate back and forth, it rotates continuously in one direction like most others motors. The rotational motion is converted to the back and forth wiper motion by a series of mechanical linkage. This type of motor is called a gear head or motor end has advantage of having lots of torque. The dc motor works on 12volt D.C. battery.

Powering the motor -

Voltage- the standard voltage requirement for the motor is 12v DC. The electrical system in a running automobile usually puts out between 13 and 13.5 volts, so it's safe to say the motor can handle up to 13.5 volts with no problem. I wouldn't recommend any voltages higher than that.

Current -

The minimum required current for the motor is 1.6 amps 70 rpm, 0.9 amps at 41 rpm. These current ratings are for the motor spinning with no load. As you add mechanical load, these numbers can increase dramatically, doubling or even tripling under a heavy load. This factor must be taken into account when selecting a power supply. Since the motor will only use what it needs when it comes to current, it's best to provide a source with a higher current rating than you think you might need.

Switch Button -

In electrical engineering,a switch is an electrical component that can break an electrical circuit, interrupting the current or diverting it fromone conductor to another. The most familiar form of switch is a manually operated electromechanical device with one or more sets of electrical contacts, which are connected to external circuits. Each set of contacts can be in one of two states: either "closed" meaning the contacts are touching and electricity can flow between them, or "open", meaning the contacts are separated and the switch is nonconducting. The mechanism actuating the transition between these two states (open or closed) can be either a "toggle" (flip switch for continuous "on" or "off") or "momentary" (push-for "on" or push-for "off") type.

A switch may be directly manipulated by a human as a control signal to a system, such as a computer keyboard button, or to control power flow in a circuit, such as a light switch. Automatically operated switches can be used to control the motions of machines, for example, to indicate that a garage door has reached its full open position or that a machine tool is in a position to accept another workpiece. Switches may be operated by process variables such as pressure, temperature, flow, current, voltage, and force, acting as sensors in a process and used to automatically control a system. For example, a thermostat is a temperature-operated switch used to control a heating process. A switch that is operated by another electrical circuit is called a relay. Large switches may be remotely operated by a motor drive mechanism. Some switches are used to isolate electric power from a system, providing a visible point of isolation that can be padlocked if necessary to prevent accidental operation of a machine during maintenance, or to prevent electric shock.

An ideal switch would have no voltage drop when closed, and would have no limits on voltage or current rating. It would have zero rise time and fall time during state changes, and would change state without "bouncing" between on and off positions.

Practical switches fall short of this ideal; they have resistance, limits on the current and voltage they can handle, finite switching time, etc. The ideal switch is often used in circuit analysis as it greatly simplifies the system of equations to be solved, but this can lead to a less accurate solution.

Micro controller (Arduino Controller) -

A **micro controller** (sometimes abbreviated **µC**, **uC** or **MCU**) is a small computer on a single integrated circuit containing a processor core, memory, and programmable input/output peripherals. Program memory in the form of NOR flash or OTP ROM is also often included on chip, as well as a typically small amount of RAM. Microcontrollers are designed for embedded applications, in contrast to the microprocessors used in personal computers or other general purpose applications. Microcontrollers are used in

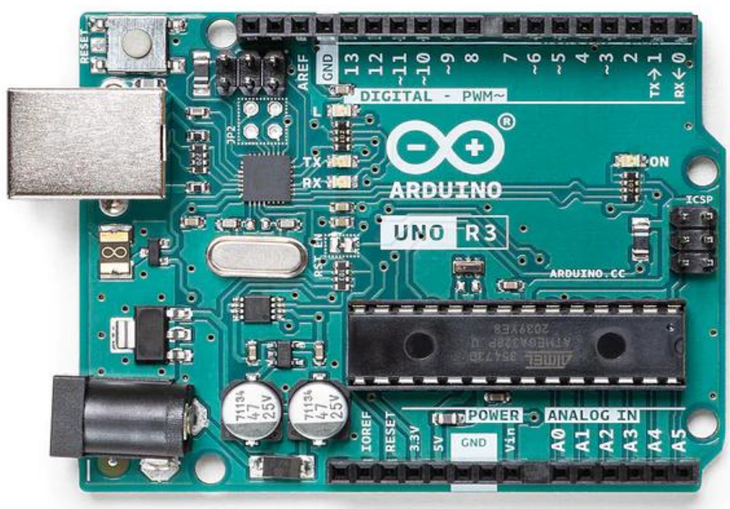

automatically controlled products and devices, such as automobile engine control systems, implantable medical devices, remote controls, office machines, appliances, power tools, toys and other embedded systems. By reducing the size and cost compared to a design that uses a separate microprocessor, memory, and input/output devices, Micro controllers make it economical to digitally control even more devices and processes. Mixed signal micro controllers are common, integrating analog components needed to control non-digital electronic systems.

Side Stand -

A Side stand is a device on a bicycle or motorcycle that allows the bike to be kept upright without leaning against another object or the aid of a person. A "smaller, more convenient" kickstand was developed by Joseph Paul Treen, the father of former Louisiana Governor, Dave Treen. A kickstand is usually a piece of metal that flips down from the frame and makes contact with the ground. It is generally located in the middle of the bike or towards the rear. Some touring bikes have two: one at the rear, and a second in the front.

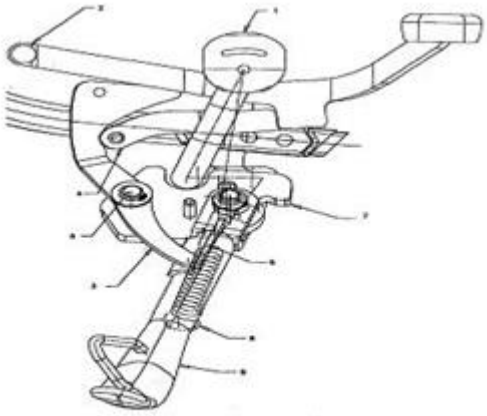

Fig 2.2 - Side stand

A side stand style kickstand is a single leg that simply flips out to one side, usually the non-drive side, and the bike then leans against it. Side stands can be mounted to the chain stays right behind the bottom bracket or to a chain and seat stay near the rear hub. Side stands mounted right behind the bottom bracket can be bolted on, either clamping the chain stays or to the bracket between them, or welded into place as an integral part of the frame.

Buck convector -

A buck converter (step-down converter) is a DC-to-DC power converter which steps down voltage (while drawing less average current) from its input (supply) to its output (load). It is a class of switched-mode power supply (SMPS) typically containing at least two semiconductors (a diode and a transistor, although modern buck converters frequently replace the diode with a second transistor used for synchronous rectification) and at least one energy storage element, a capacitor, inductor, or the two in combination. To reduce voltage ripple, filters made of capacitors (sometimes in combination with inductors) are normally added to such a converter's output (load-side filter) and input (supply-side filter).[1] It is called a buck converter because the voltage across the inductor "bucks" or opposes the supply voltage.

Switching converters (such as buck converters) provide much greater power efficiency as DC-to-DC converters than linear regulators, which are simpler circuits that lower voltages by dissipating power as heat, but do not step up output current.

The efficiency of buck converters can be very high, often over 90%, making them useful for tasks such as converting a computer's main supply voltage, which is usually 12 V, down to lower voltages needed by USB, DRAM and the CPU, which are usually 5, 3.3 or 1.8 V.

The conceptual model of the buck converter is best understood in terms of the relation between current and voltage of the inductor. Beginning with the switch open (off-state), the current in the circuit is zero. When the switch is first closed (on-state), the current will begin to increase, and the inductor will produce an opposing voltage across its terminals in response to the changing current. This voltage drop counteracts the voltage of the source and therefore reduces the net voltage across the load. Over time, the rate of change of current decreases, and the voltage across the inductor also then decreases, increasing the voltage at the load. During this time, the inductor stores energy in the form of a magnetic field.

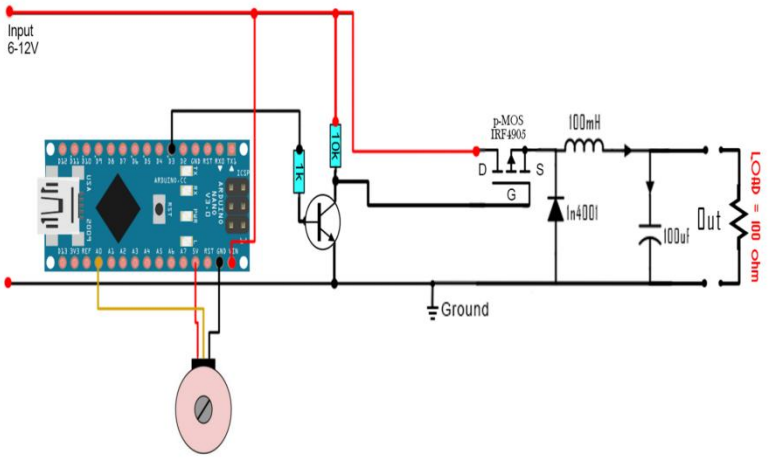

If the switch is opened while the current is still changing, then there will always be a voltage drop across the inductor, so the net voltage at the load will always be less than the input voltage source. When the switch is opened again (off-state), the voltage source will be removed from the circuit, and the current will decrease. The decreasing current will produce a voltage drop across the inductor (opposite to the drop at on-state), and now the inductor becomes a current source. The stored energy in the inductor's magnetic field supports the current flow through the load. This current, flowing while the input voltage source is disconnected, when appended to the current flowing during on-state, totals to current greater than the average input current (being zero during off-state).

Toggle Switch -

In electrical engineering, a **switch** is an electrical component that can disconnect or connect the conducting path in an electrical circuit, interrupting the electric current or diverting it from one conductor to another.[1][2] The most common type of switch is an electromechanical device consisting of one or more sets of movable electrical contacts connected to external circuits. When a pair of contacts is touching current can pass between them, while when the contacts are separated no current can flow.

Switches are made in many different configurations; they may have multiple sets of contacts controlled by the same knob or actuator, and the contacts may operate simultaneously, sequentially, or alternately. A switch may be operated manually, for example, a light switch or a keyboard button, or may function as a sensing element to sense the position of a machine part, liquid level, pressure, or temperature, such as a thermostat. Many specialized forms exist, such as the toggle switch, rotary switch, mercury switch, push-button switch, reversing switch, relay, and circuit breaker. A common use is control of lighting, where multiple switches may be wired into one circuit to allow convenient control of light fixtures. Switches in high-powered circuits must have special construction to prevent destructive arcing when they are opened.

III STEP INVOLVED FOR MAKING AUTOMATIC SIDE STAND FOR TWO WHEELER

STEP1 - CONSTRUCTION OF FRAME

Firstly we are made a general layout of side stand frame according to dimension given in present time of two wheeler. for making frame, we are used mild steel rod and with the help of manufacturing process be prepare a rectangular frame the manufacturing process include for making side stand frame are cutting, welding , grinding ,and super finishing .this figure shows the mild steel rod for making side steel frame.

STEP 2 - MAKING PLATE FOR PIVOTED SIDE STAND FROM FRAME

In this stage we are made plate on which side stands are pivoted. The dimension of this plate is given according to motorcycle specification. The plate consists of hole for bolted the side stand and a upper hook are welded to connect the one end of the spring. This plate is welded with the frame inclined to the frame axis.

STEP 3 – MAKING A TENSION SPRING

In this step we take a spring wire and with the help of lathe machine we form a tension spring. The material of the tensile spring is stainless steel. After lab test we found the stiffness of spring. 1.732 N/mm.

STEP 4 – MAKING A MECHANICAL BUSH

In this step we make we make a mechanical bush from a solid rod of stainless steel with the help of of the lathe machine. Firstly we have done turning operation for finding the desire dimension and after that we have made a hole with the help of drill bit. The main function of mechanical bush is to connect the motor shaft to the pivoted bolt of side stand.

STEP 5-FINAL ASSEMBLY

In this step all the component of side stand are assembled in proper manner.

the presented mechanism consist of a D.C motor powered by motorcycle's battery ,connected to the side stand through a worm and worm gear mechanism to gain speed reduction of motor and multiply the torque . The motor is actuated by the sensor mounted on the front wheel through the Micro controller. A presser switch is also mounted on the stand bracket to sense full disengagement of stand. When the vehicle starts moving the sensor on front wheel sends a signal to the micro controller to actuate the motor causing them to move disengaged position. When the stand is fully disengaged it presses the pressure switch which again sends a signal the micro controller which stops the motor.

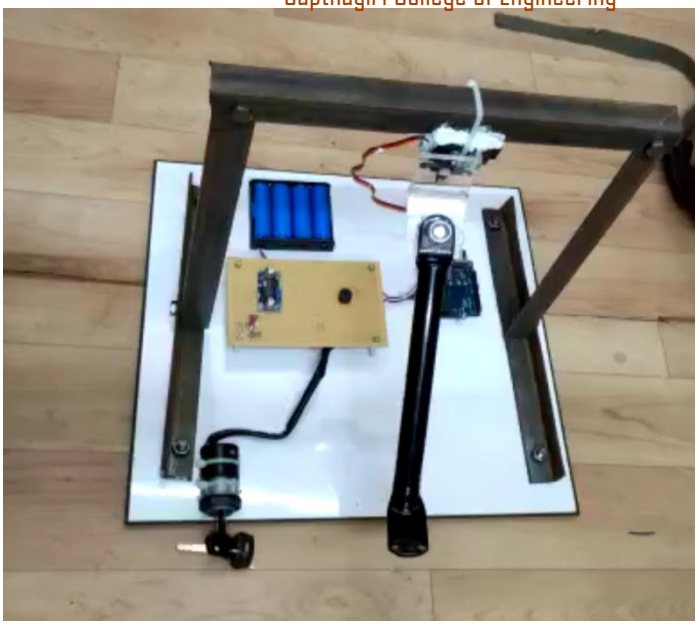

Fig -final assembly

IV. SYSTEM ANALYSIS

Calculation -

Wire diameter = 3 mm = 0.003 m
Coil outer diameter (d) = 27 mm = 0.027m
Coil inner diameter = 21mm = 0.021m
No. of coils (n) = 17
Free length of spring (L) = 휋dN
3.14x0.027x17=1.44126 m
Span weight = 0.056+0.400 kg
= 0.456 kg
F = K × X
F = 1.732x1.21536
F = 2.105 N

TORQUE –

T = FXR
T =2.105X0.11
T =0.2315 N-m
Torque due to stand weight
Stand weight = 400 gm
Spring weight = 56 gm
Combined weight of spring and stand = 400+56 gm
= 0.456 kg
Force due to stand weight =
mg sin θ = 0.456x9.81xsin50$_0$
= 3.4267 N
Torque due to stand weight
= F x R
= 3.4267x0.11
= 0.3769471
Total torque (T_a)
= 0.2315+0.376947
= 0.6087 N-m

IV. CONCLUSION

We observe that from the design and analysis Servo motor and other component like as micro controller and speed sensor ,switch are occupies less space and this space is easily available into the mechanical frame of the motorcycle . After analysis of torque the required torque to raise the side stand is 6076 N-m. So after calculation of torque we determined the power required to raise the side stand which is 19.078 Watt. So we design automatic side stand for maximum frictional torque. Hence we used 12V DC geared motor which draws 2 amp current and 24W power.
Automatic stand is presently in use and quite successful. Although it has certain disadvantages

When the rider pushes the button then the kick stand is disengage from the road.
And secondly the stand is not engage with road by the use of push button.
We are working to remove this two disadvantages. For removing these two disadvantages we use the speed sensor and micro controller and push button, when bike take some RPM then the sensor sense the signal and sends to the Micro controller and according to the C programming the Micro controller actuate the DC motor, and the dc motor automatically disengage the side stand from the road. Through this arrangement the both disadvantages are removed.

V. REFERENCES

1. Everett, S.A., Shults, R.A., Barrios, L.C., Sacks, J.J., Lowry, R. and Oeltmann, J. (2001) Trend and subgroup differences in transportation related injury risk and safety behaviors among high school students.

2. Reeder, A.I., Chalmers, D.J. and Langeley, J.D. (1996) The risky and protective motorcycling opinions and behaviors of young on road motorcyclist in New Zealand

3. Sabey, B.E. and Taylor, H. (1980) The known risk We run: The Highway.

4. Hurt, H.H., Ouellet, J.V. and Thom, D.R. (1981) Motorcycle accident cause factors.

5. Grayson, G. and Hakkert, A. (1987) Accident analysis and conflict behaviour. In J. Rothengatter and R. de Bruin (eds) Road user and traffic safety.

6. Malaterre, G. (1990) Error analysis and in- depth accident analysis.

7. Yin, R.K., (1984) case study research, Applied Social research Methods vol. 5. London Sage Publication.
1891- Frederick G.Taylor and R.L GRANSTON, “bicycle support”, U.S.patent 456,347

BIG DATA AND ARTIFICIAL INTELLIGENCE IN AGRICULTURE

[1]Shwetha B S , [2]Santhosh H C, [3]Parshwanath.P
Department of Mathematics, Sapthagiri College of engineering
#14/5Chikkasandra,Hesaraghattamain road,Bangalore-57 India
[1]shwethabs@sapthagiri.edu.in, [2]santhoshhc@sapthagiri.edu.in, hodmaths@sapthagiri.edu.in

Abstract *- Agriculture plays breath taking role during pandemic situations, what human community is facing and experiencing in 2020. Crop yielding depends on several parameters which is nothing but data. When the data is more or big, it helps in analysis and decision making process. In this case farmers take decisions based on various data available to them. To make farmers life easy, data analytics plays a vital role and big data technology is the key technology to be used. Along with this, Artificial intelligence can be used to analyse various parameters helping farmers in completing the process of cultivation with good and accurate results.*

In this work, we study on various approaches of implementing big data and Artificial technology to address problems faced by farmers and find out solutions by defining problems which can be implemented practically. We also try to find out the challenges, tools to face challenges and solutions for these challenges.

Key words:

Big data, ArtificialIntelligence(AI), Agriculture, crop development

I. INTRODUCTION

Approximately 26.5% of the world's population work in agriculture.

The agricultural industry is looking at different solutions to meet these challenges, one of which is data analytics. Big Data analytics is seen as the fourth technological revolution in agriculture and it is hoped that it will provide a solution to our growing food demands

Big Data today dominates many fields, but scientists at the science congress think agriculture will also soon be driven by data analytics and artificial intelligence (AI).

Agricultural Big Data analytics is the analysis of large datasets from a wide range of re-sources, often using artificial intelligence (AI) techniques . "With advancement of satellite and drone technology, agriculture is entering the domain of big data," said Partha P. Banerjee, Asia Pipeline Lead, Bayer Crop Science Ltd., delivering a plenary lecture at ISC 2020 on Tuesday. Incidentally, the State government has already begun experimenting with drone technology for farm data collection and crop pattern analysis.

"From mobile phones to satellites, we are producing data on the farms everyday. If tillers are fit with sensors, we can analyse the soil nutrient conditions of every inch of the farm and its applications are immense. Drone technology and data analytics are already being used to recommend advanced water irrigation strategies and diagnose disease on the farm in real time. This will help farmers understand which part of the farm needs more water or where the disease is spreading from, so that it can be tackled," he said.

Yield of a crop is a function of seed and plant genetics, environment and climate, and farm practices. To each of these, we have data layers, for instance, soil health, temperature, humidity, and rainfall for climate input. We have identified 40 key decisions a farmer makes from sowing to harvest. Data analytics can help farmers make informed decisions based on three larger parameters the yield is a function of," he said. "We are still in the prescriptive analytics stage and science will move towards predictive analytics,".

II. Role of data analysis in agriculture

Application of science and new technologies is currently lacking within this space. Many companies and start-ups are looking to fill this information gap. If Big Data has made serious advancement in fields like information technology, healthcare, education and even sports, there is an obvious need for it in the agricultural industry too.
While the vast majority of farmers and ranchers did great work for maintaining and increasing soil health using conservation practices alone, measurement tools will be instrumental in ensuring a sustainable farming future.
To maintain yields and meet the food demands of a growing population while also protecting natural resources required, making additional changes and data tools can help determine what these changes should be.
The end result of gathering data is to analyse it and come up with actionable solutions with better results. For example, a satellite image of a plot of land has several layers of data embedded into a single spectrum giving us a tonne of information to analyse. The geospatial approach and satellite monitoring of farms have led to major advancement in how farmers and companies make their decisions.

III. AI in Agriculture – An Overview

Essentially, AI in agriculture is segmented into robotics, soil and crop management, and animal husbandry, and is designed to make farming easier, more accurate, more profitable, and more productive for the farmer. It is estimated that AI and connected farm services can impact 70 million Indian farmers by 2020, thereby adding US$ 9 billion to farmer incomes. In 2017, the global AI in agriculture market size was US$ 240 million, and is expected to reach US$ 1.1 billion by 2025 (Maher, 2018). Furthermore, issues such as population growth, climate change, and food security demand innovative ways to improve crop yield. Therefore, understanding the use of AI in agriculture becomes compelling

IV . Applications of AI in Agriculture

to farmers in efficiency gains and higher incomes. The world needs to produce 50% more food by 2050. However, only 4% of additional land will come under cultivation to meet this demand (Bagchee, 2018). AI holds the promise of driving an agricultural revolution at a time when the world must produce more food using fewer resources. This essay briefly discusses key applications of AI in agriculture along different stages of the cropping cycle that have the potential to pay dividends

- **Soil Analysis and Monitoring**

AI can be used to monitor soil health with the help of sensors, cameras, and infrared rays that scan the soil for its nutritional properties (Sennaar, 2019; Baruah, 2018). This also helps in understanding the reaction of specific seeds to different soils, the impact of weather changes on the soil, and the probability of the spread of diseases and pests (Irimia, 2016). With such data in hand, the efficiency of crop inputs is improved, leading to cost savings and productivity gains for farmers. Currently, an average of 207.56 kg of chemical fertilisers are used per hectare in Haryana annually (one of the highest among Indian states). Besides being costly for farmers, fertilisers also introduce harmful substances into the food chain through crops and the water table (Indian Fertiliser Scenario, 2013).

Case Study: AI-backed soil health monitoring used in Raleigh, North Carolina, USA, led to huge efficiency gains in the use of agro-inputs by cutting the use of chemical fertilisers by nearly 40% (Sennaar, 2019). Furthermore, the spatial analysis capabilities of geographic information system (GIS) technologies helps in efficient water management during irrigation. For instance, in Alfalfa in Riverdale, California, GIS technologies in irrigation helped to increase the per acre crop output by up to 37.5%, and reduced water usage by 20% (Fictchett, 2013).

Therefore, AI in analysing and monitoring soil health helps to improve the sustainability of a given piece of arable land.

- **Crop Sowing**

AI in crop sowing is used essentially to drive predictive analytics to determine when and how to sow. It helps in making predictions on the right time to plant, apply fertilisers, harvest, bale, till, etc. based on climate data, historical conditions, market conditions for

Case Study: In 2016, Microsoft, in partnership with ICRISAT (The International Crop Research Institute for the Semi-Arid Tropics), initiated a pilot project in DevanakondaMandal in the Kurnool district of Andhra Pradesh. The pilot had a sample base of 175 farmers who were alerted on their mobile phones about suitable cropping dates, land preparation, and soil test-based fertiliser utilisation. This helped increase crop output by around 30%. In 2017, this project was expanded to cater to approximately 3,000 farmers in Karnataka and Andhra Pradesh during the *Kharif* cycle for a host of crops like groundnut, *ragi*, maize, rice, and cotton, among others. The increase in crop yield following the AI intervention ranged from 10-30% across all crops (Nagpal, 2017).

Therefore, AI in crop sowing has the potential to increase per acre crop output as well as decrease input costs for farmers.

- **Weed and Pest Control**

Average losses of up to 90% of the total crop production have been reported due to the infestation of weed (Meena, 2015). Similarly, average losses of up to 19% have been reported due to pests (Dhaliwal *et al.*, 2015). This leads to a greater use of pesticides, further contaminating the soil and groundwater.

As of today, there are 250 identified species of weeds which have become completely resistant to herbicides (Sennaar, 2018), presenting a severe threat to the sustainability of crop production. Pesticide resistance is also on the rise. The purchase of insecticides and pesticides contribute approximately 5% to the total cost inputs in agriculture, and this cost is on rise both in percentage and absolute terms (Price Policy for *Kharif* crops, 2017-18; Price Policy for *Rabi* Crops, 2014-15).

Case Study: AI helps to optimise on weed and pest management by reducing up to 80% of weedicides and pesticides used currently (Sennaar, 2019). According to a Bloomberg report (2018), a project was undertaken by the Blue River Technologies (now under John Deere & Co.) to evaluate the effectiveness of AI-supported weed controlling technologies. The 'See & Spray' technology tested under this project in Marianna, Arkansas, USA, reduced the expenditure on weedicides by around 90% reducing the need for weedicides used per acre from 20 to just 2 gallons (Little, 2018).

Therefore, AI finds great application in precision weed and pest management**.**

- **Crop Harvesting**

An estimated 40% of annual agriculture costs go into the employment of labour, predominantly for sowing and harvesting (Sennaar, 2019). AI-enabled robots for harvesting can lead to huge cost savings by reducing the need for approximately 4 agricultural labourers per acre of land (Panpatte, 2018). Furthermore, crops can be sorted according to pre-identified grades at the time of harvest, saving time and enhancing the quality of crops. However, AI is likely to change the way labour is employed in agriculture. Although conventional manual jobs will be replaced, AI presents new opportunities for job creation.

Case Study: AI-enabled robots are being widely deployed on tomato farms in Japan, and have reduced the on-field labour time by 20% (Panasonic, 2018).

Therefore, AI-enabled robots for crop harvesting save the resources of labour and time for farmers.

V. Supply Chain Management

Policymakers have not yet been able to tackle the agricultural supply chain challenge. On the one hand, farmers either do not receive a suitable price for their produce that continues to rot in *mandis* (or marketplace), and on the other, food consumers either end up paying exorbitant prices or are malnourished. Although AI in agricultural supply chain management is yet to make major inroads, its informed application in supply chain planning and optimisation, including demand forecasting and logistics, can lead to huge cost savings for farmers, and solve the information asymmetry problem for buyers.

Case Study: Platforms like Jivabhumi's 'Foodprint' aggregates and traces farm produce, and offers a digital marketplace. It uses blockchain technology to connect farmers and institutional buyers via an efficient and traceable supply chain (Baruah, 2019).

Therefore, AI has the potential to improve the agricultural supply chain efficiency and reduce spoilage.

Big data can help in Agriculture to increase the production By

1) Boosting productivity and innovation

2) Managing environmental challenges

3) Cost savings and business opportunities

4) Better supply chain management

VI. Advantages of data analysis in agriculture

Data helps debt-laden farmers, insurance agencies, loan banks, seed companies, machine industry and every big and small player. Data analysis not only creates greater awareness and more accurate knowledge, but it can also plug the lacunae in the supply and marketing chain of the industry. Information is power, and the industry can now have access to it for more informed decision making. These are the ways in which data analysis can help:

Development of new seed traits - Access to the plant genome with new ways to measure, map and drive information betters products.

Precision farming - Big data takes advantage of information derived through precision farming in aggregate over many farms. The resulting analytics, insights and better decisions can then be deployed through precision farming techniques

Food tracking - Use of sensors and analytics to prevent spoilage and food-borne illnesses

Effect on supply chains - Seismic shifts in the supply chain of seed, crop inputs and food driven by the democratisation of technology and information

The big data revolution is in its early days and most of the potential for value creation is still unclaimed. But it has set the industry on a path of rapid change and new discoveries. Stakeholders committed to innovation will likely be the first to reap rewards. If the farmers would have been concerned about the infirmities in terms of data-based farming, production could be increased.

VII. Big Data Applications in Agriculture

Let's look at a real-life example of the application of big data. Yanmar, a Japanese manufacturing company, set out to create a

sustainable 'smart' greenhouse infrastructure to increase process efficiencies .Cameras objectively track plant growth. Yanmar then utilizes Amazon Web Services to document, track, and analyze this video feed to understand the various stages of a crop's progress. Once certain growth milestones are achieved, Yanmar uses its newly found data intelligence to intuitively adjust the water and nutrient balances that the plants receive to optimize their overall growth. This pattern of growth tracking and nutrient balancing allows Yanmar to create tangible data around which method of agricultural nurturing is best and develop new methodologies for farming specific types of plants while maintaining resource-conserving practices.

VIII. Conclusion

Big data and artificial intelligence are in a mutually exclusive relationship — as one advances, the other benefits. As it benefits, it progresses, and the cycle continues to evolve both technologies. In more applicable terms, the use of big data collecting activities in smart agriculture will create more resilient and useful AI models, as with Blue River Technologies. The deployment of these models will create more efficient methods of smart agriculture processes, as we see with companies such as Yanmar. That, in turn, will generate more data to be understood and optimized.

The implementation of big data and AI in smart agriculture has already had profound effects on a small scale, and its global impact will assuredly be even more insightful in years to come.

VIII. References:

1.Ethics of Using AI and Big Data in Agriculture: The Case of a Large Agriculture Multinational

2. Artificial Intelligence in Indian Agriculture - An Industry and Startup Overview

3.Big Data in Smart Farming – A review

4. Smart Agriculture Gets a Boost from Big Data and AI

BLIND SPOT MONITORING

(FOR INDUSTRIAL APPLICATIONS)

Amar Singh[1], Ashish HG[2], Bharat S Hegde[3], M V Gagan[4], Basavaraju S[5]

[1-4]UG Students, Department of Mechanical Engineering, Sapthagiri College Of Engineering
#14/5 Chikkasandra, Hesaraghatta Main Road,Bangalore- Karnataka-560057, India
[1]amar.ssingh08@gmail.com
[2]ashishhg5@gmail.com
[3]bharatshegdechipgi00@gmail.com
[4]mvgagan615@gmail.com

Abstract - The mechanical area is enhancing day with the aid of using day. Lots of modern thoughts are stepping into the area. This task file is certainly to endow with a comprehensive examine of the technical and theoretical factors of "Blind spot monitoring" all of the subjects blanketed on this file are critical for the entire know-how and survey of the title "Blind spot monitoring". In the task we've studied and changed the product. The reports engrosses different chapter and every layout is in the prepared style. Covering primary introduction, specification, application, and its makes use of in numerous industries.

I. INTRODUCTION

To remove blind spots caused by the A-pillar in an automobile, we placed a digital camera on the automotive below the hood of the vehicle that feeds live pictures to a projector placed simply in front of the driver on the dashboard or on top of the driver's head when the steering is rotated to a certain angle. The projector projects the image on to the the screen on the dashboard or that is placed over the driver, which can also line with a retro reflective fabric. When the steering is rotated to a certain angle , it triggers the Arduino which in turn activates the sensors attached to the camera which further sends the signal to the display placed on the dashboard in front of the driver by which the driver can track the real time road path more efficiently. The illustration shows the yellow car turning right at a T-junction with the red shaded areas representing the blind spot areas caused as a result of the A-pillars.

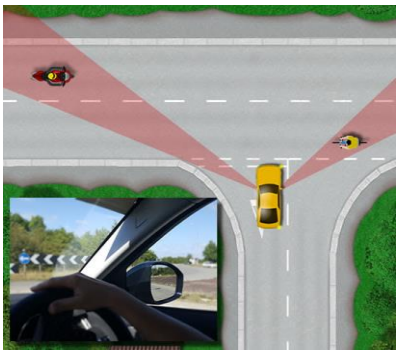

Figure: Blind Spot View

II. MATERIALS AND METHODS

A model that we are building with a pure intention to find an alternate for the blind spot caused by the A-pillar in an automobile. This mainly consists of a night vision camera with an exclusive built quality which can sustain extreme weather conditions, a display that receives signals from the camera placed a under the bonnet outside the vehicle, an Arduino that triggers based on the rotation of the steering to a certain angle, angle sensors that will be attached to the steering rod in the steering hub.The display which we use can be the inbuilt one which comes with the car (for certain cars) , or a new display can be fixed on the dashboard according to the need of the driver.It can be done for both left and right views but the actual problem arises from the one pillar which is nearer to the driver.

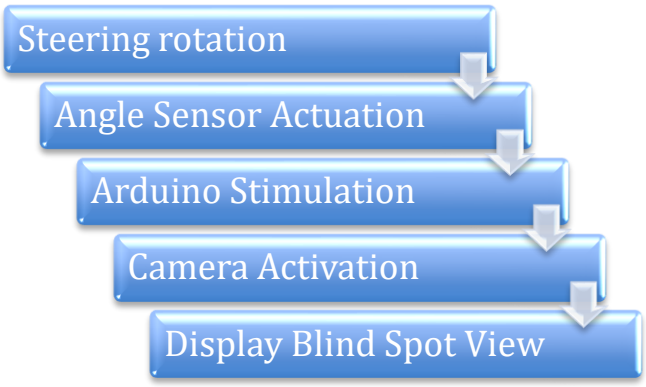

Flowchart: Methodology

III. WORKING

To get a proper output from this project, we can make use of two approaches. These two approaches are as follows:
1. By steering rotation angle method

2. By indicator switch method

In order to obtain highly efficient blind spot removal process, in this project we are making use of steering rotation angle method. For successful working of this project we made use of angle sensor along with Arduino. When the driver makes a turn rotating the steering, at certain angle (which can be fixed according to the steering ratio) ,at which the driver actually gets the blind spot the monitor gets activated. The angle sensor fixed at the steering hub base senses this critical angle and sends signal to the Arduino. The Arduino is programmed according to the need. As the Arduino gets the signal from the angle sensor it activates the camera which is fixed outside of the A-pillar or at the front end of the car. This camera which must have night vision capabilities, to make it efficient during night time, in turn gives the view for the blind spot through the display present in the car. But a monitor on the right end of the dashboard is more preferred in order to get the driver the vision more naturally without having to turn his head away losing control.

Figure: Blind Spot Monitoring

IV. APPLICATION

Blind-spot monitoring (BSM) does exactly what it sounds like: it monitors the area just outside your vehicle's rear quarters. Because many drivers incorrectly set their outboard mirrors, these blind spots can conceal a vehicle approaching in an adjacent lane. As a result, merging into that lane frequently results in a crash. According to the National Highway Traffic Safety Administration (NHTSA), changing lanes or merging causes approximately 9% of all reported vehicle crashes each year. When BSM detects a vehicle about to enter a blind spot, it alerts you that an adjacent lane is not clear. The warning light is usually located somewhere on the outboard rear view mirror on whichever side of the oncoming car is involved. Instead, it could be displayed on your vehicle's A-pillar (the pillar between the windshield and either front door), driver-information display, or head-up display.

V. CONCLUSION

Within the confines of our limited knowledge, this project has provided us with a plethora of opportunities and experiences. It not only enlightened us with theoretical knowledge, but it also instilled practical knowledge in us

about planning, purchasing, assembling, and machining. It is a source of great joy and pride for us to have completed this project successfully in such a short period of time. We accomplished everything in the best way possible by overcoming various constraints and utilising all available amenities.

ACKNOWLEDGEMENT

We would like to expres our sincere gratitude to the Management , Principal of Sapthagiri College Of Engineering Bengaluru for the facilities provided and their support. Also we would like to thank the Head of the Department of Mechanical Engneering and faculties for their encouragement and support.

REFERENCES

- Ian Y.Noya, David Shinarb, William J.Horreya, Automated driving: Safety blind spots, Volume 102, February 2018, Pages 68-78, https://doi.org/10.1016/j.ssci.2017.07.018
- Yuk Ki Cheng, Koon Hung Wong, Chi HangTao, Cheok NingTam, Yiu YanTam, Cheuk NamTsang, Front blind spot crashes in Hong Kong, Volume 266, September 2016, Pages 102-108, https://doi.org/10.1016/j.forsciint.2016.05.013
- Moonsoo Ra, Ho Gi Jung, Jae Kyu Suhrc, Whoi-Yul Kima, Part-based vehicle detection in side-rectilinear images for blind-spot detection, Volume 101, 1 July 2018, Pages 116-128, https://doi.org/10.1016/j.eswa.2018.02.005
- Christian Häne, Lionel Heng, Gim Hee Lee, Friedrich Fraundorfere, Paul Furgale, Torsten Sattler, Marc Pollefeys, 3D visual perception for self-driving cars using a multi-camera system: Calibration, mapping, localization, and obstacle detection, Volume 68, December 2017, Pages 14-27, https://doi.org/10.1016/j.imavis.2017.07.003

CHARACTERIZATION OF GLASS FIBER & GRAPHENE-REINFORCED POLYMER COMPOSITES

CHETHAN H N[1], TEJASWI N K[1], AKHILBABU[1], NITHESH S[1], BASAVARAJ GANIGER[2], RAMESH N G[2]

[1] U G Scholar, Department of Mechanical Engineering, S.C E Bangalore

[2] Assistant Professor, Department of Mechanical Engineering, S.C E Bangalore

Chethangowdru2001@gmail.com

Abstract

The present study is to investigate the mechanical properties of glass fiber reinforced polymer composites (GFRPCs). Glass fibers and graphene have reinforced into epoxy matrix to prepare the composites by hand lay-up technique. The mechanical properties have been studied through tensile, flexural and hardness test as per ASTM standards. The results have been shown that mechanical properties are increased with increase in the percentage of glass fiber in epoxy matrix.

Keywords: Glass Fibres, Graphene nano particles, Epoxy matrix and mechanical properties.

1. INTRODUCTION

Recently, fiber reinforced polymer composites (FRPC) have been considered as the most promising structural materials in the sustainable engineering technology on account of high strength-weight ratio, higher stiffness, cost effectiveness and good reproductively. In FRPCs, high strength fibres are reinforced into low modulus continuous polymeric matrix to make the composites [1,3 &5]. In the case of FRPCs, reinforcement may be either synthetic fibres (glass, carbon, aramid or basalt) or natural fibres (banana, jute, sisal, hemp, bamboo, coir, kenaf and so on), while matrix materials may be thermosets, thermoplasts or bio polymers. Fibres are the backbone of the FRPCs and verify the strength of the composites [2 &4]. The properties of FRPCs mainly depend upon strength and stiffness of fibres, polymer matrices, fibres loading, fibres sizes, fibres orientations, adhesion between fibres and polymeric matrices [6].

Glass fibres are being used in many industries such as automotive, aerospace, construction and military due to their unique properties such as lightweight, high strength and modulus, good availability, recyclability, high strength and toughness, and ease of processing . Glass fibres are the most frequently used reinforcement for

polymeric matrix to prepare its composites. The E-glass and S-glass are the most common and commercially used glass fibres. E-glass is the least expensive than other glass fibres and having a wide range of applications in plastic industry. On the other hand, S-glass shows the higher tensile strength and modulus than E-glass. However, E-glass fibre is very popular as compare to S-glass due to its low cost. Alkali-resistant glass fibres have a small amount of zirconium which helps to prevent corrosion by alkali attacks. Nowadays, GSRPCs have been used in electronics parts such as circuit board, televisions, radios, computers and phones [7, 8 & 9].

Epoxy resin is one of the most used thermosets polymers due to its excellent properties such as good interface, low curing time, high stiffness, better mechanical properties, lower moisture absorption and ease processing at room temperature. They are transparent, light amber color and have very little shrinkage [10].

2. MATERIALS AND METHODS

2.1 Materials

Woven glass fibers are used as reinforcement and epoxy resin as a matrix in this work. Glass fibres and epoxy matrix were purchased from the local resource. Epoxy resin refers to a type of reactive prepolymer and polymer containing epoxide groups. These resins react either with themselves in the presence of catalysts, or with many co-reactants like amines, phenols etc. it was manufactured by araldite with commercial name Epoxy LY 556 (Epoxy Monomer) and Hardener HY-951.were Supplied by zenith industrial supplier, Bengaluru . Graphene nano particles were supplied by Ultra nanotech Pvt ltd. Bengaluru their purity was higher than by 99%. The average Size of Nano particles is 5nm. The details of epoxy matrix and grapheme reinforcements have given in **Table 2.1 & Table 2.2.**

Table: 2.1

Details of Epoxy Matrix

Material -Epoxy LY 556	
Aspect (visual)	Yellow viscous liquid
Viscosity at 25 °C	10000 – 12000 [MPa s]
Density at 25 °C	1.15 – 1.20 [gm/cm3]

Table: 2.1

Details of Graphene

Material –Graphene	
Purity	Greater than 99%
Thickness	5–10 nm
Length	5-10 micron
Density	3.1 g/cm3

2.2 Methods

In this study, manual hand layup method is used for preparing composite laminates as shown in **Fig. 2.1**. First of all, a release gel is sprayed on the mould surface to avoid the sticking of epoxy to the surface. Thin plastic sheets are used at the top and bottom of the mould plate to get a good surface finish of the product. Reinforcement in the form of Graphene nano particles .Then epoxy in liquid form is mixed thoroughly in suitable proportion with a prescribed hardener (curing agent) and poured onto the surface of mat already placed in the mould. The epoxy is uniformly spread with the help of the brush and a roller is moved with a mild pressure on the Graphene-epoxy layer to remove any air trapped as well as the excess epoxy present. After placing the plastic sheet, release gel is sprayed on the inner surface of the top mould plate which is then kept on the stacked layers and the pressure is applied. After curing either at room temperature or at some specific temperature at 60˚C - 80˚C, the mould is opened and the developed composite part is taken out and further processed. For epoxy based system, normal curing time at room temperature is 24 - 48 hours.

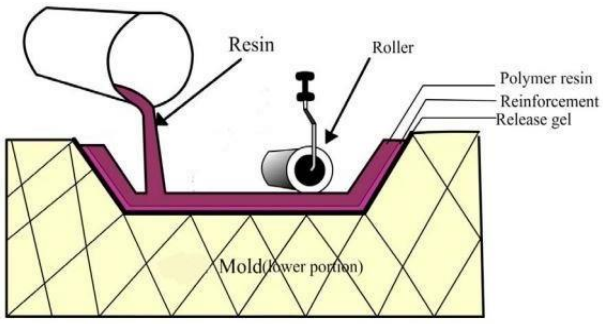

Fig. 2.1 Hand Layup Fabrication.

2.3 Testing of Composites

The tensile test is done by cutting the composite specimen as per ASTM: D638 standard (sample dimension is 216 × 19 × 3 mm^3). A universal testing machine (UTM) (Model: KIC-2-1000-C) is used for testing with a maximum load rating of 100 KN. Composite specimens with different fiber combinations are tested, which are shown in Figure 2.31. In each case, three samples are tested and the average is determined and noted. The specimen is held in the grip and load is applied and the corresponding deflections are noted. The load is applied until the specimen breaks and break load, ultimate tensile strengths are noted. Tensile stress and strain are recorded and load vs length graphs are generated.

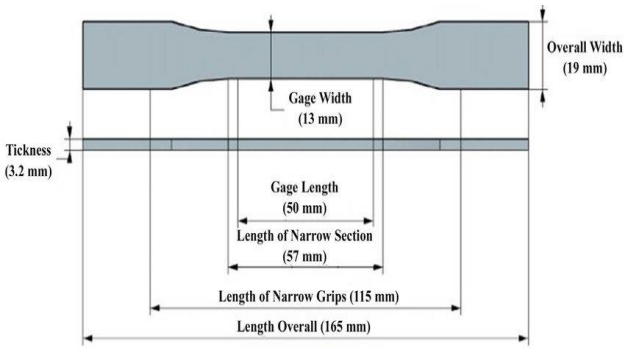

Figure 2.2 3Schematic diagram of Tensile test sample

The flexural test is done in a three point flexural setup as per ASTM: D790 standard (sample dimension is 150 × 12.7× 10 mm^3). When a load is applied at the middle of the specimen, it becomes bends and fractures as shown in Figure 2.32. This test is carried out in the UTM from which the breaking load is recorded and load vs length graphs are generated.

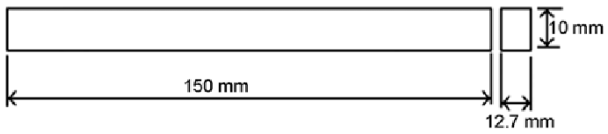

Fig. 2.3Schematic diagram of Flexural test sample

Hardness is the resistance to permanent indentation or penetration. Hardness of materials like polymer, elastomer and rubbers is measured by Shore D scale. Durometer has an indenter loaded by a calibrated spring. The hardness is determined by the penetration depth of the indenter under the load. Hardness test is done by preparing the specimen as per ASTM: D2240 standard.

3. RESULT AND DISCUSSION

ASTM standard specimens were prepared for tensile testing and the average values of calculated tensile strength of different samples were tabulated in **Table 3.1**

Table 3.1

Tensile Test results

Sl. No	Sample	Tensile Strength (N/mm^2)
1	Epoxy	34.6
2	98% Epoxy +1% Glass Fibers+ 1% Graphene	22.99
3	96% Epoxy +2% Glass Fibers+2% Graphene	27.84
4	94% Epoxy +3% Glass Fibers+ 3% Graphene	30.60

From the results, it was observed that the Graphene nano particle and Fiber reinforced with Epoxy specimen possessed higher tensile strength than that of plain Epoxy specimen. It is also concluded that tensile strength of the polymer composite increases with the increase in reinforcement material.

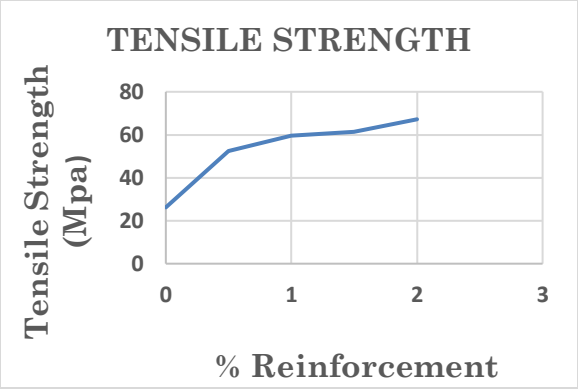

Fig. 3.1: Variation of Tensile Strength with reinforcement

It was also seen that the specimen had the peak value of tensile strength obtained at 2 wt % of Reinforcement as shown in Figure 3.1.

Flexural strength is the ability of composites or materials to resist bending deflection when energy is applied to the structure.

Table 3.2

Flexural Test results

Sl.No	Sample	Flexural Strength (N/mm^2)
1	Epoxy	37.2
2	99 % Epoxy+0.5% Glass Fibers +0.5% Graphene	56.23
3	98 % Epoxy +1% Glass Fibers+ 1% Graphene	61.58
4	97 % Epoxy +1.5% Glass Fibers+1.5% Graphene	63.4
5	96 % Epoxy +2% Glass Fibers+ 2% Graphene	67.6

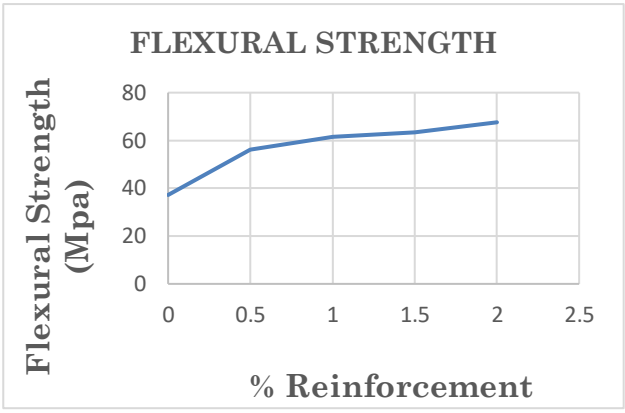

Fig. 3.2: Variation of Flexural Strength with reinforcement

It was also seen that the specimen had the Flexural strength obtained at 2 wt % of Reinforcement as shown in **Fig. 3.2.**

Hardness number is resistance to penetration, indentation or abrasion when load is applied on the materials. The increase in the hardness number of the material shows the resistance to penetration.

Table 3.3

Hardness Test results

Sl. No	**Sample**	**Shore Hardness Hs**
1	Epoxy	59
2	99 % Epoxy+0.5% Glass Fibers +0.5% Graphene	75
3	98 % Epoxy +1% Glass Fibers+ 1% Graphene	82
4	97 % Epoxy +1.5% Glass Fibers+1.5% Graphene	84
5	96 % Epoxy +2% Glass Fibers+ 2% Graphene	78

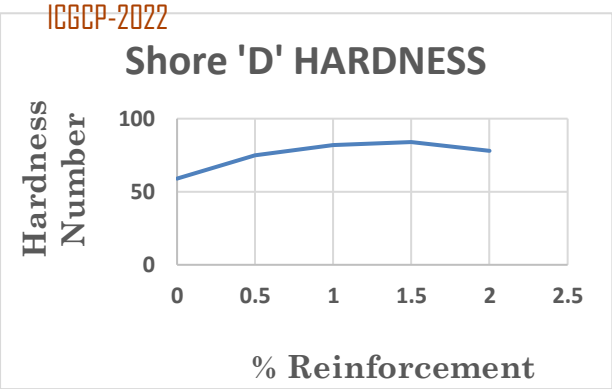

Fig. 3.3: Variation of Hardness with reinforcement

It was seen that hardness number did not much increase with increase of Reinforcement content.. Higher hardness number 84 was obtained at 1.5 wt % of Reinforcement as shown in Figure.

4. CONCLUSIONS

The prepared glass composites are tested for water absorption, mechanical and thermal properties and following conclusions are drawn:

1. The mechanical properties such as tensile, found to be maximum for glass Fiber Reinforced composite with maximum % wt of glass fibres.
2. The mechanical properties such as flexural strength, found to be maximum for glass Fiber Reinforced composite with maximum % wt of glass fibres.
3. The mechanical properties such as Hardness, found to be maximum for glass Fiber Reinforced composite with maximum % wt of glass fibres.

References

1. Gupta M K, Srivastava R K. Mechanical properties of hybrid fibres-reinforced polymer composite: A Review. Polym-Plast Technol Eng. 2016, 55: 626-642

2. Gupta M K, Srivastava R K, Kumar Sushil, Gupta Suresh, Nahak Binayak. Mechanical and water absorption properties of hybrid sisal/glass fibre reinforced epoxy composite. American J Polym Sci Eng. 2015, 3: 208-2019

3. Chow W S. Water absorption of epoxy/glass fiber/organo-montmorillonite nanocomposites. eXPRESS Polym Lett. 2007, 2: 104-108

4. Kornmann X, Rees M, Thomann Y, Necola A, Barbezat M, Thomann R. Recent Advances in Polymer Nanocomposites: Synthesis and Characterisation. Compos Sci Technol. 2005, 65: 2259-2268

5. Xie H-Q, Zhang S, Xie D. An efficient way to improve the mechanical properties of polypropylene/short glass fiber composites. J Appl Polym Sci. 2005, 96: 1414-1420.

6. Morye S S, Wool R P. Mechanical properties of glass/flax hybrid composites based on a novel modified soybean oil matrix material. Polym Compos. 2005, 26: 407-416

7. Mishra S, Mohanty A K, Drzal L T, Misra M, Parija S, Nayak S K, Tripathy S S.

Studies on mechanical performance of biofibre/glass reinforced polyester hybrid composites. Compos Sci Technol. 2003, 63: 1377-1385

8. Sathishkumar T P, Satheeshkumar S, Naveen J. Glass fiber-reinforced polymer composites – a review. J Reinf Plast Compos. 2014, 33: 1258-1275

9. Mathew M T, Naveen Padaki V, Rocha L A, Gomes J R, Alagirusamy R, Deopura BL, Fangueiro R. Tribological properties of the directionally oriented warp knit GFRP composites. Wear. 2007, 263: 930-938

10. Lopez F A, Martin M A, Alguacil F J, Rincon J Ma , Centeno T A, Romero M. Thermolysis of fibre glass polyester composite and reutilisation of the glass fibre residue to obtain a glass ceramic material. J Anal Appl Pyrolysis. 2012, 93: 104-112

Experimental Investigation on Properties of Self Compacting and Self-Curing Concrete Using Light Weight Aggregate, M-Sand and Fly Ash as a Mineral Admixture

[1]Pallavi G A, [2]C.H Bhavya

#1,2Assistant Professor, Dept. of Civil Engg., SCE
Bangalore-560057, India
pallaviga@sapthagiri.edu.in, bhvyach civ@sapthagiri.edu.in

Abstract - Self-compacting concrete (SCC) is considered as a concrete which can be placed and compacted under its self-weight with little or no vibration effort and which is at the same time cohesive enough to be handled without segregation or bleeding of fresh concrete. This study presents an experimental investigation on Self-Compacting and Self-Curing Concrete (SCCM) with fine aggregate replacement of a M-Sand (0, 10, 20, 30, 40%) with 10% and 15% LWA constant and addition of mineral admixture Fly Ash. Mix proportions of SCCM for M40 grade concrete were arrived. For each concrete mix nine 150×150×150 mm cubes, 150×300 mm cylinders were cast and left for Self-Curing for 7, 28 and 56 days and results are compared with Self-Compacting Concrete (SCC). The Slump Flow, J-Ring, U Box, L-Box and V- Funnel test is carried out on the fresh properties of SCCM and in harden concrete Compressive Strength, Split Tensile Strength were determined. The flow properties on SCC with cement, Fly Ash as additional for cementitious material and various proportions of M-Sand has been performed and found that the values of Slump flow, V-Funnel, U-Box, L-Box and J-Ring were within the limits prescribed by EFNARC. From overall study, it was concluded that SCC with Quarry Dust found satisfactory.

Keywords - Self Compacting Concrete (SCC), Fly Ash, Light Weight Aggregates and M-Sand.

I. INTRODUCTION

The self-compacting concrete (SCC) is the newest innovating category of high-performance concrete, characterized by its ability to spread and self-consolidation in the formwork exhibiting any significant separation of constituents. Elimination of vibration for compacting concrete during placing with the use of SCC leads to substantial advantages related to better homogeneity, enhancement of working-environment and improvement in the productivity by increasing the speed of construction. One of the disadvantages of SCC concrete is its cost, associated with the use of high volume of Portland cement and use of chemical admixtures. One alternative to reduce the cost of SCC is the use of mineral admixtures such as fly ash, which is finely, divided material added to concrete during mixture procedure. When this mineral admixture replaces a part of the Portland cement, the cost of SCC will be reduced especially if the mineral admixture is waste or industrial by-product. Moreover, the use of mineral admixture in the production of self-compacting concrete not only provides economic benefits but also reduces heat of hydration. SCC is not a new material, but rather new and improved way of executing the concreting operation. SCC, similar to CVC (conventional vibrated concrete), has a wide variety of properties to achieve specific targets. A wide number of definitions can be found in the literature, but all of them describe SCC in the common way: SCC is a concrete that is able to flow under its own weight and completely fill the formwork and encapsulate the reinforcement, while maintaining homogeneity and can consolidate without the need for vibration compaction. The use of SCC offers benefits in the key areas such as construction process, concrete quality, energy conservation, health and safety. There are many advantages of using SCC especially when the material cost is minimized. These include:

1. Reducing the construction time and labour cost.
2. Eliminating the need for vibration.
3. Reducing the noise pollution
4. Improving the filling capacity of highly congested structural members.
5. Facilitating construability and ensuring good structural members.

SCC consists of the same components as conventionally vibrated concrete, which are cement, aggregates and water, with the addition of chemical and mineral admixtures in different proportions.

II. OBJECTIVES OF STUDY

1. To study the fresh properties for all mix proportions such as:

Slump Flow

J-Ring Test
U-Box Test
V-Funnel
L-Box

To determine the different strength parameters such as compressive strength, split tensile strength of the Self-Compacting and Self-Curing Concrete (SCCM) in comparison to Self-Compacting Concrete (SCC).

Some of the terms frequently used in the present investigation are defined as follows:

Self-Compacting and Self-Curing Concrete (SCCM). It is the self-compacting and self-curing concrete produced by replacing coarse aggregate with 10% and 15% of light weight aggregate (LWA) and fine aggregate by 0, 10, 20, 30 and 40% of M-Sand.

Self-Compacting Concrete (SCC): It is a composite product produced by mixing cement, fine aggregate, coarse aggregate and water in suitable proportions.

SCCM0: It is the self-compacting and self-curing concrete produced by replacing coarse aggregate with 10% of light weight aggregate (LWA).

SCCM1: It is the self-compacting and self-curing concrete produced by replacing coarse aggregate with 10% of light weight aggregate (LWA) and fine aggregate by 10% of M-Sand.

SCCM2: It is the self-compacting and self-curing concrete produced by replacing coarse aggregate with 10% of light weight aggregate (LWA) and fine aggregate by 20% of M-Sand.

SCCM3: It is the self-compacting and self-curing concrete produced by replacing coarse aggregate with 10% of light weight aggregate (LWA) and fine aggregate by 30% of M-Sand

SCCM4: It is the self-compacting and self-curing concrete produced by replacing coarse aggregate with 10% of light weight aggregate (LWA) and fine aggregate by 40% of M-Sand.

SCCM5: It is the self-compacting and self-curing concrete produced by replacing coarse aggregate with 15% of light weight aggregate (LWA).

SCCM6: It is the self-compacting and self-curing concrete produced by replacing coarse aggregate with 15% of light weight aggregate (LWA) and fine aggregate by 10% of M-Sand.

SCCM7: It is the self-compacting and self-curing concrete produced by replacing coarse aggregate with 15% of light weightaggregate (LWA) and fine aggregate by 20% of M-Sand.

SCCM8: It is the self-compacting and self-curing concrete produced by replacing coarse aggregate with 15% of light weightaggregate (LWA) and fine aggregate by 30% of M-Sand

SCCM9: It is the self-compacting and self-curing concrete produced by replacing coarse aggregate with 15% of light weightaggregate (LWA) and fine aggregate by 40% of M-Sand.

Self-curing or internal curing is a technique that can be used to provide additional moisture in concrete for more effective hydration of cement and reduced self-desiccation. There are two major methods available for internal curing of concrete. The first method uses saturated porous lightweight aggregate (LWA) in order to supply an internal source of water, which can replace the water consumed by chemical shrinkage during cement hydration. The second method uses poly-ethylene glycol (PEG) which reduces the evaporation of water from the surface of concrete and also helps in water retention. In the present study the first method is being adopted. The use of fly ash, blast furnace slag and silica fume in SCC reduces the dosage of superplasticizer needed to obtain similar slump flow compared to concrete mixes made with only Portland cement.

III. EXPERIMENTAL PROGRAM

In this investigation 99-cube, 99-cylinders are tested to investigate concrete compressive strength and split tensile strength of SCC with the combination of M-Sand Fly Ash and light weight aggregate. All test specimens of cube with 150 mm size and cylinders with diameter 150 mm and 300 mm in length.

IV. MATERIALS USED IN THIS EXPERIMENT

1) Cement (C)

In this experimental study, Ordinary Portland Cement conforming to IS: 8112-1989 was used. The physical and mechanicalproperties of the cement used are shown in Table 1

TABLE-1: PROPERTIES OF CEMENT

Physical properties	Results
Fineness	2%
Normal consistency	31%
Vicat initial setting time (minutes)	30
Vicat final setting time (minutes)	400
Specific gravity	3.1

2) Light Weight Aggregate (LWA)

It is highly porous light weight aggregate. Its density is approximately 0.25g/cm^3. It is typically light colored and translucent bubble walls.

3) FLY ASH

Fly ash or pulverized fuel ash is the residue of the combustion of finely ground coal used in thermal power plants. It is removed by the dust collection system as fine particle residue from the flue gases before they are discharged into atmosphere. These micron-sized earth elements consist primarily of silica, alumina and iron. When mixed with lime and water the fly ash forms a cementations compound with properties very similar to that of Portland cement. Because of this similarity, fly ash can be used to replace a portion of cement in the concrete, providing some distinct quality advantages. Fly Ash is also known as Coal Ash, Pulverized Fuel Ash and Pozzolana. Fly Ash is the most commonly and abundantly available artificial pozzolana. Large proportion of fly ash, which is produced in India, can be advantageously used in cement and concrete. It is the most widely used pozzolanic material all over the world. The importance and use of fly ash in concrete has grown so much that it has almost become a common ingredient in concrete, particularly for

making high performance and SCC.

4) AGGREGATES

Locally available natural sand with 4.75 mm maximum size was used as fine aggregate (FA). Coarse aggregate (CA) of maximum
12.5 mm was used. Table-3 gives the Physical properties of fine & coarse aggregate.

5) SUPER PLASTICIZER (SP)

Master glenium-Ace 30(JP) from BASF Bangalore was used.

TABLE-2: PHYSICAL PROPERTIES OF FINE & COARSE AGGREGATE

Property	Fine Aggregate (FA)	Coarse Aggregate (CA)
Specific gravity	2.5	2.84
Fineness modulus	3.37	7.1
Surface texture	Smooth	--
Particle shape	Rounded	Angular
Crushing value	--	17.4
Impact value	--	12.5

6) M-SAND

Basalt fines, often called quarry or rock dust are by products of the production of concrete aggregates by crushing of rocks. The addition of quarry dust to normal concrete mixes is limited because of its high fineness. The addition of quarry dust to fresh concrete increases the water demand and consequently the cement content for given workability and strength requirement however potential benefits to using quarry dust is the cost having, because the material cost varies depending on the source.

7) WATER

Ordinary portable water is used.

V. SCC MIX DESIGN

Several methods exist for the mix design of SCC. We have adopted Nan-Su method.Mixing procedure for SCC is described as follows:

- Binder and aggregates are mixed for one minute.
- The 1st part (70%) of water was added and mixed for two minutes.
- SP and VMA along with 2nd part (30%) of water was added and mixed for two minutes.
- The mix was stopped and discharged for SCC tests.

VI. RESULT AND DISCUSSION

This chapter consists of test results and discussions on workability, compressive strength, split tensile strength Self-Curing Concrete (SCCM) for different fine Aggregate (Natural Sand) and coarse aggregate (LWA) replacement levels. The test results are compared with Self Compacting Concrete (SCC).

A) Properties of Fresh state SCC

The workability is measured by flow properties as per EFNARC. The values of flow properties with constant water/binder ratio for Self-compacting self-curing concrete for different mixes were measured.

B) Properties of hardened SCC

The properties of hardened SCC were measured in terms of Compressive Strength obtained from Compression test confirming to IS 516-1959.Tests were conducted at different curing periods of 7, 28 and 56 days. The tensile strength is one of the basic and important properties of concrete. Hence, the tensile strength of concrete is obtained indirectly by subjecting concrete cylinders to the action of compressive force along two opposite generators of a concrete cylinder placed with its axis horizontal between the compressive platens. Due to the compression loading a fairly uniform tensile stress is developed over nearly 2/3 of the loaded diameter as obtained from the elastic analysis. The split tensile test is carried out as per IS: 5816-1970. The magnitude of tensile stress was evaluated using the relation $\sigma SP = 2P/ \pi DL = 0.637P/DL$. The results of variation in compressive strength and tensile strength with various curing periods are as shown in table and figure.

TABLE-3: DETAILS OF SELF-COMPACTING AND SELF-CURING CONCRETE (SCCM) AND SELF-COMPACTING CONCRETE (SCC) SPECIMENSCONSIDERED FOR STRENGTH PARAMETERS.

Sl no	Type of concrete	Designation	Cementitious material		Fine aggregate contents		Coarse aggregate conctents	
			Cement	**Fly Ash**	**Sand**	**Quarry Dust**	**CA**	**LWA**
1	Self-Compacting Concrete	SCC	79%	21%	100%	0%	100%	0%
2	Self-Compacting and Self-CuringConcrete (SCCM)	SCCM0	79%	21%	100%	0%	90%	10%
3		SCCM1	79%	21%	90%	10%	90%	10%
4		SCCM2	79%	21%	80%	20%	90%	10%
5		SCCM3	79%	21%	70%	30%	90%	10%
6		SCCM4	79%	21%	60%	40%	90%	10%
7		SCCM5	79%	21%	100%	0%	85%	15%
8		SCCM6	79%	21%	90%	10%	85%	15%
9		SCCM7	79%	21%	80%	20%	85%	15%
10		SCCM8	79%	21%	70%	30%	85%	15%
11		SCCM9	79%	21%	60%	40%	85%	15%

TABLE-4: COMPRESSIVE STRENGTH OF SCCM CONCRETE AND SCC

Sl no	Designation	Fine aggregate contents		Coarse aggregate contents		Average compressive strength, N/mm^2 at Differentages		
		Sand	M-Sand	**CA**	**LWA**	**7 Days**	**28 Days**	**56 Days**
1	SCC	100%	0%	100%	0%	26.8	46.4	51.2
2	SCCM0	100%	0%	90%	10%	27.2	46.6	51.7
3	SCCM1	90%	10%	90%	10%	28.1	46.8	52.3
4	SCCM2	80%	20%	90%	10%	31.0	48.1	54
5	SCCM3	70%	30%	90%	10%	32.3	50.2	54.5
6	SCCM4	60%	40%	90%	10%	32.1	50	53

Sl no	Designation	Fine aggregate contents		Coarse aggregate conctents		Average compressive strength,N/mm^2 at Different ages		
		Sand	M-Sand	**CA**	**LWA**	**7 Days**	**28 Days**	**56 Days**
1	SCC	100%	0%	100%	0%	26.8	46.4	51.2
2	SCCM5	100%	0%	85%	15%	27.3	46.8	52.7
3	SCCM1	90%	10%	85%	15%	28.5	48.0	54.1
4	SCCM2	80%	20%	85%	15%	31.8	48.6	54.8
5	SCCM3	70%	30%	85%	15%	33.3	50.8	56.1
6	SCCM4	60%	40%	85%	15%	32.7	50.0	54.1

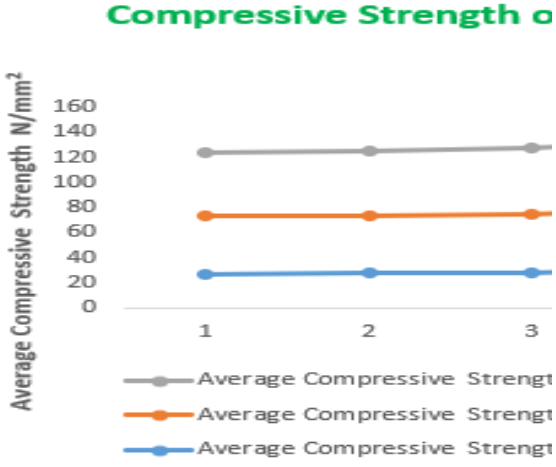

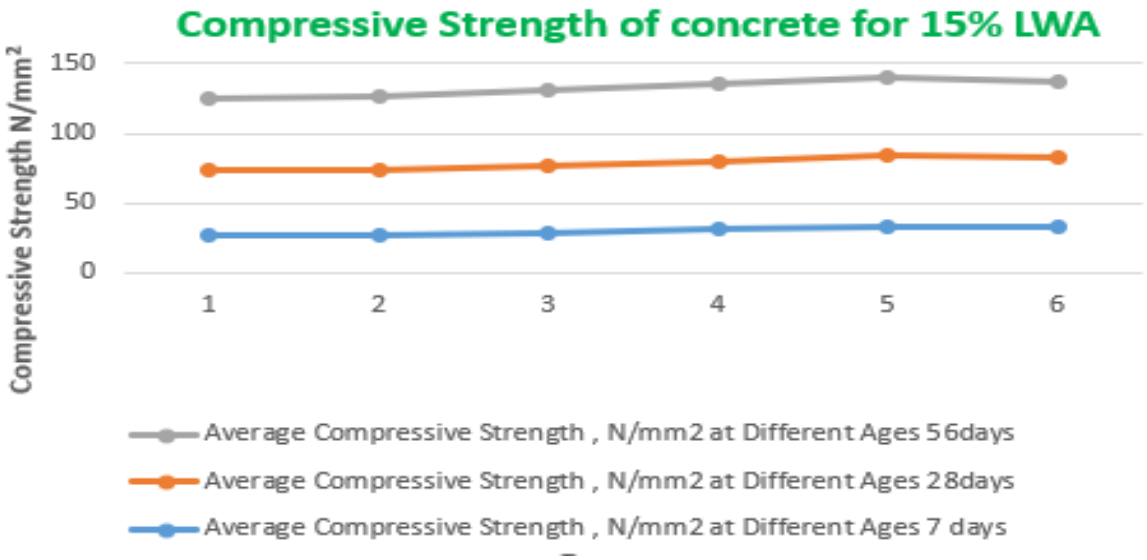

VII OBSERVATION AND DISCUSSION

1. By increasing the percentage of M-Sand, the compressive strength goes on increasing at all levels. The maximum strength is observed for 30% replacement of M-Sand in both cases 10% LWA and 15% LWA replacements to CA internally cured and were water sprinkled.
2. It observed that the strength increases up to 30% replacement of M-Sand. Three standard cubes each for various mixes were tested to determine 7 days, 28 days and 56 days compressive strength.
3. The increase in the compressive strength which is maximum for SCCM3 concrete is 21%, 9% ,7% at 7, 28, 56 days respectively in comparison to that of SCC (water cured) at laboratory condition.
4. The increase in the compressive strength which is maximum for SCCM8 concrete is 24%, 9%, 9% at 7, 28, 56 days respectively in comparison to that of SCC at laboratory condition.
5. The decrease in the compressive strength was generally 2-3% was observed in the compressive strength for 40% Replacement of quarry dust for SCCM9 and SCCM4 as compared to that of SCCM3 and SCCM8.
6. This shows that it is possible to use M-Sand in place of natural sand up to 40% if Cement is supplemented by the addition of fly ash and also subjected to internal curing at the point of scarcity of water and sprinkling of water by replacing with appropriate percentages of coarse aggregate with that of light weight aggregate.
7. The compressive strength substantially increased made with combination of Light Weight Aggregate and Normal Weight Aggregate.
8. The amount of increase in Compressive Strength substantially increases with increasing the portion of Normal Weight Aggregate.

TABLE-5: SPLIT TENSILE STRENGTH OF SCCM CONCRETE AND SCC

Sl no	Designation	Fine aggregate contents		Coarse aggregate conctents		Average Split tensile strength, N/mm² at Differentages		
		Sand	M-Sand	**CA**	**LWA**	**7 Days**	**28 Days**	**56 Days**
1	SCC	100%	0%	100%	0%	2.6	3.2	3.9
2	SCCM0	100%	0%	90%	10%	2.63	3.27	3.92
3	SCCM1	90%	10%	90%	10%	2.68	3.30	4.0
4	SCCM2	80%	20%	90%	10%	2.71	3.48	4.14
5	SCCM3	70%	30%	90%	10%	2.8	3.61	4.20
6	SCCM4	60%	40%	90%	10%	2.69	3.60	4.19

Sl no	Designation	Fine aggregate contents		Coarse aggregate conctents		Average Split Tensile strength,N/mm^2 at Different ages		
		Sand	M-Sand	**CA**	**LWA**	**7 Days**	**28 Days**	**56 Days**
1	SCC	100%	0%	100%	0%	2.6	3.2	3.9
2	SCCM5	100%	0%	85%	15%	2.71	3.43	3.93
3	SCCM1	90%	10%	85%	15%	2.77	3.47	4.13
4	SCCM2	80%	20%	85%	15%	2.83	3.60	4.23
5	SCCM3	70%	30%	85%	15%	2.87	3.66	4.27
6	SCCM4	60%	40%	85%	15%	2.81	3.60	4.20

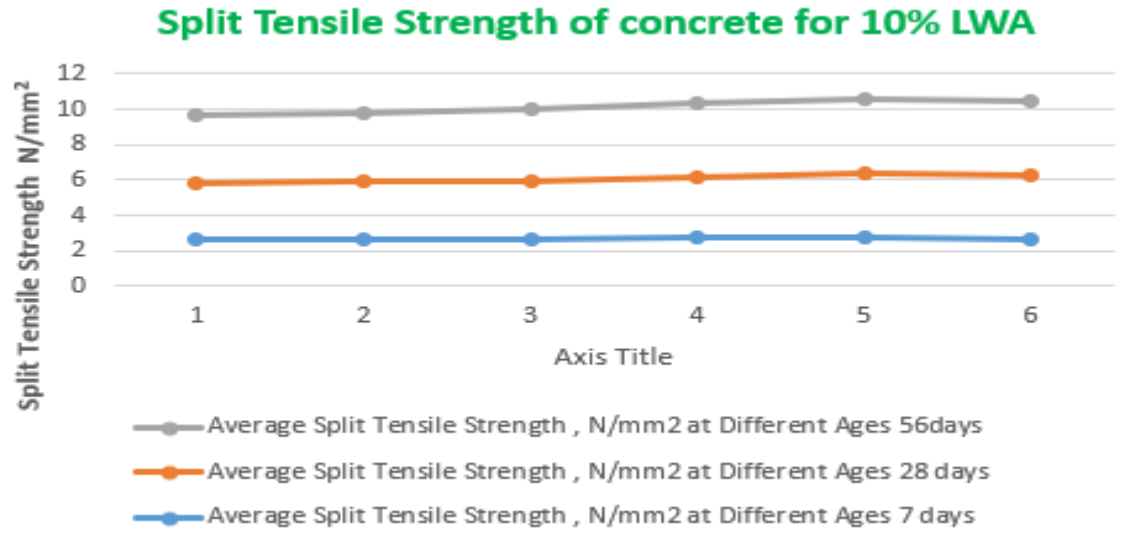

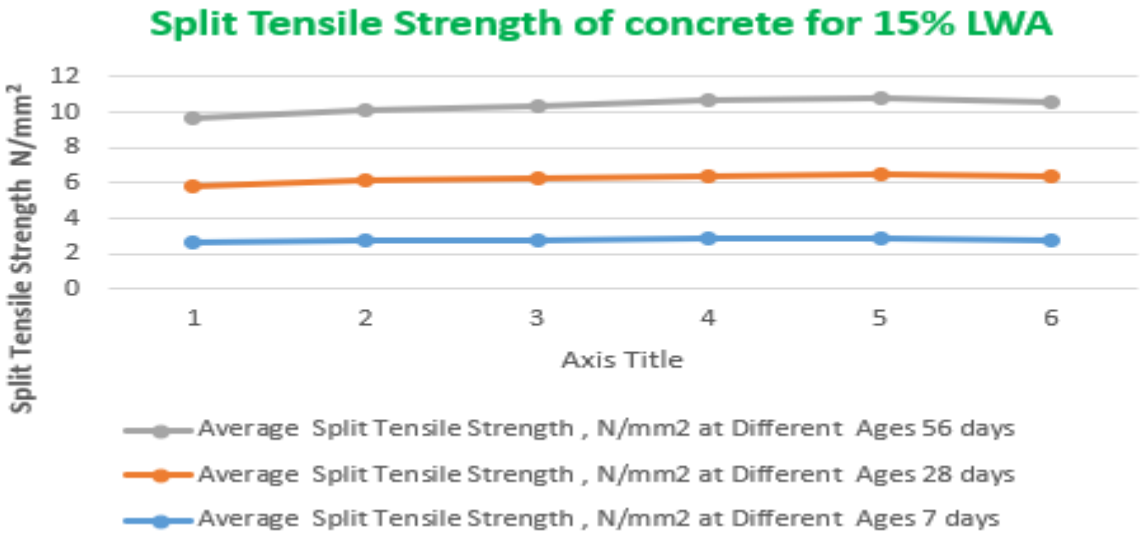

VIII OBSERVATION AND DISCUSSION

1. By increasing the percentage of M-Sand, the split tensile strength goes on increasing at all levels. The maximum strength is observed for 30% replacement of M-Sand in both cases 10% LWA and 15% LWA replacement to CA.
2. It can be seen that strength increases up to 30% replacement of M-Sand. Three standard cubes each for various mixes weretested to determine 7 days, 28 days and 56 days split tensile strength.
3. The increase in the split tensile strength which is maximum for SCCM3 concrete is 7%, 13% ,8% at 7, 28, 56 days respectively in comparison to that of SCC for 10% coarse aggregate replaced by LWA subjected to internal curing at laboratory condition.
4. The increase in the split tensile strength which is maximum for SCCM8 concrete is 10%, 15% , 10% at 7, 28, 56 days respectively in comparison to that of SCC for 15% coarse aggregate replaced by LWA subjected to internal curing at laboratory condition.
5. This shows that it is possible to use M-Sand in place of natural sand if Cement is supplemented by the addition of fly ash.
6. This shows that it is possible to use M-Sand in place of natural sand up to 30% if cement is supplemented by the additionof fly ash and also subjected to internal curing at the point of scarcity of water and sprinkling of water by replacing with appropriate percentages of coarse aggregate with that of Light Weight Aggregate.
7. The split tensile strength substantially increased made with combination of Light Weight Aggregate and Normal Weight Aggregate.
8. The amount of increase in split tensile strength substantially increases with increasing the portion of Normal Weight Aggregate.

IX CONCLUSION

The study examines the properties of freshly poured Self-Compacting Concrete with fixed water cement ratio of 0.45 in which cement is added with fly ash and natural sand replaced by various percentage quarry dust in weight ratios of 0, 10, 20, 30, 40%the following observations are made:

1. The fresh properties of SCCM mixes in terms of passing ability, filling ability and segregation containing different proportions of quarry dust and light weight aggregate formed that the values are within the limits prescribed by EFNARC.
2. The results showed that the slump flow varied with replacement ratio of M-Sand for natural sand and LWA
3. The average compressive strength of SCCM having 30% M-Sand for both 10% LWA and 15% LWA internally cured ascompared to SCC water cured was increased by 9% for 28 days.
4. The average split tensile strength of SCCM having 30% M-Sand for both 10% LWA and 15% LWA internally cured ascompared to SCC water cured was increased by 13% and 15% for 28 days.
5. It is been indicated that SCCM mixes at all replacement levels of M-Sand has higher compressive strength and split tensile strength subjected to internal curing with addition filler material fly ash.
6. Hence it is possible to successively utilize waste M-Sand and fly ash for replacement of natural sand and at point ofscarcity of water may be subjected to self-curing by proper replacement of LWA due to its absorbed mechanical advantages.
7. The employment of waste mineral admixture and by self-curing improved the economic feasibility of SCC production on aunit strength basis.

REFERENCES

[1] K. Ozawa and H. Okamura, “Development of the High-Performance Concrete”, Proceedings of JSI, Vol. 11, No.1, 1989, pp. 699-704.

[2] Nan Su, Kung-Chung Hsu, His-Wan Chai, “A Simple Mix Design Method for Self-Compacting Concrete”, Cement and Concrete Research, Vol. 31, 2001, pp. 17991807.

[3] Jagadish Vengala and Ranganatha R.V, “Effect of Fly Ash on long term strength in Self Compacting Concrete”,International conference on recent trends in conference in Concrete Technology and structures, INCONTEST 2003, Coimbatore, 10-12, September 2003, pp. 341-347.

[4] Naveen Kumar C. and Kiran, “Self-Compacting Concrete with Fly Ash and Metakaolin”, April. 2006, pp. 33-39.

[5] Choi, et. al., “Experimental research on the fluidity and mechanical properties of high strength lightweight Self- Compacting Concrete”, Cement and Concrete Research, Vol. 36, pp. 1596-1602.

APPLICATION OF SOLID WASTE MANAGEMENT IN KANIVENAHALLI

PAVAGADA TALUK TUMKUR DISTRICT

J SURAJ, NAIRA N, TEJAS GV, ANKITH KUMAR B

Department of civil Engineering, Sapthagiri College of engineering

#14/5 chikkasandra, Hesaraghatta main road, Bangalore-560057

1surajj1999@gmail.com

2neshasarikaanjan@gmail.com

3tejudowney4329@gmail.com

4ankithkumar7676@gmail.com

5.hodcivil@sapthagiri.edu.in

Abstract- The solid waste land fill site selection is a relatively delicate process. In this study, the suitability of solid waste land fill site selection for the city of kanivenahalli pavagada city will help the urban local bodies' people. This paper covers an introduction to project, study area, status of the existing solid waste management system and recycling of solid waste use in mechanical recycling techniques that are presented. From this study leads to the represents a necessary environmental protection as well as an economic opportunity

1. INTRODUCTION

Municipal Solid waste Management has always been a great challenge and is one of the important Obligatory functions of the urban local bodies (ULBS) in Municipal authorities. However, most of them are currently unable to fulfil their duty to ensure the environmentally sound and sustainable ways of dealing With waste generation, collection, transport, treatment, and disposal. The failure of municipal solid waste management (MSWM) can result in serious health problem and environmental degradation. Because of deficient services, uncollected waste often also mix with human and animal excreta is Dumped indiscriminately in the streets and in drains, thereby contributing to flooding, breeding of insect and rodent vectors, and spreading of diseases. A sustainable amount of this waste is extremely danger to the living organisms including human beings. To overcome this problem, efficient solid waste management must be implemented. The objective of solid waste management to control, collects, process, utilize and dispose of solid waste in such an economical way which protects health of human being and natural environment

2. STUDY AREA

Pavagada is a town in pavagada taluk in Tumkur district, in the Indian state of

Karnataka as shown in figure 1 .It is a taluk headquarter. It lies between 14.1°Nand 77.27°E with an average elevation of 646 meters (2119 feet).The town of pavagada has population 34,522 and an area of 6.75KM the Pavagada city where it is relatively hot. The year may broadly be classified into four seasons. The dry seasons are from January to February, followed by hot weather from March to May. The SW monsoon season is from June to September and the NE monsoon period from October to December. The sum of average annual precipitation in pavagada city is 665mm.The monthly temperature for pavagada city 36°C during April. Similarly, the minimum temperature falls in the year 2021 is 17C during January. The following table1 shows number of sources and the average waste generated in each source based onthe waste estimation. Amount of waste generated from Residents (7.34tons), commercial establishments (2.10tons), markets (0.29tons), Meat/chicken (0.21tons), hotels and restaurants (0.32tons), street sweeping (1.26tons) and in Miscellaneous (0.34tons) and overall wastes generated is (11.56tons).

Figure1. Map showing pavagada city

TABLE 1. ESTIMATION OF QUANTITY FROM WASTE GENERATION

SL no	Waste	No of generators	Avg. waste per day in kg	Total waste in kg	Total waste in tons
1	Household	6699	1.0	6699	6.70
2	Slum household	709	0.9	638.1	0.64
3	Shops	887	1.6	1392	1.39
4	Meat	18	11.6	0.95	0.21
5	Petty shop	57	1.49	208	0.08
6	Hotel	35	9.2	84.93	0.32
7	Markets	1	290	322	0.29
8	Institution	26	2.1	219	0.05
9	Marriage halls	8	35	280	0.28
10	Street sweeping				
	A	17.5	60	452.4	0.45
	B	17.5	30	526.5	0.53
	C	16.3	14	228.0	0.23
	D	8.9	5.6	49.9	0.05
11	Miscellaneous waste	5%		335.31	0.34
TOTAL				**11562.24**	**11.56**

3. METHODOLOGY:

The pavagada town has setup municipal solid waste management disposing sites at kanivenahalli which is located 4km away from the town. The total area of landfill site is about 10.27acres.This site is being is used for dumping of municipal solid waste generated in the town .The facilities has been provided with the security Shed, storerooms, composite pit,

compound wall and electricity connections. The disposal sites are not being provided with watchman and weighing bridge. The collected waste directly dumped into landfill site, presently there is no processing and handling of waste.

THE RECYCLING TECHNIQUES THAT ARE PROPOSED: REVISED PRICE SCHEDULE:

SL NO.	DESCRIPTION	PRICE
1	supply of equipment as per details attached MSW 50 TPD	**RS.1,04,36,000/-**
2	Vertical baler machine	**R 3,15,000/-**
3	Twin shaft shredder Model 250	**Rs7,25,000/-**
4	TROMMEL MACHINE	**RS6,50,000/-**

3A. ALFA THERM-MSW 50 TPD COMPOST PLANT

Figure2. MSW 50 TPD COMPOST PLANT

The weight of all incoming vehicles containing MSW shell be recorded with electronic weigh bridge at the entry gate, where after it shell be unloaded and tipping floor and visually inspected and large in at material shell be removed there from. Composting is one of the promising technologies for managing municipal solid waste. Though it is a natural process which transforms decomposable organic material in to carbon dioxide, water and stabilizes organic matter, intervention with specific control measure to established and maintains the composting process is utmost necessary The fermented waste is subjected to mechanical screening in dual rotary sieves of 35mm and16mm screen with a set of conveyors-feeding, undersize and oversize the screen material is transferred and stacked in the curing section. The oversize + 35 and 16mm content is transferred to the land fill/RDF The fermented and screen waste is stacked in the curing section for 14days for further stabilization and moisture control. Additives can be added to improve the quality of the final project. The shed requires proper ventilation.The compost is now subjected to screening in a Trommel with 4mm opening followed by refinement removing the impurities like dust, stones, glass etc.in a DE stoner from the finished product The high quality compost thus produced can either be packed in bags of appropriate weight, suggested 50kgs, or can be directly be loaded to tractor trolleys. Packed bag shall be sealed using portable stitching machine and finally stacked in the finished goods store room with a three day storage facility. The recyclable material shall also be stored appropriately.

3B.VERTICAL BAILER MACHINE

Figure3. Waste Compactor/Bailer Machine

Recycling and green business have been in the fore front of the news in the few years, and all corporation, large and small, are required to do their parts, environmental regulation compliance is of prime importance and also the need to reduce the load on the landfills. Vertical balers are one such technology to bale the material and make it economically to transport/store and fit and extraordinary well in a modern efficiency plan. A vertical baler is large machine that takes use amount of card board, plastic and paper, aluminium etc. and compact them together in a bale of a recyclable materials. This method of removals saves the storage space and makes the complete process efficient. Instead of having to analyse and place the recyclable material as they come in, there are all placed in to the baler before being compacted and loaded on to the trucks for the further transportation. This method of recycling can make a costly land fill process in to a profitable business. No one wants to see recyclable materials go to waste in a land fill, but a corporation has to deal with this large issue any way possible. With the use of recycling an vertical balers, this to goals do not need to be a at odd with each other. Vertical balers are easy to use and also help in moisture removal from the waste. The leachate is collected at the bottom of the unit in a tray. Power consumption is lesser and hence the leaching baling cost also reduces.

3C.TWIN SHAFT SHREDDER CAPACITY-5 TONS PER DAY

Figure4. Twin Shaft shredder.

Twin shaft shredders are multipurpose shredders that can shred a variety of bulky materials in either the primary or secondary stages. The shredders are exceptionally tough, with a solid support system that can bear any load. Electrical and hydraulic drive systems for shredders are plentiful. Conveyors for feeding and discharging are available. The housing is welded together and made of solid materials. The bearing unit is separate and well-sealed to prevent damage from liquids and solids, extending its life. Low speed, high torque, low noise, low dust, and low maintenance are all characteristics of the shredders. When the shredder is overloaded and foreign objects are caught in the cutting unit, the rotor comes to a halt and slides backward before returning to its previous position. The twin shaft shredders are used for shredding of Medical Waste, Municipal Solid Waste, Wood, Tyres, Plastic, E-waste, Packing material, textile, Drum,

Metals, oversize bulky waste, industrial waste, General Waste, Hazardous Waste, end of life equipment and other difficult to shred items. The heavy-duty shredders manufactured by us have capacities up to 20 tons/hr. capacity

3D.TROMMEL SCREEN

Figure5. Trommel Screen.

A trommel screen is a rotary screen that separates materials based on their size. It is mostly employed in the solid waste processing and mineral processing sectors. The material that is oversize is separated from the material that is undersized. The trommel℃℃ screen is made out of a large cylindrical drum with several holes/openings of the desired separation size. The perforations aid in material classification, and when the drum rotates, only material that is smaller than the size of the holes falls through, while bigger materials flow out the other side of the trommel.

4. RESULT AND DISCUSSION:

- In this study we attempt to identify the land fill site using the collected data.
- The 50 TPD compost plant helps in the recycling the food waste, market waste, yard waste, plastic products and other miscellaneous solid waste
- Vertical Bailer machine which helps to take the huge amounts of amounts of cardboard, plastic and paper, aluminium etc. And compost them together in a bale recycling materials.
- The twin shaft shedder are most used technique as it segregate medical waste, E-waste drum, metals and oversize bulky.
- Trommel screen which helps to seperate the materials based on their size.
- Proposed the new technics to the pavagada city which leads to have a clean environment.
- From the proposed mechanical technique we can give the job opportunity to the un employed people

5. CONCLUSION:

The solid waste management in pavagada city appears to be inadequate and needs up gradation. The solid waste has to be disposed of scientifically through sanitary landfill and recyclable portion of the waste should be salvaged. Segregation of recyclable material would also leads to reduction in quantity of solid waste for final disposal. Higher priority needs to be assigned to the management of municipal solid waste by the local authority and a system approach needs to be adopted for optimizing the entire operation of SWM encompassing segregation at source, timely and proper collection, transportation routes and types of vehicles and development. Here we attempt to introduce the new technologies like 50 TPD compost plant, Vertical Bailer, Trommel screen and Twin shaft shredders. These technologies are more convenient ways to the disposal of Solid waste. The selection of land fill site in kanivenahalli leads to a lot of changes to the urban local bodies, as waste will be not dumped in road side. This leads to have a better opportunity's for the further solid waste management.

ACKNOWLEDGMENT:

We would like to express our sincere gratitude to the management, Principal Sapthagiri College of Engineering Bengaluru for the facilities provided and their support. Also we would like to thank Head of the department Civil Engineering and faculties for their encouragement and support.

6. References

[1] G.V.Rathnamala, R.M.Ashwini.Domestic Environmental Destructions Due to lack of Solid Waste Management in Rural Areas.(Advances in Mathematics: Scientific Journal 10) Vol-3(2021),no.3,Pp.1807-1819

[2] Sabrin Ara, Rabea khatun, Mohammed salh Uddin. Urbanization challenge: Solid waste Management in Sylhet City, Bangladesh.(International Journal of Engineering Applied Science and Technology) Vol-10 (2021),Pp.20-28

[3] Basavarajappa HT, Jeevan L, Manjunath M C. Suitable waste disposal site selection in Tumkur City using Geomatics application. (International Journal of Civil Engineering and Technology) Vol-6 (2015),Pp.133-146

[4] Muheeb Majid and Bashir Ahamed Mir. Landfill site selection using GIS based multi criteria evaluation technique of Srinagar city. ELSEVIER(Environmental Challenge.) VOL-3 on (2021).10031

[5]Abhishek Nandan, Bikarama Prasad Yadav, Soumyadeep Baksi. Recent Scenario of Solid Waste management in India.(World Scientific News) 66(2017),Pp.56-74

[6] Picture Source : ALPHA-THERM LIMITED

"IMPROVING THE COMPRESSIVE STRENGTH OF CONCRETE BY USING CRUSHED AGGREGATE - GRANITE POWDER AS FILLER MATERIAL."

YASHAS. M[1], *DARSHAN.N*[2], *ABHISKEK MOHAN*[3],*VIVEK HEGDE*[4], *KAVYA H P*[5]
[1,2,3,4] *Student, Dept of Civil Engineering, Sapthagiri College Of Engineering, Bengaluru, Karnataka-560057, India*
[5]*Assistant Professor ,Dept. of Civil Engineering , Bengaluru, Karnataka-560057, India*
Yashasm09@gmail.com
darshan.ngowda21@gmail.com
abhishekmohan011@gmail.com
vivekvhegde2@gmail.com
kavyahp@sapthagiri.edu.in

***ABSTRACT* — The use of recycled concrete aggregates as an alternative source of coarse aggregates for the production of new concrete can help to solve the problem of depleting natural resources and that of growing waste disposal crisis. There is recycling could be decreases the concrete performance, particularly for recycled aggregate. To compensate for this decreases, cement content can be adjusted hence, the environmental interest of RA (Recycled aggregate) has to be assessed. From the strength point of view, the uses of RA induces a decreases of RAC (Recycled aggregate concrete) performance, which is proportional to their content. This decreases can be compensated for by increasing cement content. For 50% of RA dosage, a 16% of additional cement is necessary to achieve the compressive strength of NAC (Natural aggregate concrete) when RA is used. From the research point of view granite powder as a cementious property hence we are using a 16% of granite powder to achieve workability and more over increases density, hence increasing the durability of concrete.**

INTRODUCTION:

Construction and demolition are the procedure that works simultaneously. The demolished buildings are rubble in India generally goes to waste in landfills. After few years buildings and demolition waste will be more than half of the national total waste in the most nations of the world so recycling of these concrete waste materials from building demolition can provide a solution to this problem.

In construction field concrete is main construction material across the world and is mostly used in all type of civil engineering works. An aggregate represents the about 70-80% of concrete components so it will be beneficial to recycle the aggregate for construction works and also to be solve the environmental problems. To minimize the problem of excess of waste material it is good step to utilize the recycled aggregates provided that the desired final product will meet the standards. The cost of recycled concrete aggregate may be less than 20-30% less than natural aggregates in some regions.

Protection of environments is a basic factor which is directly connected with the survival of the human race. Parameters like environmental consciousness, protection of natural resources, sustainable developments play an important role in modern requirements of construction works. Due to modernization, demolition materials are dumped on land not use for any purpose such situation affect the fertility of land.

The first large scale use of demolition rubble as aggregate occurred after the second world war. A review of overseas literature carried out as part of this project, shows that research into using recycled concrete aggregate with granite powder for new concrete began in earnest in the mid to late 1970's. Work was carried out in both North America and Europe. The main reasons generally given for carrying out the research were (Buck. 1977: Frondistou-Yannas, 1977).

- A shortage of readily available, high grade conventional aggregates.
- Environmental concerns, including lack of landfill sites for disposal of demolition rubble, and the environmental impact of transporting conventional aggregates greater and greater distances.
- Economic concerns, which parallel the environmental concerns, As aggregate supplies and rubble disposal sites become more scarce, the cost of these services increases, making recycling a cost effective option.

Stringers are attached to the top and bottom skin panels and run through the span-wise direction of the wing. Stringers stabilize the skin against buckling by means of providing longitudinal stability and carry bending stresses. An aircraft has at least two spars, front and rear spars, which run through the span of the wing and from top to bottom. Spar acts as an end member for the wing box and carries wing bending loads.

Figure 1. Granite powder

METHODOLOGY:

- Plain cement concrete and reinforce cement concrete is collected from sites.

- This collected material is crushed by hammer to separate the aggregates and reduce their sizes in smaller fraction.
- On these separated aggregates various testes are conducted in laboratory as per Indian Standard code & their results are compared with natural aggregates.
- Recycled aggregate reduces the impact of waste on environment. By using some percentage in construction sector, cost is saved, due to reduction of transportation and manufacturing process.

TESTS ON MATERIAL

Tests on cement

a. Field test

b. Laboratory test

1. Normal consistency
2. Specific gravity.
3. Initial & final setting time

Figure 2. Cement

Test on granite powder

a. Specific gravity test

b. Sieve analysis

Figure 3. Crushed granite powder

Test on fine aggregate

a. Specific gravity test

b. Sieve analysis

Figure 4. Fine aggregate

Test on Coarse aggregate

a. specific gravity test

b. impact test

c. abrasion test

d. crushing test

e. water absorption test

Figure 5. Coarse aggregate

MIX DESIGN FOR M25 GRADE CONCRETE :

(According to IS: 10262 2009)

• Stipulations for proportioning

1. Grade designation : M 25
2. Type of cement – 1989: OPC 43 grade conforming IS: 8112
3. Maximum nominal sine of aggregate: 20 mm (Table 5 of IS: 456-2000)
4. Minimum cement content : 250Kg/m3 (Table 5 of IS: 456 -2000)
5. Maximum water-cement ratio:0.45 (Table 5 of IS: 456 —2000)
6. Workability: 100 mm (slump)
7. Exposure condition: Mild (for reinforced concrete)
8. Method of concrete placing: Conventional.
9. Degree of supervision: Good
10. Type of aggregate: Crushed angular aggregate
11. Maximum cement content: 450 Kg/m3

Test data for materials

i Cement used : : OPC 43 grade conforming IS: 8112 -1989

ii. Specific gravity of cement : 3.04

iii Chemical admixture :Super-plasticizer (conplast SP430 DIS)

iv. Specific gravity

a. coarse aggregate : 2.77
b. Fine aggregate : 2.69

v. Water absorption

a. Coarse aggregate: 0.88%

ISBN: 979-88-35073-61-0

b. Fine aggregate: 1.00%

vi. Free (surface) moisture

a. coarse aggregate : Nil

b. Fine aggregate Sieve analysis: Nil

Figure 6. Cubes casted at laboratory

CONCLUSION

- The possible outcomes is based on the test results obtained.
- Depending upon the compressive strength achieved for 7 days,14 days ,21 days & 28 days of the concrete cube mould with addition of crushed aggregate.
- For what percentage of recycled aggregates is added and amount of granite powder the compressive strength is achieved.
- It is observed that compressive strength of concrete reduces with the recycled aggregate percentage increases.
- Percentage of granite powder increases, compressive strength also increases.
- For the percentage of granite powder increases, the workability of concrete decreases.

- It is observed that concrete produce by replacing natural sand by demolition waste exhibit higher shear strength has compared to concrete produce by natural sand. This is true for all percentage replacement level. This is due to fact that recycled aggregate observes more water results in the low workability.

REFERENCES

[1] Arumugam K, Ilangovan R, James Manoha "A study on characterization and use of Pond Ash as fine aggregate in Concrete" international journal of civil and structural engineering volume 2, Feb. 2011

[2] Kadam M.P Dr.PatiI.Y.D. "Effect Of Coal Bottom Ash As Sand Replacement On The properties Of Concrete With Different W/C Ratio" International Journal of Advanced Technology in Civil Engineering, Volume-2, 2013

[3] Bahoria B.V, Dr.Parbat.D.K Dr.NaganaikP.B P.B. Dr.Waghe U.P "Comprehensive literature review on use of waste product in concrete" Volume 2,Issue 4, April 2013

[4] Yogesh Aggarwal, Paratibha Aggarwal"Prediction of Compressive Strength of SCC Containing Bottom Ash using Artificial Neural Networks"

[5] Mark Whittaker, Rachel Taylor, Qui Li, Shuangxinli Li and Dr. Leon Black "The Effects of Bottom Ash as a Partial Cement Replacement."

[6] Tarun R. Naik, Rudolph N. Kraus, and Bruce W. Ramme "Development Of Dry-Cast And Wet cast Concrete Products Utilizing Fly Ash, Bottom Ash, And Used Foundry Sand"

[7] Zhengyueren and Lijiuwan "High Fly Ash Content In Concrete With Dipy Construction Formwork" School of Civil and Hydraulic Engineering, Dalian University of Technology, Dalian.

TRANSLUCENT CONCRETE

Khalid Maqsood Mir [1], Ishaque Ahmed KM [2], Vinay R [3], Sanjay Sharma [4], Kavya H P [5]
Department of Civil Engineering, Sapthagiri College Of Engineering, Bengaluru, Karnataka-560057, India
[5]Assistant Professor ,Dept. of Civil Engineering , Bengaluru, Karnataka-560057, India

Khalidmaqoodmir2000@gmail.com
Ishaqueahmed5905@gmail.com
Vinay2000@gmail.com
Ssharma3761@gmail.com
Kavyahp@sapthagiri.edu.in

Abstract

Translucent concrete allows light to pass through it because of the presence of optical fibre within the opaque concrete wall. Light is transmitted from one surface of the said wall to the other, because of the presence of optical fibre strands along the width of the wall, which allows light to pass through. The work presented in this project reports an investigation on the behaviour of concrete and mortar with optical fibre. Concrete and mortar cube are casted with fibres to study the properties and to compare the compressive strength between normal mix concrete with optical fibre and normal mortar with optical fibre.

I. INTRODUCTION

Translucent lightweight Concrete is a new material with various applications in the construction field, architecture, decoration and even furniture. As can be imagined, concrete with the characteristic of being translucent will permit a better interaction between the construction and its environment, thereby creating ambiences that are better and more naturally lit, at the same time as significantly reducing the energy consumption. India consumes 20% of total electrical energy for lighting the buildings. At present, green structures are greatly focusing on saving energy with indoor thermal systems. However, in area of illumination field, there is little research offering relevant solution. Research on intrinsic characteristic material which transmit the light from one surface to another surface is used as construction material which transmit the light from one surface to another surface is used as construction material, known as optical fibres. Due to its outstanding light guiding and sensing advantages, such as anti-electromagnetic Interference capability, small dimensions, distributed measurement and anticorrosion characteristics, optical fibres have been widely adopted in the communication and sensing fields.

II. METHODOLOGY

Material Specification

The basic material used for manufacture of transparent concrete are cement, aggregate and optical fibre

Material Specifications

1.Cement 53 Grade
2.Fine aggregate Passing through 2.36mm sieve
3.Optical fibre 2% - 4%

In the process of making light transmitting concrete, the first step involved is preparation of mould. The mould required for the prototype can be made with different materials which can be of either tin or wood. In the mould preparation, it is important to fix the basic dimensions of mould. The standard minimum size of the cube according to IS 45 2000 is l5cm x l5cmx l5cm for concrete. In the mould, markings are made exactly according to the size of the cube so that the perforated plates can be used. Plates made of sheets which are used in electrical switch boards is used which will be helpful in making perforations and give a smooth texture to the mould, holes are drilled in to the plates .The diameter of the holes and number of holes mainly depends on percentage of fibre used.

Figure 1 Optical fibres

Ratio	Compressive strength	
	Normal concrete	Translucent concrete
1:2 28 days	24.15 N/mm^2	24.03 N/mm^2

The manufacturing process of transparent concrete is almost same as regular concrete. Only optical fibres are spread throughout the aggregate and cement mix. Small layers of the concrete are poured on top of each other and infused with the fibres and are then connected. Thousands of strands of optical fibres are cast into concrete to transmit light, either natural or artificial. Light transmitting concrete is produced by adding 2% to 4% optical fibres by volume into the concrete mixture. The concrete mixture is made from fine materials only it does not contain coarse aggregate. Thickness of the optical fibres can be varied between 2 µm and 2 mm to suit the particular requirements of light transmission. Automatic production processes use woven fibres fabric instead of single filaments. Fabric and concrete are alternately inserted into moulds at intervals of approximately 2mm to 5mm.Smaller or thinner layers allow an increased amount of light to pass through the concrete. Following casting, the material is cut into panels or blocks of the specified thickness and the surface is then typically polished, resulting in finishes ranging from semi-gloss to high-gloss

III.TEST CONDUCTED

A.Compressiontest

By definition, the compressive strength of a material is that value of uniaxial compressive stress reached when the material fails completely. The compressive strength is usually obtained experimentally by means of a compressive test. The compressive strength of the concrete is determined by cast the cubes of size 150mm x150mm x150mm.

Compressive strength = load/area

IV. RESULT

Table 1

Ratio	Compressive strength	
	Normal concrete	Translucent concrete
1:2 7 days	15.08 N/mm^2	14.05 N/mm^2

Table 2

APPLICATIONS

- Transparent concrete blocks suitable for floors, pavements and load-bearing walls.
- Facades, interior wall cladding and dividing walls based on thin panels.
- Partitions wall and it can be used where the sunlight does not reach properly.
- In furniture for the decorative and aesthetic purpose.
- Light fixtures.
- Light sidewalks at night.
- Increasing visibility in dark subway stations.
- Lighting indoor fire escapes in the event of a power failure.
- Illuminating speed bumps on roadways at night.

Advantages and Disadvantages

The main advantage of these products is that on large scale objects the texture is still visible - while the texture of finer translucent concrete becomes indistinct at distance.

- When a solid wall is imbued with the ability to transmit light, it means that a home can use fewer lights in their house during daylight hours.
- It has very good architectural properties for giving good aesthetical view to the building.
- Where light is not able to come properly at that place transparent concrete can be used.
- Energy saving can be done by utilization of transparent concrete in building.
- Totally environment friendly because of its light transmitting characteristics, so energy consumption can be reduced.
- The main disadvantage is these concrete is very costly because of the optical fibres.
- Casting of transparent concrete block is difficult for the labour so special skilled person is required.

V. CONCLUSION

Translucent concrete blocks can be used in many ways and implemented into many forms and be highly advantageous. Yet, the only drawback would be its high cost. That doesn't stop high class architects from using it. It's a great sign of attraction and artistic evolution. Any structure with a small hint of translucent concrete is bound to make heads turn and make them stand in awe. The compressive strength of Light transmitting concrete is equal to the strength of the ordinary concrete and it has the

property to transmit light. If the percentage of the optical fibres increased than the strength of the concrete starts decreasing so we can conclude that the strength of translucent concrete is inversely proportional to light transmittance. Only fine aggregates are used because if we use coarse aggregates then it may destroy the optical fibres and changes their properties. Transparent concrete achieves maximum effect when used in an environment with a high degree of light contrast, such as this illuminated table in a dimly lit room. The strength results of decorative concrete are correlated with results of ordinary plain cement concrete. The results evidently show that the decorative concrete also performance based on the strength aspect is also considerably high. Hence the application of optical fibre will make the concrete decorative as well as can make the concrete structural efficient

VI. REFERENCES

[1] Momin, A., Kadiranaikar, R., Jagirdar, V. & Inamdar, A.,"Study of Light Transmittance of Concrete Using Optical Fibers and Glass Rods," Proceedings: International Conference on Advances in Engineering&Technology–2014.
[2] He, J., Zhou, Z. & Ou, J., "Study on Smart Transparent Concrete Product and Its Performances," Proceedings: The 6th International Workshop on Advanced Smart Materials and Smart Structures Technology – 2011.
[3] Zhou, Z., Ou, G., Hang, Y., Chen, G. & Ou, J., "Research and Development of Plastic Optical Fiber Based Smart Transparent Concrete," SPIE, vol. 7293, no. F, 2009
[4] Shanmugavadivu, P., Scinduja, V., Sarathivelan, T. & Shudhesamithronn, C., "An Experimenal Study of Light Transmitting Concrete," IJRET, vol. 3, no. 11, 2014.
[5] Germano, J., "Translucent Lightweight Concrete". Europe Patent EP2410103, 2012.
[6]. Soumyajit Paul, Avik Dutta"Translucent Concrete", International Journal of Scientific and Research Publications, Volume 3, Issue 10, 2013, pp.
[7]. Aashish Ahuja, Khalid Mosalam, Tarek Zohdi"Computational Modeling of Translucent Concrete Panels", American Society of Civil Engineers, 2014.
[8]. R. Pradheepa,S. Krishnamoorthi"An Experimental Study on Translucent Concrete", International Journal for Scientific Research &Development,Vol.3,Issue03,2015,pp.174-177
[9]. Saber Rahimi "Investigating the Use of Fibre Optic Sensors in Ferro concrete Structures", Technical Journal of Engineering and AppliedSciences,2013,pp.2796-2798
[10]. Bhavin Kashiyani, Varsha Raina, Jayeshkumar Pitroda, Bhavnaben Shah"A Study on Transparent Concrete: A Novel Architectural Material to Explore Construction Sector", International Journal of Engineering and Innovative Technology (IJEIT),Volume 2, Issue8,2013,pp.83-87
[11]. Anurag Shukla, Trushik Poriya, Jigar Zala "An Experimental Work On Light Transmitting Concrete", International Journal of Advance Engineering and Research Development (IJAERD) Volume 1,Issue 5, 2014.
[12]. F. Ansari " Practical Implementation of Optical Fibre Sensors in Civil Structural", Health Monitoring Journal of Intelligent Material SystemsandStructures,2007.
[13]. Shakir Ahmed Salih, Hasan Hamodi Joni, Safaa AdnanMohamed "Effect of Plastic Optical Fibre on Some Properties of Translucent Concrete", Eng. &Tech.Journal, Vol. 32,Part (A), No.12,2014, pp. 2846-2861.
[14]. Jianping He, Zhi Zhou, Jinping Ou "Study on Smart Transparent Concrete Product and Its Performances", The 6th International Workshop on Advanced Smart Materials and Smart Structures Technology, ANCRiSST2011, Dalian, China,2011.
[15]. Zhi Zhou, Ge Ou, Ying Hang, Genda Chen, Jinping Ou "Research and Development of Plastic Optical Fibre Based Smart Transparent Concrete", Center for Infrastructure Engineering Studies, Missouri Univ. of Science and Tech., Rolla,USA,2009.
[16]. A. Momin, R. Kadiranaikar, Vakeel Jagirdar, Arshad Inamdar "Study on Light Transmittance of Concrete Using OpticalFibresandGlass Rods", International Conference on Advances in Engineering & Technology (ICAET-2014),2014,pp.67-72
[17].https://illumin.usc.edu/245/translucent-concrete-an-emerging-material/

PHYSICO-CHEMICAL CHARCTERISTICS OF GROUND WATER QUALITY ANALYSIS AT MUNICIPAL SOLID WASTE DISPOSAL SITE

Mamatha H K[*1,] *Beeresh C M* [*2]

Department of Mechanical Engineering, Sapthagiri College of engineering #14/5 Chikkasandra, Hesaraghatta main road, Bangalore- 57 India.

mamatha_hk@sapthagiri.edu.in
beereshcm22@gmail.com

----------***----------

Abstract - *Inadequate and improper management of municipal solid waste disposal sites poses serious environmental threats to their surrounding and nearby residents due to groundwater contamination, pollution issues, and health risks. The current investigation was carried out to assess groundwater contamination caused by waste dumping at a landfill site in the Tumkur district's Ajjagondanahalli region, by water quality index. The ground water samples were tested for physicochemical parameters such as Calcium, Magnesium, Chloride, Sulphate, Total Hardness, Fluoride, Nitrate, Total Dissolved Solids, Alkalinity, pH, Biological oxygen demand, dissolved oxygen, iron, zinc, color and odour. The samples were collected from 16 different locations surrounding the the dump site. Water quality index (WQI) is a valuable and unique rating that depicts the overall water quality status in a single term, which aids in the selection of appropriate treatment techniques to address the issues at hand. The findings revealed that many water samples were contaminated. As a result, this landfill poses a risk to the environment as well as to the local community and the government*.

Key Words: water quality index,landfill,geospatial technique,groundwater quality,physicochemical

1.INTRODUCTION

Water state under earth's surface is referred to as groundwater quality. Groundwater can collect between soil particles and in fissures in subterranean rocks. There is a risk of contamination with harmful substances because certain compounds can dissolve in water and others can be suspended in water. Petroleum, hydrocarbons, insecticides, minerals, and disease-causing microbes are only a few examples.(jameel et.al)

Because toxins must transit through the earth to reach the water, groundwater is less susceptible to contamination than surface waterways such as streams, rivers, and lakes. Contamination can still happen, especially if there are fissures in the surrounding soil and rock that allow poisonous substances to flow more easily. (przydatek et.al)

Groundwater in India is getting poisoned as a result of different human activities. Improper management of solid waste is the most valuable drivers of contamination, with groundwater quality around landfills worsening (ayeni et.al).

2. STUDY AREA

Ajjagonadanahalli, a 40-acre municipal solid waste disposal site in Tumkur district. It's located between the north latitude of 12048′39.63′′ and the east longitude of 76000′24.22′′. 76000′24.22′′ Tumkur is a Karnataka administrative district. It is 70 kilometres to the north west of Bangalore and is located on National Highway No. 4. Figure 3.1 depicts the situation.

The MSW management activities in all 35 wards of Tumkur City Municipal Council (TCMC) have been outsourced. Street cleaning, debris collections, primary transportation, bulk garbage collection, and supplementary transportation are among the activities that have been outsourced. The primary collecting of MSW is done by SHGs. Dumping MSW into RCC bins / masonry bins and on the roadside (open collection sites) is a frequent practice in Tumkur. TCMC uses open dumping as a method of disposing of MSW.

Under the Karnataka Municipalities Act, 1964, the Town Municipal Councils are required to handle MSW. The MSW Rules also make it essential for an urban local government to process and dispose of MSW in a scientific manner.

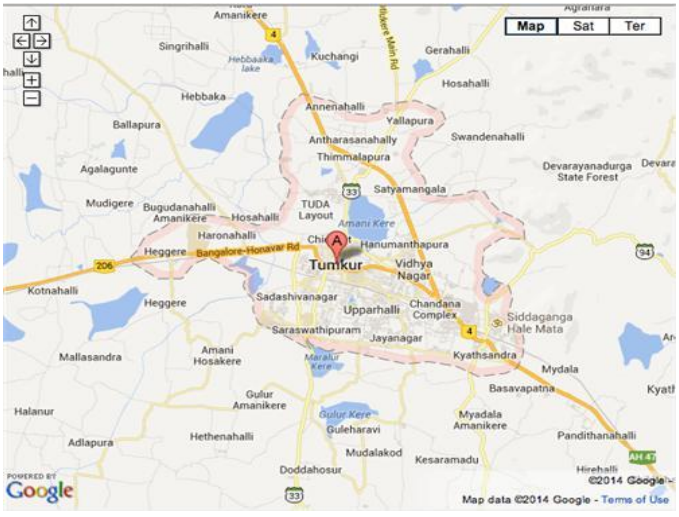

Fig -1: tumkur city map

Fig 2: Location of sampling points

3. MATERIALS AND METHODOLOGY

SAMPLING

Samples were collected from borewells in one litre plastic bottles as per standard procedure (is 3025 part 1).samples collected

3.2 Water quality index

The common index of water quality technique is created by choosing characteristics with considerable care, establishing a standard tables, and allocating weights. The National Sanitation Foundation (NSF) took the efort, in way to compute the index quality of water of several highly contaminated bodies of water. Temperature, pH, turbidity, faecal coliform, dissolved oxygen, biochemical oxygen demand, total phosphates, nitrates, and total soids are among the nine water quality indicators in technique for distincting the aquatic quality of different aquatic locations. The information on aquatic quality is taken down and exported to a curve of weighing table, from which a worth for Qi is calculated.The mathematical formula is given by,

$$WQI = \frac{QiWi}{\sum Wi}$$

Qi = quality parameter of water of sub-index *Qi* or ith;
Wi= quality parameter of water associated with weight;
n = quality parameters numbers

The quality rating scale (Qi) for each parameter is calculated by using this expression:

$$Qi = 100\left(\frac{Vi - Vo}{Si - Vo}\right)$$

Vi is estimated concentration of ith parameter in the analysed water
Vo is the ideal value of this parameter in pure water
Vo = 0 (except pH =7.0 and DO = 14.6 mg/l)
Si is recommended standard value of ith parameter The unit weight (Wi) for each water quality parameter is calculated by using the following formula:

$$Wi = \frac{K}{Si}$$

Where,
K= proportionality constant and can also be calculated by using the following equation:

$$K = \frac{1}{\sum \frac{1}{Si}}$$

4. Results and discussions

the physical and chemical parameters of 16 bore wells that encompass the study region have been determined using standard methods in order to expose the water quality. In table 4.0, they have been listed in a systematic manner. The physical characteristics of the ground water under the study region are determined by the metrics pH, total dissolved solids, turbidity, and electrical conductivity. The parameters total hardness, total hardness, iron, fluoride, nitrate, calcium, chloride, sulphate, and alkalinity are used to determine the chemical properties of the ground water in the research region.

Ground water quality
pH
The pH of the sub surfacewater is neutral or close to it, ranging from 6.9 to 7.8, which is within the allowed limits of 6.5-8.5 set by Indian Standards and also meets the WHO guideline of 7.0-8.0. One of the important goals of pH management is to create aqua that is resistant to both corrosion and incrustations. Comosite interaactivitybetween pH and other several factors , such as dissolved particles, disolved gases, hardnes, alkaliniity, and temperature, occur in these method, which can create significant harm to aqua delivery process. Figure 4.1 depicts the pH changes over the research period.

Turbidity
The research area's groundwater levels turbidity ranges from 0.4 to 1.8 NTU. As depicted in Figure 4.3. Turbidity is a metric for how cloudy water is. It is used to indicate the quality of the water as well as the performance of the filtration system. Increased levels of turbid are linked to higher numbers of illness microorganisms such viruses, parasites, and bacteria.

TDS
The level of sub surface aqua of total dissolved solids 284-807 mg/L, it is higher than 500 mg/L an 1000 mg/L. Tds a term that refers to the inorganic compounds that are the quality of potable water are determined by the quantities of its constituents. Mineralized water is characterised by excessive hardness, taste, mineral depositions, and corrosion. Figure 4.4 shows the total dissolved solids changes across the study period.

Conductivity
The conductivity of groundwater in study ranges from 614 - 933 s/cm.it can be used as indicator of other quality of water issues because it so easily measured. It as high contents of mineral has a higher conductivity, it is a sign that the water has a high dissolved solid concentration. As a result,

ISBN: 979-88-35073-61-0

conductivity measurements can be used to discover potential water quality issues quickly. Figure 4.2 depicts the changes in electrical conductivity across the research period.

Total hardness

As CaCO3, total hardness ranges from 340 to 458 mg/l. hardness ratings for research region was found to be difficult in all areas, and they were found to be on the higher end of the WHO guideline and Indian requirements. Figure 4.6 depicts the changes in total alkalinity and total hardness across the course of the study.

Total alkaliniyy

The samples alkalinity varies from 338 to 447 mg/l. All the samples collected have significant alkalinity values, preventing acidification of a groundwater samples. Figure 4.7 depicts the changes in total alkalinity and total hardness over time.

calcium

Calcium in water is a result of its passage through limestone, dolomite, gypsum, and calcium rocks. It is an important nutrient for the aquatic ecosystem. its carbonate in small amounts forms a protective layer on steel pipes, preventing corrosion. However, as the temperature rises, a higher concentration of calcium precipitates, forming damaging scales in boilers, pipelines, and kitchenware. Calcium has an allowance of 200 mg/l .Calcium concentrations ranges from 42 -198 mg/l in this investigation. Calcium variation in the studied area is shown in figure 4.8.

Chlorides

Chloride levels in groundwater sources tests range from 295 to 62 mg/l, greater the limit of 250 mg/l by Indian and WHO guidelines. Chloride is a widely dispersed element that can be found in various forms in all sorts of rocks. It has a strong affinity for salt. As a result, it has a high concentration in sub surface water where the temperature is more and rain is low. The porous and perm of the soil may play a role in the accumulation of chlorides. Figure 4.9 depicts the fluctuation in chlorides across the period of the study.

Sulphates

The content of sulphate in obtained groundwater samples varied between 30-48 mg/l, well within the allowed 200 mg/l under norms and 250 mg/l. Concerns about sulphate in drinkable water are being raised in light of reports linking diarrhoea to the consumption of water having high amounts of sulphate. Figure 4.10 represents the variation in Sulphate across the observation period.

Nitrates

Nitrate levels in the study region varies from 4.0 to 13.0 mg/l, within which the allowed value of 45 mg/l under norms and 50 mg/l under guidelines. The capacity of these to infiltrate groundwater is determined by the soil and rock present, as well as the depth and structure. Figure 4.11 depicts the variance in Nitrate over the course of the study.

Fluorides

Fluoride values in underground tests ranging from 0.4-0.92 mg/l, which would be significantly less than the permitted value of 1 mg/l set by Indian regulations. The time period of low temperature with soil conditions, rainfall, and the chemical reaction. Figure 4.12 depicts the Fluoride fluctuation over the observation period.

Total iron

Groundwater in the research area have iron concentrations ranging 0.3-0.84 mg/l, with desirable level of 0.3 mg/l and permitted to 1.0 mg/l for iron in potable water (BIS, 1991). As a result, is well within the permitted range. Figure 4.13 depicts the iron fluctuation across the course of the study.

D O

The levels of dissolved oxygen ranges from 4.1-5.7 mg/l. Figure 4.14 shows how dissolved oxygen concentrations varied minimally between locations in the current investigation. The greatest concentration of dissolved oxygen was 5.7 mg/L, while the lowest was 4.1 mg/l. most essential in determining quality of water is dissolved oxygen, which represents the biological and physical activities taking place in the water. For aquatic life and the chemical features of the environment, dissolved oxygen is critical.

B O D

BOD levels varies from 2.6 to 3.5 ppm. BOD is an amount of consumption oxygen utilized by pathogenic organisms during the degradation of biological matter in aerobic circumstances at a specific temperature the samples analyzed for heavy metals like zinc and chromium in which they are characterized as an undesirable in the subsurface water as there concentrations availed to be below the standard range. This shows that these can be absorbed by the soil or organic matter.

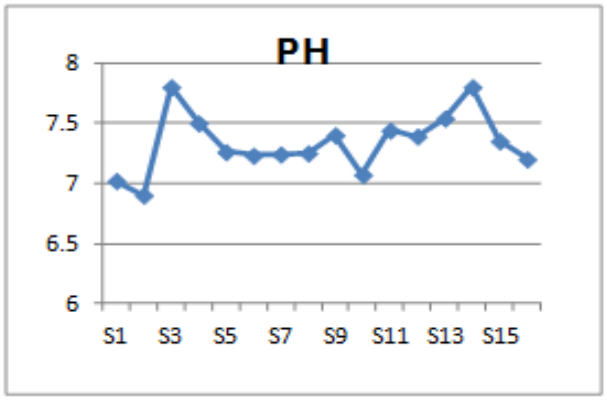

ISBN: 979-88-35073-61-0

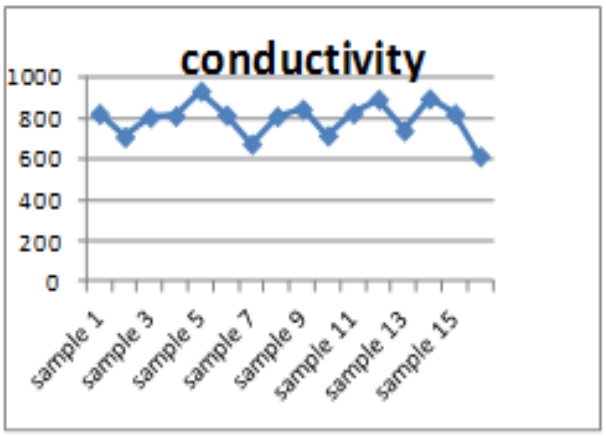

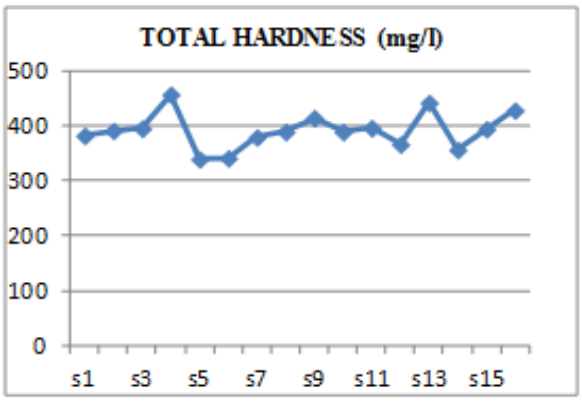

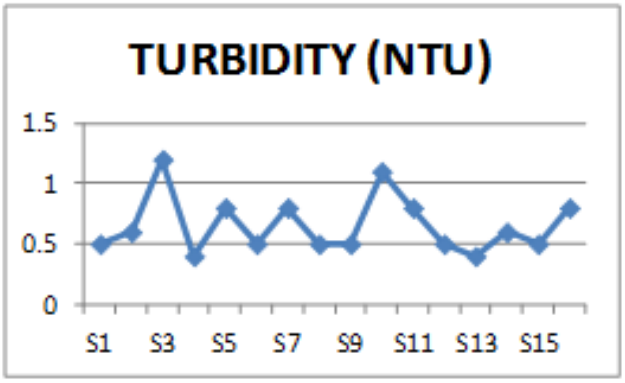

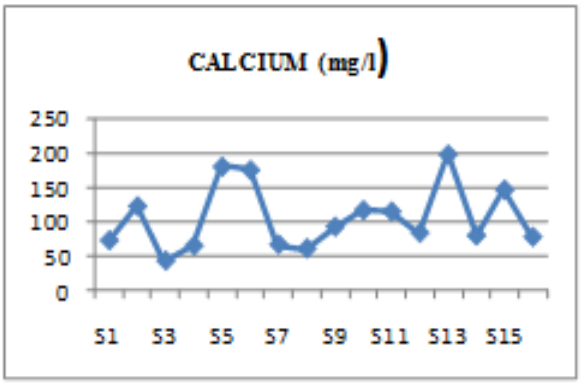

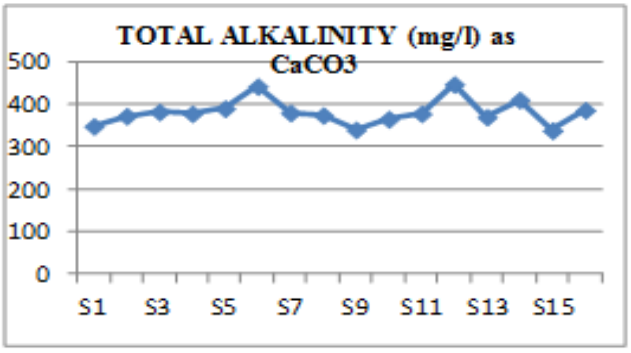

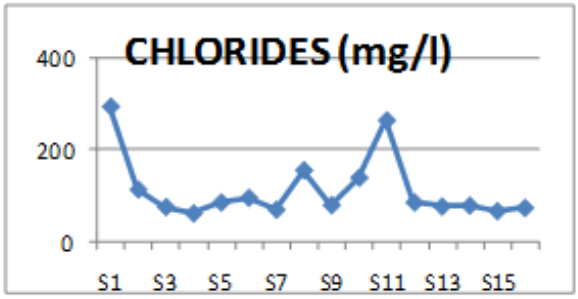

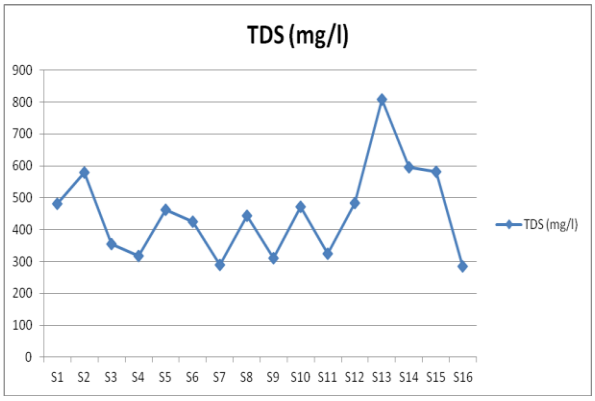

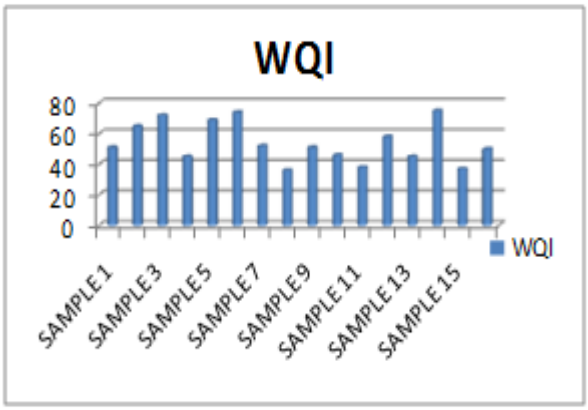

ISBN: 979-88-35073-61-0

CONCLUSIONS

According to the results of the current study of physico-chemical examination of subsurface water in the vicinity of municipal solid waste dumping sites, seven of a sixteen locations have good water quality and the others have poor water quality.Some of the metrics exceed the limitations set by the Indian Standard for Drinking Water (BIS-10500:1991) and the World Health Organization. The greater TDS concentration indicates that landfill leachate has gotten into the subsurface water and polluted it. As a result, we may conclude that landfill has a negligible effect on the quality of groundwater water at the moment.

Even though the water performance is improved, it must be protected in the future against pollution caused by municipal solid waste dumping sites. To reduce ground water pollution, more focus will be placed on improving waste management techniques and constructing appropriately managed landfill site.

REFERENCES

1.Abdul Jameel A & J Sirajudeen (2006) : *"Risk Assessment of Physico-Chemical Contaminants in Groundwater of Pettavaithalai Area, Tiruchirappalli, Tamilnadu – India".* Environmental monitoring and assessment volume 123, pages299–312(2006)

2.Bernard , Nurudeen Ayeni (2012) *"Physicochemical Analysis of Groundwater Samples of Bichi Local Government Area of Kano State of Nigeria Emmanuel". Research gate,*World Environment 2012, 2(6): 116-119 DOI: 10.5923/j.env.20120206.02

3.Bureau of Indian Standards, Specification for drinking water. IS: 10500, New Delhi, India, 2012.

3.Guidelines for Drinking-water Quality, Fourth Edition, World Health Organization ISBN 978 92 4 154815 1. 2012. Guide Manual: Water and Waste Water, Central Pollution Control Board, New Delhi. http://www.cpcb.nic.in/upload/Latest/Latest_67_guidemanualw& wwanalysis.pdf (Accessed 12 July 2013).

4.Grzegorz Przydatek & Włodzimierz Kanownik (2019) ; *"Impact of small municipal solid waste landfill on groundwater quality".* Environmental impact and assessment volume 191, Article number: 169 (2019).

5.Hamed soleimani et.al., (2018) *"Data on assessment of groundwater quality for drinking and irrigation in rural area Sarpol-e Zahab city, Kermanshah province, Iran". Environmental Monitoring and Assessment* volume 190, Article number: 417 (2018).

6.Hossein najafi saleh,et.al., (2020) *"Assessment of groundwater quality around municipal solid waste landfill by using Water Quality Index for groundwater resources and multivariate statistical technique". Springer, Environmental Geochemistry and Health* volume 42, pages1305–1319(2020).

7.Implimentation of integrated municipal solid waste management system in Tumkur, Karnataka.

8.IS 10500 : 2012 *indian standard "*drinking water — specification", *(second revision).*

*9.*Jain C K et.al., (2018) "*Physico-chemical characteristics and hydrogeological mechanisms in groundwater with special reference to arsenic contamination in Barpeta District, Assam (India)". Environmental Monitoring and Assessment* volume 190, Article number: 417 (2018)

10.Jacob Vincent, Green Chemistry & Technology.*"Physico chemical analysis of ground water near municipal solid waste dumping sites in arumuganeri, thoothukudi district, tamilnadu, india",*Green Chemistry & Technology Letters Vol 2, No 1, January 2016, pg 35-37 eissn: 2455-3611, doi: 10.18510/gctl.2015.217 www.greenchemistry.in 35

*11.*Jemal fito et.al .,(2019*) "Physicochemical and heavy metal constituents of the groundwater quality in Haramaya Woreda, Oromia Regional State, Ethiopia".* International Journal of Energy and Water Resources volume 3, pages23–32(2019)

12.Longe E O and M R Balogun (2010*) "Groundwater Quality Assessment near a Municipal Landfill".* Research Journal of Applied Sciences, Engineering and Technology 2(1): 39-44, 2010 ISSN: 2040-7467 © Maxwell Scientific Organization, 2009

13.Mohd Saleem et al Civil & environmental engineering research article, "analysis of groundwater quality using water quality Index: a case study of greater noida (region), uttarPradesh (u.p), india". International Journal of Energy and Water Resources https://doi.org/10.1007/s42108-021-00117-5

*14.*Prem sudha R et al (2016) *"assessment of groundwater quality using wqi method around vellalore municipal solidwaste disposal site in coimbatore, tamilnadu, india.* Research gate, int. J. Chem. Sci.: 14(1), 2016, 229-243 issn 0972-768x.

15.Rakesh Kumar Pandey et al *IOSR Journal of Mechanical and Civil Engineering* "*Physico-Chemical Analysis of Subsurface Water in the Vicinity of Municipal Solid Waste Dumping Sites of Satna District, India*" (IOSR-JMCE) e-ISSN: 2278-1684,p-ISSN: 2320-334X, Volume 13, Issue 1 Ver. I (Jan. - Feb. 2016), PP 37-42 www.iosrjournals.org DOI: 10.9790/1684-13113742 www.iosrjournals.org 37 | Page

*16.*Rima Chatterjee et al (2009) *"Groundwater quality assessment of Dhanbad district, Jharkhand".* Bull Eng Geol Environ (2010) 69:137–141 DOI 10.1007/s10064-009-0234-x

17.Salve P R et al (2008*) "Assessment of Groundwater Quality with Respect to Fluoride".* Bull Environ Contam Toxicol (2008) 81:289–293 DOI 10.1007/s00128-008-9466-x

18.Shankar B S et.al ., (2007) *"Impact of industrialization on groundwater quality – a case study of Peenya industrial area, Bangalore, India".* Environmental Monitoring and Assessment volume 142, pages263–268(2008)

19.SachinMishra ,et .al,.(2019) *" Impact of Municipal Solid Waste Landfill leachate on groundwater quality in Varanasi, India".* Elsevier, Bioresource Technology Reports, Volume 6, 2019, pp. 198-206

20.Shivaprasad H et al Int. Journal of Engineering Research and Applications, . **"***A Study on Physico-Chemical Characteristics of Borewell Water In Sugar Town, Mandya City, Karnataka State, India".* www.ijera.com ISSN : 2248-9622, Vol. 4, Issue 7.July 2014, pp.112-123

21.United State EPA 816-F-09-004, May 2009, http://water.epa.gov/drink/contaminants/upload/mcl-2.pdf (Accessed 12 July 2013.

ANALYSIS AND DESIGN OF G+4 RESIDENTIAL BUILDING USING ETABS

[1]Adhya NK, [2]Ankith KC, [3]Bharath P, [4]Madhusudan BS, [5]Pallavi GA
[1,2,3,4] Student &[5] Faculty, Department of civil engineering
Sapthagiri College of Engineering
Bengaluru,India
[1]adhyank0202@gmail.com , [2]ankithkc04@gmail.com , [3]bharathpgr123@gmail.com , [4]madhusudanbshivanna@gmail.com, pallaviga@sapthagiri.edu.in

***Abstract*: ETABS stands for Extended Three-Dimensional Analysis of Building Systems. The most purpose of this software is to design a multistoried structure in a veritably methodical process. The effective design and construction of structures have great significance far and wide in the world. This design presents a multistoried residential building anatomized and designed using ETABS. This design is meant as per INDIAN CODES- IS 1893-part2:2002, IS 456:2000.**

Keywords: ETABS Software Tool, Multi-Storied Residential Building

INTRODUCTION

ETABS is that the present-day leading design software within the request. Numerous design companies use this software for their project design purpose. So, this paper substantially deals with the relative analysis of the results attained from the analysis of a multi-storied building structure when anatomized manually and using ETABS software. Structural response to earthquake depends on the dynamic characteristics of the structures and intensity, duration, and frequency content of being ground stir. Structural analysis means a determination of the overall shape and all the specific confines of a particular structure so that it performs the function for which it is created and will safely repel the influences which will act on it throughout its useful life.

This design presents the analysis and design of multi-storied residential structures using ETABS software. This design is designed as per INDIAN CODES- IS 1893-part2:2002, IS 456:2000. The structure is proposed to have an Ordinary RC moment-defying frame and the Response Reduction Factor(R) is 3.0 Design illustration of a six-storey structure: In this paper, from the plinth to the certain height of the building the column size may differ that is it would be more when compared to the upper columns because to reduce the failure in the structure. The diaphragm is rigid. The main beams rest on the columns to avoid local eccentricity. As the load is more at the bottom when compared to the top floors, there is no need of furnishing large sizes at the top. Scrimping the column by means of column exposure in a longer span longer direction will reduce the quantum of bending, as a result, there are of the steel is reduced.

DESCRIPTION OF THE STUDY MODEL

Project Details

1. Purpose of the building: Residential
2. The shape of the building: Regular (rectangular)
3. No. of stories: (G+5)
4. Type of wall: Solid concrete block wall
5. Height of stories: 3m. (Similar stories)
6. Depth of foundation: 1.5m.
7. Area of plot: 24.5m (80'5") x 12.3m (40'6") = 301.35m² (7215.5ft²)

Material Properties:
Grade of concrete: M25
Grade of steel: Fe 500

Column and beam dimensions:
Beam size:

i. 150mm x 450mm
ii. 200mm x 450mm
iii. 200mm x 600mm
iv. 450mm x 150mm (Concealed beam 1)
v. 600mm x 150mm (Concealed beam 2)

Column size:

i. 150mm x 600mm
ii. 200mm x 600mm
iii. 200mm x 750mm

Description of Loads

• All moving loads come under live loads.
Live load (on floors): 2kN/m², (IS 875:1987 – Part -2)
Live load (on the roof): 1.5kN/m², (IS 875:1987 – Part -2)
• Floor finishes are the superimposed dead loads.
Floor Finishes: 1.5kN/m
• Wall loads are loads of bricks used in construction.
For an 8" wall (External wall): 10.59kN/m²
For a 6" wall (Inner wall): 7.94kN/m²
Parapet wall: 3.97kN/m²

AutoCAD plan:

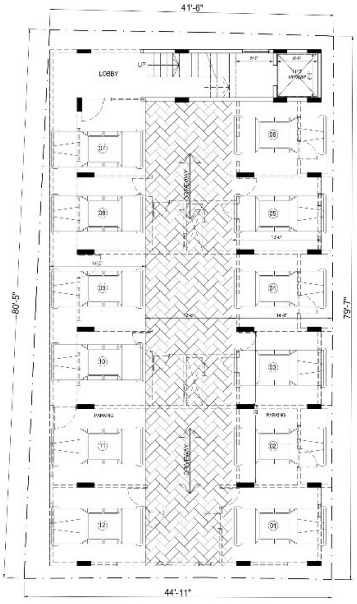

Ground Floor Plan
The dimensions of the building are 23.0m x 12.0m.
Consists of 12 Car parking space.

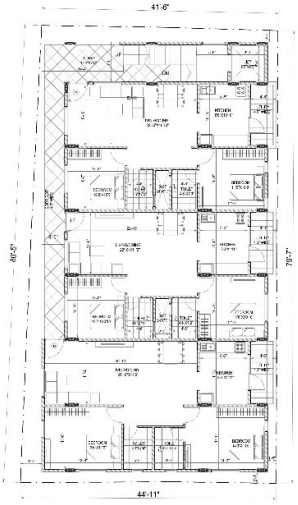

Typical Floor Plan (5 Floors)
All the floor consists of 3 Flats of 2BHK.

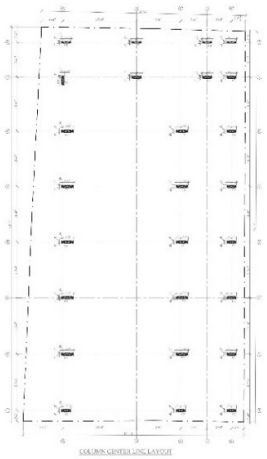

Centerline Column layout

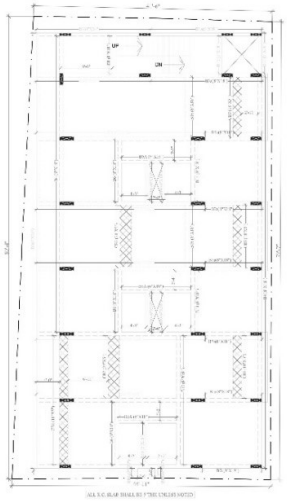

Beam Layout

Modelling in Etabs:
Modelling is done by importing the drafted AutoCAD plan into Etabs.

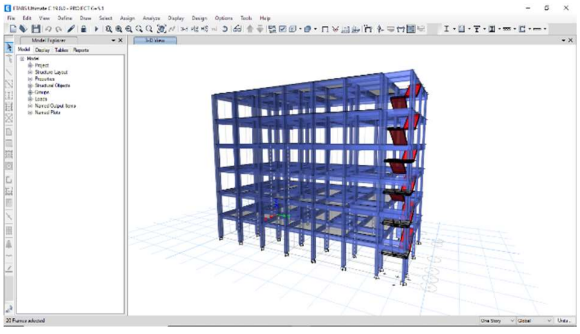

3D Model

Assigning of loads:

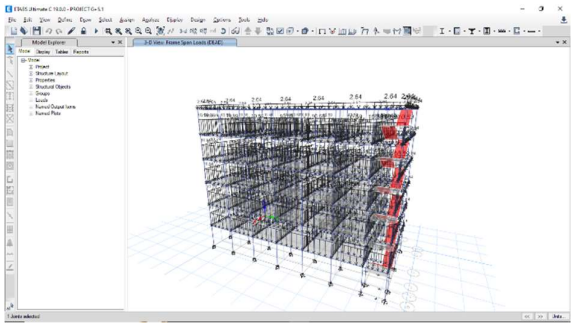

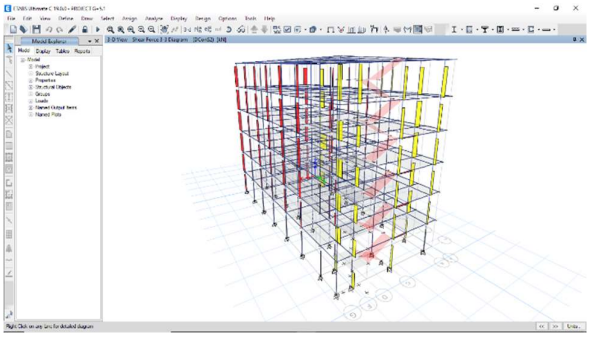

Bending Moment Diagram

Load Combinations:

1. DL 1.5 + LL1.5
2. LL 1.5
3. DL 1.6 + LL 1.2
4. LL 1.4
5. DL 1 + LL 1
6. LL 1.2
7. LL 1.4

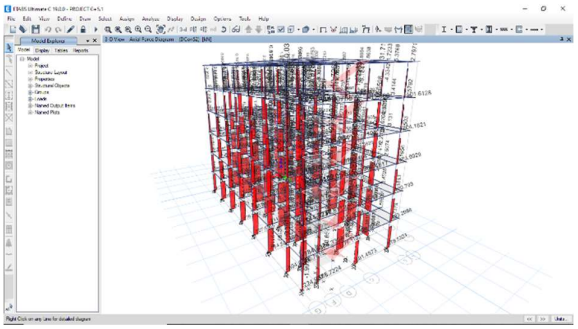

Axial Force Diagram

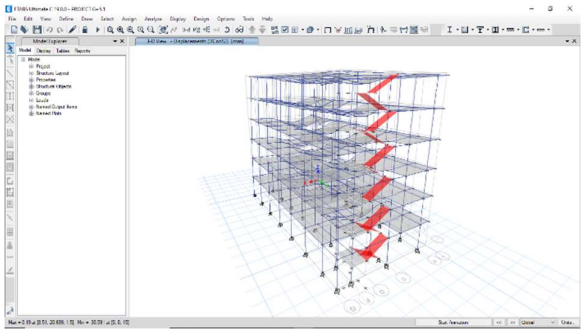

Deflection Diagram

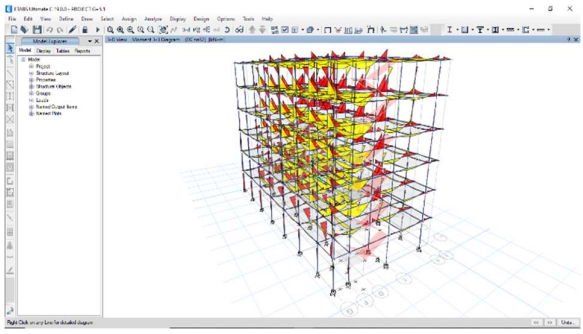

Shear Force Diagram

Reinforcement Details:

Column Reinforcement Details:

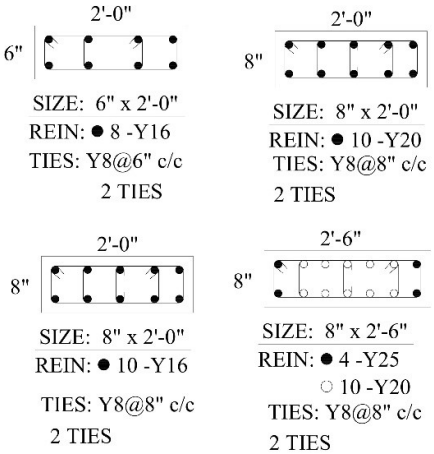

C/S of Columns

Beam Reinforcement Details:

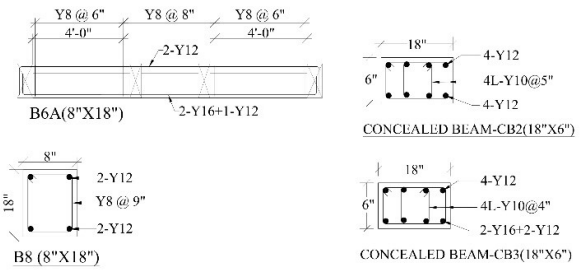

C/S of Beam

Slab Reinforcement Details:

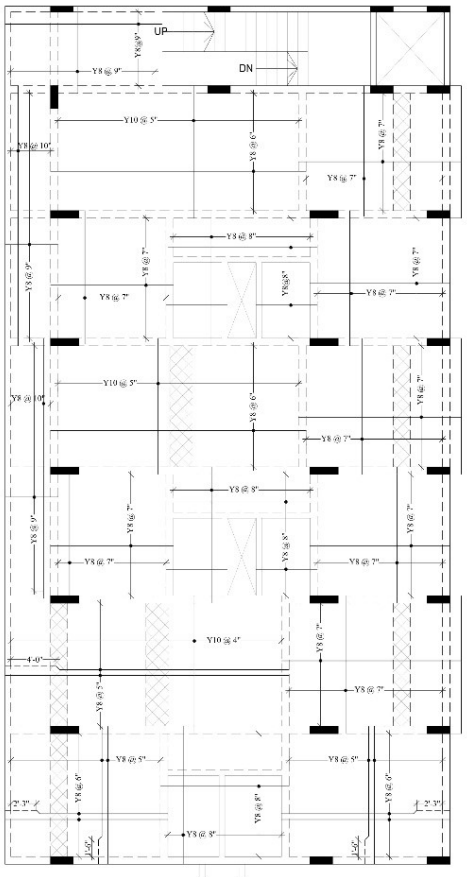

Slab Reinforcement Plan

Staircase Reinforcement Details:

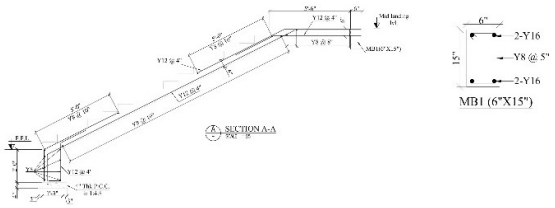

C/S of Staircase

Isolated footing Reinforcement Details:

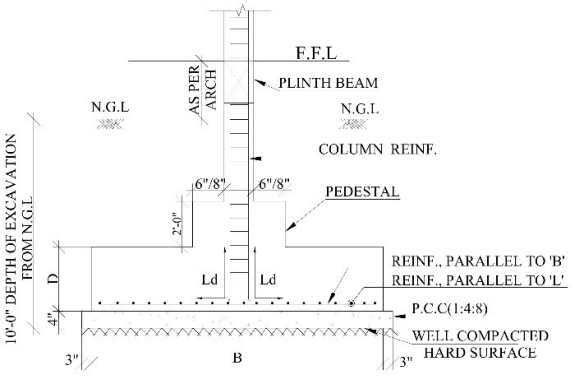

C/S of Isolated Footing

Combined footing Details:

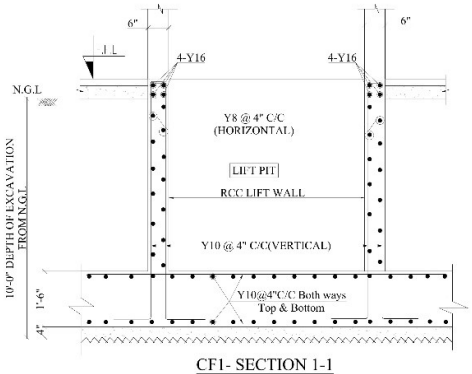

CF1- SECTION 1-1
(COMBINED FOOTING)

CONCLUSION

1. The structure is designed according to IS Codes based on Etabs.
2. AutoCAD is used for drafting the plan.
3. The designed structure provides acceptable strength, serviceability, and durability besides economy.
4. All the reinforcement details of Beams, Columns and Slab has been verified.
5. The displacement, shear force, bending moment variations has been shown.

REFERENCES

1. Chinmay Padole, Samiksha Bansod, Taniya Sukhdeve, Abhishek Dhomne, **"Analysis & Design of G + 4 Resedential Building using Etabs"**, April 2021.
2. Manoj U. Deosarkar, Dhanashree R.Ballewar, Rutuja R.Chitte Punam B Swami Nilima S. Shirasath , **"Analysis And Design of Multistoried Building by Using Revit BIM"** , June 2021.
3. Ms. Priyanka Soni, Mr. Purushottam Lal Tamrakar , Vikky Kumhar, **"Structural Analysis of Multistory Building of Differentshear Walls Location and Heights"**, February 2016.
4. *Tatiana* Zolina, *Natalya* Kupchikova, **"Influence of vibration impacts from vehicles on the state of the foundation structure of a residential building",** 2019.
5. **IS: 875 (PART I) – 1987**
   Code of practice for design loads (other than earthquake) for buildings and structures
   Part 1 dead loads - unit weights of building materials and stored materials
6. **IS: 875 (PART 2) – 1987**
   Code of Practise for Design Loads (Other than Earthquake) for Building and Structures
   Part 2 Imposed Load

Analysis and Design of Multi-Level Car Parking

Tilak H S[1], Sachin K C[2], Dhanush K L[3], Harish S R[4], Shobha Y N[5]

[1,2,3,4]*Under graduate students, Dept. of Civil Eng., SCE Bangalore-560057, India*
[1]tilakgowda4@gmail.com
[2]sachinkc893@gmail.com
[3]dhanushlingappa@gmail.com
[4]harishsr81232@gmail.com

[5]*Assistant Professor, Dept. of Civil Eng., SCE Bangalore-560057, India*
shobhayn_civ@sapthagiri.Edu.in

***Abstract* — The world's population continues to grow, especially in cities and metropolitan areas. The increase in population and the proliferation of urban centers leads to an increase in vehicle ownership and an increase in the need for mobility for a variety of purposes. We cannot leave the car on the road or in unsafe places. Proper parking of the vehicle if not used "parking" is required. There were more than 80 lakh registered vehicles in the southern city of Bengaluru at the end of the 2019 financial year. Due to the increase in the number of vehicles especially cars in Bangalore city, it needs more parking so it can be controlled by building a multi-level car park near the designated areas.**

High-quality parking comes with many advantages as it has many advantages such as efficient use of spaces, so that drivers are comfortable as the pressure to struggle for the parking space is removed and added security.

The project introduces an analysis and design of a multi-level car park (G + 3) to reduce road challenges in public places. The total area of the building is 40mX60m (2400 m2). The program was originally developed using AutoCAD and 3D modeling was done using REVIT Software. The design approach involves analyzing the entire structure in ETABS. The ramp, stairs, and isolated footing are designed manually. The design approach involved in ETABS is limit state design confirming to IS codes of practice.

Keywords - Multi-level car parking, Analysis, Design, ETABS, REVIT and Ramp.

I. INTRODUCTION

Nowadays every day the number of vehicles on the road increases. It is very difficult to park a car on the road or when a vehicle is moving. But, when the car stops, we can't leave the car on the road either an unsafe place. For proper maintenance of the car if not used 'parking space' is required. For everyone storage space is important both where you are going and where you are staying. When the one has to stop on the road for some reason other than traffic, the car needs to stop in that location, without interfering with traffic flow. Such place is called parking lot. It is also noteworthy that a private car travels about 2 to 3 hours a day, while the remaining time is 'parked' at the residence or destination and sometimes on the road. With the growth of ownership and use of private cars, parking has become a staple in recent years, especially in urban areas Thus, with the increase in population, the demand for cars increases and we need more parking so the controlling space by building a multi-level car parking.

II. OBJECTIEVES

1. To reduce the parking space by providing a multi-level car parking structure.
2. To provide a safe and secure environment for parked vehicles.
3. To reduce the traffic congestion.
4. Proposing a multi-level car parking in Bangalore region.

III. LITERATURE REVIEW

1. Design and Analysis of Multistory Parking

B Vamsi, Dr. Dumpa Venkateswarlu, Dr. D V Rama Murthy [Ijrsae].
This project aims to design an effective parking system and it helps to reduce parking in the city. To control parking problems they suggested a parking lot for many issues in this area. This multi-story parking lot provides power parking, and thus reduction environmental degradation. Here, they have provided parking of 277 cars according to design. To determine the Requirements for such a parking system, they were designed for G + 3 floor structure.

2. A Study of Analysis and Design of Multilevel parking

Upendra singh dandotia , Rakesh Gupta, Mukesh Pandey [Ijedr]
In this research paper they have built a parking space for a capacity of 600 cars and 550 bicycles. Multilevel parking consisting of G + 2 + 2 Basement with 13 story's on the ground floor and its structure is based on a framed building. In this work they designed various multi-level parking components namely raft foundation, retaining walls, beams, column and flat slab using STAAD-Pro, portable foundations and AUTO-CAD software for creating various architectural drawings.

3. Analysis and Design of Multi-level car parking structure using seismic zone III

Babitha Rani.H, Voleti Vyshnavi [Ijirt]
In this study paper, the construction of Multi-Level Car Parking involving G + 4 floors is modeled, modified and designed in such a way that each floor can accommodate 46 cars. The multi-level car parking system is developed using AutoCAD and the structure is analyzed to determine the seismic behavior of the building under zone III and is designed using STAAD PRO software. The design was based on the standard Indian code IS 456: 2000.

4. Analysis of Multi-storied parking building using STAAD PRO software

Patil.S.S , Devtale.M.K, Jadhav Bhushan D, Navadkar Sunil R, Jadhav Santosh L, Patil Amrutrao E, Kalam Akshay A and Pawar Govind M [Ijmter]
In this paper an analysis of the multi-story G + 1 building used for the parking system. They discussed the problems faced during parking, and then offered a solution to the Parking Problem. In the study of seismic load analysis and rear load analysis according to the IS seismic code 1893 (Part1): 2002 performed. In buildings, the asymmetric in the structure of the G + 1 building compares the conditions in which building column numbers and the effort are made to study the impact of earthquake loads on them and determine the duration of exercise, base shear and time using response spectrum method.

IV. METHEDOLOGY

The process was as follows:

1. First the plan is prepared using AutoCAD.
2. External 3D modelling is performed using REVIT software by importing the model from ETABS.
3. Analysis and design is done using computer software ETABS 2018 except footing. The building was modelled and analysed.
4. After analysis the detailing was done using AutoCAD.

V. PLANNING IN AUTOCAD

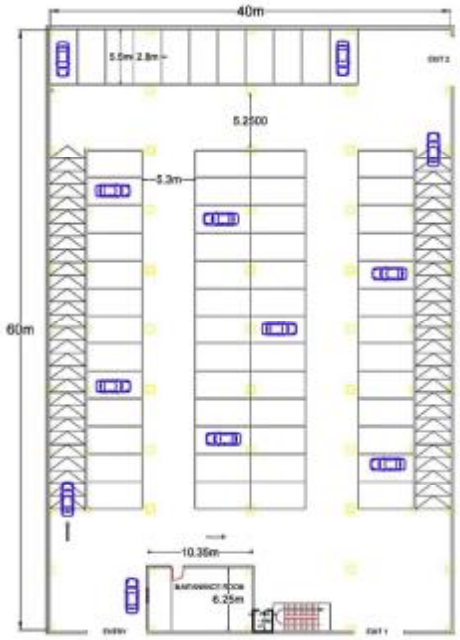

Fig1. Ground floor plan

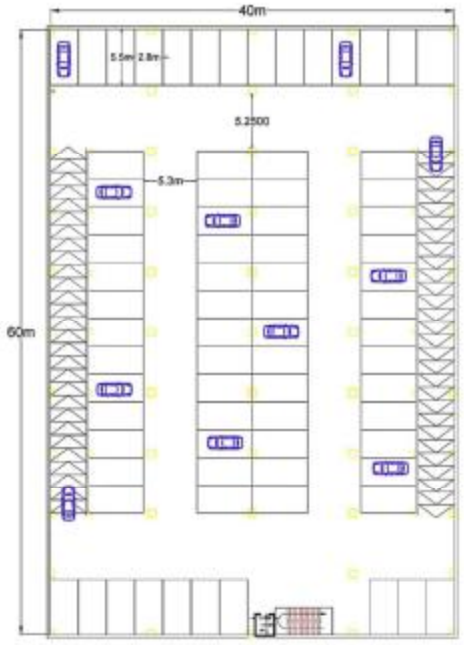

Fig2. Plan of 1st, 2nd and 3rd floor

VI. EXTERIOR MODELING IN REVIT

Fig3. 3D Modeling in Revit

Bay Size:
The car bay dimension is rated 5.5m x 2.8m.

Head room:
The recommended minimum length is clear either headroom, normal height measurement for vehicles is 2.10m. Additional permissions are usually required on gradient changes as ramps. The floor height is considered as 3.5m which is satisfactory minimum height recommended for headroom which includes ventilation, lighting, obstacle controls and other possibilities ratings.

Parking angle:
Placing bays at associate degree at angle less than 90° is very convenient for drivers but exact 90^0 may be a convenience for drivers since it facilitates entry and exit. This successively improves the 'dynamic and turnover capacity' of the aisle. Here parking angle is of 90o

Car parking gridlines:

This building contains 4 spans of 10-meter in X-direction and 11 spans of 6-meters in Y-direction. For the ramps we have provided a projection of 3.75m from the beginning and end of the width in the x-direction. The total height of the building is 14m. The building plan measures 40m x 60m as shown in fig (4).

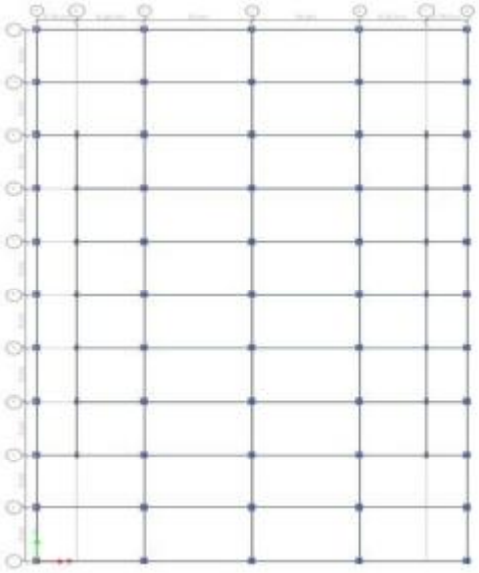

Fig4. Grid lines of parking building

VII. ANALYSIS IN ETABS

Design information:
The building was built in line with the Indians Standard 1893 (Part I): 2002 (Indian Decision Code Earthquake Resistance). And IS: 875 Part III (Wind load consideration). Story height is considered to be 3.5m. The buildings are to be fixed at the base. The floor of all the buildings acts as the diaphragms are sturdy and they are analyzed and designed by using ETABS v18.0.2 software of the city of Bengaluru (i.e. Zone II).

The material grades taken are M30 for concrete and Fe 415 for steel. Live load is taken as 5 KN/m2 and floor finish as 1 KN/m2. Thickness of slab is calculated as per clause 23.2.1 of IS 456: 2000 and also sizes of beams and columns are decided by using criteria as per IS 13920: 1993 (Ductile Detailing of Reinforced concrete structures) Sizes of the column is taken as (750X750) mm. For the ramp column size is taken as (300X750) mm.

According to IS 1893(Part1): 2016 and IS 875 (part III): 2015 Load combinations used are:

1. 0.9DL-1.5EQX
2. 0.9DL-1.5EQY
3. 0.9DL-1.5WLX
4. 0.9DL-1.5WLY
5. 0.9DL+1.5EQX
6. 0.9DL+1.5EQY

7. 0.9D+1.5WLX
8. 0.9DL+1.5WLY
9. 1.2(DL+LL+EQX)
10. 1.2(DL+LL+EQY)
11. 1.2(DL-LL-WLX)
12. 1.2(DL+LL+WLY)
13. 1.2(DL+LL-EQX)
14. 1.2(DL-LL-EQY)
15. 1.2(DL-LL-WLX)
16. 1.2(DL+LL-EQY)
17. 1.5(DL+EQX)
18. 1.5(DL+EQY)
19. 1.5(DL+LL)
20. 1.5(DL+WLX)
21. 1.5(DL+WLY)
22. 1.5(D-EOX)
23. 1.5(DL-EQY)
24. 1.5(DL-WLX)
25. 1.5(DL-WLY)
26. 1.5DL

As per IS 1893 (Part I): 20016

Natural Time Period: $T_a = (0.09*h) / \sqrt{d}$
In X-direction, $T_{ax} = (0.09 * 14) / \sqrt{40} = 0.213$ sec.
In Y-direction, $T_{ay} = (0.09 * 14) / \sqrt{60} = 0.174$ sec.
Importance Factor: I = 1.0
Response Reduction Factor: R= 5.0
Soil Type = medium
Zone Factor: Z = 0.1 (Zone II).

As per IS 875 (part III): 2015
Basic wind speed, V_b = 33 m/s
Risk coefficient, k_1 = 1
Terrain roughness and height factor, k_2= 0.8
Topography factor, k_3 = 1
Importance factor for the cyclonic region, k_4 = 1
Design wind speed (V_z) = $V_b*k_1*k_2*k_3*k_4$ = 33*0.8*1*1 = 26.4m/s.

Analysis results:

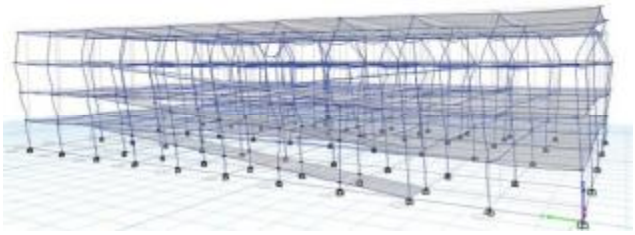

Fig5. Displacement due to combinations of load

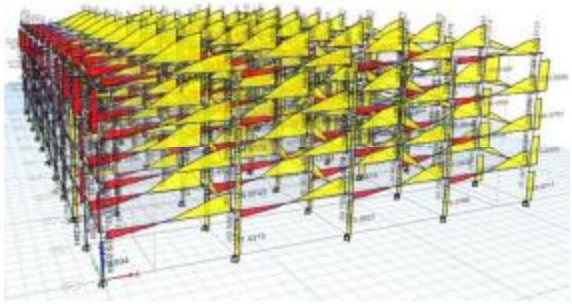

Fig6. Shear force diagram

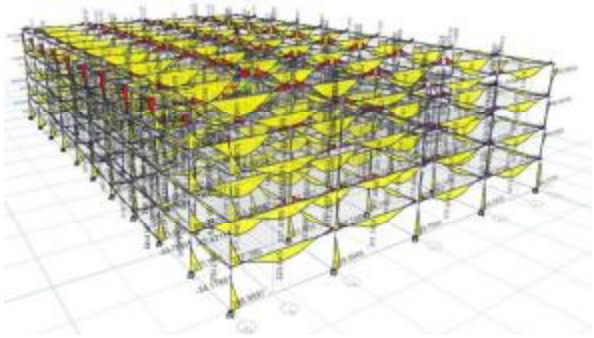

Fig7. Bending moment diagram

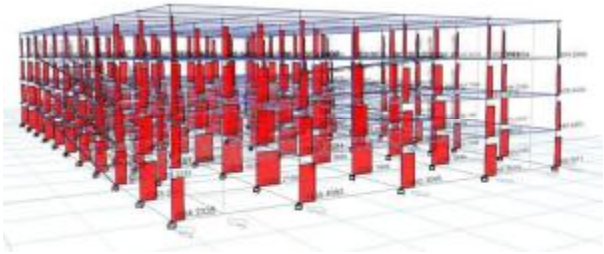

Fig8. Axial force diagram

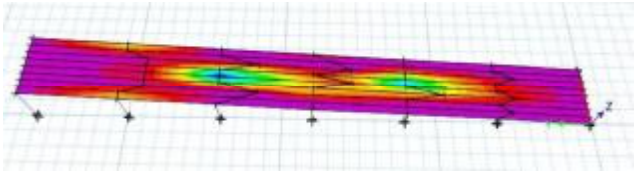

Fig9. Resultant bending moment of the Ramp

VIII. DESIGN OF SLAB

Slab dimension: 10m x 6m
Concrete grade: M30
Steel used: Fe 415

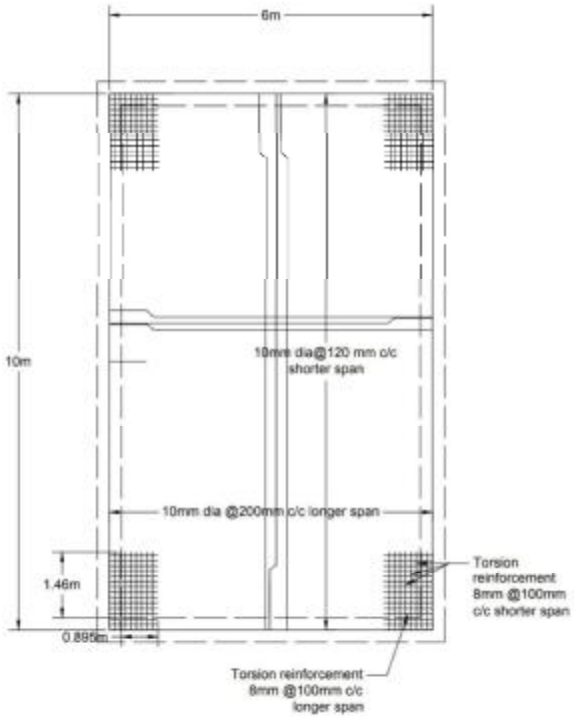

Fig10. Reinforcement details of Two-way Slab

IX. DESIGN OF BEAM

Beam dimension: 450mm x 700mm
Concrete grade: M30
Steel used: Fe 415

1. For 10m span

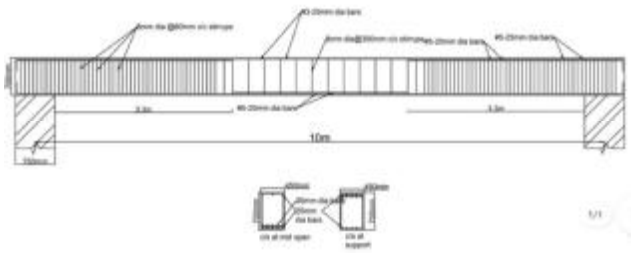

Fig11. Reinforcement details of beam for 10m span

2. For 6m span

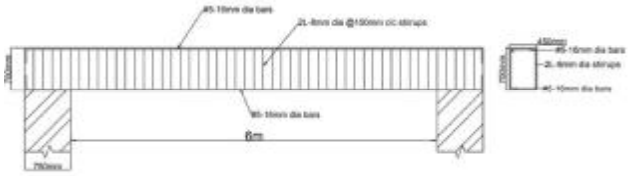

Fig12. Reinforcement details of beam for 6m span

X. DESIGN OF RAMP

Ramp slab dimension: 3.75m x 6m
Slope: 1: 10.3
M30 concrete & Fe 415 steel used

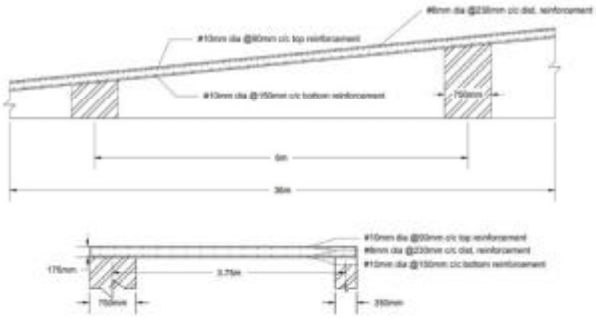

Fig13. Reinforcement details of Ramp

XI. DESIGN OF INCLINED BEAM FOR RAMP

Beam dimension: 300mm x 500mm
Concrete grade: M30
Steel used: Fe 415

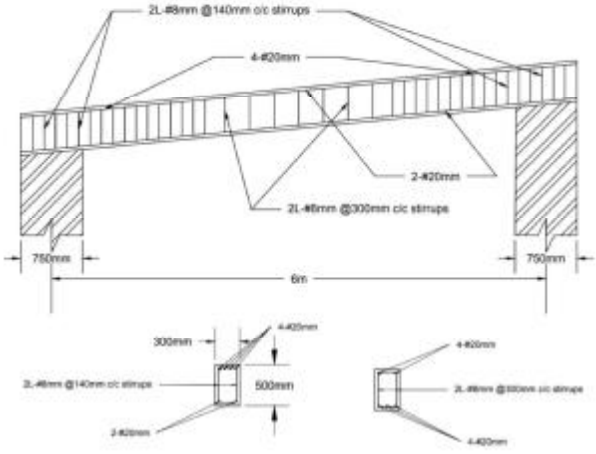

Fig14. Reinforcement details of Inclined Beam

XII. DESIGN OF COLUMN AND FOOTING

1. Column: 750mm x 750mm
Footing: 3m x 3m
M30 concrete & Fe 415 steel used

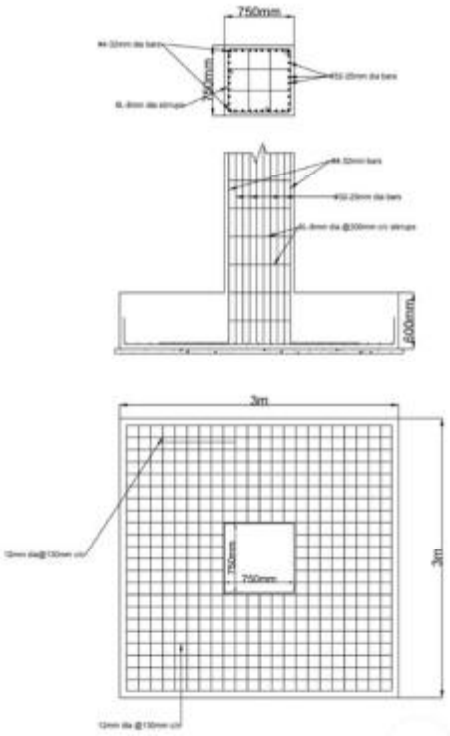

Fig15. Reinforcement details of footing

2. Column: 350mm x 750mm
Footing: 1.75m x 2.8m
M30 concrete & Fe 415 steel used

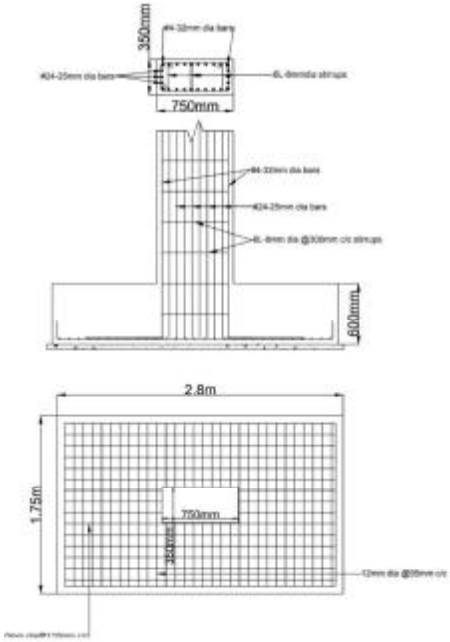

Fig16. Reinforcement details of footing

XIII. DESIGN STAIRCASE

M30 concrete & Fe 415 steel used

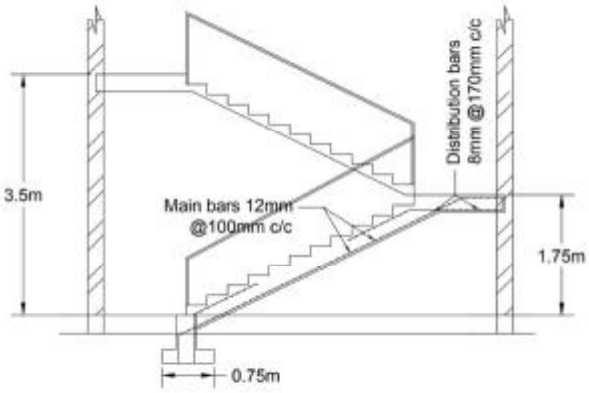

Fig17. Reinforcement details of Doglegged Staircase

XIV. CONCLUSION

From our present parking studies the traffic congestion problem can be regulated by providing multi-level car parking

at BENGALURU. We hope this project will serve as a solution to various traffic congestion problems and can be used as a model in the development of multi-level car parking's. We have designed the multilevel parking building consisting of G+3 which will survive the purpose of traffic congestion. In ground floor having a car parking capacity of 63 and the 1st, 2nd and 3rd floor having a capacity of more than 75 cars each. This system can help in economy and security based aspects for the society. It is a currently, management information system play an important part in the life, however many of the rules are poor and need to be progress. This project has been focus on improving the Bangalore parking system to be suitable for the life style.

REFERENCES

[1] B Vamsi, Dr. Dumpa Venkateswarlu, Dr. D V Rama Murthy "Design and Analysis of Multistory Parking", Ijrsae

[2] Upendra singh dandotia , Rakesh Gupta, Mukesh Pandey, "A Study of Analysis and Design of Multilevel parking", 2016 IJEDR, Volume 4, Issue 2, ISSN: 2321-9939.

[3] Babitha Rani.H, Voleti Vyshnavi., "Analysis and Design of Multi-level car parking structure using seismic zone III", November 2019 IJIRT, Volume 6, Issue 6 , ISSN: 2349-6002.
[4] Patil.S.S , Devtale.M.K, Jadhav Bhushan D, Navadkar Sunil R, Jadhav Santosh L, Patil Amrutrao E, Kalam Akshay A and Pawar Govind M,"Analysis of Multi-storied parking building using STAAD PRO software" March 2017, Volume 04, Issue 03,IJMTER, Issn 2349–9745.
[5] Dr. P. S. Pajgade[1], Radhika A. Dahane[2]. "Design of multi-level car parking", Volume 3 , Special Issue 1, ICSTSD 2016, IJIERE.
[6] M R Rajashekara[1], Mohammed Kalandar Khan[2], Nikita Anil Moodi[3] "Demand assessment of multi-level car parking in garuda mall", Volume 03 Issue 07 | Jul 2014 | IJRET.
[7] Nirmal S. Mehta[1], Urmi D. Modi[2], Parth R. Patel[3], Rutvik M. Prajapati[4], "Analysis and design of multi storey residential building using ETABS",2018 JETIR , November 2018, Volume 5, Issue 11.
[8] Shradhesh Rajuji Marve[1], Abhijit Nanaji Chalkhure[2], Sarvesh Rajendra Jumde[3], Rohit Murlidhar Khobragade[4], Ankit Gurudas Chunarkar[5], Shubham Maroti Thakre[6] ., "Design and analysis of multy storied car parking building (G+2)." Volume 9, Issue 4, April 2020 JIRSET.

EXPERIMENTAL STUDY OF DENSE BITUMINOUS MACADAM USING CRUMB RUBBER

RAVIKAUMAR*[1], SUNIL YADAV[2], TEJAS N[3], TEJAS S RAM[4]
Department of Civil Engineering, Sapthagiri College of engineering
#14/5 Chikkasandra, Hesaraghatta main road, Bangalore- 57 India
STUDENTS OF CIVIL ENGINEERING DEPARTMENT

[1] sunilyadav20244@gmail.com [2]ravikumartelgur@gmail.com [3] tejasnayaka168@gmail.com
[4]tsr17500@gmail.com

Abstract **-** Human existence fashion and growth in populace has prompted an growth in stable waste consisting of rubber. Rubber wastes are constantly growing with the growing call for of producing of transportation vehicles. The usage of waste substances like rubber with inside the method of avenue creation affords many benefits.

The abundance and growth of waste tyre disposal is a extreme main disaster that ends in environmental pollution. Crumb rubber acquired from shredding of these scrap tires has been verified to beautify the residences of simple bitumen for the reason that 1840s. It may be used as a reasonably-priced and environmentally pleasant change method to limit the harm of pavement because of growth in carrier visitors density, axle loading and occasional protection offerings which has deteriorated and subjected avenue systems to failure extra rapidly.

I. INTRODUCTION

India is a rustic of villages and roads are the first-class manner of connectivity for shipping. Increasing the variety of roads and enhancing its high-satisfactory enables withinside the sizable improvement of any country. Due to the speedy upward push in shipping thru roads the use of motors is significantly increased. Hence the use of rubber tyres is unexpectedly increased. Replacement of car tyres is important for about 20000 km – 60000 km of transportation relying at the sort of car. Due to this extra amount of waste tyres are produced. It has been envisioned that extra or much less billions of heaps of waste tyres are produced globally each year. The ever growing tyre waste and its disposal is a severe hassle that ends in environmental pollution. The shredded Crumb rubber received from the scrap tyres has been proved to decorate the houses of simple bitumen for the reason that 1840s.

The high-satisfactory of pavement is imbibed relying at the sort of substances selected for its making. Pavements are typically of classes primarily based totally on structural performance – Flexible pavements and Rigid pavements

A bendy pavement is the only which has a bitumen coating on pinnacle and inflexible pavements that are stiffer than bendy ones which have PCC or RCC on pinnacle. The bendy pavements are constructed in layers and it's miles ensured that below utility of load not one of the layers are overstressed. The most depth of pressure takes place at pinnacle layer, for this reason they may be crafted from advanced cloth specially bitumen.

The blend layout have to intention at a cost-effective combination with right gradation of aggregates and ok percentage of bitumen in an effort to satisfy the preferred houses of blend that are stability, durability, flexibility, skid resistance and workability. Mix layout strategies have to intention at figuring out the houses of aggregates and bituminous cloth which could deliver a combination with those houses. The layout of asphalt paving combos is a multi-step system of choosing binders and mixture substances and proportioning them to offer the best compromise amongst numerous variables that have an effect on aggregate behavior, thinking about outside elements which include site visitors loading and weather conditions. In the development of bendy pavements,

ISBN: 979-88-35073-61-0

bitumen performs the position of binding the mixture collectively with the aid of using coating over the mixture. It additionally enables to enhance the energy of the road. But its resistance closer to water is poor. Anti-stripping sellers are being used. Bitumen is a sticky, black and particularly viscous liquid or semi-strong which may be determined in a few herbal deposits or received as byproduct of fractional distillation of crude petroleum. It is the heaviest fraction of crude oil, the only with maximum boiling point (525°C) .Various Grades of Bitumen used for pavement purpose:30/40, 60/70 and 80/100. The suited houses of bitumen for pavement are:

- Excellent binding belongings with aggregates, each cohesive and adhesive in nature.
- Repellent to water.
- Thermoplastic in nature (stiff while cold, liquid while hot) [Athira and Sowmya, 2015].

An notably used technique to enhance the high-satisfactory of bitumen is with the aid of using enhancing the Engineering houses of bitumen with the aid of using mixing with natural artificial polymers like rubber. They can go back to the earth as useful components in bitumen roads

II. MATERIALS & METHODS

2.1 Bitumen

VG30 bitumen turned into used on this research to put together the samples. Table 1 indicates the check consequences of fundamental houses of bitumen.

Table 1: Basic Properties of Bitumen

Properties Results

Properties	Results
Specific gravity	1.02
Penetration	36 mm
Softening point	37°C
Flash point	330°C
Fire point	350°C
Ductility	79 mm
Viscosity	60/70

2.2. Fine Aggregate

Aggregates of length underneath 4.seventy five mm as in line with MORTH Specifications (fifth revision) [Anonymous, 2013] have been used as excellent aggregate. Table 2 indicates the check consequences of fundamental houses of excellent aggregates.

Table 2: Basic Properties of Fine Aggregates

Properties Results

Properties	Results
Specific gravity	2.64
Water absorption	1.45%

2.3. Coarse Aggregate

Aggregates of 20mm as in line with MORTH Specifications (fifth revision) [Anonymous, 2013] down length have been used as Course aggregate. Table three indicates the check consequences of fundamental houses.

Table 3: Basic Properties of Coarse Aggregates

Properties Results

Properties	Results
Specific gravity	2.67
Impact value	18.75%
Water absorption	0.39%

2.4. Crumb Rubber

Uniformly shredded Rubber portions have been used withinside the study.

Crumb rubber passing 150µm and preserving 300µm turned into used.

Table 4: Basic Properties of modifiers

Properties Results

Properties	Results
Specific gravity	0.707

Methodology:

3.1 Marshall Stability Test

The Marshall Stability and flow test provides the performance prediction measure for the Marshall Mix design method. The original Marshall Method is applicable only to hot asphalt paving mixes. Marshall Stability of a test specimen is the maximum load required to produce failure when the specimen is preheated to a prescribed temperature placed in a special test head and the load is applied at a constant strain (50.8 mm/minute).

ISBN: 979-88-35073-61-0

While the stability test is in progress dial gauge is used to measure the vertical deformation of the specimen. The deformation at the failure point expressed in units of 0.25 mm (0.01 inch) is called the Marshall Flow value of the specimen.

The 'Marshall Stability' of the bituminous mix specimen is defined as a maximum load carried in kg at the standard test temperature of 60°C when load is applies under specified test conditions. It involves mainly 2 processes:

Preparation of Marshall Samples

Marshall Test on samples

3.2 Preparation of Marshall Samples

- For DBM mixes the coarse aggregates, fine aggregates and filler were mixed with bitumen and modifier used according to the adopted gradation, such that each aggregates are weighed and added.
- This will be about 1200 g referring to Rothfutch's graph results.
- Each material is graded, weighed and placed in an oven until a uniform temperature of 60°C is attained.
- Nominal bitumen mix specimen is prepared; Course aggregate is added to a preheated pan and stirred.
- When they heat up to around 100°C, melted bitumen is added and mixed thoroughly.
- When the mixture shows well coated by bitumen, fine aggregate and cement (filler material) is slowly added.
- The ingredients are heated until they reach 130°C.
- The CRMB samples are obtained by following the above procedure; the only change being the variation in crumb rubber which is heated and melted along with bitumen before the hot liquid mix is poured over coarse aggregate.

FIG.1 PREPARATION OF SPECIMEN

FIG.2 CASTING THE SPECIMEN INTO THE MOULD

ISBN: 979-88-35073-61-0

FIG.3 UNMOULDING SPECIMEN AFTER 24 HOURS OF CASTING

3.3 Marshall test on samples

Marshall Stability test is conducted on compacted cylindrical specimens of bituminous mix of diameter 101.6 mm, thickness 63.5 mm. The load is applied perpendicular to the axis of the cylindrical specimen through a testing head consisting of a pair of cylindrical segments, at a constant rate of deformation of 51 mm per minute at a standard test temperature of 60°C. The 'Marshall Stability' of the bituminous mix specimen is defined as a maximum load carried in kg at the standard test temperature of 60°C when load is applies under specified test conditions. The flow value is the total deformation of Marshall Test specimen at the maximum load, expressed in mm units.

In the Marshall method of mix design, each compacted test specimen is subjected to the following tests and analysis.

Bulk specific gravity (Gb) determination

Stability and Flow test and

Void analysis

- Bulk specific gravity (Gb) determination
- Bulk specific gravities of saturated surface dry specimens are determined.

Stability and flow tests

After determining the bulk specific gravity of the test specimens, the stability and flow tests are performed. Place the specimen centrally on the lower testing head and fit upper head carefully. Fix the flow meter with zero as initial reading. The load is applied at a constant rate of deformation of 51 mm (2 inches) per minute. The total load at failure is recorded as its Marshall Stability Value. The reading of flow meter in units of 0.25 mm gives the Marshall Flow value of the specimen. The entire testing process starting with the removal of specimen from bath up to measurement of flow and stability shall not take more 30 seconds. While the stability test is in progress, hold the flow meter firmly over the guide road and record.

Density and voids analysis

After completion of the stability and flow test, a density and voids analysis is done for each set of specimens. The calculations are given in section 5. Average the bulk density is determined for asphalt content. This average value of Gb is used for further computations in void analysis. (a) Determine the theoretical density (Gt) for at least 2 bitumen contents nearer to the optimum binder content. (b) Vv, VMA and VFB are then computed using the standard equations.

Fig.4 Marshall Stability testing Machine

ISBN: 979-88-35073-61-0

III. RESULTS & DISCUSSIONS

1. The use of rubber in roads can solve the problem of environmental damage which can be caused by their disposal.
2. The presence of crumb rubber reduces the air voids which prevents the moisture absorption and also prevents oxidation of bitumen due to entrapped air. This result shows enhancement of Marshall Stability value, stripping and other design parameters and this may prevent formation of potholes.

IV. CONCLUSIONS

1. The aim of the study was to utilize the waste materials i.e. crumb rubber waste for mass scale utilization such as in highway construction in an environmentally safe manner.
2. As in the first part of the study, an attempt was made to assess the stabilization of the bitumen containing crumb rubber waste in shredded form by performing basic tests such as Ductility Test, Penetration Test, Softening Point Test, Viscosity Test and Flash & Fire Point Tests.

V. REFERENCES

1. Anonymous (2013) Specification for Road and Bridge Works (Fifth Revision). Indian Roads Congress, MORTH, New Delhi. Pp: 174-179.
2. Athira R Prasad and Sowmya NJ (2015) Bitumen Modification with Waste Plastic and Crumb Rubber. International Journal of Engineering Research & Technology (IJERT) 4(5): 1586-1591.

ISBN: 979-88-35073-61-0

STUDY ON STORM WATER RUNOFF

KIRAN HN[1], VISHWAS R[2], BHUVAN S[3], KRISHNA KANT SAHU[4], KAVYA H P[5]
[1,2,3,4] *Student, Dept of Civil Engineering, Sapthagiri College Of Engineering, Bengaluru, Karnataka-560057, India*
[5]*Assistant Professor ,Dept. of Civil Engineering , Bengaluru, Karnataka-560057, India*
Kiranhn2605@gmail.com
Vishu322001@gmail.com
Bhuvanbhuvi783@gmail.com
Krishnakantnew14@gmail.com
kavyahp@sapthagiri.edu.in

ABSTRACT- urban runoff from traffic area is major source of pollution that degrades the quality of adjacent surface waters. Green infrastructure provided by the substantial amount of road side land at the urban fringe areas can be used to better manage and infiltrate this urban runoff. For the urban green areas, recycled materials should be preferred in order to achieve economically feasible and environmentally responsible solutions.

I.INTRODUCTION

Bengaluru capital also known as Silicon Valley of India is failing to cope with the inexorable urbanization and population growth. Failing to cope with the inexorable urbanization and population growth. Unplanned urbanization, land development through filling encroachment of water bodies and lack of maintenance is changing the ecological balance of the city). Inhabitants of Bengaluru are paying the price of rampant unplanned urbanization in form of Insufficient coverage and delivery of urban facilities like water supply, garbage disposal and proper drainage sewar logging in Bengaluru IS one of the adverse pieces of evidence of unplanned urbanization which IS getting hilarious day by day. This study focuses on the pluvial flooding or water logging which is induced by high intensity rainfall runoff in the urban area Extensive impervious surface, inadequate drainage channels, lack of drainage system maintenance and encroachment of wet lands and natural drainage system, reduce the runoff concentration period and increase the peak flow which cause severe water logging This complex issue cannot be solved in blink of Various governmental organizations. urban designers and landscape architects have much more to contribute to the city rather than mere beautification.

II.CAUSES

Population growth, unplanned development and encroachment

Ever increasing population has led to unplanned urban land development and unauthorized land filling that results the

disappearance of natural drainage pattern. This phenomenon interrupts the drainage network and reduces detention basins, which have aggravated the water logging problem.

A natural drainage system consists of canals, ponds, lakes and reservoirs. Unplanned development and encroachment of natural water bodies make the remaining canals and ponds to quickly transform into black and smelly waters- To improve the environmental and traffic condition, many of these canals were transformed into box culverts and connected to underground drainage network.

Small drainage sections In Inlets and outlets without appropriate lining of slopes in storm sewer network reduce the drainage capacity and cause the long-term pluvial flooding situation for BANGALORE. Due to the limitation of resources and proper waste management system. Rainwater washes away the wastes and creates gridlock situation in the inlets of surface drains

Disappearance of soak able green areas

Unplanned development and encroachment are making Bangalore a concrete ungle with very little green space and soil. As a consequence, rainwater remains on the surface and takes a long time to penetrate into the ground.

Figure 1. Topograhy

Due to the topographic condition, the rainwater cannot discharge to the lakes, canals, retention areas and surrounding rivers smoothly and remains stagnant in low lying areas. Moreover, people have a tendency to develop comparatively in higher ground through raising the ground level. This keeps the existing road networks in lower level which receive the rainwater from the surrounding areas.

Impacts of water logging

Impacts of water logging range from interruption of day-to-day life to the extent of severe damage to resources. The associated impacts of water logging on urban life are discussed below,

Disruption of Traffic-flow

Rapid urbanization causes unbearable traffic congestion In BANGALORE even in the dry season, the situation Becomes worst when it rains heavily. The victims of this phenomenon are not only the pedestrian users but also

Impairment of structures and infrastructure

Prolonged water logging and water infiltration decreases the longevity of the floor and walls, brick foundations! and substructures of the buildings in low lying areas: It also causes the problem of subsidence, dampness and other damage of infrastructure and impairs underground utility services such as water, gas, sewerage pipelines etc. Moreover, roads are damaged which lead to movement problem even after the water has subsided.

Contamination of water bodies and transmission of water borne diseases

Strom water is often contaminated by mixing with the wastes from hospitals, Industries and overflowing latrines as well as garbage in the streets and drams. This polluted storm water runoff contaminates ground water and the receiving water bodies like the canals, rivers and detention areas. This stagnant polluted water results in Inconvenience, odour, breeding sites for disease vectors, water borne diseases, skin diseases and sometimes disruption of blood transmission and therefore triggers health hazards and misery).

Damage to Flora and Fauna

Prolonged stagnant water and continuous release of wastewater causes harm to the habitat of flora and faunas Contaminated storm water imbalances the ecology of the habitat by polluting the soil and water bodies This causes depletion in the quantities of trees, aquatic plants and animals.

Rise of construction and maintenance cost

Water logging not only exerts the physical, social and environmental problem, but also become a massive economic burden. Damage of infrastructure such as road, service utilities not only hamper the regular life of citizen, but also demand an enormous or the replacement and maintenance of the damaged amenities: Owner of the households faces huge financial losses due to the damage of substructure. brick foundations, local house. During the water logging

Decrement of income potential

The deleterious effects of water logging include direct financial costs, loss of Income potential in various ways During the water logging disaster commercial activities nearly come to a standstill in BANGALORE. Shopping malls, restaurants even the banks have least customers and witness unusually low transaction. Poor people are the worst sufferers as Inundated roads directly disrupt livelihood of the poor people. The income of rickshaw puller, street vendors and daily labour greatly depends on the weather condition since people avoid moving in knee-deep water level without emergency.

III INCLUSION OF LANDSCAPE DESIGN AS A PROBLEM-SOLVING TOOL

Micro Scale Solution:

Since macro scale intervention is a long-term expensive process, urban designer can contribute greatly to micro scale solution These solutions are comparatively less expensive and can be implemented immediately.

Due to rapid urbanization and population growth, BANGALORE public space is diminishing gradually. Protecting these open spaces not only contributes to the physical and mental health of the citizen but also solves the water logging problem. These green spaces infiltrate the water into the ground. Parks, wet lands, open fields can serve as detention ponds if these are preserved and designed properly During the heavy rainfall a concave section of the green open field will retain water for a while which will alleviate burden on urban drainage.

These seasonal detention ponds during the monsoon can also serve as public space re-establishing the human-water relationship.

To solve the water logging problem, pipe should be continued underneath the footpath to the green parks. 100mm rainfall infiltration through green or infiltration wells that can greatly lessen the pressure on urban drainage

Banks of canal and lake have to be widened up to 2-3 meters with pedestrian path ways, greenbelts and tree plantation. Pedestrian walkways around the water bodies will help to protect them from encroachment and these have to be constructed with permeable material such as permeable surface bricks, tiles avoiding the present trend of using impermeable materials. Excavation of the canal and raising the bank of the water bodies are two main ways to protect the city from water logging. Two sides of the canals should have green and permeable surface, if the sides are made with hard surfaces eventually it becomes drain.

The approaches like rain water harvesting, roof gardening, water plazas, rain garden, grassed swales can be easily adopted in community or individual level to alleviate water logging problem. These approaches not only improve the water logging situation but also enhance the environmental quality. Ram water harvesting can contribute both ways: reduce the water in street and this harvested water can be used for household activities, car washing, and gardening. But ram water harvesting has to be planned properly- green roofs can exert a significant Impact in minimizing pluvial flood by retaining rainwater. Roof gardening concept is getting popular in recent days as it alleviates heat stress, ameliorates air quality, beautifies the city, and increases building's insulation.

Revival of canal networking

The chief of the Biodiversity Unit of the World Conservation Union (IUCN) indicates that, densely populated city like BANGALORE requires 25 per cent wetland for ecological balance and sustainability of habitats. But BANGALORE has less than 10 per cent wetland, which too is threatened.

Extending the connections between sewerage and drains with natural water bodies makes a drainage network. A canal rather than its retention activity, collects water from neighbour areas, evaporates and percolates water and is connected with the drainage system. Therefore, it is much needed to re-excavate the existing canals with proper design depth to increase its retention capacity and revitalize the missing connections for proper drainage network.

Development of Retention and Detention Areas

A wetland cannot be considered as a wasteland as it gives much more than money can buy. A wetland's hydrological function lies in serving as recharge source or discharge area of groundwater, flood storage and slowing drowning the erosion of water waves. The bigger the wetland is, the greater its water-logging storage capacity is. Therefore, water project management of wetland strengthens the urban drainage planning, by this bangalore can be protected from frequent flooding.

IV. CONCLUSION

Bangalore in the process of rapid urbanization, is facing a massive pressure on its land and the city is trying to meet the demand by Initiating encroachment of water bodies, unplanned development and the wetlands grabbing According to this study, these are the main reasons behind water logging disaster Hence for an effective permanent solution, government has to take strong stand against such Issues. Both micro and macro solution to water logging disaster require a comprehensive synchronization government authority. Beyond the traditional measures of flood control, urban drainage planning strategy should incorporate urban design tools like roof garden, park, rain water harvesting which will not only contribute to the solutions of water logging problem but also improve the physical and environmental quality of the city. Therefore, current research recommends the solutions which require less resources rather more public awareness and community participation and above all implementation of law.

V.REFERENCES

[1] "e-Governance in Bangalore Water Supply & Sewerage Board", India Governance Knowledge Centre , accessed 11 August 2007 Archived 2007-10-19 at the Wayback Machine. Note that other sources indicate 1964 as the year of the Board's formation. Literally everybody living in Bangalore wastes so much water

[2] "Cauvery water for new areas soon", *The Hindu*, 20 June 2007, accessed 11 August 2007

[3] "Bangalore team visits RWH structures in city", *The Hindu*, 3 August 2007, accessed 11 August 2007

[4] "It pours, but T G Halli reservoir remains dry", *Deccan Herald*, 27 June 2007, accessed 11 August 2007

[5] *"Government of Karnataka Notification No. FEE 215 ENV 2000". Archived from the original on 27 September 2007. Retrieved 12 August 2007*

[6] BWSSB Sewerage System overview

Study of strength characteristics of cladding material using cement as the base material and plastic from bio medical waste as replacement

***Abstract* – Cladding material is used to provide a degree of thermal insulation and weather resistance, and to improve the appearance of buildings. Bio medical plastic waste is incorporated with cement and quarry dust.**

Keywords- Biomedical plastic waste, quarry dust, sustainability, recycled plastic.

INTRODUCTION

Biomedical waste disposal into landfills and oceans has created serious issue in human and marine life. Recycling of biomedical waste generated from hospitals, labs, veterinary and other sectors have a great impact on reducing the risk of human health diseases, marine life and improved rate of sustainable development which promotes economy of the nation. In this report the importance of recycling, economic development rise and sustainability is discussed.
The importance of waste disposal management is a very important and major part of any health care institute. CPCB (Central Pollution Control Board) is one the major recycling organization in India since 22 September 1974. On world environment day 2021 it is shown that India produced 45,308 tones of Covid-19 bio-medical waste in from 2020 to 2021. According to CPCB, India is been generating nearly 146 tones of bio-medical waste everyday due to diagnostic waste and treatment of Covid-19 patients. This biomedical waste generation alone has increased 17% because of pandemic. There's always room for improvement to reduce our environmental impact, one such is RECYCLING OF BIO MEDICAL WASTE IN INDIA. Recycling is a traditional form of modern waste reduction. The future of our country relies on innovative solution. Often the materials used on construction sites are a mixture of raw materials and a level of recycled materials. Improvement in wellbeing of the nation, meeting all the economic crisis, providing basic needs to all humans in the country is always a responsibility of any project.

The replacement of natural fine aggregate by using quarry dust leads to consumption of generated quarry dust, the requirement of land fill area can be reduced and solves the natural sand scarcity problem. The sand availability as a fine aggregate at low cost which needs the reason to search as a alternative material. Even it causes saddle to dump the crusher dust at one place which causes environmental pollution. The chemical analysis, specific gravity, sieve analysis and compressive strength is identified for various percentage and grades of concrete by replacement of sand with quarry dust.

Real-time problem faced is high disposal of plastic in Bengaluru, especially during the pandemic 2020-2021. In this study we will be doing cladding material facade using cement as base material and plastic obtained from biomedical waste as replacement with other additives to improve texture and aesthetic view. Conducting physical characteristic tests like compression test, flexural strength, tension test and others to meet the requirements. The other objective of the study is to improve the ease of installation, low maintenance, warranty, fire resistant and increase the percentage of recyclability of the same material.
The cladding material is eco-friendly and provides an aesthetic view.
Achieving required strength using bio-medical waste as a replacement to coarse aggregate.

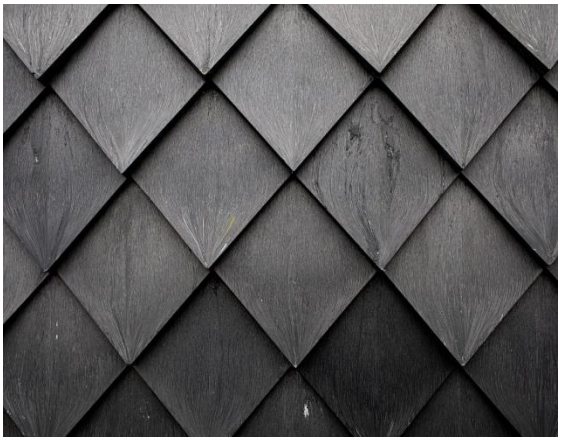

Fig1. Cladding material sample design(wall façade)

METHODOLOGY

Procurement of materials

Materials of the cladding materials were collected from the available areas and shops.

Fig 2. Materials used.

Batching of materials

Measurements of materials for making cladding material is called batching. After collection of material unwanted waste was removed from the collected material and plastic was segregated according to the sizes required for the material.

Mixing

Mixing of material is essential for attaining uniform strength of material. The mixing has to be ensured that the mass becomes homogenous, uniform in color and consistency. Generally there are two type of mixing hand mixing and mechanical. in this project we adopt hand mixing.

Moulding

After completion of proper mixing we place mix into required mould. In this project we used brick size (7cm*7cm*7cm)

.

COMPOSITION OF MOULD

The normal consistency of cement is 30%.
The cement and quarry dust ratio in 1:3.
Plastic percentage varying in 8%, 10%, 12%.
The mix design is done as per the IS code book.

Sl no	Weight of motar cube(gm)	Cement (gm)	Quarry dust (gm)	Plastic (gm)
1	600	150	450	-
2	600	138	414	48
3	600	135	405	60
4	600	132	396	72

RESULT

Sl no	Composition of mould	No. of days	Compression strength in N/mm²
1	Cement+ Quarry dust	7	17.55
2		14	20.86
3		21	23.98
4	Cement+ quarry dust+ plastic (8%)	7	16.56
5		14	19.94
6		21	20.56
7	10%	7	20.00
8		14	18.96
9		21	17.23
10	12%	7	16.21
11		14	15.2
12		21	13.85

CONCLUSION

From the obtained result it is found that mortar cube with composition of quarry dust and cement mould has a increased amount of compression strength to the mortar cubes replaced with reusable PPE plastic in varying proposition of 8%, 10%, 12%.

Though strength of motar cube obtained from varying percentage of 8%, 10%, 12% is less but can be reffered to places like interior and exterior wall facade (cladding material), architectural indoor and outdoor articraft.

The mortar cube using plastic is sustainable and economic.

ACKNOWLEDGMENT

We would like to express our sincere gratitude to the Management, Principal of Sapthagiri College of Engineering, Bengaluru for the facilities provided and their support. Also, we would like to thank the Head of the Department of civil Engineering and faculties for their encouragement and support.

REFERENCES

[1]. Pretty plastic -Hester van Dijk,
[2]. Nuance studio – Srinivas Kumar, Banglore.
[3]. Karthikeyan Muniraj – utilisation of waste plastic in concrete. April 2019
[4]. A.O. Awoyera – case study of plastic waste to construction products, volume 12, June 2020.
[5]. Hegger – exterior cladding panels as an application of textile reinforced concrete, volume 224- page 55to 70, January 2004.
[6]. K Shyam Prasad – strength characteristic of quarry dust in replacement of sand 2017.
[7]. Uma Devi R – Effective utilization of biomedical waste in construction industry, vol 8 issue 3 march 2019.
[8]. Ibrahim Almeshal – Eco friendly concrete containing recycled plastic as partial replacement for sand, 2022.
[9]. Mohan T harish – sustainable approach for the utilisation of PPE biomedical waste in construction center, 2021.
[10]. Baboo Rai – Study of waste plastic mix concret with plasticizer, 2012.

RETROFITTING OF COLUMN BY RC JACKETING

YASHWANTH T P, AKSHATH GOWDA N K, ABHISHEK R, DHRUVA KUMAR DL ,PRAMOD K R

Department of civil engineering, SAPTHAGIRI COLLEGE OF ENGINEERING
#14/5 chikkasandra, Hesaraghatta main road, Bengaluru-560057 INDIA
yashuyashwanth172@gmail.com
akku3111@gmail.com
dhruva0013@outlook.com
abhishek.rgowda4545@gmail.com
pramodkr@sapthagiri.edu.in

Abstract-

Abstract External confinement using jackets can definitely growth the electricity and ductility of the reinforced concrete rectangular columns. This paper encompasses an experimental investigation for reading the effectiveness and suitability of concrete mixes as a retrofitting material and its use as jacket for square columns. The experimental programme included improvement of concrete blend and its use in retrofitting of square column specimens which have been both intact or distressed in advance to sure level. The experimental programme consisted of testing 8 control specimens, repairing, and retrofitting prior to trying out. The manage specimens had been of diameter one hundred fifty mm and top three hundred mm, forged in M30 conventionally vibrated concrete, reinforced longitudinally with 4 bars of eight mm diameter and five lateral ties of four mm diameter as transverse reinforcement. Two exclusive concrete mixes, had been used for jacketing across the columns. The jacket was bolstered with slight metal welded wire mesh (WWM) 50 mm × 50 mm manufactured from 3 mm diameter cord. The retrofitted specimens have been tested after 7 days, 28 days of curing. The take a look at consequences revealed the effective use of in part changed concrete as retrofitting cloth. The concrete jacket with WWM as reinforcement will increase the closing load wearing ability of column specimen. The ductility component is likewise calculated after the retrofitting with concrete mixes.

INTRODUCTION: -

The energy of constructing reduces, it may reduce by using overloading, herbal disaster (earthquake/floods), hearth environmental consequences. This leads the structure to fail. Failure of the maximum vital shape elements results in the whole fall apart of the body structure. During our survey at the failures leading to retrofitting of the member, it was noticed that the failure of compression member (column), because of the preferred compressive power of concrete was now not executed. Hence, selected the retrofitting of the column with via the RC Jacketing and have made

In case of RC columns partially or totally damaged a want for repair method to repair the unique column potential (with none increase in original power) is strongly wished. This technique includes the addition of a layer of bolstered concrete within the form of the jacket the use of longitudinal steel reinforcement and transverse steel ties outside the perimeter of current member. The thickness of jacket usually exceeds 10cm a good way to permit the casting of the concrete

MATERIALS AND METHODS: -

The columns were retrofitted by means of 7- wire strands, which were placed at every 150mm, starting at 75mm from the column base Hollow steel sections (HSS 31.8x31.8x6.35mm) were placed on each face with three semi-circular disks welded on them, forming a frame around the column at each strand location. The height and location of semi-circular raiser disks were 6calculated to make transverse forces as equally distributed as practically possible. The anchor was placed on one of the steel hallow sections, replacing one of the semi-circular disks, while enabling the prestressing of strands.

The materials used here in this project are, Portland cement, M-sand, 20mm course aggregate, GGBS, fly-ash, zeolite.

The first pair of columns were prepared with M30 grade concrete mix design. The remaining 3 pairs of columns were casted by replacing cement by GGBS, fly-ash, zeolite in 5% and 10% in content.

The experimental work herein aims to research the bonding some of the column cores and their

jacketing and the remaining load-carrying potential and axial displacement of uniaxial loaded square RC columns repaired and strengthened the usage of two jacketing types with 3 techniques of floor roughening. The acquired effects are as compared with the ones of the reference columns.

The procedure includes testing the column's compressive strength prepared with concrete were the cement is partially replaced with GGBS, Fly-ash and zeolite. The project also aims to prove that the column made of concrete, where the cement is partially replaced with GGBS, Fly-ash and zeolite have same strength has the concrete made of cement without replacement of other materials.

PARTICULARS	EXPERIMENTAL RESULTS	IS LIMITS (IS:8112-1989)
Specific gravity	3.14	-
Initial setting	115	Not less than 30 min
Final setting	205	Not more than 600 min

METHODOLOGY:

1. Material testing
2. Mix design
3. Compressive strength of original column and jacketed column
4. TESTS ON AGGREGATES:
    - Crushing Test- to determine crushing strength.
    - Los Angeles Abrasion Test- to determine hardness.
    - Impact Test- to determine toughness.
    - Specific gravity Test.
5. TESTS ON CEMENT:
    - Fineness Test of cement.
    - Setting Test of cement.
    - Soundness Test of cement.
    - Specific Gravity Test of cement.
6. TESTS ON ZEOLITE:
    - X -RAY Diffraction test.

Constituent Material:

Concrete: -

Concrete is specially a mixer of materials composed of water combination and cement. Aggregates, Fine and Coarse mixed occupy about 70% voids in a special mass of concrete and residual 30% voids are occupied through water, cement and air voids. To acquire the preferred physical homes of completed materials, generally supplementary cementitious substances are brought in a concrete aggregate.

Cement: -

Ordinary Portland cement (OPC) is the most favoured binder in the production of concrete due to its properly adhesive and cohesive houses that facilitate it's bonding with other materials. Locally acquired Ordinary Portland cement of 53 grade of the ACC cement Branch conforming to ISI standards is used and fashionable exams have been performed in line with IS:8112-1989. The bodily and chemical elements of cement are given in Table 2.

Ground Granulated Blast Furnace Slag: -

GGBS is accumulated from Steel Mill Karachi. Blast furnace slag is a by-product left as a residual product after the burning of coke, limestone and ore of iron in an aggregate at 1500 C. Molten iron and molten slag are received after heating the mix. The low-density molten slag comes up on the surface and without difficulty separated from rest of the mass. Afterwards its miles cooled down through the action of water. The water stress during the cooling method breaks down the slag right into a length less than five millimetres. Blast furnace slag powder is then received via grinding the

dried slag mass. The chemical and physical houses of BBFS are proven in Table 2.

GGBS is derived from pig iron production technique. When the molten slag cools, its adjustments right into a satisfactory, granular, nearly fully non-crystalline, glassy form referred to as granulated slag. It has latent hydraulic houses. The finely ground slag, when combined with Portland cement (PC), offers excellent binding houses. It has same chemical houses as that of cement, however it's far much less reactive than Portland cement (PC). It hydrates on including water just like the Portland cement and primarily in aggregate with Portland cement, normally within the range 60 to forty percentage GGBS, depending at the utility. The blends can both be manufacturing facility made or formed in the mixer by means of including Portland cement and GGBS each from its very own silo. Concrete containing GGBS/PC blend may be gradual in reacting than natural PC concrete, however it has progressed sturdiness. The chemical and physical homes of BBFS are proven in Table 2

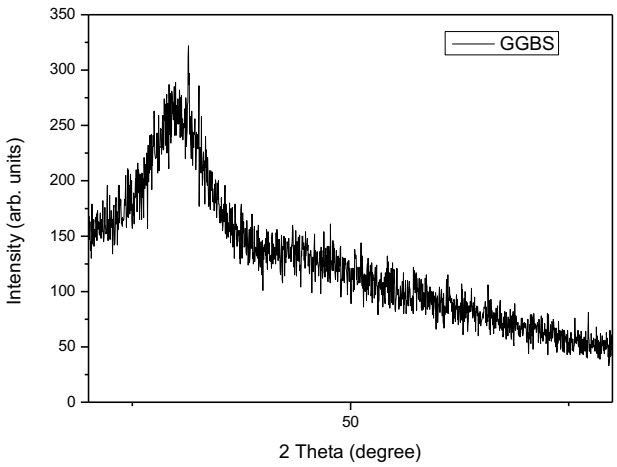

Table 2. Physical and Chemical Properties of GGBS and Fly Ash

Properties	Cement	GGBS	Fly Ash
Specific gravity	3.16	2.78	2.41
$SO2$	20.1	34.9	63.4
$Al2O3$	4.12	9.12	11.21
$fe2O3$	3.5	2.59	5.22
CaO	62.4	44.2	14.72
MgO	2.42	4.53	1.82
$SO3$	3.21	2.36	0.38
$Na2O$	_	0.62	0.41
$K2O$	_	0.25	0.1
LOI	1.81	1.33	2.22

Fly ash: -

Fly Ash is the alternative choice. Locally to be had (Jamshoro, Pakistan) Class F Fly Ash became used. It was accumulated from Lakhra Power House, Jamshoro. It is acquired from coal strength flora [19]. It creates critical environmental, disposal and health troubles. Its grains are round in form and are used in aggregate with ordinary cement to enhance the concrete workability. Also, it increases durability and power of hardened concrete. The chemical and bodily houses of Fly Ash are proven in Table 2.

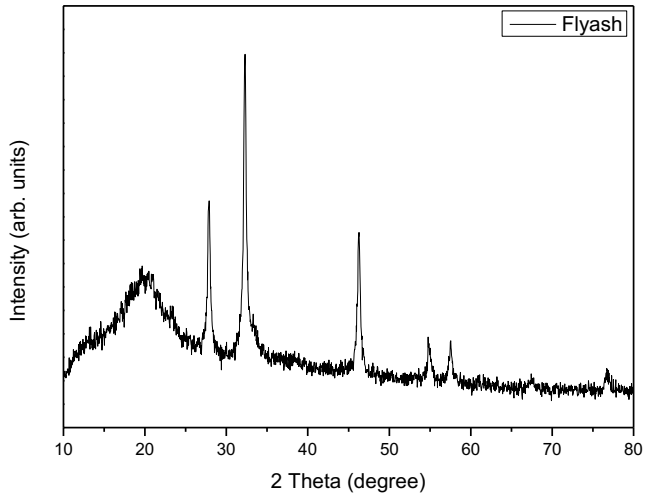

Locally to be had river sand that is loose from organic impurities is used and conformed to

Fine and Coarse Aggregates: -

grading zone 2 as according to IS: 2386 (Part-I – 1963). Sand passing via sieve is 4. Seventy-five

mm and maintaining on IS sieve no. A hundred and fifty μ is used on this look at. Sieves are very well wiped clean earlier than use.

The coarse combination used within the experiments have most length of 20 mm. IS 383:1970 turned into used to discover the percentage mix of coarse aggregate, with 60% 10 mm size and 40% 20 mm. The bodily residences are proven in Table 3.

Table 3. Physical properties of Fine aggregate and Coarse aggregate

Properties	Fine aggregate	Coarse aggregate
Specific gravity	2.68	2.792
Water absorption	2.1%	1%
Free surface moisture	2.3%	Nil

Water: -

Higher water content imparts higher workability to the concrete mix. When water is added to the concrete, hydration response takes place, and hardening of the paste begins, in the end. Water should have a pH price inside the variety 6-8. Water must no longer contain salt in it if used for strengthened concrete, because it can reason the reinforcement metallic material to corrode.

Zeolite: - -

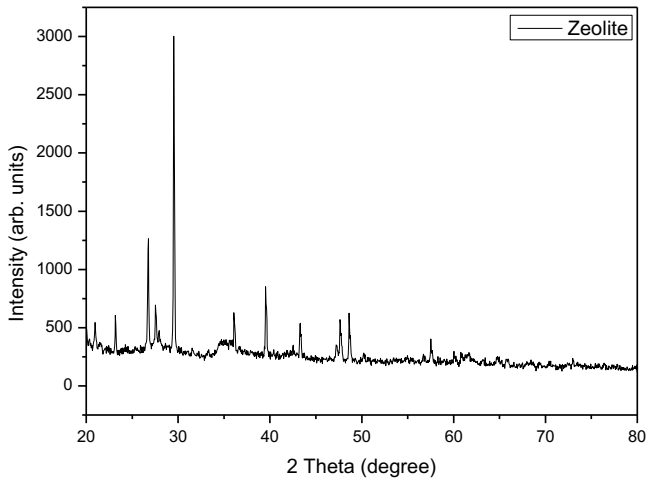

Determination of Load Carrying Capacity: -

A RC column of 300mm length having a move phase of a hundred and fifty×150 mm with 1% place of reinforcement has been designed and its load sporting capability has been calculated as in line with the limit country technique. The strength of the column is decided from the following equation with admire to IS 456:2000 phase 39.Three:

$$P = 0.\text{Four} \times fck \times Ac + 0.\ 67 \times fy \times Asc \quad (1)$$

Where; fck: Characteristics compressive power of the concrete (20 MPa); fy: Characteristic energy of compressive reinforcement (415 MPa); Ag: Gross region of the column (22500mm2); Asc: Area of longitudinal reinforcement required for the column (1% of Ag = 900 mm2); Ac : Area of concrete ($Ag - Asc$= 21600 mm2); Reinforcement furnished = 4 - 8Φ, i.E..

P = 0.Four×20×21600+ 0.Sixty seven×415×900 = 423.Half KN Using a element of protection as 1.5, the closing load carrying ability (Pu) could be:

Pu = 1.5 × 423.1/2 = 634.56KN.

Design of the Jacket: -

The design for the jacketing of the columns is primarily based at the provisions and specifications made in IS 15988:2013. The minimal specifications required for jacketing a column are: 1. Strength of the brand-new materials that shall be used should be as a minimum equal to or greater than those of the existing Column. The energy of latest concrete shall be extra than that of the present concrete by using as a minimum 5 MPa.

2. For columns in which no additional longitudinal reinforcement is required, at least 12 Φ bars have to be furnished on the 4 corners with 8Φ ties @ a hundred c/c spacing.

3. Minimum jacket thickness that shall be supplied is one hundred mm.

4. Minimum diameter of ties that shall be supplied is eight mm and no longer less than one-third of the longitudinal bar diameter.

5. The spacing of vertical ties must no longer exceed 100 mm. If viable, the spacing of ties shall not be greater than the thickness of the jacket or 2 hundred mm whichever is much less. The design for the jacketing of the columns is primarily based at the provisions and specs made in IS 15988:2013. $Ac = Ag - Asc$ (2) But $Asc = 0.01Ag$; Therefore, $Ac = 0.99Ag$ So: 1354.Fifty six × one thousand = $0.41 \times 25 \times$ zero.$89Ag + 0.57 \times 415 \times 0.01\ Ag \rightarrow Ag$ = 117920 mm2 Since the cross phase is a rectangular, consequently: B = D =√117920 mm2 = 328 mm; so, allow B = D = 350 mm. Therefore, thickness of the jacket = (350−300)/2 = 25 mm. But According to IS: 15988-2013, Minimum thickness of the jacket ought to be 100 mm; i.e. B = D = 500 mm. Agj = (500 × 500) – (a hundred and fifty × a hundred and fifty) = 160000 mm2 $Ascj$ = zero.$01Agj$ =1600 mm2.

But as in step with IS 15988, clause eight.5.1.1 (e); $Ascj$= (4/3) × $Ascj$ received (3) =1.33×1600 = 2128 mm2 . So, offering 16- 14Φ bar for the main reinforcements (Figure 2). Asc Provided = 2463 mm2 > 2128 mm2 . (Pu) Jacket = 0. Four × 25 × 157537 + zero.Sixty seven × 415 × 2463 = 2360.20 KN Therefore; (Pu) Jacketed column = Pu + (Pu) Jacket = 1544.Fifty six KN+ 2360.20 KN = 3764.Seventy six KN. Hence, percentage boom in load sporting potential is = ((Pu) Jacketed−Pu)/Pu×a hundred = 84.46%.

Load carrying capacity	Initial column	Jacketed column	Percentage increase in strength
As per design(KN)	634.56	1171.65	84.46
As per Simulation (KN)	936.4	1600.56	92.3

Results and Discussion: -

The statistics and results of this observe is provided in tabular shape. The values of final load ability were acquired from the simulation plots.

Table 4. Percentage increase in energy after jacketing Load Carrying Capacity

Table 4

Jacketed column Percentage boom in power As according to Design (KN) 634.5 1171.65 804.

46% As in line with Simulation (KN) 936.1 1600.56 92.3%

From the above outcomes it can be talked about that the proportion boom in axial load carrying potential as in step with layout is greater than that received after simulation. The primary cause for this distinction is the impact of bonding among the vintage current concrete surface and the new jacket floor. For the layout technique the burden sporting capacity of the preliminary column and the jacket portion had been calculated one by one and they had been summed up assuming a really perfect bond among the antique and new surfaces. While at some stage in the simulation floor to floor bond between vintage and new concrete became mounted the use of TIE constraint. Since the evaluation is based on the assumption of a a hundred percent bond at the interface, the best bond among the jacket and the column turned into simulated by means of merging the nodes of existing column with the nodes of the jacket at the interface.

Conclusion: -

Strengthening of column on this look at changed into an try to growth the burden carrying capacity of it in an current building that wishes to be retrofitted to fulfil the desired purpose. The energy of the column member subjected to concentrically axial compressive load will increase considerably after RC jacketing. As in step with effects noted in Table, the boom inside the load sporting potential of the jacketed column as according to layout is eighty four.46% while it is ninety two.3% as in step with simulation performed in ABAQUS. From the test performed inside the past, the growth in load wearing capacity was determined to be around a hundred and ten% under uniaxial load [14] for 50 mm jacket thickness. So the distinction and huge boom within the load carrying capability for the existing examine can be attributed to using thick jackets around the four sides that is 100mm as well as the TIE constraint used within the modelling which imparts best floor to floor bond between the existing concrete and the jacket.

REFRENCES:

1.“Design and Detailing of RC Jacketing for Concrete Columns”

Nikita Gupta1, Poonam Dhiman2, Anil Dhiman3 1,2, three(Department of Civil Engineering,

Jaypee University of Information Technology, Himachal Pradesh, India)

IOSR Journal of Mechanical and Civil Engineering (IOSR-JMCE) e-ISSN: 2278-1684, p-

ISSN: 2320-334X. PP 54-58

2.“RC columns externally bolstered with RC jackets”

G. Campione • M. Fossette • C. Giacchino • G. Minafo

Materials and Structures (2014) forty-seven:1715–1728 DOI 10.1617/s11527-013-0146-x

Received: 2 October 2012 / Accepted: 9 July 2013 / Published online: 19 July 2013 RILEM 2013

3.“Experimental examine of the effectiveness of retrofitting RC columns using concrete jackets”

R. Dubey, Pardeep Kumar

Published 15 October 2016

Materials Science

Construction and Building Materials

DOI: 10.1016/J.CONBUILDMAT.2016.07.079

Corpus ID: 138705970

4.“Effect of Reinforced Concrete Jacketing on Axial Load
Capacity of Reinforced Concrete Column”

Praveen Anand, Ajay Kumar Sinha
a Research Scholar, Department of Civil Engineering, National Institute of Technology, Bihar,
Patna, 800005, India. B Professor, Department of Civil Engineering, National Institute of Technology, Bihar, Patna, 800005, India.
Received 28 February 2020; Accepted 29 May 2020
Kaliyaperumal, Gnanasekaran, and Amlan Kumar Sengupta.

Comparative Study on Fiber Reinforced Concrete Using Fly Ash and Granulated Blast Furnace Slag as Partial Replacement of Cement and Sand

[1]Vanishree S, [2]Chandana C, [3]Gopal Kumar P, [4]Keerthana B , [5]MD Nasrullah Faiz
1.Assistant Professor, Dept of Civil Engineering, SCE, Bangalore, Karnataka
2,3,4,5 Student, Dept of Civil Engineering, SCE, Bangalore, Karnataka
vanishree_s@sapthagiri.edu.in, chandanacnaik@gmail.com, gopalkrishnabaaghi@gmail.com, keerthanagowda5555@gmail.com, nasrullahfaiz0@gmail.com,

Abstract
Considerable efforts are being made in every part of the world to develop new construction materials. In the construction industry, concrete technology is heading towards entirely new era by the use of Fly Ash, GBFS and Fibers like Steel Fibers in concrete. While conventional concrete has poor tensile strength, low resistant to tensile cracking, so its capacity to absorb energy is limited. The weakness in tension is conventionally overcome by strengthening their matrix with steel and more recently by reinforcing with fibrous materials. Concrete when mixed with fibers, give fibrous concrete. The mechanical property of fibrous concrete is superior to that of ordinary concrete. Fly Ash and GBFS will be evaluated for use as supplementary cementitious material in cement and sand based system, the performance of Fly Ash and GBFS mixtures will be compared to controlled mixtures and mixtures incorporating Fly Ash and GBFS as partial replacement for cement and sand.

1. INTRODUCTION

Concrete is a composite material containing hydraulic cement, water, coarse aggregate and fine aggregate. The resulting material is a stone like structure which is formed by the chemical reaction of the cement and water. This stone like material is a brittle material which is strong in compression but very weak in tension. This weakness in the concrete makes it to crack under small loads, at the tensile end. These cracks gradually propagate to the compression end of the member and finally, the member breaks. So to increase the tensile strength of concrete a technique of introduction of fibers in concrete is being used. These fibers act as crack arrestors and prevent the propagation of the cracks. Portland cement is the most important constituent of concrete. Unfortunately one ton of CO_2 is released into the atmosphere during the production of 1 ton of cement.

Thus partial replacement of Portland cement by mineral by products such as fly ash (FA) can significantly reduce CO2 emission. Fly ash is used in concrete to achieve energy conservation and economic, ecological and technical benefits. It is used as pozzolanic mineral admixture in concrete. Fly ash is usually found to improve workability and contribute to strength development and hence considered to be an effective cementitious component of concrete. In India, natural river sand (fine aggregate) is traditionally used in concrete. The growing environmental restrictions to the exploitation of sand from the river beds has brought in severe strains on the availability of sand forcing the construction industry to look for an alternative construction material. Thus granulated blast furnace slag (GBFS) appear as an attractive alternative to natural fine aggregates for concrete. GBFS is totally different from natural river sand. It has been found that concrete made with GBFS achieved compressive strength equal to or higher than concrete made with natural sand, reducing the void content of the aggregates, there by lubricating the aggregate system without increasing the water requirement of the mixture. Most of the previous investigators were mainly engaged in replacing FA and GBFS with ordinary Portland cement. This research is an attempt on fiber reinforced concrete with FA and GBFS as partial replacement of cement and natural sand for various percentages 10, 20, 30 and 40 with a constant w/c ratio of 0.35.

LITERATURE REVIEW

Mohammed Maslehuddin et. al., [1]: This research has Specific Significance to the Corrosion-resisting characteristics of concrete mixtures in which fly ash are used as an admixture. The date developed in this investigation indicates that concrete sample with fly ash as an admixture exhibit higher compressive strength gain and corrosion resistance compared to plain concrete. The compressive strength of 20% and 30% cement replaced fly ash concrete samples was higher than the plain concrete samples at all ages tested. The strength differential between the fly ash concrete samples and plain concrete samples became more distinct after about 28 days of curing. The fly ash concrete samples follow the water-cement ratio law, indicating that the strength contribution attributed to the fly ash increased as the water cement ratio was decreased.

Vasudev R and Dr. B G Vishnu ram. [2]: This paper aims to have a comparative study between ordinary reinforced concrete and steel fiber reinforced concrete. The fibers which were used in the study were the hooked end steel fibers. The Experimental investigations and analysis of results were conducted to study the compressive & tensile behavior of composite concrete with varying percentage of such fibers added to it. The concrete mix adopted were M20

and M30 with varying percentage of fibers ranging from 0, 0.25, 0.5, 0.75 & 1%. On the analysis of test results the concrete with hooked end steel fibers had improved performance as compared to the concrete with conventional steel fibers.

Alhozaimy A.M et. al., [3]: This study carried out experimental investigations on the effects of adding low volume fractions (<0.3%) of calculated fibrillated polypropylene fibers in concrete on compressive and impact strength with different binder compositions They observed that polypropylene fibers have no significant effect on compressive strength, while flexural toughness and impact resistance showed increased values. They also observed that positive interactions were also detected between fibers and pozzolans.

L. Zeghichi et. al., [4]: Experimented on substitution of sand by GBF crystallized slag. Tests carried out on cubes of concrete showed the effect of the substituting part of sand by granulated slag (30% & 50%) and the total substitution on the development of compressive strength. Compressive strength test results at 3, 7, 28, 60 days and 5 months of hardening concluded that the total substitution of natural coarse aggregate with crystallized slag affects positively on split tensile, flexural and compressive strength of concrete. The partial substitution of natural aggregate with slag aggregates permits a gain of strength at long term but entire substitution of natural aggregates affects negatively the strength (a loss in strength of 38%).

M.S. Rao et. al., [5]: This paper highlights a case study of Granulated Blast Furnace Slag (GBFS/GBS) sand application as a partial substitute of Crushed Stone Sand (CSS) in cement concrete. Laboratory Studies were conducted for different grades of concrete viz. M30 to M70 using blend of crushed stone sand and granulated slag sand in the ratio of 50:50 of total fine aggregate in concrete. From this study it is observed that GBS sand and CSS blend could be used as alternative construction material for natural sand in cement concrete applications.

OBJECTIVES

The objectives of this research project are:

1. The objective of the present investigation is to find the optimum mix design for M30 grade concrete with regards to the amount of material constituents.
2. To study the workability of concrete for various replacement level of FA and GBFS.
3. To investigate the strength characteristics such as compressive strength, split tensile strength and flexural strength for concrete mixes of grade M30 by replacing FA and GBFS as a partial replacement of cement and sand respectively with addition of 0.5% steel fibers
4. Compare the strength properties of steel fiber reinforced concrete with various percentage replacement levels of FA and GBFS with conventional concrete.
5. Compare the durability properties of steel fiber reinforced concrete with various percentage replacement levels of fly ash and GBFS with conventional concrete.
6. To determine the usage level of industrial wastes such as fly ash and GBFS.

METHODOLOGY

The aim is to determine the characteristics of constituent materials and strength of concrete produced by replacing cement by FA and natural sand by GBFS with the addition of steel e fibers. Several experimental works are carried out. Thus work study is laboratory oriented.

1 The materials such as fly ash, GBFS, fine aggregate, coarse aggregate, super plasticizer, M30 grade concrete and required slump are chosen.
2. The materials have been collected from a specific location and properties have been studied.
3. Using these properties, mix design is carried out with suitable w/c ratio of M30 grade concrete.
4. Required slump is obtained experimentally by slump cone test.
5. Concrete cubes were casted to study the compressive strength of concrete. Then the cubes were tested in compression testing machine.
6. The compressive strength of the concrete will be determined by using 150mmconcrete cubes specimens. The specimens will be tested at 7 and 28 days age, in200tons capacity hydraulic type compression-testing machine. The cube compressive strength will be obtained by considering the average of three specimens at each age.
7. Cylinders of size 150mm by 300mm cylinders were casted to study the split tensile strength of concrete. The specimens were tested at 7 and 28 days age, in 200tons capacity hydraulic type compression-testing machine. The tensile strength will be obtained by considering the average of three specimens at each age.
8. Beams (150mm×150mm×700mm) were casted to study the flexural strength of concrete.
9. Then the beams were tested in single point loading and deflections under the load points will be recorded.
10. All the beams will be tested in a universal testing machine of 1000kN capacity at a constant rate of displacement.
11. The density of FA and GBFS concrete will be observed and compared.
12. Using these test results suitable graphs is plotted.
13. Conclusions are drawn based on test results.

CHARACTERIZATION OF CONSTITUENT MATERIALS

Ordinary Portland Cement

The cement used in this experimental investigation is Birla Super 53 Grade OPC conforming to IS: 12269-1987.

Table 1 Physical properties of cement

Properties	Obtained Values	Requirements as per IS: 12269-1987
Fineness	4.8%	Not more than 10%
Soundness	1mm	Not more than 10 mm
Initial setting Time	48min	Not less than 30 min
Final setting Time	240min	Not more than 600min
Standard	33%	-

Consistency		
Specific Gravity	3.14	-

Fine Aggregate

The material have used as fine aggregate in this project is locally available clean river sand passing IS Sieve No.480 (4.75mm) have been used with water absorption of 1.5%. The results of sieve analysis conducted concluded is tabulated in Table 4.3 and it confirms to Zone II as per the specifications of IS: 383-1970 (Reaffirmed 2007).

Coarse Aggregate

The material whose particles are of size as are retained on I.S Sieve No.480 (4.75mm) is termed as coarse aggregate. The size of coarse aggregate depends upon the nature of work. The coarse aggregate used in this experimental investigation are of 20mm, 12mm sizes, crushed angular in shape having water absorption of 0.5%. The aggregates are free from dust before used in the concrete. The sieve analysis of combined aggregates confirms to the specifications of IS: 383-1970 (Reaffirmed 2007) for graded aggregates.

Water

Water is an important ingredient of concrete as it actively participates in the chemical reaction with cement.

Fly Ash

Fly ash is an industrial by-product, generated from the combustion of coal in the thermal power plants. The size of fly ash particle is largely dependent on the type of dust collection equipment.

GBFS

The physical and chemical properties of GBFS are verified .It contains more calcium oxide (CaO) compared to fly ash. Since it contains aluminum oxide and silica oxide. Specific gravity of GBFS 2.785 is used for this investigation work

Table 2Physical properties of GBFS

Properties	Results
Color	Light gray
Form	Granular
Plasticity	Non plastic
Specific gravity	2.88

Chemical Admixture

Super plasticizer GLENIUM 8233 of M/s. BASF Construction Chemicals (I) Pvt. Ltd, confirming to IS: 9103: 1999 has been used.

EXPERIMENTAL INVESTIGATIONS

Workability Test

Slump Test: Slump test is the most commonly used method for measuring consistency of concrete which can be employed either in laboratory or at site of work. It is not a suitable method for very wet or very dry concrete. It is used conveniently as a control test and gives an indication of the uniformity of concrete from batch to batch.

Table.3 Workability Test Results of M30 Grade Concrete

Mix Proportions	Slump Values Using 0.5% SF (mm)
CC	100
FRC 10%	100.80
FRC 20%	99.80
FRC 30%	98.71
FRC 40%	97.61

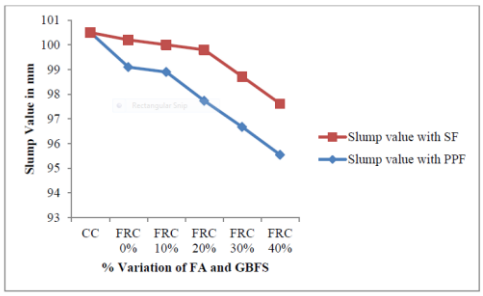

Split Tensile Test

FRC cylinders of size 150mm (dia) x 300mm (height) casted and test results are compared with that of conventional concrete.

Where,

P is the compressive load on the cylinder

l is the length of the cylinder

d is diameter of the cylinder.

Table 4 Split Tensile Strength of M30 SFRC for 7 Days in N/mm²

SL. No.	%Variation of FA and GBFS with 0.5% SF	Split Tensile Strength for 7 Days (N/mm)
1	CC	2.09
2	10% FA & 10% GBFS	2.64
3	20% FA & 20% GBFS	2.33
4	30% FA & 30% GBFS	1.93
5	40% FA & 40% GBFS	1.40

Table 5 Split Tensile Strength of M30 SFRC for 28 Days in N/mm²

SL. No.	%Variation of FA and GBFS with 0.5% SF	Split Tensile Strength for 28 Days (N/mm²)
1	CC	3.43
2	10% FA& 10% GBFS	3.63
3	20% FA & 20% GBFS	3.34
4	30% FA & 30% GBFS	3.00

5	40% FA & 40% GBFS	2.60

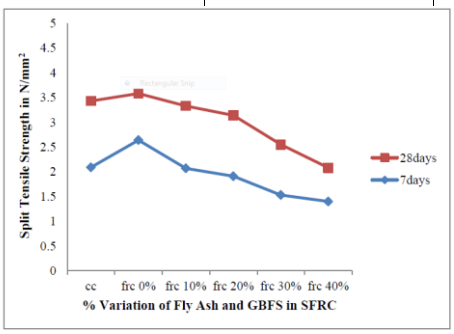

Cube Compression Test

This test was conducted as per IS 516-1959. The cubes of standard size 150x150x150mm were used to find the compressive strength of concrete. Specimens were placed on the bearing surface of CTM, of capacity 200tones without eccentricity and a uniform rate of loading of 140kg/sqcm per minute was applied till the failure of the cube. The maximum load was noted and the compressive strength was calculated for normal concrete mix and fiber reinforced concrete mixes with FA and GBFS at 7 and 28 days. The results are tabulated in Table 6 and 7 and has been graphically represented in figures

Cube compressive strength (fc) in N/mm2 = P/A
Where,
P= Cube Compression Load in kN
A= Area of the Cube on Which Load is Applied (150 x 150 = 22500 mm2)

Table 6Compressive Strength of M30 SFRC for 7 Days in N/mm²

Sl. No.	% Variation of FA and GBFS with 0.5% SF	Compressive Strength for 7 Days (N/mm²)
1	CC	25.14
2	10% FA & 10% GBFS	25.92
3	20% FA & 20% GBFS	24.84
4	30% FA & 30% GBFS	23.20
5	40% FA & 40% GBFS	20.22

Table 7 Compressive Strength of M30 SFRC for 28 Days in N/mm²

Sl. No	% Variation of FA and GBFS with 0.5% SF	Compressive Strength for 28 Days (N/mm²)
1	CC	42.04
2	10% FA & 10% GBFS	43.00
3	20% FA & 20% GBFS	41.15
4	30% FA & 30% GBFS	38.62

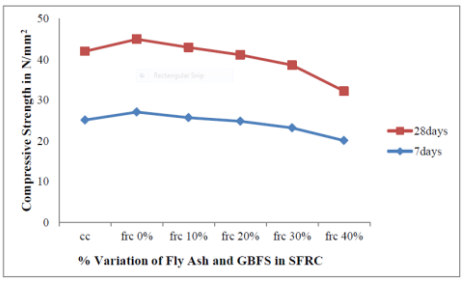

Flexural Strength

The test results of flexural strength of design mix M30 on standard 150x150x700 mm beams (with and without reinforcement) at 28 days age obtained are tabulated and the results are graphically represented for fly ash and GBFS concrete with addition of steel and polypropylene fibers.

Table 8 Flexural strength of M30 FRC without reinforcement for 28 days in N/mm2

% Replacement of FA & GBFS	Addition of fibers in (%)	Flexural Strength (N/mm²)
CC	0.5% steel fiber	5.40
10% FRC	0.5% steel fiber	5.52
30% FRC	0.5% steel fiber	4.86
40% FRC	0.5% steel fiber	4.21

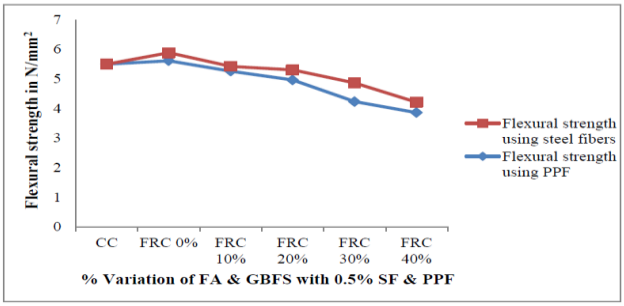

Conclusion

Based on the results of the investigation conducted on fly ash and GBFS based concrete made with various levels of cement and sand replacement and cured for various curing periods 7 and 28 days, the following conclusions can be drawn:

1. The fiber reinforced concrete mix with addition of mineral admixtures has shown considerable improvement in all the properties of concrete when compared to conventional concrete.
2. The workability of fiber reinforced concrete has been slightly reduced with increase in the percentage of FA and GBFS.
3. Fly ash and GBFS based steel fiber reinforced concrete mix having various cement and sand replacement level upto 30% exhibited satisfactory results for both compressive and split tensile strength.

4. The optimum FA and GBFS content is observed to be 30% of cement and sand.
5. By analyzing the experimental results of fiber reinforced concrete it has been observed that there is an appreciable improvement in flexural strength when steel reinforcements are used while comparing it with the beams without steel reinforcement.
6. Use of high volume fly ash and GBFS in any construction work as a replacement of cement and sand provides lower impact on environment (reduce CO2 emission) and judicious use of resources (energy conservation, use of by-product)
7. Use of fly ash reduces the amount of cement content as well as heat of hydration in a concrete mix and the use of GBFS as a partial replacement of sand overcome the problem arise due to sand scarcity. Thus, the construction work with fly ash and GBFS based concrete becomes environmentally safe and also economical.

REFERENCES

[1] Mohammed Maslehuddin, Abdulaziz I. AL-Mana, Mohammed Shamim and Huseyin Saricimen., "Effect of sand replacement on the early-age strength gain and long term corrosion resisting characteristics of fly ash concrete", ACI Materials Journal, 1989.
[2] Vasudev R and Dr. B.G Vishnuram,"Studies on Steel Fiber Reinforced Concrete- A Sustainable Approach", International Journal of Scientific and Engineering Research Vol. 4, No. 5, 2013.
[3] Alhozaimy A.M "Mechanical Properties of Polypropylene Fiber Reinforced Concrete and the Effects on Pozzolonic Materials", Cement and Concrete Composite Journal, Vol. 18, No. 2, 1996, pp.85-92
[4] L. Zeghichi, "The Effect of Replacement of Naturals Aggregates by Slag Products on the Strength of Concrete," Asian Journal of Civil Engineering (Building and Housing), Vol. 7, 2006, pp. 27-35.
[5] M.S. Rao "Application of Blast Furnace Slag Sand in Cement Concrete–A Case Study", International Journal of Civil Engineering Research. Vol. 5, No. 4, 2014, pp. 453-458.
[6] Ramadevi.K, Sindhubala.S, "Determination of Optimum Percentage Replacement of Fine Aggregate in Concrete Using GBFS (Granulated Blast Furnace Slag)", International Journals of Engineering vol.2, No.3, 2014.
[7] Md.Moinul Islam and Md.Saiful Islam "Strength Behaviour of Concrete using Fly ash as Partial Replacement of Cement", vol.1, No.3, 2010.
[8] M C Nataraja, P G Dileep Kumar, "Use of Granulated Blast Furnace Slag as Fine Aggregate in Cement", International Journals of Structural and Civil Engineering Vol.2, No.2, 2013.
[9] Mohammed Nadeem and Pofale A D ,"Replacement of Natural Fine Aggregate with Granular Slag – A Waste Industrial By-Product in Cement Concrete Applications as Alternative Construction Materials", International Journal of Engineering Research and Applications, Vol. 2, No. 5, 2012, pp. 1258-1264.

SELF COMPACTING CONCRETE

CHETHAN GOWDA D, POOJA S, SUSHMA M, PUSHPALATHA H S

Department of civil engineering, Sapthagiri college of engineering.

#14/5 Chikkasandra, Hesaraghatta main road, Bengalore-57

chethansonic@gmail.com

poojaspoojas98@gmail.com

Sushmamanjunath0502@gmail.com

pushpalathahr18@gmail.com

INTRODUCTION

Cement products make up almost all of the man-made products and are therefore the most important design products, in fact they are likely to continue to have the same value in the future. However, these products and anatomist products need to meet new and larger needs. As soon as you are fighting production problems, the whole economy, high quality and suspension, weather resistance takes other design products such as plastic goods, building materials and timber. The only place in this development is usually to self-compacting concrete (SCC), a type of improved product that will pass, and incorporate intoxication by its body weight.

It should find non-compliant housing with a large circulation capacity and a strong level of resistance to resistance. That consistency is due to the effect of dissolving a high-pressure water-cooled mixture (super plasticizer) mixed with a mixture produced by high concentration of allergies in additional filling products. The key elements that control this fine-tuning are often in line with local physics and chemistry which is why, SCC is often heavily influenced by game combinations, as well as the large available space for written content for payments. The new SCC, like all cement products, is the formation of medium particles and a range of measuring particles (from 10- so you can reach 25 mm target concrete). This allergy is influenced by a

combination of complex particles electronic.

ABSTRACT:

Self-adhesive concrete is a liquid mixture that is suitable for depositing in structures with high density without vibration. The self-adhesive concrete development should ensure a good balance between deformity and stability. Also, cohesion is affected by the properties of the materials and the dimensions of the mix; it becomes necessary to change the SCC hybrid design process. The paper introduces the experimental process of designing concrete mixtures that combine them. A coarse surface found in the area of 20 mm and 12.5 mm, sand M as the ideal amount used in this exploration activity. The water concentration was adjusted to 0.31. Alccofine is used as a cement substance over cement. Different track combinations were fixed with C. A: F. A separate and add a growing percentage of super plasticizer to obtain a better SSC mix. Test results for concrete acceptance signals such as downhill, V-funnel and L-Box are displayed. Examples of cube sizes 150mmX150mmX150mm are prepared for pressing concrete mixtures. Strength is

limited to 7 years and 28 days of treatment period.

It is very liquid and is able to pass through the affected areas and fill all the nooks and corners without the risk of mud or other external fragmentation ingredients, at the same time there are no air pockets or closed stones. This type of concrete mix does not they require any congestion and save time, labor and energy.

Bonding Concrete.

The impact of fly ash (FA) on compound concrete (SCC) materials is being investigated. Portland Cement (PC) was replaced by 0–80% FA. The water level in the binder was kept at 0.36 in all mixtures. Properties included performance, compressive power, ultrasonic pulse speed (V), absorption and shrinkage. The results show that high volume FA can be used in SCC to produce high strength and low shrinkage. Replacing 40% of PCs with FA resulted in power over 65 N / mm2at 56 days. Higher absorption rates are achieved with a growing FA value, however, all FA concrete shows less than 2% absorption. There is a systematic decrease in fat as FA content rises and with FA content of 80%, a 56-day decrease is reduced by two-thirds compared to controls. The linear relationship exists between a 56-day reduction and FA content. Increasing the admixture content above a certain level leads to a decrease in energy and an increase in absorption. The relationship between energy and absorption indicates a significant decrease in energy as absorption increases from 1 to 2%. After 2% absorption, the energy decreases by a very slow rate.

MATERIALS AND METHODS

Cement, sand, course aggregates, V funnel fly ash, L box, U box research work related to the various uses and methods used to test Concrete made from different cement materials and mixtures is discussed. This chapter provides a comprehensive review of the work done by various researchers in the field of Self-compacting Concrete.

EXPENDITURE

CEMENT

The bond is a fine, dark powder. It is compacted with water and building materials, for example, sand, stones, and pebbles to form concrete. Bond and water are a layer of glue that holds other things together as the cement hardens. Normal concrete consists of two basic fixes especially argillaceous and calcareous. In the structures of argillaceous mud is abundant and in shiny materials calcium carbonate prevails. The basic part of the bond is shown in.

LIMITS OF FORMATION OF PORTLAND CEMENT

The Ultra Tech Grade 43 bond was used to throw shapes and chambers into every solid combination. The concrete had the same shade, i.e. black and light green shade and had no solid bumps. Highlights of the various bond-led assessments are provided under Table.

GOOD AGGREGATES

The sand used for the exploration program was purchased locally and complied with the standard Indian IS: 383-1970. The sand was first filtered through a 4.75 mm filter to remove any particles larger than 4.75 mm and then washed to remove dust. The properties of the positive amount used in the experimental work are drawn in Table. The aggregates are filtered through a set of filters to obtain a filter analysis and the same is shown in Table. Penalty rates were for grade III sinners.

SOLID INTEGRATION

Items stored in IS sieve no. 4.75 is called a strong aggregate. Crushed stone is commonly used as a coarse stone. The quality of the work determines the maximum size of the solid aggregate. A

coarse amount of locally available 10 mm was used in our work. Aggregates were washed to remove dust and dirt and then dried to make them appear dry. Aggregates tested as per IS: 3831970. The results of various tests performed with solid aggregate are given in Table 3.5 and Table 3.6 shows the results of filter analysis.

WATER

Generally, drinking water is good for concrete use. Water from lakes and streams containing seafood is generally suitable. If water is available from the above sources, no sampling is required. If it is suspected that water may be sewage, mine water, or waste from industrial plants or tins, it should not be used in concrete unless the test shows that it is satisfactory. Water from such wells should be avoided as the water level may change due to the groundwater or tap water used for pumping.

COMBINATION

Complast SP430 complies with IS: 9103: 1979 and BS: 5075 Phase 3 and ASTM-C-494 Sort "F" as the maximum width of the dehydration compound. Conplast SP430 is available in light Sulphonated Napthalene Polymers and is supplied as a cocoa liquid that dissolves rapidly in water and is specifically described as providing a 25% reduction in water loss without loss of performance, Special Gravity 1.22 to 1.225 At 30 °

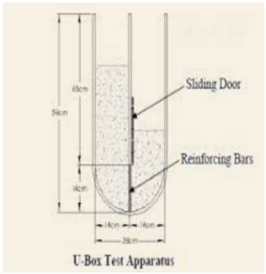

U-BOX APPARATUS

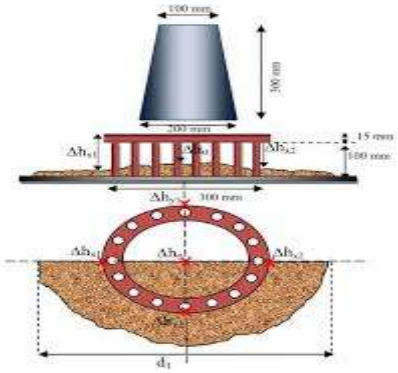

SLUMP CONE

V FUNNEL

METHODOLOGY

Checked that the SCC flows alone under its dead weight to the level, being affected externally and compacting itself without the passage of additional density and without unknown separation. Due to the

high powder content, SCC may show more plastic wrinkles or abrasion than conventional cement mortar. These views should therefore be considered between defining and determining the SCC. The knowledge of Ebb and the flow of these angles is restricted and this area mandates further research. The solid compound should be called Self-adhesive cement if the requirements of all three components are met.

• Completion capacity: The ability to complete a form function entirely under its own weight.

• Passing Ability: Ability to overcome obstacles under its own weight without interruption. Obstacles e.g. little support and openness and more.

ACCEPTANCE CRETERIA FOR SELF COMPACTING CONCRETE:

 In a situation where a test result is not achievable, there may be different reasons. The unthinkable reason can be found with more certainty by looking at the quality of other testing systems and independently evaluating performance characteristics. By following these lines the best unimaginable problem-solving work can be achieved. Table 2.3 and Table 2.4 provide a list of possible activities and the most frequent impacts of cement. It is clear that the impact depends on the size of the work and on the actual performance and creation of the solid compound. Each task can have a positive or negative impact on a variety of strong qualities.

 In the event that test results between different piles or loads change significantly, the reason may be varied:

 Attributes of cement

 Additional attributes

 Aggregate moisture content setting,

 Temperature

 The process of integration

 Test time

Test Methods: -An existing test of new SCC Mixes:

U-Box Test:

U-Box Testing: Of the many test methods used to test personal cohesion, the U-sort test (Fig 4.3.1) proposed by Taisei combination is the most suitable, due to the small amount of cement used, compared to others (Ferraris, 1999). In this test, the level of storage capacity can be determined by the condition the cement reaches after going through the obstacles. Concrete with a filling stem greater than 300 mm can be judged as a joint for you. A few organizations consider a solid bond around you if the filling stem is more than 85% of the maximum length imaginable.

The Slump Flow Test:

The critical gear used is the same with respect to the standard Droop test. The test system differs from the traditional way in which the solid template inserted into the skin is not folded and when the magnetic cord is removed the sample collapses. The rate of sample expansion is measured, i.e. the level separation is dead. set there is a specific split in the standard Droop test. The Droop Stream test can provide Proof of compliance, filling capacity and SCC performance. SCC is expected to have a decent filling capacity and consistency if the spread diameter reaches between 650mm to 800mm.

FLly Ash:

Fly ash (FA) is the result of the burning of piped coal in hot power plants. It emits a layer that collects dust from the power plants of fossil fuels such as smooth, smooth circles from thermal gases before being released into the atmosphere. The length of the particles depends largely on the type of hardware that collects dust. The distance between the particles of flammable debris is flies from less than 1-150 micrometer. For the most part it is better than Portland concrete. Their surface area is usually 300 to 500 m / kg, although some fly cylinders can have an surface area of up

to 200 m / kg and a height of 700 m / kg. The flammable waste is primarily a silicate glass containing silica, alumina, iron, and calcium. The relative size or specificity of the fly slag and the maximum width somewhere in the range of about 1.9 and 2.8 and tracking a large part of the black or tans (Halstead, 1986). The composite form of fly powder is governed by the related types and proportions of non-combustible materials used in coal. The most important synthetic elements in fly slag are silica, alumina and oxides of calcium and iron. As a result of its fineness and pozzolanic and sometimes natural cement environment, fly slag is widely used as part of bond and cement.

RESULT

COMPRESIVE STRENGTH 1	RESULT
7 DAYS	18.9 N/mm^2
14 DAYS	27.0 N/mm^2
28 DAYS	38.9 N/mm^2

CONCLUSION

It can be concluded that the SCC helps to improve the environment of construction sites (reducing the noise produced by plants and construction sites) and to reduce workers' exposure (staff reduction) when concrete is concrete. In other words, SCC is a suitable type of concrete that can be used for small reinforcement spaces and sections that require structures, or, more commonly, for all building applications where they require higher efforts to achieve sufficient density. In addition, it can be seen that the SCC offers many other precast benefits, compressed concrete sector and surface construction such as removed issues related to vibration, rapid construction, high strength gain and better concrete quality after hardening.

AKNOWNLEDMENT

This paper is supported by the project "Improving the quality of doctoral studies in engineering science in order to develop a knowledge-based society QDOC" number contract. POSDRU / 107 / 1.5 / S / 78534, a project funded by the European Social Fund through the Human Resource Operational Program 2007-2013

REFERENCE

- SUBRAMNIAN.S. CHATTOPADHYAY.D. "Experiments for mix- proportioning of self- compacting concrete", The Indian Concrete Journal, Jan 2002.
- Indian Standard Codes for Concrete & Guidelines.
- CHAMPION, J. M. and JOST, P., 'Self-compacting concrete: Expanding the possibility of Concrete Design and Placement', Concrete International, Vol.22, No.4, pp. 159-178, June 1998.
- HEINE, HANS J. "Saving Dollars Through Sand Reclamation - Part 1," Foundry Management and Technology. (May, 1983), pp.
- HENDERSON, N. "Self-compacting concrete at Millenium point",

CONCRETE, vol.34, No. 4, April 2000, pp.26- 27.

- KAMESWARA RAO, C.V.S (1983) "Analysis of Some Common Workability Tests". Indian Concrete Journal. Ø KATHY STANFIELD, "Self-compacting concrete a Growth area", The Str.Engg., Vol. 76, Nos 23 and 24
- NAGATAKI, S. and FUJIWARA, H. "Self-compacting property of Highly-Flowable Concrete" ICI Journal July-September 2002.
- KLAUS HOLSCHEMACHER, "Structural Aspects of Self-compacting concrete", NBM & CW, July 2002

DETERMINATION OF OPTIMUM BINDER CONTENT FOR BITUMINOUS CONCRETE

CHANDANA M
Dept of Civil Engineering
Sapthagiri College Of Engineering
chandurgouda26@gmail.com

POOJA S
Dept of Civil Engineering
Sapthagiri College Of Engineering
poojasiddeswara@gmail.com

PRAGATHI R
Dept of Civil Engineering
Sapthagiri College Of Engineering
pragathir148@gmail.com

SINDHU C
Dept of Civil Engineering
Sapthagiri College Of Engineering
sindhumenan2000@gmail.com

***Abstract*—** 98% highways constructed in flexible pavement road. Bituminous Concrete mix design emphasizes to determine the proportion of bitumen, filler, fine aggregates, and coarse aggregates to produce a mix which is workable, strong, durable and economical. Bituminous concrete mix is the most common material used for flexible pavement road construction. It primarily consists of bitumen binder and aggregates. Bitumen binder acts as an adhesive agent that binds aggregate particles into a cohesive mass. One thing is of major considerations in this regard –pavement design. Our project emphasizes on the mix design consideration to find out the optimum binder content. In this design we have studied Marshall Stability test method.

***Keywords*—** Bitumen, Aggregate, Bituminous Concrete, Optimum Binder Content, Marshall Stability

I. INTRODUCTION

Most of the roadways in India constructed with flexible pavement having surfacing course with bituminous concrete. Bituminous concrete should be constructed to satisfy the recommendation and requirements of Ministry of road transport and highways Section 509. This clause specifies the construction of Bituminous Concrete, for use in surfacing and profile corrective courses. During 1900's, the bituminous paving technique was first used on rural roads – so as to handle rapid removal of fine particles in the form of dust, from Water Bound Macadam, which was caused due to rapid growth of automobiles [Roberts et al. 2002]. At initial stage, heavy oils were used as dust palliative. An eye estimation process, called pat test, was used to estimate the requisite quantity of the heavy oil in the mix. By this process, the mixture was patted like a pancake shape, and pressed against a brown paper. The first formal mix design method was Hubbard field method, which was originally developed on sand bitumen mixture. Mixes with large aggregates could not be handled in Hubbard field method. India being the second largest growing economy in the world, in par with other developmental activities, road infrastructure is developing at a very fast rate. Large scale road infrastructure developmental projects like National Highway Development Project (NHDP) and Pradhan Manthri Gram Sadak Yojna (PMGSY) are in progress. The spurt in the growth of traffic and overloading of vehicles decreases the life span of roads laid with conventional bituminous mixes. This also leads to the reduction in the riding quality resulting in exorbitant vehicle operating costs and frequent maintenance interventions due to premature failure of pavements. Providing durable roads has always been a problem for a country like India with varied climate, terrain condition, rainfall intensities and soil characteristics. A good amount of research is going on all over the country in this field to solve the problems associated with pavements. It is observed that Stone Matrix Asphalt mixture is an ideal mixture for long lasting Indian Highways. The literature pertaining to the bituminous mixtures is reviewed in this chapter with a detailed discussion of SMA mixtures.

II .MARSHALL METHOD

During World War II, the U.S. Army Corps of Engineers (USCOE) began evaluating various HMA mix design methods for use in airfield pavement design. Motivation for this search came from the ever-increasing wheel loads and tire pressures produced by larger and larger military aircraft. Early work at the U.S. Army Waterways Experiment Station (WES) in 1943 had the objective of developing:

"…a simple apparatus suitable for use with the present California Bearing Ratio (CBR) equipment to design and control asphalt paving mixtures…"

The most promising method eventually proved to be the Marshall Stability Method developed by Bruce G. Marshall at the Mississippi Highway Department in 1939. WES took the original Marshall Stability Test and added a deformation measurement (using a flow meter) that was reasoned to assist in detecting excessively high asphalt contents. This appended test was eventually recommended for adoption by the U.S. Army because:

1. It was designed to stress the entire sample rather than just a portion of it.
2. It facilitated rapid testing with minimal effort.
3. It was compact, light and portable.
4. It produced densities reasonably close to field densities.
5. WES continued to refine the Marshall method through the 1950s with various tests on materials, traffic loading and weather variables. Today the Marshall method, despite its shortcomings, is probably the most widely used mix design method in the world. It has probably become so widely used because (1) it was adopted and used by the U.S. military all over the world during and after WWII and (2) it is simple, compact and inexpensive.

III.MARSHALL MIX DESIGN PROCEDURE

The Marshall mix design method consists of 6 basic steps:

1. Aggregate selection
2. Bitumen binder selection
3. Proportioning
4. Sample preparation (including compaction)
5. Stability determination using the Marshall stability
6. Marshall properties calculations
7. Optimum asphalt binder content selection

Aggregate Selection

Although Marshall mix design did not specifically develop an aggregate evaluation and selection procedure, one is included here because it is integral to any mix design. A typical aggregate evaluation for use with either the Marshall mix design methods includes three basic steps.

ISBN: 979-88-35073-61-0

SIEVE ANALYSIS TEST RESULTS

IS Sieve Size in mm	% Passing		
	A	*B*	*C*
37.5	100	100	100
26.5	95	100	100
19	-	78	100
13.2	-	68.5	100
4.75	-	-	56
2.36	-	-	37.3
03	-	-	22
0.075	-	-	3.2

1. **Determine aggregate physical properties**: This consists of running various tests to determine properties such as:
   - Toughness and abrasion
   - Gradation and size
   - Specific gravity and absorption
   - Cleanliness and deleterious materials
   - Particle shape and surface texture

2.

SL NO	TEST ON COARSE AGGREGATES		
	TEST NAME	*TEST RESULTS*	*STANDARD VALUE AS FOR IRC*
1	Aggregate crushing value	25.21%	Max 30%
2	Aggregate impact value	17.78%	Max27%
3	Los Angeles abrasion value	26.4%	Max35%
4	Water absorption	0.675	2%
5	Specific gravity	2.76	25-30%
6	Flakiness and Elongation	15%,17%	Max 30%

2. Determine bitumen binder properties

SL NO	TEST ON BITUMEN		
	DESCRIPTION OF TEST	*TEST RESULTS*	*STANDARDS AS PER IRC*
1	Penetration test	67	60-70
2	Specific gravity	1.02	0.99
3	Ductility in cm	76.3cm	45-55
4	Softening point	47	40(min)
5	Viscosity test	42min	40(min)

3. Bitumen Binder Evaluation

SL NO	Composition of bituminous concrete pavement layer		
	GRADING(SIEVE SIZE)	*GRADE-I*	*MID LIMIT*
1	26.5	100	-
2	19	79-100	89.5
3	13.2	59-79	69
4	9.5	52-72	62
5	4.75	35-75	45
6	2.36	28-44	36
7	1.18	20-34	27
8	0.6	15-27	21
9	0.3	10-20	15
10	0.15	5-13	9
11	0.075	2-8	5
12	Bitumen content,% weight of total mix	5.0-6.0	

Proportioning of aggregates

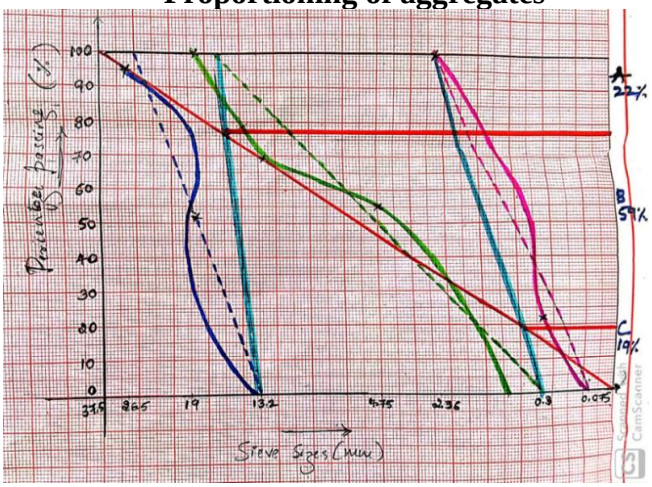

Figure 1. Rothfuch's graph as per obtained sieve analysis results

Material A = 22 % , Material B = 59 % ,Material C = 19%

Sample preparation

The Marshall method, like other mix design methods, uses several trial aggregate-asphalt binder blends (typically 5 blends with 3 samples each for a total of 15 specimens), each with a different asphalt binder content. Then, by evaluating each trial blend's performance, an optimum asphalt binder content can be selected. In order for this concept to work, the blends must contain a range of asphalt contents both above and below the optimum asphalt content. Therefore, the first step in sample preparation is to estimate an optimum asphalt content. Trial blend asphalt contents are then determined from this estimate .Based on the results of the optimum asphalt binder content estimate, samples are typically prepared at 0.5 percent by weight of mix increments, with at least two samples above the estimated asphalt binder content and two below.

- The aggregates and filler are mixed together in desired proportion as per the IRC standards to produce specimen of 63.5mm approx.
- A total of approx 1200g of aggregates and filler mix is taken and heated at a temperature of 175-190·c
- The bitumen binder is heated to a temperature of 120-165·c(till it attains pouring consistency).
- The weighed quantity of bitumen is added to the heated aggregate and the mixture is thoroughly mixed at specified temperature (<160·c).
- The mix placed in pre heated mould and compacted.

ISBN: 979-88-35073-61-0

Compaction with the Marshall Hammer

Each sample is then heated to the anticipated compaction temperature and compacted with a Marshall hammer, a device that applies pressure to a sample through a tamper foot (Figure 1) Some hammers are automatic and some are hand operated. Key parameters of the compactor are:

- Sample size = 102 mm (4-inch) diameter cylinder 64 mm (2.5 inches) in height (corrections can be made for different sample heights)
- Tamper foot = Flat and circular with a diameter of 98.4 mm (3.875 inches) corresponding to an area of 76 cm^2 (11.8 in^2).
- Compaction pressure = Specified as a 457.2 mm (18 inches) free fall drop distance of a hammer assembly with a 4536 g (10 lb.) sliding weight.
- Number of blows = Typically 35, 50 or 75 on each side depending upon anticipated traffic loading.
- Simulation method = The tamper foot strikes the sample on the top and covers almost the entire sample top area. After a specified number of blows, the sample is turned over and the procedure repeated.
- The compacted specimen is allowed to dry for 24 hours in air and the average dia , thickness and its weight is measured
- The specimen to be tested are kept immersed in water bath maintained at 60·c±1·c for about 30-40min.

Figure 1. Marshall drop hammers.

The standard Marshall method sample preparation procedure is contained in: AASHTO T 245: Resistance to Plastic Flow of Bituminous Mixtures Using the Marshall Apparatus

- The Marshall stability and flow test provides the performance prediction measure for the Marshall mix design method. The stability portion of the test measures the maximum load supported by the test specimen at a loading rate of 50.8 mm/minute (2 inches/minute). Basically, the load is increased until it reaches a maximum then when the load just begins to decrease, the loading is stopped and the maximum load is recorded.

- During the loading, an attached dial gauge measures the specimen's plastic flow as a result of the loading (Figure 2). The flow value is recorded in 0.25 mm (0.01 inch) increments at the same time the maximum load is recorded

fig2.Marshall stability testing apparatus.

One standard Marshall mix design procedure is:

Density and Voids Analysis

All mix design methods use density and voids to determine basic HMA physical characteristics. Two different measures of densities are typically taken:

1. Bulk specific gravity (G_{mb}).
2. Theoretical maximum specific gravity (G_{mm}).

These densities are then used to calculate the volumetric parameters of the HMA. Measured void expressions are usually:

- Air voids (V_a), sometimes expressed as voids in the total mix (VTM)
- Voids in the mineral aggregate (VMA)
- Voids filled with asphalt (VFA)

Generally, these values must meet local or State criteria.

Design Requirements of Bituminous Mixes for pavement layers (as per MORTH)

1. Marshall stability value, kg(min)=900
2. Marshall flow value, mm units=2-4
3. Air voids in total mix, Vv%=3-6
4. Voids filled with bitumen, VFB%=65-75
5. Voids in Mineral Aggregates, VMA% should fulfill the following requirements.

Nominal max size of the aggregates in the mix,	Min VMA% for design air voids of 3-5% in the mix
12.5	13-15
19,0	12-14
25.0	11-13
37.5	10-12

Table -5

Marshall Stability Test

Bitumen content%	Total air voids(Vv%)	Voids filled with mineral aggregates VMA%	Voids filled with bitumen VFB%
4.0	3.38	12.791	73.575
4.5	2.2	12.788	82.796
5.0	0.99	12.75	92.235
5.5	-	12.94	-
6..0	-	14.11	-

selection of Optimum Bitumen Binder Content

The optimum asphalt binder content is finally selected based on the combined results of Marshall stability and flow, density analysis and void analysis (Figure 3). Optimum asphalt binder content can be arrived at in the following procedure:

1. Plot the following graphs:
   - Asphalt binder content vs. density. Density will generally increase with increasing asphalt content, reach a maximum, then decrease. Peak density usually occurs at a higher asphalt binder content than peak stability.
   - Asphalt binder content vs. Marshall stability. This should follow one of two trends:
   - * Stability increases with increasing asphalt binder content, reaches a peak, then decreases.
   - * Stability decreases with increasing asphalt binder content and does not show a peak. This curve is common for some recycled HMA mixtures.
   - Asphalt binder content vs. flow.
   - Asphalt binder content vs. air voids. Percent air voids should decrease with increasing asphalt binder content.
   - Asphalt binder content vs. VMA. Percent VMA should decrease with increasing asphalt binder content, reach a minimum, then increase.
   - Asphalt binder content vs. VFA. Percent VFA increases with increasing asphalt binder content.

   Determine the asphalt binder content that corresponds to the specifications median air void content (typically this is This is the optimum asphalt binder content.

2. Determine properties at this optimum asphalt binder content by referring to the plots. Compare each of these values against specification values and if all are within specification, then the preceding optimum asphalt binder content is satisfactory. Otherwise, if any of these properties is outside the specification range the mixture should be redesigned.

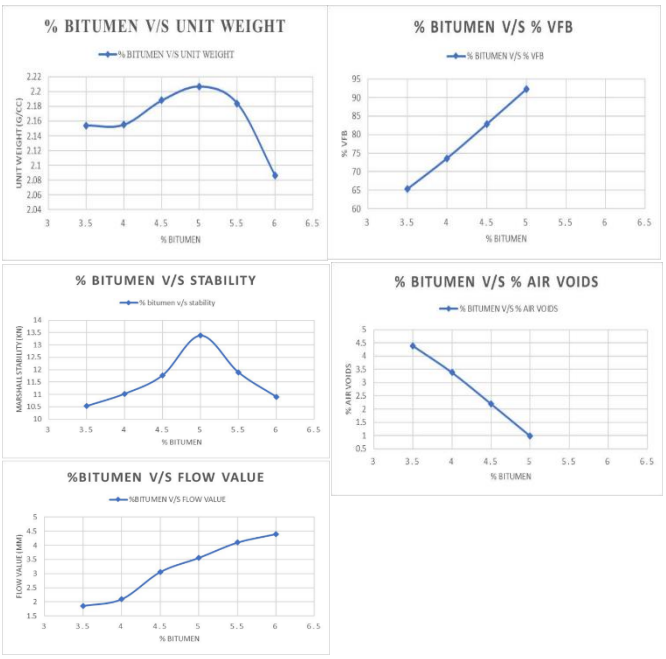

Marshall properties at optimum binder content

Marshall properties	Results of BC grade -I	Standard specification as per MORTH
Optimum Binder Content%	4.83%	Min4.5%
Stability(kg)	12.93KN	9KN
Flow value(mm)	3.73 mm	2 to 4mm
Bulk dsity(g/cc)	2.145g/cc	-
Air voids(Vv)	3.5	3 to 6
VMA(%)	21.87 %	Min 12.5%
VFB(%)	68.1 %	65 to 75%

ISBN: 979-88-35073-61-0

CONCLUSION

On the basis of the results of this project work the following conclusions can be drawn:

- Results of physical properties of the aggregates used in this study were tested and are presented in table-2 and test results are satisfying the requirements as per Table 500-8 of MoRTH(IV revision) specifications.
- The physical properties of the plain binder used for this study was tested and are presented in table-3 respectively and test results are satisfying the requirements as per IS: 73-2002 for plain Bitumen.
- For Marshall mix design ,optimum bitumen content was 4.83% per BC mix and it was meeting the requirement as per the MORTH specifications table 500-11.

REFERENCES

[1] Highway engineering by S.K KHANNA, C.E.G JUSTO and A VEERARAGAVAN.

[2] Revised 5th edition 2019.

[3] Nem Chand & bros., Roorkee 247 667, India

[4] Principles and practice of highway engineering (Including Express ways and Airport Engineering)

[5] By Dr L.R KADIYALI, and N.B LAL

[6] Khanna publishers, New Delhi-6

[7] Ministry of Road Transport and Highways (4th revision)

[8] IS:2386 (part 4)-1963 “Crushing strength test, Abrasion test, Impact test” on aggregates

[9] IS: 2386 (Part 1)-1963 “Shape test” on aggregates.

[10] IS: 2386 (Part 3)-1963 “Specific gravity” on aggregates

[11] IS: 1203-1978 “Penetration Test” on bitumen

[12] IS: 1208-1978 “Ductility test” on bitumen

[13] IS: 1205-1978 “Softening point test” on bitumen

[14]IS: 1202-1978 “Specific gravity” on bitumen

Study on Breathe Bricks

Abstract **-Breathe brick is a masonry system that filters the polluted outdoor air to improve the indoor air quality. This system does not use any filtration technique for separating suspended particles. The air itself creates the filtration effect. The brick is modified to have a faceted shape to direct the airflow into the brick. The pressure and temperature differentials are considered for directing the particle-laden air to the brick. Cyclonic separator, which is the cheapest and efficient type of separator is adopted as the major component of breath brick. The efficiency of cyclonic separator depends on particle size and velocity. It shows 70-80% efficiency in solid separation, if the fluid contains large number of solid particles the separation efficiency exceeds 99%. The existence of life on earth is impossible without air. The quality of air is an important factor, which requires special consideration in the current scenario. Degradation of air quality leads to many problems that affect humans as well as environment.**

INTRODUCTION

Air has been source for our living planting to breathe. It is the mixture of gases that fills the atmosphere and gives life to plants and animals. But when the air is being polluted it affects larger proportion of our living system. Filtration of the breathing air has become important for the comfort and safety of the people inside the buildings.

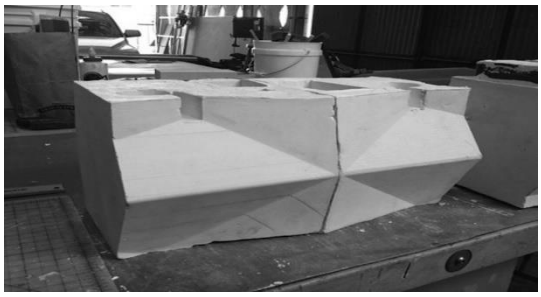

Breathe brick

By the effective utilization of technical knowledge, the pollution can be prevented in greater extent. Commercial structures such as office buildings often have heating and air conditioning systems that pull in the air from outside the building.

Most single-family homes and many apartment buildings have no such air filtration systems, as outside air is introduced through screen windows which may block insect from screens. But it may be exposed to dust which may cause allergies. To prevent that these, breath bricks are introduced to the exterior walls of the buildings. It has a cyclone separator technique which separates solid particles from gases hence air will healthier to breathe. Hence this type of systems is very helpful for average income families living in city Centre. If this system is effectively taken into usage more people will be benefitted especially in India region where cities like Delhi are prone to air pollution, so people can easily afford since it doesn't require electricity or other major energies to operate. Air filtration for domestic dwellings are usually carried out by pleated'' flow through filter'' system.

PRESENT SCENARIO OF BREATHING WALL

The countries located closer to equator have inherited problem of hotter climates. They also receive comparatively lesser rainfall. Geographical context and rich or poor in the economic prosperity framework. Changing climate resulting in global warming arising from extensive and uncontrollable use of fossil fuel has considerably magnified the thermal comfort problem. In winters, it is intensely cold and summers are intense too making newer hottest. The records every year passing says that, oil producing countries may be able to provide cheaper fuel to their citizens but the countries that must import fuel for energy are facing increasing energy cost thereby a difficulty to provide a comfortable living environment for their inhabitants. It is worth mentioning that extreme climates have resulted in many deaths all over the planet Earth. Many die due to lack of heating and many due to in sufficient cooling. Economic activity relationship is adversely affected by increasing fossil fuel prices. This aspect alone is forcing the poor communities to switch to alternate methods of making homes comfortable. Cost of energy and carbon footprint are increasing in the construction industry in manufacturing construction materials like steel, cement, glass, plastics and other numerous supplementary and complementary building materials etc. A quick look in the supply chain will show that before the building materials reach the site, much of fossil fuel energy has used and consequent carbon has been produced.

METHODOLOGY

Collection of materials

The materials of these bricks are properly collected from the available areas and also shops.

Batching of materials

Measurement of materials for making brick is called batching. After collection of materials, we separate and remove any other waste presented in the collected material and check that any water content in sample collected.

Mixing

Mixing of materials is essential for the production of uniform and strength for brick. The mixing has to be ensure that the mass becomes homogeneous, uniform in color and consistency. Generally, there are two types of mixing, Hand mixing and mechanical mixing. In this project, we adopted hand mixing. Until the entire lime content required for water added.

Moulding

After completion of proper mixing we place mix into required mould. In these projects we use the different brick sizes(15x15x4 cm). After 2 days remove the brick from the mould and then done curing.

Burning

The test specimens after moulding were allowed to dry for a period of 24 hours. The specimens were kept in burning at 120oC and a period of 8 hours.

BASIC TESTS ON LIME

1. VISUAL TEST: It is performed from the physical appearance of a lime. If the lime colour is off white then the lime is class A lime or hydrated lime.If the is slightly clear than off white then it is class B lime. If the colour is perfectly white then the lime is class C lime or fat lime.

2. BALL TEST: In a ball test, water is added in lime and stiff lime is formed. Then from stiff lime a ball of about 40mm diameter are made and kept as it is for 6 hours the undisturbed ball are kept in a basin of water. If there is slow expansion and slow disintegration of ball within a minute then it show class C lime.If there is very small or no expansion and numerous crack then it indicates class B lime. If it remains in its shape and ball crack then the lime is class A.

3. SOUNDNESS TEST: Aim of the soundness test is to find disintegration or unsoundness of the lime. It is performed using Le Chatelier's apparatus where lime is properly tested. Cement, hydrated lime and sand is thoroughly mixed in the proportion of 1:3:12 and then this mix is filled in a cylinder of a Le Chatelier's apparatus. Cylinder is covered by a glass plate and kept for 1 hour and the distance between the two ends of indicator is properly measured and noted. This apparatus is kept for 48 hours in damp air and then kept for 3 hours in steam. Then the temperature is cooled down to room temperature, The distance of the two end of indicator is again measured and noted down. The distance between the two distances is found out and it should not be more than 10mm.

MIX DESIGN

In order to find the breathe bricks that they possess high compressive strength with various mix proportions are made and they are tested on compressive testing machine (CTM). The mix proportions of the breathe bricks are as follows:

Table no-1: Mix Proportion

S. No	LIME (Kg)	WHITE CEMENT (g)	CALCIUM NITRATE (g)	C2H6O2 (ml)	WATER (%)
1	0.5	50	50	50	250
2	0.5	100	50	100	300
3	0.5	150	50	150	350

The polluted air enters the breath brick unit via coupler. The air moves through the baffles to reach the cyclonic chamber. The cyclonic separator with a cylindrical upper part(barrel) and conical lower part admits the particle laden air tangentially through the top of barrel. The air induces a swirling motion when it reaches the chamber. The inertial force of the gas particles gets transformed to centrifugal force by means of vortex generated by the swirling effect of the particles.

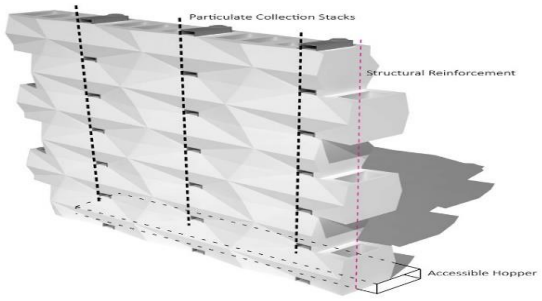

Sample No.	Lime Percentage	Water Absorption %
1	0	0.2
2	5	0.12
3	10	0.11
4	15	0.009
5	20	0.0073

As the diameter of cone decreases the velocity of flow of particles increases, which results in increase in centrifugal force. When the particle hits the wall of separator the particle losses their energy and falls down due to gravitational force. The density of air get reduced as the particle is separated from the air. As a result the purified air moves towards the barrel by forming inner vortex and it is released from the breathe brick unit. The dust particles move through the dust collector shaft and it finally reaches the collection hopper kept at the bottom of wall. The hopper is cleaned periodically by sweeping or vacuuming.

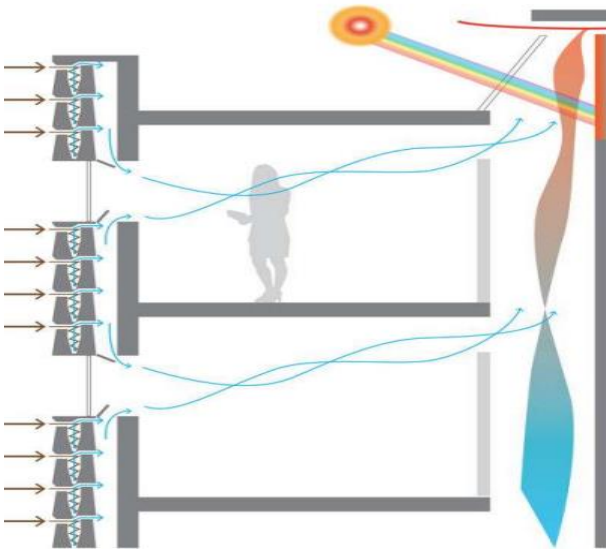

Aerodynamics of Breathe Brick

RESULTS

Table no-2: Compressive Strength Test

Sample No.	Normal Brick Strength	Breathe brick Compressive strength (N/mm2)
1	3.5	3.1
2	3.5	3.1
3	3.5	3.3
4	3.5	3.3
5	3.5	3.3

Table no.3: Water Absorption test

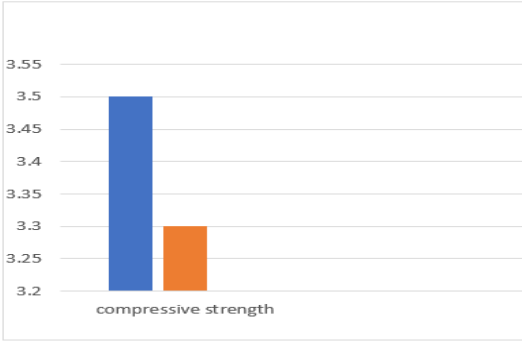

Chart -1: Compressive strength test

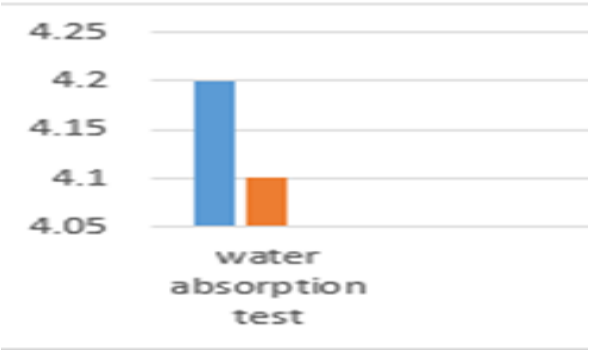

Chart – 2: Water absorption test

CONCLUSION

The compressive strength of these brick is equal to ordinary brick. The water absorption is better than normal brick. And the other tests like efflorescence, Hardness, Soundness etc., gives the same result. The Breath brick is a capable of capturing dust particles at a variety of pressure, temperature and velocity of air. The applications of this in those building systems would be in the locations where the currently no air filtration is used, and the removal of dust particles without an output of fossil fuel energy .Encouraged to create beauty in their dwellings, the chances of the surviving is improved .Enables natural Ventilation with improved indoor air quality .Environmentally friendly architecture that turns a building into its own air filter.

ACKNOWLEDGMENT

We would like to express our sincere gratitude to the Management, Principal of Sapthagiri College of Engineering, Bengaluru for the facilities provided and their support. Also, we would like to thank the Head of the Department of civil Engineering and faculties for their encouragement and support.

REFERENCES

[1]. U. S department of Energy – Building energy data book-2012
[2]. MadehIzat Hamakareem – Building technology guide by editing at constructor.org
[3]. Scott Rory – The innovative pollution absorbing brick from Arch daily-2015
[4]. Kate Hajash – Design and research of breath brick book-2015
[5]. Barbosa. S – Perspective of double skin facades for ventilated buildings-2017

"STUDY OF HIGH-DENSITY CORRIDOR OF SELECTED STRETCH IN BENGALURU CITY"

Akshay J
Assistant Professor ,
Department of civil engineering
Sapthagiri College of Engineering
Bengaluru, India
akshayaradhya89@gmail.com

Hemanth Kumar N
Post-Graduate Student
M.S Ramaiah University of Applied Sciences
Bengaluru, India
hemanthkumar2798@gmail.com

***Abstract*—** Bengaluru population has been growing at a rate of 3.25% per year in the last decade. There has been a phenomenal growth in the population of vehicles as well especially the two and four wheelers in this period due to rising household incomes. The number of motor vehicles registered has already crossed 36 Lakhs. In the absence of adequate public transport system, people are using the personalized modes which is not only leading to congestion on limited road network but also increasing environmental pollution. An average citizen of Bengaluru spends more than 240 hours stuck in traffic every year. Such delays result in loss of productivity, reduced air quality, reduced quality of life, and increased costs for services and goods. Road network capacity is inadequate. Most of the major roads are with four lane or less with limited scope of their widening.
There are many high-density corridors in and across the Bengaluru city in which the commission has allocated to study the stretch of Tumkur road corridor to Gorguntepalya (Via Sangolli Rayanna circle, Okalipuram, Sujatha Talkies, Dr. Rajkumar Road, Sandal soap factory, Yeshwanthpur railway station, RMC Yard) which is an 9km Stretch.

Keywords*— *Traffic congestion, road capacity, Geometric Features.

I. INTRODUCTION

There are social, convenience, economic, and environmental benefits of living in places of higher density if they are designed to be mixed-use, walkable, and pedestrian scale. Higher density is critical for creating lively places with many services. It allows for beautiful public spaces, for lots of people walking, low car use, and makes life opportune and enjoyable by providing many amenities within close proximity of each other. Having a number of good corner stores, restaurants, cafes, and other personal services within walking distance of most homes delivers a higher quality of life to all residents of a town or city. Increased density greatly reduces driving, traffic congestion, and huge amounts of air pollution that come with it. Nationally, there is a growing consumer preference for places of higher density providing desired urban facilities.
The people who lived in villages had started to move to big cities in search of jobs. So the cities became denser. With increasing immigration, the quality of life in the city started to degrade and environmental pollution increased. The cities gradually became too dense and the price of land increased. A greater concern was the lack of necessary infrastructure to support the densities that occurred. Once this happened, people started to move outside of cities for their housing although they needed to be close to cities to work in factories. Traffic volume is the number of vehicles passing a given stretch of road or traffic lane in per unit time. Traffic volume studies are executed to determine the count, movement and classification of roadway vehicles at a given site so as to become attentive of the peak hours of the day when the traffic volume is highest on the road. India's traffic is heterogeneous in nature and varies continuously during 24 hours of duration in a day. This tends to raise problem like congestion of traffic responsible for increase accidental condition during peak hours so it is necessary to study the junction between the moving vehicles over an extensive array of roadway and traffic conditions. Traffic volume study also considers traffic safety by examining sites of roadways with high accidental rate and developing countermeasure to reduce crashes and accidents. In Traffic volume study Heterogeneous traffic has been addressed by exchanging the different types of vehicles into equivalent passenger cars and expressing the volume in terms of Passenger Car Unit (PCU) per hour. The PCU is the universally adopted unit for measurement of traffic volume, derived by taking the passenger car as the standard vehicle. Traffic volume study which include traffic stream, flow rate, direction distribution, peak hour flow and annual average daily traffic (AADT) provide input for planning, design and operation of highway in maximum of the industrialized countries. If traffic volume isn't measured continuously transportation system may miscarry to manage and additionally face a difficulty of traffic jam and accidental proven conditions. As per report of world health organization report 2018 number of yearly road traffic death reached to 1.35. Road traffic injuries are now the leading killer of people aged 5-30 years. As per media statistics, in India one person dies in a road accident every four minutes. The main reasons for India's high percentage of on- road defect are bad road conditions, careless user behavior, defective road planning and designing, poor control of

traffic rules and emergency services. After all the surveys and observations solution and suggestions are provided for better traffic condition and safeguard of users for smooth functioning of transportation system and conquer future requirement.

II. LITERATURE REVIEW

Birva B. Shah, Prof. N. G. Raval (2016) [1]
Concluded that Estimation of traffic volume is fundamental to planning, design and operation of the roads. It helps in improving new and existing transportation facilities for safe and time efficient movement of vehicle on roads. In their studies, they found out the suggested traffic volume capacity by Indian road congress (IRC) is nearly 16% less that the observed at C.G. Road of Ahmadabad city. Due to urbanization and increased population traffic is increased rapidly in the urban area which is highly dynamic in composition. They suggest, design service volumes are required to update in the highly congested cities which At this level, will be around 0.7 times the maximum traffic volume required for design of road.

Hall & Pendleton (1990) [2]
Examined the connection between hourly crash rates and also the ratio of traffic volume to capacity on rural highways. They found that the speed of traffic crashes on roadway sections increases with increasing traffic volume. However, data which was needed in order to support this relationship were highly scattered. According to the authors, the idea of a relationship between traffic crash rates and traffic volume is valid but the exact nature of the connection is unknown.

Ashish Dhamaniya & S. Chandra (2013) [3]
Mixed traffic flow is transformed to equivalent flow in passenger car units (PCUs). These PCU values are utilized to convert highly dynamic traffic volume to homogeneous volume in PCU per hour. New concept of stream equivalency factor (SEF) is presented in this study and denoted by K. It is the ratio of traffic volume in PCU to volume in vehicles per hour which related to traffic composition and volume on a road and study through the regression analysis method. A micro simulation program is used to generate the traffic flow data for various categories of vehicles in the traffic stream used to present a generalized solution for defining the value of K for any combination of traffic composition and volume on a road.

Nabanita Roy, Rupali Roy, Hitesh Talukdar & Pritam Saha (2017) [4]
These research focus on how heterogeneity in traffic mix affect on two-lane road traffic. It examine the effects of such traffic on capacity, traffic flow characteristic and factors affecting it. Here, traffic flow characteristics equation developed using green shield modal which show capacity and free-flow speed changes with the traffic composition and largely affected by the presence of low performance vehicles including non-motorized ones. It clarifies the requirement of announcing the concept of dynamic passenger car unit which would lighten the current implication on capacity standards of two-lane roads under heterogeneous mixed traffic.

Pothula sanyasi Naidu, Gundu Navya, Chukka Deepika, Mahesh Yamala [5]
This research presents important features of capacity evaluation for road designing by using PCE In place of PCU. Utilization of Mathematical model is done by using IRC specifications and regression analysis is performed for obtaining capacity values of traffic flow on road. Relations between traffic volume and geometric cross section of road are identified, which derives the capacity effecting zones. This relation helps in studying variation in capacity with respect to various widths of road elements. Impact of geometrics and road elements on capacity is measured and capacity is derived on the basis of PCE and road geometric factors, which results inaccurate prevailing road capacities.

Sai Kiran M. & Ashish Verma [6]
The primary objective of this research is to review on various mixed traffic characteristics in developing economies, identify their limitations and supply guidelines for the long run research. Also, a detailed methodology of the simulation process for the mixed traffic is given, reflecting the ‘‘gap- filling’’ instead of the traditional ‘‘car-following’’ behavior. A comparison of the past modelling approaches is additionally presented and therefore the accuracy of their implementation is discussed.

Joseph. O. Ukpata, Anderson A. Etika, et al.,[7]
Their study has highlighted some remedies to improve traffic congestion in Nigeria. Good road network, encouragement of mass transport system, proper traffic planning/management, regular road maintenance, construction of interchanges and regular education of road users are among the recommendations to reduce traffic congestions. The various state governments controlling most of these cities affected by congestion should encourage the use of reliable mass transit buses to reduce the number of vehicles on their urban roads. Proper and consistent bus stops which are not too far apart should be sited across each city, including provisions for enforcing compliance by bus drivers. The Federal and State governments should initiate plans for the introduction of other forms of urban transportation such as Metro and Trains which supports mass movement of people.

Olusina, J.O. and Samson, A.P., et al., [8]
Studied that Traffic congestion always have negative effects on lives and environment. This work has been directed at identifying causes of congestion on some selected routes in Lagos Metropolis. Questionnaires were administered. Results revealed that bad access road is the highest cause of traffic congestion, and that cars are the highest mode of transportation. For Recurrent Congestion the data on traffic

volume were used to develop a generalized polynomial of n order. From the generalized model, a response (dependent) variable y for any route can be determined for any predictor (independent) variable x. Spatial queries of the various volume of traffic on these roads revealed more routes are congested between 7.00 – 8.00hrs in the morning peak period and between 16.00 – 17.00hrs and 18.00 – 19.00hrs in the evening peak period.

Babitha Elizabeth Philip, Jaseela K. H, et al., [9]
Stated that Traffic congestion is a serious problem facing today. The causes, effects and solutions of traffic congestion vary according to the location. In this paper a model is developed to eliminate the traffic congestion to a considerable extent. Different samples are selected for the study and traffic survey was conducted. From the survey data, it was analyzed whether the selected samples are congested or not and hence the samples were finalized. A study on traffic congestion was conducted. The general causes, effects and solutions for the traffic congestion were discussed. The model as a solution for traffic congestion and to obtain an efficient movement of traffic was developed. The model for a straight link is developed in this paper.

Dr. Benjamin O. Uwadiegwu, et al., [10]
Stated that Traffic problems along route ways in Nigerian cities cannot be adequately addressed without proper identification of the factors responsible for the problem. For the purpose of identifying factors responsible for traffic congestion along city roads in Nigeria, 20 variables organized into 4 factors suspected to be relevant factors were articulated in a questionnaire. Relative Factor Index (RFI) for the 230 respondents across their responses was computed which yielded variable loadings which determined the relevant factors. Factors identified include physical, technical, land use and human factors. Some management measures were recommended which include improvement in terminal facilities, land use relocation, traffic education and traffic personnel improvement. Apart from making reference to some secondary sources, data for this study were mainly primary in origin. Two major methods were adopted for data sourcing. This includes fieldwork and questionnaire administration.

Saleem-ullahLar, Xiaofeng Liao and SongtaoGuo, et al.,[11]
Stated that TCP steady-state Performance is affected by the congestion in the network and to select an appropriate data for the available capacity (bottle-neck link) is an open issue. This congestion is mainly arises when a large amount of flow (FTP transaction) is to be sent. The aim of this paper is to solve these issues up to the maximum level using simulation approach in already defined algorithms. The simulation result shows that the proposed schema can achieve higher throughput and lower delay, full and always link utilization with minor packet loss which will be controlled by using some TCP New Reno already defined mechanism and modifying slow start and congestion avoidance algorithms.

Amudapuram Mohan Rao1, KalagaRamachandra Rao, et al.,[12]
published a CRRI journal Congestion - both in perception and in reality - impacts the movement of people. Traffic congestion wastes time, energy and causes pollution. There are broadly two factors, which effect the congestion; (a) micro-level factors (b) macro-level factor. That relate to overall demand for road use. Congestion is ‘triggered’ at the ‘micro’ level (e.g., on the road), and ‘driven’ at the ‘macro’ level. The micro level factors are, for example, many people want to move at the same time, too many vehicles for limited road space. On the other side, macro level factors are e.g., land-use patterns, car ownership trends, regional economic dynamics, etc. This paper gives an overview and presents the possible ways to identify and measure metrics for urban arterial congestion.

Prof.Gopal R. Patil, et al.,[13]
Studied They studied the traffic flow entering and leaving the IIT Bombay campus, a traffic volume count survey was conducted on 29th January 2015. A classified traffic volume count survey was performed at all three gates (Main gate, Market gate and lakeside gate) IIT Bombay campus from 7 AM to 10 PM. Classified volume count survey was also conducted at many locations inside IIT Bombay from 7:00 AM to 11:00 AM.

III. METHODOLGY

A. Selection of Route

High-density corridors in and across the Bengaluru city in which the commission has allocated to study the stretch of Tumkur Road corridor to Gorguntepalya (Via Sangolli Rayanna circle, Okalipuram, Sujatha Talkies, Dr. Rajkumar Road, Sandal soap factory, Yeshwanthpur railway station, RMC Yard) which is an 9km Stretch.

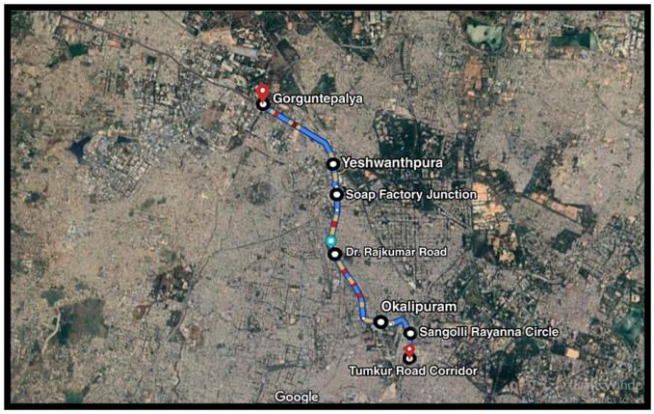

Fig 1: Selection of Route

B. Selection of Junctions

The Junctions were selected based on the Place where amount of traffic volume & Congestion is more and the studied information of every junction is noted below.

The information of each and every junction is collected from the traffic police who were taking care of traffic signal and the residence of the area and the shops in the study area.

Shantala Junction

KSR Railway station

Sangolli Rayanna Circle (Towards Okalipuram)

Okalipuram Bus stand and signal

Sujatha Talkies

Dr. Rajkumar Road

Sandal Soap factory

Yeshwanthpur Railway station

RMC yard

Goraguntepalaya

C. Data Type, Geometric Features and Remarks

SL NO	DATA TYPE	MEASUREMENTS	REMARKS
1	WIDTH OF THE ROAD	29m	Width of road has to be increased in order to avoid congestion.
2	CONDITION OF THE ROAD	Moder ate	Condition of road is Moderate, but still some potholes are present.
3	FOOTPATH	2.9m	Footpath as variable width and encroachment of foot path can be seen throughout the stretch.
4	PARKING	-	Since the parking is not provided vehicles are parked at the side of the can be seen.
5	NO OF INTERSECTIONS	1	Proper Traffic signals and traffic signs are being provided.
6	BUS BAYS	Not present	No separate lane for buses.
7	PEDESTRAIN MOVEMENT	Heavy	
8	SPEED BRAKERS	-	No speed breaker provided. There is need of speed breakers.
9	NOISE LEVEL	75Db	Noise level is moderate.

Fig 2A: Manhole at varying heights with respect to road surface

Fig 2B: Footpath encroachment

SL NO	DATA TYPE	MEASURMENTS	REMARKS
1	WIDTH OF THE ROAD	3.5m	No need of increase of width of road.
2	CONDITION OF THE ROAD	Under construction	Proper width is provided at junction but after this continuation road width is very less that is around only 18mt.
3	FOOTPATH	-	Due to the construction of road, carriage way width as reduced resulting in no footpath.
4	PARKING	-	No parking facilities available.
5	NO OF INTERSECTIONS	-	As per the plan of government, construction of road is done to make a signal free.
6	BUS BAYS	-	
7	PEDESTRAIN MOVEMENT	-	No pedestrian movement can be observed.
8	SPEED BRAKERS	-	No speed breaker available.
9	NOISE LEVEL	72Db	Noise level is moderate.

Fig 3A: Potholes Fig 3B: Construction in Progress

- Road construction started 4 years ago but not yet completed. There is a very slow progress in construction.
- Traffic umbrella has deteriorated. maintenance required.
- Medians are properly placed
- In some stretch a speed breaker sign is provided but no speed breaker present

SL NO	DATA TYPE	MEASURMENTS	REMARKS
1	WIDTH OF THE ROAD	24m	No need of increase of width of road.
2	CONDITION OF THE ROAD	Moderate	Construction of road can be observed with width 7m on one side road. Potholes can see.
3	FOOTPATH	3.2m	Good condition of foot path
4	PARKING	No parking facilities can seen	
5	NO OF INTERSECTIONS	1	Road markings not provided and traffic signals are not design to resist the heavy traffic, use Webster's method of signals system.
6	BUS BAYS	Not present	No separate bus lane is provided. Bus stop shelter is also not provided.
7	PEDESTRAIN MOVEMENT	Moderate	Sky walk or underpass must be provided.
8	SPEED BRAKERS	No speed breaker	There is no need of speed breaker.
9	NOISE LEVEL	86Db	Noise level is moderate.

Fig 4: Poor condition road fully deteriorated

- Any break down of single vehicle causes heavy road congestion
- In an 8mt lane width on one side around 2 to 3m of the road is used for parking. This is one of the major drawbacks of the road which causes delay.
- Foot path encroachment can be clearly seen due to presence of petty shops and construction work materials on poured hence pedestrians cannot walk safely.
- No umbrellas are provided for the traffic police
- There is a need of road markings and road signs throughout the stretch.
- As information's collected from the road users in the stretch, we have noticed there are many accident blackspots throughout they have be clearly studied and remedial measures need to be given.

SL NO	DATA TYPE	MEASURMENTS	REMARKS
1	WIDTH OF THE ROAD	28mt	No need of increase of width of road.
2	CONDITION OF THE ROAD	Good	Condition is good but some undulations are present
3	FOOTPATH	2m	Width may need to be increased if the pedestrian movement is observed
4	PARKING	Available	
5	NO OF INTERSECTIONS	Nil	
6	BUS BAYS	Good	
7	PEDESTRAIN MOVEMENT	Moderate	No need of sky walker
8	SPEED BRAKERS	Not present	Speed brakers are required because of falling gradient in road.
9	NOISE LEVEL	73.2Db	Noise level is moderate.

Fig 5: No Footpath

SL NO	DATA TYPE	MEASURMENTS	REMARKS
1	WIDTH OF THE ROAD	16mt	Width must be increased
2	CONDITION OF THE ROAD	Poor	At Some places potholes and undulations are present
3	FOOTPATH	3.5m	Condition is bad width is not uniform throughout and at some places it is in under construction
4	PARKING	Not available	Parking on streets is clearly visible hence increases the congestion. Particular sign boards should be provided.

5	NO OF INTERSECTIONS	4	More than 4 intersections are clearly visible and proper road markings are not specified
6	BUS BAYS	Not present	Bus enters into normal lane which causes delay
7	PEDESTRAIN MOVEMENT	Heavy/Moderate	Zebra crossing and walk signal needs to be Provided.
8	SPEED BRAKERS	Not required	-
9	NOISE LEVEL	78Db	Noise level is moderate.

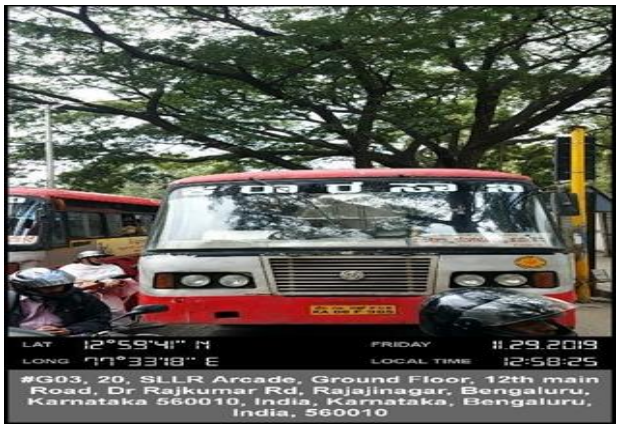

Fig 6: Breakdown of any single causing congestion

Fig 7: Parking of vehicles along Rajkumar road

- Any break down of single vehicle causes heavy road congestion
- In an 8mt lane width on one side around 2 to 3m of the road is used for parking. This is one of the major drawbacks of the road which causes delay.
- Foot path encroachment can be clearly seen due to presence of petty shops and construction work materials on poured hence pedestrians cannot walk safely.
- No umbrellas are provided for the traffic police
- There is an need of road markings and road signs throughout the stretch.
- As information's collected from the road users in the stretch, we have noticed there are many accident blackspots throughout they have be clearly studied and remedial measures need to be given.

SL NO	DATA TYPE	MEASURMENTS	REMARKS
1	WIDTH OF THE ROAD	30m	Width is not uniform throughout
2	CONDITION OF THE ROAD	Bad	Presence of potholes is more and proper alignment is not done
3	FOOTPATH	2-3m	Footpath is not uniform throughout and it is worn out at some places
4	PARKING	Not provided	Cars and 2-wheelers are parked on road side which causes congestion
5	NO OF INTERSECTIONS	3	Markings should be provided
6	BUS BAYS	Present	Bus stop signs must be provided at stop.
7	PEDESTRAIN MOVEMENT	High	Sky walker is under construction
8	SPEED BREAKERS	Present	Speed breakers are present wherever needed.
9	NOISE LEVEL	70Db	Noise level is moderate.

Fig 8: Road under construction, no road marking

SL NO	DATA TYPE	MEASURMENTS	REMARKS
1	WIDTH OF THE ROAD	42m including service road	No need for increased width.
2	CONDITION OF THE ROAD	Moderate	Potholes are present and undulations can be seen
3	FOOTPATH	3m	Not in good condition and it is worn out at some places
4	PARKING	Absent	Vehicles are parked on road side causes delay and congestion proper sign board must be implemented
5	NO OF INTERSECTIONS	-	-
6	BUS BAYS	Present	-
7	PEDESTRAIN MOVEMENT	Moderate	Sky walker are present.

8	SPEED BRAKERS	Not present	Not required
9	NOISE LEVEL	85Db	Noise level is moderate.

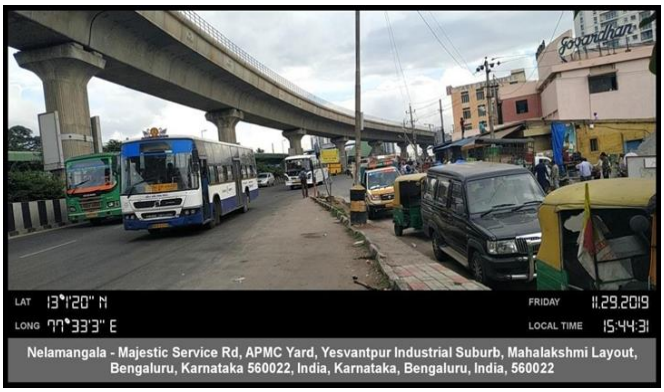

Fig 9: No proper median and parking on road

SL NO	DATA TYPE	MEASURMENTS	REMARKS
1	WIDTH OF THE ROAD	3.4m	Width is not uniform throughout
2	CONDITION OF THE ROAD	moderate	Potholes and undulations are more.
3	FOOTPATH	Absent	Footpath must be provided as pedestrian movement is high
4	PARKING	Absent	All trucks and heavy loaded vehicles are parked in the street which causes congestion
5	NO OF INTERSECTIONS	-	-
6	BUS BAYS	Present	These are occupied by trucks and other vehicles
7	PEDESTRAIN MOVEMENT	High	Footpath should be provided and sky walker is necessary as market is present.
8	SPEED BRAKERS	Absent	-
9	NOISE LEVEL	80Db	Noise level is moderate.

Fig 10: Truck parking on road side and their movement in RMC yard

SL NO	DATA TYPE	MEASURMENTS	REMARKS
1	WIDTH OF THE ROAD	36m	Width needs to increased due to the congestion in peak hours.
2	CONDITION OF THE ROAD	Moderate	Potholes everywhere can be observed.
3	FOOTPATH	1-3m	Width is not uniform throughout and footpath condition is poor.
4	PARKING	Absent	Vehicles are parked at road side which causes traffic congestion.
5	NO OF INTERSECTIONS	3	Proper markings and sign boards not present and Traffic signal time must be altered.
6	BUS BAYS	Present	But Trucks and heavy loaded vehicles enter into bus lane which causes delay and congestion.
7	PEDESTRAIN MOVEMENT	High	No provision of sky walker and road markings.
8	SPEED BRAKERS	Absent	Required at some places.
9	NOISE LEVEL	103.7Db	Noise is very high in this junction.

Fig 11: Noise level measured by sound level meter.

IV. CONCLUSION

In this research we have worked on Congestion problem for such special areas which have dense traffic density. The system works on traffic related problems such as traffic jam; un reasonable latency time of stoppage of vehicle, emergency vehicles or forcibly passing, etc.., can be solved. By using this system configuration, we try to reduce the possibilities of traffic jams, caused by traffic lights. Number of passing vehicle in the fixed time slot on the road decide the density range of traffics and on the basis of vehicle density calculation, microcontroller decide the traffic light delays.

REFERENCES

[1] Birva B. Shah, Prof. N. G. Raval, "Estimation of Capacity for Arterial Road of Urban Area" International Journal of Innovative Research in Technology, 2016, 63-64.

[2] Ashish Dhamaniya, and S. Chandra.2013. "Concept of Stream Equivalency Factor for Heterogeneous Traffic on Urban Arterial Roads." Journal of Transportation Engineering/Volume 139, Issue 11/2013.

[3] Nabanita Roy, Rupali Roy, Hitesh Talukdar, PritamSaha, "Effect of Mixed Traffic on Capacity of Two-Lane Roads: Case Study on Indian Highway"10th International Science Conference Transbalita, 2017.

[4] Pothula sanyasi Naidu1, Gundu Navya2, Chukka Deepika3 , Mahesh Yamala4, "Capacity of Road with vechile Characteristics and Road Geometrics Interface Modelling", SSRG International Journal of Civil Engineering (SSRG-IJCE) – volume 2 Issue 10 October 2015.

[5] SaiKiran M.1 & Ashish Verma2," Review of Studies on Mixed Traffic Flow: Perspective of Developing Economies" Springer International Publishing Switzerland 2016 and Technology, 2018, e-ISSN-2395- 0056.

[6] Amudapuram Mohan Rao, KalagaRamachandra Rao, Measuring Urban Traffic Congestion-A Review, International Journal Traffic and Transport Engineering, August 2012, 2(4): 286-305.

[7] Ashish Padshala, Traffic Studies of Urban Mid Block Section: A Case Study of Pragatinagar to Akhbarnagar & Akhbarnagar to Ranip Cross Road, International Journal of Research in Engineering and Technology, June-2014, Vol. 03. Issue 6, ISSN: 2321- 7308.

[8] Babitha Elizabeth Philip, Jaseela K. H,Traffic Flow Modeling and Study of Traffic Congestion, International Journal of Scientific Engineering and Research, January 2016, Vol. 4. Issue 1, ISSN 2347- 3878.

[9] Dr. Benjamin O. Uwadiegwu, Factors Responsible for Traffic Congestion in Nigeria-A Case Study, Journal of Environment and Earth Science, 2013, Vol. 3, No.3, ISSN 2225-0948.

[10] Joseph. O. Ukpata, Anderson A. Etika,Traffic congestion in Major Cities of Nigeria, International Journal of Engineering and Technology, August 2012, Vol. 2 No. 8, ISSN 2049-3444.

[11] M. AbsarAlam and Faisal Ahmed, Urban Transport System and Congestion – A Case Study, Transport and Communications Bulletin for Aisa and the Pacific,2013, No. 82.

[12] Olusina, J.O. and Samson, A.P., Determination of Predictive Models for Traffic Congestion in Lagos Metropolis, International Journal of Engineering and Applied Science, July 2014, Vol. 5. No. 2, ISSN 2305-8269.

[13] Prof.Gopal R. Patil, Traffic Volume Count Survey in IIT Bombay Campus, Indian Institute of Technology Bombay, February 2015.

[14] Saleem-ullahLar, Xiaofeng Liao and SongtaoGuo, Modeling TCP NewReno Slow Start and CongestionAvoidance using Simulation Approach, International Journal of Computer Science and Network Security, January 2011, Vol. 11. No.1.

[15] A. K.Vidhya, "International Journal of Innovative Research in Science, Engineering and Technology," Density Based Traffic Signal System , vol. Volume 3, no. Issue 3, 2014.

[16] Inam Ullah Khan, Shaheen Ahmad, Nazia Azim, Syed Bilal Hussain Shah," Wireless sensor networks & Applications in Different Technologies", International Journal of Mechanical Engineering and Computer Applications, IJMCA, Vol. 5, No. 2, March – April.

[17] Whittemore AH and BenDor TK (2019) Exploring the acceptability of densification: How positive framing and source credibility can change attitudes. Urban Affairs Review 55(5): 1339–1369.

[18] Yadavalli A, McFarland CK and Rainwater B (2018) State of the cities 2018. Available at: www.nlc.org/resource/state-of-the-cities-2018 (accessed 1 March 2019).

[19] Patterson KL, Ranahan M, Silverman RM, et al. (2017) Community benefits agreements (CBAs): A typology for shrinking cities. International Journal of Sociology and Social Policy 37(3): 231–247.

[20] Perrone C (2019) 'Downtown Is for People': The street-level approach in Jane Jacobs' legacy and its resonance in the planning debate within the complexity theory of cities. Cities 91: 10–16.

[21] O'Connell L (2009) The impact of local supporters on smart growth policy adoption. Journal of the American Planning Association 75(3): 281–291.

UTILIZATION OF BLACK COTTON SOIL IN THE MANUFACTURE OF BRICKS

Pruthviraj S, Renuka prasad T, Prajwal S Gowda, Kiran H.D

UG students

Department of Civil Engineering

Sapthagiri college of Engineering, Hesaraghatta main road, Bangalore, Karnataka, India

ASTRACT – With depletion of natural resources due to increase in constructional activities, the construction industry has found new alternatives to meet the sustainable infrastructural requirements. Alternative materials for use in brick has evolved over decades, lately research is done in use of black cotton soil in manufacture of bricks. In this study, an attempt as been made to manufacture bricks with black cotton soil and their properties are compared with red soil bricks. Since the bearing capacity of black cotton soil is moderately less compared to red soil, some admixtures like coal powder, lime powder, rice husk powder are added in order to increase the compressive strength of bricks. It is seen that a ratio of 92.5% of black cotton soil, 2.5% of coal powder, 2.5% of lime powder and 2.5% of rice husk powder has resulted in stronger brick. From the results, it can be seen that both compressive strength of bricks made up of black cotton soil is stronger compared to the strength of normal bricks.

INTRODUCTION

A brick is a solid block which is used to build walls, pavements and other elements in masonry construction. The term 'brick' denotes ''block composed of dried clay''. But now, some chemically cured construction blocks are used in the place of clay.

Bricks are produced in numerous classes, types, materials, sizes, produced in bulk quantities, Varies with region and time period.

The process of manufacturing of bricks from clay involves preparation of clay, molding and then drying and burning of bricks in kilns. Bricks are building materials which are generally available as rectangular blocks. The bricks do not require any dressing and brick laying is very simple compared to stone masonry.

A brick is most artefact thing required to build walls, pavements and parts of masonry construction. Usually, bricks are unit stacked along or set as brick work along with mortar to build a permanent structure. Within the world Asia produces 87 of the overall production of the brick. Brick are the unit generally made in common or normal size in bulk quantities they need to be considered one in all the longest enduring and strongest artefact employed in twentieth century.

What do you know about BLACK COTTON SOIL?

- Black cotton soil has very low bearing capacity, high swelling

capacity and shrinkage characteristics than other soils which is used for construction.

- Black cotton soils are expansible soils and are inorganic clays of high to medium compressibility.
- They are highly compressible.
- It is inorganic clay formed in regions having poor drainage conditions.
- It is mainly known as black cotton soil because this soil is most suitable for cotton crop.
- Black cotton soil is basically found in MAHARASTRA, SAURASTRA, MALWA, MADHYA PRADESH and CHATTISHGARH.

Finally, the question is, is it possible to manufacture bricks from BLACK COTTON SOIL? the answer is YES. According to some sources, by adding some impurities it is possible to manufacture bricks from black cotton soil and it is cheaper and the manufacture procedure will be easier compared to normal bricks.

OBJECTIVES

- To make an eco-friendly and economical brick.
- Try to increase the compressive strength of the brick.
- Make use of huge amount of black cotton soil in local areas.

Materials

1. Black cotton soil.
2. Rice husk.
3. Coal powder.
4. Lime powder.

Fig(i) Black cotton soil

Black cotton soil [fig(i)] is a clayed type of soil also known as “EXPANSIVE SOIL”. It has very low bearing capacity, high swelling and shrinkage characteristics. Hence stabilization is needed for this soil before subjecting it to any construction purpose.

Fig(ii) Rice husk powder

Rice husk[fig(ii)] is the hard protecting coverings of grains of rice. In the addition to protecting rice during the growing season, rice

husk can be put to use as an INSULATION material, fertilizer or fuel etc. It is used in its powder form.

Fig (iii) Coal powder

This is the powdered form of coal[fig(iii)]. which is created by crushing of coal. This is product obtained during mining. Coal powder is used in concrete. This is used to give stability to soil in brick manufacture.

Fig (iv) Lime powder

Lime powder[fig(iv)] is obtained by calcination of limestone. It has cementing capability. It can be used in concrete as cementitious material. Lime is used in manufacture of cement.

TESTS CONDUCTED ON BLACK COTTON SOIL

- Specific gravity test
- Liquid limit test
- Plastic limit test
- Standard proctor compaction test

SPECIFIC GRAVITY TEST:

Specific gravity of soil is defined as the weight of soil to weight of equal volume of water.

It tells how much heavier or lighter the material is than the water. This test covers the determination of specific gravity of soil.

The standard value is 2.65.

Fig (v) Soil in pycnometer

DETERMINATION	TRIAL 1	TRIAL 2
Weight of pycnometer (W1)g	648	648
Weight of pycnometer + dry soil (W2)g	848	847
Weight of pycnometer + soil + water (W3)g	1600	1659
Weight of pycnometer + water (W4)g	1471	1489
Specific gravity	2.81	2.31
Average Specific Gravity	2.56	

LIQUID LIMIT TEST

Fig (vi) Liquid limit test

The liquid limit is the moisture content at which the soil passes from the plastic state to the liquid state as determined by the liquid limit test.

TRIAL	1	2	3	4	5
% Water added	20%	25%	30%	35%	40%
No of blows	34	30	25	22	18
Empty weight of container (W1)	33	31	32	36	30
Weight of wet soil + container (W2)	37.6	33.7	34.38	37.69	33.16
Weight of oven soil + container (W3)	39.6	34.8	35.2	38.2	34.3
Weight of wet soil	4.6	2.7	2.3	1.6	3.1
Weight of dry soil	6.6	3.8	3.2	2.2	4.3
Water content	69.76	70.94	73	74.12	75.5

Average water content of soil 72.68

PLASTIC LIMIT TEST

Fig (vii) Plastic limit test

The plastic limit is the moisture content that defines where the soil changes from a semi-solid state to the plastic state.
It may also defined as that water content at which soil starts crumbling when rolled into threads of 3mm dia .

DETERMINATION NUMBERS	1
Container number	28
Weight of the container W1(g)	30
Weight of the soil + wet soil (W2)g	34.5
Weight of container + oven dry + soil (W3)	33
Weight of Wet soil	1.5
Weight of dry soil	3
Water content	50

STANDARD PROCTOR COMPACTION TEST

Compaction is the application of mechanical energy to a soil so as to rearrange its particles and reduce the void ratio. it is applied to improve the properties of an existing soil or in the process of placing fill such as in the construction of embankments, road bases runways, earth dams

Water Content

Container no	34	22	21
Mass of container(W1)	30	32	29
Mass of container + wet soil (W2)	42.2	41.7	38.4
Mass of Container + dry soil (W3)	40.9	39.5	37.5
Water Content	11.9	19.6	10.5

DETERMINATION	1	2	3
Mass of mold + compacted soil(g)	6938	7053	7208
Mass of mold	4554	4554	4554
Mass of compacted soil (g)	2384	2509	2654
Bulk Density g/cm3	2.52	2.65	2.81
Dry density g/cm3	2.14	2.16	2.18

METHODOLOGY

- Impurities present in the soil must be removed .
- After removing the impurities, lumps should be blended and water should be added homogeneously.
- It should be left for 3 days.
- Admixtures like coal powder, lime powder, rice husk powder should be added to the soil and it should be mixed properly.
- The mixture should be poured into the brick mold.
- Bricks should be burned in kilns.

ISBN: 979-88-35073-61-0

Fig (ix) Bricks made with black cotton soil

Fig (x) Bricks made with admixtures

COMPRESSION STRENGTH TEST

The average compressive strength of brick made from black cotton soil is 5.68 N/mm^2.

The compressive strength of brick made from red soil is 4.25 N/mm^2

COMPRESSION STRENGTH CHART:

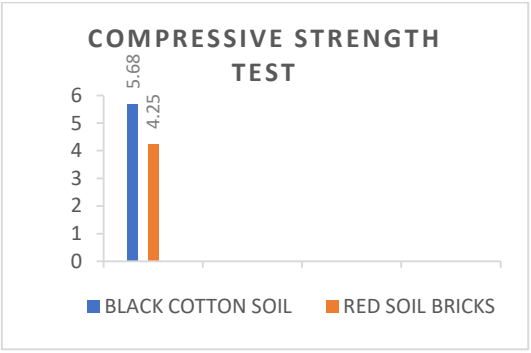

RESULT AND DISCUSSION:

- The specific gravity test for the black cotton soil is conducted according to IS-2720, the standard value for black soil lies between 2.57 to 2.35 respectively, in practical laboratory test we obtained the value of 2.56, hence the results are within the limits and the soil can be used for manufacturing of bricks.
- In standard proctor compaction test as per IS-2720, for different percentage of moisture content and corresponding values of dry density of soil are observed. The maximum dry density obtained is 2.16 gm/cc at optimum moisture content of black cotton soil at 21% of water. This results shows that soil gives better strength at the water content of 21%.
- Values of liquid limit and plastic limit used to classify fine grained soil. It gives us information regarding the state of consistency of soil. The values obtained for liquid limit is 72.68% and plastic limit is 50% for the soil sample.
- As per IS code provisions the standard dimensions of first class

brick is 19cm x 9cm x 9cm. In the laboratory test the dimensions of black cotton soil bricks are 22cm x 11cm x 8cm .

- In the laboratory test as we performed the maximum compressive strength of brick using black cotton soil obtained is 5.68 N/mm^2. But the red soil brick compressive strength is 4.25 N/mm^2. Hence the compressive strength of black cotton soil is more than red soil brick, so we can use this bricks in construction works.

CONCLUSION :

Bricks are normally prepared from red soil or cementitious materials such as fly ash, GGBS etc. The researches on the production of bricks using black cotton soil is done very rarely. But, the bricks made from black cotton soil are highly effective compared to normal bricks. Black cotton is a type of soil which is having high bonding strength when it is mixed with admixtures. It has more adhesive property compared to red soil. The strength of bricks is expected more compared to normal bricks. Since, the bricks are more economical, soil is easily available in local areas and it is stronger. It is a good idea to use black cotton soil in the manufacture of bricks in places where black cotton soil is highly available.

REFERENCES

1. Maruthi Balekatti, et al.,(2018), paper entitled as “UTILIZATION OF BLACK COTTON SOIL IN THE MANUFACTURE OF BRICKS”.

2. Patel Adit Kanti bhai, et al.,(2018), paper entitled as “APPLICATION OF BLACK COTTON SOIL BRICK IN CONSTRUCTION INDUSTRY”.

3. Hubli Kiran, et al.,(2018), paper entitled as “A STUDY ON MANUFACTURING OF BRICKS USING BLACK COTTON SOIL AND RED SOIL”.

4. Pragati Saha, Kshama singh,(2018), paper entitled as “COMPACTION OF BLACK COTTON SOIL BRICK WITH NORMAL CLAY BRICK”.

5. Panchal Darshan, et al.,(2014), paper entitled as “COMPARISION OF BRICK MADE FROM BLACK COTTON SOIL WITH VARIOUS ADMIXTURE TO THE NORMAL BRICK”.

A Review Paper on Study on Properties of Concrete using Waste Rubber Tire pieces as Replacement

Neha Murthy G, Abhishek D , Moksha Lakshmi B R, Darshan R , Nagarjun Gowda B S (Assistant Professor)
Department of civil Engineering

Sapthagiri College of Engineering

Bengaluru, India
nehamurthy1824@gmail.com ,abhishek29gowda@gmail.com ,mokshalakshmibr@gmail.com ,darshanbharadwaj7777@gmail.com

ABSTRACT

The tire is one of the major pollutants which release greenhouse gases when burnet, causing air pollution and depletion in ozone layer. Due to this a proper method should to be adopted for the tire disposal . Rubber is thought to be a potential material for use in concrete technology. The ductile behaviour will enable the concrete material to have the capacity to deform and support flexural and tensile loads, even after initial cracking . Tyres cut into pieces with maximum size of 20 mm to use as coarse aggregate, and crumb rubber tyres used as fine aggregate .As this scrap rubber waste is an elastic material having less specific gravity, energy absorbent material can be used as a replacement material for obtaining lightweight concrete. It can be used as one of the alternatives for the natural aggregates used as structure and structural members. The concrete is a predominate material used in construction and it competes with all other major construction materials. The load bearing capacity of such structures is low. This has the additional advantages of saving in natural aggregates used in the production of concrete which are becoming increasingly scarce. In this paper we will study about compression strength of concrete containing recycled tyre or rubber material aggregates, to assess its suitability as a construction material.

KEYWORDS

Concrete, waste rubber tyres, compressive strength ,Aggregate

I.INTRODUCTION

The concrete is a predominate material used in construction and it competes with all other major construction materials such as cement, coarse aggregate and fine aggregate. Aggregates used in concrete serve as filler and densify the material. Concrete is the most widely use material for construction due they are ease in workability and its availability. There are many drawbacks on aggregates in concrete when used in large scale. The aggregates are obtained by quarry and crushing of rocks and mountains; these processes are hazardous and a dd a negative impact on environment. The waste can be used as a replacement of aggregates in concrete. Waste tire is one of the most significant environmental hazards in most of countries. Worldwide, the production of rubber increases every year. Burying scrap tyres in landfills is not only wasteful, but also costly. Research have shown that scrapped rubber tyres contain materials that do not decompose under environmental conditions and cause serious problems. Using the tier as a replacement cannot obtain the compression strength as of the ordinary concrete but a suitable strength still can be obtained for the use in structures. Crumb rubber modified bitumen (CRMB) is used annually in road construction. New regulations introduced in 2016 allow for import of waste tyres for recycling.

II. Literature Review

- **Ground Waste Tire Rubber as a Total Replacement of Natural Aggregates in Concrete Mixes: Application for Lightweight Paving Blocks Matteo Sambucci and Marco Valente.2021**

It observed that , according to American society for testing and materials (ASTM) C 109/109M standard method [39], the test was performed by using a Z150 (150 kN load cell) testing system (Zwick – Roell, Ulm, Germany). The preload was 5 N, and the loading rate was 1 mm / min. The compressive strength reduction in rubberized concrete or mortars is evidence unanimously shared by researchers operating in this field [6,10,17- 22,46,47,51 – 53].A negative effect of ground tire rubber (GTR) on mechanical performance is absorbed. . Furthermore, by balancing the content of the two polymer fractions it was possible to achieve suitable mechanical properties for the reference applications proposed in this work. Indeed, RP50-RG50 sample yield a compressive strength (17.9 MPa) within the range recommended by Eurocode 2 standard for paving unit applicable in driveways, garages, or sidewalks.

- **The use of recycled polymers and rubbers in concrete Felipe J A et.al.2004**

Ordinary Portland cement , Fine aggregates was replaced with the weight % of rubber used was 5%,10% with the particle size of 0.25MM and 0.59MM,scrap rubber was used untreated with a solution of NaOH, W/C-0.53.Strength reduction of 50% was absorbed for a mix with 14% replacement study. This concrete can be used for constructing low load carrying structures.

- **Recovery and Modification of Waste Tire Particles and Their Use as Reinforcements of Concrete Eduardo Sadot Herrera-Sosa et.al.2015**

The research is absorbed that the compressive strength values vary as a function of size and concentration of waste tire particles. It is observed that when increasing the waste particle concentration and adding large particles more air content is obtained. Moreover, all these kinds of concretes have lower values than those for control concrete, namely, 24.1MPa. Only 10% of tire particles of 2.8mm showed higher values than those for control concrete, up to 23% of improvement. . It can be seen that concrete with concentrations no greater than 10% of particles of 2.8 mm show the highest values compared to those for the control concrete for compressive strength.

- **Use of waste rubber tyres as aggregate in concrete Abubaker M. Almaleeh.2016**

The report was prepared for the replacement of the rubber tyres particles as aggregates in the conventional concrete was undertaken in three phases. In the first phase, fine rubber tyres aggregates were used to replace 50% of the normal sand. This replacement was done to check the influence of the fine rubber tyres in the behaviour of the normal concrete. The second phase consisted of 50% replacement of normal gravel by coarse rubber tyres. All samples were cured for 7 days. The compressive strength as showed decreased significantly in both BS and ACI method. The concrete in BS method lost up to 80% of the strength, when the fine rubber tyres aggregates were added. In the ACI method, the rubberized concrete strength dropped by 85% of the control strength. Compressive strength of rubberized concrete is suitable for footpaths. At lower replacement, the strength was about 5 MPa which it could be enough.

- **Effects of Concrete by Using Waste tyre Rubber (Solid Waste) Shanmugapriya M 2015**

In the research its reported that ordinary Portland Cement (OPC) of 53 Grade was used for the entire investigation. The specific gravity of ordinary Portland cement is 3.15.Waste tyre was procured and specific gravity was 1.18 and unit weight 1150 kg/m^3 and the tyre is cut into pieces with a grading of 12 to 20 mm size aggregate. The specimen is tested after 28 days curing. The control specimen C, 3RA, 6RA, 9RA and 12RA in each 3 number of specimens is tested. The value of compressive strength even though comes to a value of 21.20 N/mm^2 this value is very much higher than the prescribed strength of the Light Weight Concrete. The reduction in compressive strength is up to 42% but the compressive strength at 12% of rubber content gives a compressive strength of 21.11N/mm2 which is more than the requisite compressive strength of Light Weight Concrete.

- **Impact of Chemically Treated Waste Rubber Tire Aggregates on Mechanical, Durability and Thermal Properties of Concrete Yih Chen Khern et.al.2020**

In the research, compressive strength at 7 and 28 days is carried out. At 7 days , untreated rubber aggregate concrete (R8) showed around 8% lower compressive strength compared to the reference concrete (REF).However, when rubber aggregates were pre-treated, the compressive strength of concrete for R8-W2h, R8-W24h and R8-W72h were 5.15, 5.86, and 5.11% lower than that of REF concrete, respectively . For the rubber aggregates treated with NaOH, the compressive strength of concrete for R8- N2h, R8-N24h and R8-N72h were 4.74, 5.37, and 5.07% lower compared to the REF concrete, respectively. Similarly, when the rubber aggregates were treated with Ca(ClO)2, the compressive strength of concrete for R8-C2h, R8-C24h, and R8-C72h were 5% lower, 1.87% lower and 2.91% higher, respectively, than that of REF concrete. Replacing 8% of natural aggregates with tire rubber resulted in 18% lower compressive strength at 28 days compared to the reference mixture. On the other hand, when tire rubber aggregates were treated with NaOH and Ca(ClO)2 resulted in lower reduction of compressive strength: compared to the reference, concrete containing rubber aggregates treated by Ca(ClO)2 for 72 h resulted in strength similar to the reference concrete.

- **Re-Use of Waste Tire Rubber Pieces in the Production of Light Weight Concrete K.Charankumar et.al.2013**

As per the Journal, the compressive strengths of concrete specimens were determined after 7,28,56 days of standard curing. It is observed that as the curing increases the compressive strength also increases for every grade of concrete prepared . For rubberized concrete, the test results show that the addition of rubber aggregate resulted in a significant reduction in concrete compressive strength compared with the control concrete. This reduction increased with increasing percentage of rubber aggregate.

- **PRODUCTION OF LIGHTWEIGHT CONCRETE FROM WASTE TIRE RUBBER CRUMB Joseph Olawale AKINYELE et.al.2016**

In this research, rubber crumb was used to partially replace fine aggregates in concrete at 0 , 4 , 8 , 12 , and 16% and represented as M0 , M4 , M8 , M12 , AND M16 respectively. The 28 days compressive strength showed that there was a general reduction in strength. The work concluded that rubber crumb can be used to replace fine aggregate up to 16% , in light weight concrete. The result obtained for the compressive strength gave a positive side of the research work because the 28 days compressive strength for the M16 concrete mix is higher than the recommended compressive strength of 15 N/mm2 for reinforced light weight concrete. Hence rubber crumb can conveniently replace fine aggregate in concrete up to 16% for light weight concrete.

CONCLUTION

By reusing tire rubber for the construction purpose reduces the pollution in the environment. When the tires are to disposed it done in two ways by burning which produce Greenhouse gases which leads to the depletion of ozone layer ; And by land disposal, which takes up space in landfills. The tires in construction are used to replace fine aggregates and coarse aggregates ,they are used to produce light weight concrete. They satisfy the standardization for compression strength . These types of structures are having low load carrying capacity ;thus, they are use as partition wall ,frame works. They have good thermal conductivity so they are used to freezer construction. Due to the presence of tires, it exhibits high yield structures. The use of natural aggregates is reduced which decreases the scarcity of aggregates

ACKNOWLEGEMENT

The authors would like to thank Nagarjun Gowda B S Assistant Professor, Department of Civil Engineering , Dr. Rajeshwari HOD, Department of Civil Engineering, Dr. H Ramakrishna the Principal of Sapthagiri college of engineering , Bengaluru for their constructive comments and suggestions in preparing the manuscript.

REFERENCE

[1] K.Charankumar , Dr. S. Siddi Raju , Re-Use of Waste Tire Rubber Pieces in the Production of Light Weight Concrete , International Journal of Science and Research (IJSR) ISSN (Online): 2319-7064 Index Copernicus Value (2013): 6.14 | Impact Factor (2013): 4.438.

[2] Yih Chen Khern1 , Suvash Chandra Paul1,2 , Sih Ying Kong1 , Adewumi John Babafemi3 , Vivi Anggraini1 , Md Jihad Miah4 and Branko Šavija5 * , Impact of Chemically Treated Waste Rubber Tire Aggregates on Mechanical, Durability and Thermal Properties of Concrete, South China University of Technology,Published: 15 April 2020.

[3] Priyanka Asutkar a,⇑ , S.B. Shinde a , Rakesh Patel , Study on the behaviour of rubber aggregates concrete beams using analytical approach , a MGM Jawaharlal Nehru Engineering Collage, Aurangabad, MH, India b Sagar Institute of Research Technology and Science, Bhopal, MP, India,26 July 2016.

[4] Pooja Lamba1 · Dilraj Preet Kaur1 · Seema Raj1, Jyoti Sorout1 Recycling/reuse of plastic waste as construction material for sustainable development: a review, 6 October 2021.

[5] Shanmugapriya M , Effects of Concrete By Using Waste tyre Rubber (Solid Waste) , research Scholar, Department of Civil Engineering, Sathyabama University,Chennai, Tamilnadu, India, ISSN 0973-4562 Volume 10, Number 5 (2015) pp. 13221-13230

[6] Abubaker M. Almaleeh1,2* , Stanley M. Shitote3 and Timothy Nyomboi3, Use of waste rubber tyres as aggregate in concrete , Vol. 8(2), pp. 11-19, February 2017 .

[7] Vidat Choudhary1, Abhay Choudhary2 , USE OF TYRE WASTE IN CONCRETE: A REVIEW , International Research Journal of Engineering and Technology (IRJET) e-ISSN: 2395-0056 Volume: 04 Issue: 10 | Oct -2017 www.irjet.net p-ISSN: 2395-0072.

[8] Matteo Sambucci * and Marco Valente , Ground Waste Tire Rubber as a Total Replacement of Natural Aggregates in Concrete Mixes: Application for Lightweight Paving Blocks , : 7 December 2021 .

[9] Joseph Olawale AKINYELEa,b, Ramhadhan Wanjala SALIMa , Williams Kehinde KUPOLATIa , PRODUCTION OF LIGHTWEIGHT CONCRETE FROM WASTE TIRE RUBBER CRUMB , Tshwane University of Technology, Civil Engineering, Faculty of Engineering and Built Environment, Pretoria, 001 South Africa bFederal University of Agriculture, Civil Engineering, College of Engineeing, Abeokuta, 0022 Nigeria Received 14 May 2016; accepted 03 July 2016.

[10] Eduardo Sadot Herrera-Sosa,1 Gonzalo Martínez-Barrera,2 Carlos Barrera-Díaz,3 Epifanio Cruz-Zaragoza,4 and Fernando Ureña-Núñez5 Copyright © 2015 Eduardo Sadot Herrera-Sosa et al. , Recovery and Modification of Waste Tire Particles and Their Use as Reinforcements of Concrete , 22 June 2015.

SOLID WASTE MANAGEMENT: A case study of

Hanumantharaja S C, Gurucharan Reddy P S, Naveen Gowda K R, Dilip K S, Dr. Rajeshwari R
Department of Civil Engineering, Sapthagiri College of Engineering
#14/5 Chikkasandra, Hesaraghatta main road, Bengalore-57, India
1 rajahanumantharaja@gmail.com
2 reddygurucharana@gmail.com
3 dilipks03006@gmail.com
4 naveengowdakr148@gmail.com, hodcivil@sapthagiri.edu.in

ABSTRACT - Solid waste disposal is a major challenge in many industrialized and developing nation, both in metropolitan regions as well as rural ones. The collection and disposal of municipal waste is a serious issue faced by ~~facing~~ metropolitan areas in many nations today. An effective MSW management strategy must satisfy all of these criteria: financial viability, technical feasibility, social and legal acceptability, and ecological friendliness. For managing solid waste, we use composting, incineration and burning and landfilling technique. For organic waste we use commonly composting method.

Composting is the controlled conversion of degradable organic products and wastes into stable products with the aid of microorganisms. Composting is a long-used technology, though it has some shortcomings that have reduced its extensive usage and efficiency. The shortcomings include pathogen detection, low nutrient status, long duration of composting, long mineralization duration, and odor production. These challenges have publicized the use of chemical fertilizers produced through the Haber-Bosch process as an alternative to compost over time. Chemical fertilizers make nutrients readily available to plants, but their disadvantages outweigh their advantages. For example, chemical fertilizers contribute to greenhouse effects, environmental pollution, death of soil organisms and marine inhabitants, ozone layer depletion, and human diseases. These have resulted in farmers reverting to the application of composts as a means of restoring soil fertility. Composting is a fundamental process in agriculture and helps in the recycling of farm wastes. The long duration of composting is a challenge; this is due to the presence of materials that take a longer time to compost, especially during co-composting This review discusses the proper management of wastes through composting, different composting methods, the factors affecting composting, long duration composting, the mechanism behind it, the present trends in composting and prospects. The extraction of mono-fertilizers from compost, development of strips to test for the availability of heavy metals and pathogens as well as an odor trapping technique can go a long way in enhancing composting techniques. The addition of activators to raw materials can help to improve the nutritional quality of compost. This review further recommends that degradable organic material in which composts slowly should be assessed for their ability to mineralize slowly, which could make them advantageous to perennial or biennial crops. Viricides, fungicides, anti-nematodes, and anti-bacterial of plant or organic sources could as well be added to improve compost quality. The enhancement of composting duration will also be usefuli

INTRODUCTION

The most pressing problem faced by any urban center in India today is Municipal Solid Waste Management (MSWM). Rapid

urbanization and changing lifestyles have led to the generation of huge amounts of garbage and waste in the urban areas, so much so, over the past few years, just the handling this Municipal Solid Waste (MSW) has assumed the proportion of a major organizational, financial and environmental challenge.

Despite MSWM being a major task of the local governments, typically accounting for a sizeable portion of the municipal budget - about 20% to 50%, yet the Urban Local Bodies (ULBS) are unable to provide effective services. Most of the ULBs do not even have reliable MSW generation estimates.

An unfortunate fallout of rapid urbanization without the adequate infrastructure backup is that in all Indian cities/towns, disposal of waste is done indiscriminately, leading to stray animal menace, clogged drains and spread of diseases. The process of collection, transportation and disposal of MSW is not complete in most of the cities/towns with garbage heaps remaining unattended until the severity reaches with unmanageable proportions. Also, the high organic content of Indian MSW, compounded by the hot and humid tropical climate leads to the rapid decomposition of the uncollected waste and is an ever-present health hazard. In addition, the contamination of MSW by bio-medical and industrial hazardous waste is a growing concern.

METHODOLOGY

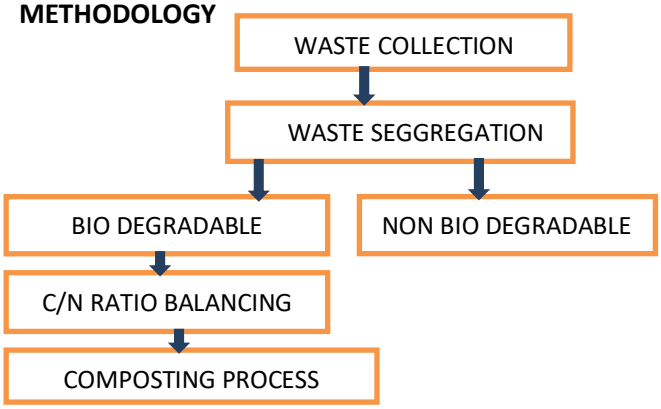

1) WASTE COLLECTION

The collection of waste is taken place in two types.

First one is door to door collection

It takes place in residential area where a waste collection vehicle can entered the residential area and collect the waste from household.

Community bins

It is placed in public places where collection of waste is more and it is mixed with all types of waste.so before treating the waste .we must first segregate the waste into different types.

2) WASTE SEGGREGATION

The segregation of waste is taken place by using IOT based techniques. In this we use some hardware material and software methodology is required for segregation of waste

Material and methods

- Inductive proximity sensor
- Dc motor
- Arduino uno r3
- Software methodology

A) Inductive proximity sensor.

It is operate under the principles of inductance. It states that when coil rotate it creates magnetic field around it.

The main components of the inductive proximity sensor have four components.

- Coil
- Oscillator
- Detection circuit

 Output circuit

When the coil starts rotating it creates magnetic field and it attracts the magnetic particle. If any particle present in solid waste.

B) DC motor

It is an electrical machine it converts electrical energy into mechanical energy.it is used to rotate the waste bin based upon required conduction.

C) Arduino UNO r3

The Arudino UNO is a microcontroller board based on ATmega328. It has 14 digital input/output, 6 analog inputs, ceramic sensors, USB connection, a power jack and reset button. It contains everything needed to support the microcontroller simply connected to the computer with USB cable.

D) Method

When waste is dumped it is sensed by inductive sensors and turns accordingly to their respective bins by using software in arudino to control speed of DC motor and non dection of empty container.

Practical working method

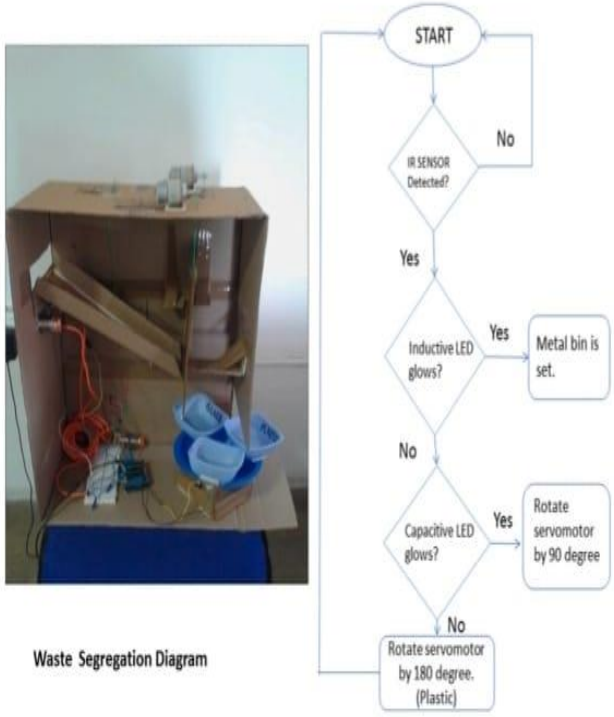

Fig. 1. Smart waste dustbin depiction with device and flow chart implementation.

2) BIO DEGRADABLE WASTE

After segregating the waste into bio degradable and non bio degradable, bio degradable waste are sent to composting process and non bio degradable waste like glass, plastic etc are sent to burning and incineration process.

4) COMPOSTING PROCESS

At present condition the waste vehicle can collect the waste from bins and dump the waste in to composting pits. And after dumping it will take to time for decaying, generally a composting pit is designed for 200 kg capacity of solid waste and it will take two and half month for complete decaying/ composting. Instead of doing this manner if we adopt some technical aspects before dumping the waste in to composting pits definitely we can manage the solid waste in good manner.

*CARBON /NITROGEN RATIO BALANCING

For good composting carbon to nitrogen ratio must be between 20:1 to 40:1 ideally it may 30:1. So before dumping we need to find the carbon percentage (USING WALK LINE METHOD) and nitrogen percentage (KJELDAHL METHOD) in waste. For every 30% of carbon 1% of nitrogen needed, the carbon content is very much required for micro organism it provides protein for micro organism to degrade the waste very fast. At the lower C:N ratio there will be excess nitrogen provided which can result in the production of ammonia. This has the unpleasant odor that many composters will experience at some time in their composting carrier. At C:N ratio of over 30:1, there will not be enough nitrogen to support sufficient microbial growth and the microbe population will be too low to produce sufficient heat with the result that the decomposition process will be very slow.

For balancing carbon content, if the carbon content is less, add CHAR COAL to waste. It contains rich carbon content, and it will help to increase the carbon content in waste and as well as it will help to absorption of carbon dioxide from atmosphere if the decomposed waste is used for fertilizer.

For check, this method is worked in practical or not, takes same weight of waste in two different bins and in first bin decomposes the waste in natural manner without balancing the C/N ratio and note down the time taken for composting. In second bin find out the C/N ratio and balance it (30:1) and note down the time taken for composting.

RESULTS AND DISCUSSIONS

SL No	Bin 1	Bin 2
Weight	2 kg	2 kg
C/N Ratio	Balanced(30:1)	Natural/Un balanced(21:1)
Time taken for composting	4 days	7 days
Contents	Good rich content in C/N and used as a good fertilizer	C/N content les compare to Bin 1
Image		

*This project work has been completed in a limited time and we are proud to announce that “SOLID WASTE MANAGEMENT” is able to fulfill the expectations.

*We successfully completed this project by ~~with~~ using new technique and we show the different path for managing the solid waste, and we are happy to announce we find the new path for managing the solid waste in good manner and quickly.

*At present condition entire world is faced waste managing problem, and it will become bigger day by day due to increasing population, just because of due to lag of this technical consideration before dumping the waste. If we adopt in practical manner definitely we can manage the waste very quickly and good manner also.

CONCLUSIONS

This project has provided us a plethora of opportunities and experiences, with in the bonds of our limited knowledge. It will give not only theoretical knowledge, it also included practical knowledge how composting process will and takes place and how the rate of composting process increases when balancing the C/N ratio and how natural process takes place. It is a matter of immense of happiness and pride for us in having been able to complete this project successfully in a limited span of time. We have done everything in the best possible way we could by overcoming the various constraints and by utilizing all the available amenities.

ACKNOWLEDGMENT

We would like to express our sincere gratitude to the Management, Principal Sapthagiri College of Engineering Bengaluru for the facilities provided and their support. Also we would like to thank the Head of the department Civil Engineering and faculties for their encouragement and support.

REFERENCES

1 Aruna, G, Kavitha, B;" An observational study on practices of disposal of waste garbage", pg 392-394 published on 2020.

2 Khan, M, Chniti, S, "Properties and internal characteristics of anaerobic bio reactor of food waste" published on 2021, 8, 319-322

3Prakash and V prabu, "IOT based waste management for smart city" volume 4, published on February 2022

4 Sigmund, G, Poyntner, C, "Influence of compost and biochar on microbial communities and the degradation" published on 2020, 354, 107-113.

SMART VILLAGE

(CASE STUDY – GUNGARAMELE VILLAGE)

HARSHITHA R, KAVYA SHREE S, SHWETHA R, SOWMYA K V

Department of Civil Engineering, Sapthagiri College of engineering#14/5Chikkasandra, Hesaraghatta main road, Bangalore-57 India

[1]harshitha7143@gmail.com
[2] kavyashree.dinnu@gmail.com
[3] shwetharaj341@gmail.com
[4]sowmyakvreddy@gmail.com
[5] hodcivil@sapthagiri.edu.in

Abstract – Smart village is built on the philosophy of a self-sustaining eco system, one that is capable of adapting to changing governance regimes and generating resources in order to augment human development. The main problems faced by rural areas are poverty, low -level of sanitation and limited access to technology. Gungaramele village in India is one of the regions that created smart concept starting from rural area. This study deals with study and development of village as a smart village. Literature reviews on smart cities, smart villages, and smart rural areas were acquired and evaluated after an initial interview in the village of Gungaramele. The initiative taken to implement smart concepts are – smart energy, smart agriculture, smart management and smart technology.

I. INTRODUCTION

The vast majority of Indians live in villages. Villages are home to over 70 percent of India's population according to the census report of 2016. Each year, however, a huge number of individuals from villages travel to cities in quest of better jobs, medical care, education, and a better quality of life. Smart City is a project that strives to improve the living conditions of city dwellers. Similarly, Smart Village is a rural development effort aimed at making villages self-sufficient.

Smart village is a new concept developed by the researches from India, N Viswanathan and Sowmya Vedula. This concept was developed in 2010, by describing the ecosystem for a village and mapping the procedures of integrated design to build a smart village.

Smart village initiatives are being undertaken in rural areas all over the world to improve the lives of people living in villages.

The objective of smart village concept is to provide benefits of urban lifestyle to the villagers while retaining valuable aspects of rural communities.

These initiatives enable inhabitants of rural communities to attain complete potential for the development by connecting to the world and earning a feasible livelihood while leading a healthy lifestyle.

Such initiatives also attempt to prevent the migration of villagers to cities by providing enormous opportunities in smart village.

According to recent literatures, sustainable development in smart cities and smart villages; An Indian prospective paper of (2022) highlights the issues and challenges that need to be overcome for sustainable development and digital transformation.

They also help to reduce the digital divide that exists between rural and urban areas.

Sustainable environment, renewable energy, health and sanitation, food and clean water, eco-friendly production-oriented enterprises, education and awareness, and finally democratic involvement of the villagers in various issues are some of the core features of smart village programs. Energy access must be linked into other programs for the development of smart village, so renewable energy production and access became the backbone of overall development process.

Another significant issue that has been considered in the development of smart communities is improving the lighting system so that children can study at night because studying is a pollution-free activity.

Similarly, households in smart villages can consume clean, safe water as well as nutritious food while reducing the cost of heating water for drinking. In the global south of India, replacing traditional biomass-based cooking stoves with cleaner fuel-based modern stoves will reduce indoor pollution.

The main objective of this study is proposal of Gobar gas and solar energy concepts in Gungaramele village, while educating the villagers about waste management process and use of hydroponics in agriculture.

II. DATA COLLECTION

The data collected during the initial interviews in Gungaramele village are: -

No of houses interviewed: - 50 houses
No of people residing: - 186 members
Total waste production- 1450 kg

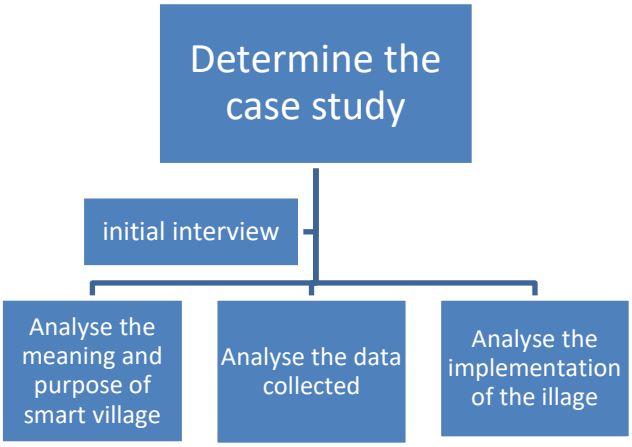

Fig 1. flowchart of initial procedure

III. METHODOLGY

The methods selected to study the smart village concept were done through preliminary interview, literature review of previous studies, books and analysis of regulations that support it are done according to fig.1
The literature review was conducted by choosing journals based on the definition of the concept and instances of smart village implementation. Analyzing the data collected while interviewing the local residing in the village, Gungaramele is studied and considerable implementations were taken. The various categories that were considered are implementation of Gobar gas, installation of solar panels, E –learning and smart education, health and sanitation, Improvements in the field of agriculture.

The categories considered in smart village are: -

1) Smart energy
2) Smart agriculture
3) Smart waste management
4) Smart technology

1) SMART ENERGY

Smart energy is the process of using devices for energy-efficiency. It focuses on powerful, sustainable renewable energy sources that promote greater eco-friendliness while driving down costs with smart energy system we can better match supply with demand, and integrate more renewable energy sources such as wind and solar into the system. These forms of generating energy create less air pollution and emit significantly less CO2 into the atmosphere.

In smart energy we considered Gobar gas production and Solar Energy.

1. GOBAR GAS

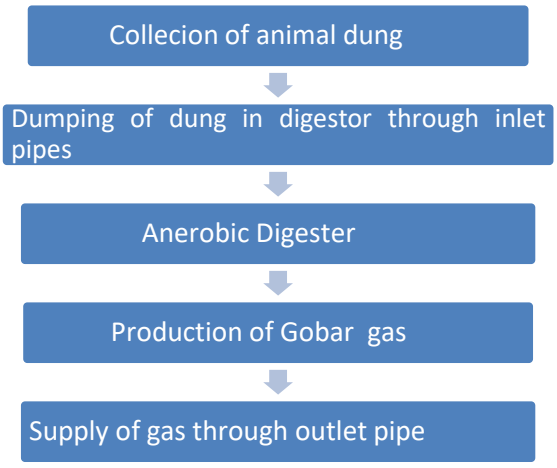

Fig 2. Production of gobar gas

- As mentioned in the above figure 2, First the animal dung is collected from every house then sent to the digester via inlet pipes at the proper temperature. Inside the digester, anaerobic digestion occurs. After a period, the gobar gas is released through the house's outlet pipes.

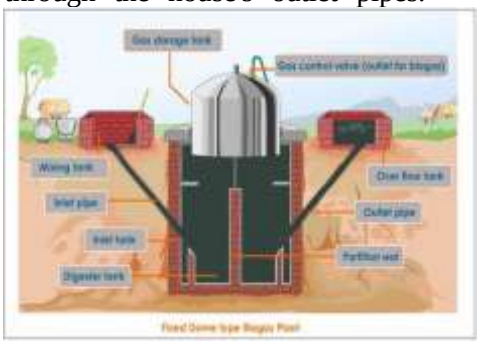

Fig 3: Typical biogas plant (source:google)

- With reference to the fig 3 and collected data for a waste production of 1450 kg, a biogas plant with a digester of 350cm and a depth of 350, a gas holder of diameter 530cm and depth13cm as well as a slurry tank of 350*350 cm.

  The plant design described above will generate 58000 liters of biogas per day.

2. SOLAR ENERGY

- Solar energy is a renewable, inexhaustible, and affordable form of energy. It can be used to cook food, heat water, and generate electricity. Furthermore, electrical energy generated from solar energy can be stored in solar cells.
- The two types of solar energy are: -

1) Active solar energy involves

ISBN: 979-88-35073-61-0

Fig 2. Production of gobar gas

equipment or an action to convert solar energy into a useful form. One example of active solar energy is the use of solar cells to convert energy from the sun into electrical energy that can be used in the home.

2) Passive solar energy does not require any specific action or equipment. An example of passive solar energy is strategically placing windows in a home to allow sunlight to enter and provide heat.

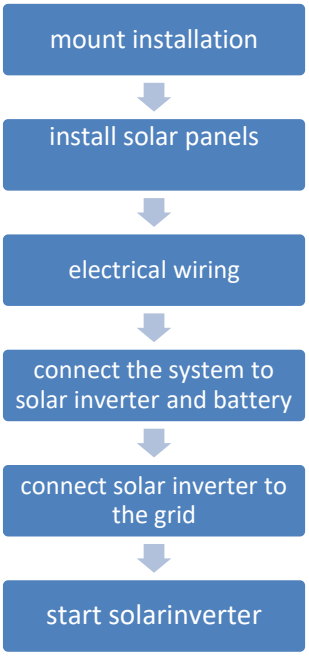

Fig 4. Installation of solar panels procedure

- The procedure outlined in the fig 4 is followed to install solar panels for every house in the village to produce lighting.
- We must install a 1kw rooftop solar system for every residence in the village.
- 1 kw of system produces 4kwh of electricity on a good day and 120 kwh a month.
- Installation of a 1kw rooftop solar system cost from 45000 to 85000.

Fig 5. Installation of solar panels(source:google)

2) *SMART AGRICULTURE*

- Smart agriculture is about using the new technologies which have arisen at the dawn of the Fourth Industrial Revolution in the areas of farming and cattle production to increase production quantity and quality, by making maximum use of resources and minimizing the environmental impact. Also, the implementation of technology in agriculture and cattle production will make it possible to boost food security throughout the world.
- By using hydroponics in agriculture, the crops can be easily grown without using large area of plantation and less usage of water.

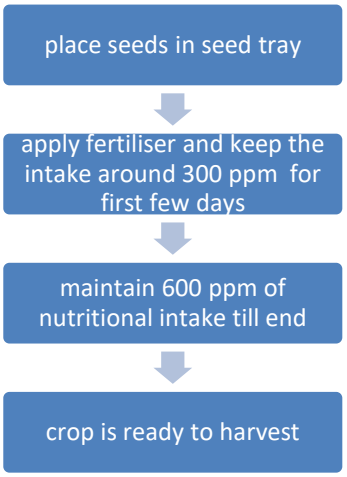

Fig 6: Hydroponics using deep water system

- The agriculture land in Gunbarrel has good water facilities; we selected hydroponics using water culture. Plant production is achieved by suspending the plant roots in a solution of nutrient rich, oxygenated water.
- The installation of hydroponics is depicted in the fig6.
- A 4*5 feet of hydroponics setup is

required for every house in the village which will cost 5500 and 27500 for 50 houses.
- The above hydroponics setup can generate 2000 to 10000 monthly profit.

3) SMART WASTE MANAGEMENT

- Smart management involves educating the villagers about the waste management. Waste management basically involves dividing the waste into dry waste and wet waste.
- Dry waste includes plastic, papers, bits of paper waste, glass, cardboard, rubber metal.
- By educating the villagers about the toxins present in plastic, instead of burning them, they can use the plastic waste in production of bricks, where small scale industries come into picture and many employment opportunities can be possible created, so that the people can avoid migrating into the urban areas.
- Wet waste includes all the kitchen waste that we produce. This can include vegetable peels, used tea, fruits, leftovers etc. instead of dumping the waste, this waste can contribute to the production of Biogas where the waste with the animal dung can be dumped in the digestor of biogas... Hence educating the villagers about the waste management and the spreading the awareness of burning of plastic plays a vital role in smart management.

4) SMART TECHNOLOGY

- Smart technology affects almost every aspect of 21st century life, from transport efficiency and safety, to access to food and healthcare, socialization and productivity. The power of the internet has enabled global communities to form ideas and resources to share easily.
- As banks is still being establishing in villages, digital money or use of net banking maybe a slow process in villages.
- Due to Jio connections and the fast-paced internet awareness can be created in the villages about the networking and the use of digital money through phones.
- Many apps like Google pay and phone pay as been used in cities of India, awareness is spreading across the villagers about net banking, people can afford banks in their phones itself rather than walking miles just for banks.

IV. RESULTS AND DISCUSSIONS

- Achieving the sustainable development of rural areas is not only a major challenge for the development of rural areas but also the vision and goal for the future development of rural areas, especially for a country such as India, where half of the population lives in rural areas.
- Biogas is generated by estimating the waste production for one day and utilizing machines such as a digestor with a depth of 350 cm and a diameter of 530 cm, as well as a gas holder and slurry are required which generates 58000 liters of biogas per day which can be used for cooking purpose.
- Solar panels will be installed, with each residence receiving at least 1KW of electricity. Up to a certain extent, solar energy can be utilized in lightening bulbs and fans.
- Hydroponics is the most ideal system recommended. A 4*5 feet of hydroponics setup for every house will provide 2000 to 10000 profit per month.
- Internet towers are suggested for Jio net installation, each user with a phone will receive 1GB of data, which can be utilized for personal and financial networking reasons.

CONCLUSIONS

- In this study, the village gunguramele is taken as a model village to propose the concepts of smart village namely smart energy, smart agriculture, smart waste management and smart technology.
- The smart energy plans and designs i.e., biogas plant helps in the vision of improving the productivity of gas having higher thermal efficiency than charcoal and kerosene.

ISBN: 978-93-25073-61-0

- Solar panels using photovoltaic effects to convert light directly into electricity as a result every house in the village will be having solar to access electricity.
- The smart agriculture considering hydroponics forming is highly profitable as it will high yield crops just in a small place in any season or in any weather condition.
- Smart waste management entails utilizing technology and data to produce a more effective waste sector, as well as optimizing resource allocations, lowering operating costs, and increasing waste service sustainability.
- Due to this cultural, economic, environmental, living standard and overall status of village increases. Because of that, the village become self-dependent and contributes towards the development of nation.

VI. ACKNOWLEDGMENT

We would like to express our sincere gratitude to the Management, Principal Sapthagiri College of Engineering Bengaluru for the facilities provided and their support. Also, we would like to thank the Head of department Civil Engineering and faculties for their encouragement and support.

VII. REFERENCES

[1] A A Aziiza and T D Susanto: IOP Conf. Ser.: Mater. Sci. Eng. 722 012011,2020

[2] E. Syaodih: Smart Village Development (The 9th International Conference of Rural Research and Planning Group) pp. 22–33,2018

[3] J. Ahlawat: Smart Villages, Information Communication Technology and Geographical Information System (International Journal of Current Trends in Science and Technology Vol. 7) No. 8, pp. 20232–20238,2017

[4]] A. M. Muke and U. Nilesh S: Use of Advanced Technology in Developing Smart Villages (International Journal of Research in Engineering Science and Technology Vol. 03) No. 04, pp. 1–6,2017

[5] B. Madintha: Design and Implementation of Smart Village Mapping Geographic Information System Based Web In The Cinunuk Village (The 2017 IEEE Asia Pacific Conference on Wireless and Mobile (APWiMob)), pp. 66–71,2017

A review on the uses of sugarcane bagasse ash as cementitious material in concrete

Thanushree V, Amrutha D, Hemanth Gowda P, Prashanth Gowda NC
Department of civil engineering
Sapthagiri College of Engineering
Bengaluru, India
amruthad222@gmail.com ,phemanthgowda@gmail.com, thanushreev361@gmail.com, prashanthgowda5859@gmail.com

Dr. Rajeshwari R
Department of civil engineering
Sapthagiri College of Engineering
Bengaluru, India

ABSTRACT

Massive development in the infrastructure sector has given an unexpected rise in the demand for cement. Approximately the world expends 30 billion tons of cement concrete every year(ref-BS Thomas , 2021). Researches around the world incisiving for several solutions for achieving the practice to stay free from carbon footprint. One among them is sugarcane bagasse ash from sugar mills. Where bagasse ash has high strength and reduces the permeability of concrete. This review represents the physical and chemical properties of sugarcane bagasse ash. It possesses pozzolanic reactivity and increases the compressive strength and also decreases thermal conductivity. Sugarcane bagasse can be replaced with concrete without disturbing its mechanical properties. 1ton SC produces approximately 26% of bagasse and 0.62% residual ash(G). The ash generated during the burning of agricultural waste at a controlled temperature of less than 700 ° C for 1 hour, converts the silica content in the ashes to the amorphous phase. Sugarcane bagasse is a lingo cellulosic material. It is generally a kind of waste, which may have some particular uses. In the analysis study the cement is partially replaced in 0%,5%,10%,15%and 20% of sugarcane bagasse ash(ref-santosh kumar meghwar ,2019).

KEYWORDS

Sugarcane bagasse (SCBA), Pozzolanic reactivity, compressive strength, workability, split tensile strength

INTRODUCTION

The husk obtained after the crushing of sugarcane is sugarcane bagasse. Sugarcane bagasse is obtained during the manufacturing of sugar. It is commonly used as fuel in boilers to generate steam and electricity. The cement industries emit an 80% contribution to the global greenhouse effect. Brazil is the highest sugarcane producer with 814.9 million tones. Second comes India with 376.1 million tones and third comes China with 138.3 million tonnes (ref-D K Ashish-2019). The scraped fibrous matter is called bagasse. Bagasse is burnt at about 500-560^{0}C (ref-S Nazar-2019). For every 10 tons of sugarcane 3 tons of bagasse are generated.

Figure 1. Land disposal of: (a) Bagasse ash and (b) Bagasse Fibres(ref-Gabriel,2019).

After the milling process for every ton of burnt sugarcane, 0.62% ash is produced. where approximate production of sugarcane bagasse yearly is 11.42MT (ref-. V. jittin -2019).

SCBA CHARACTERISTICS

Sugar cane bagasse ash was obtained by an uncontrolled bagasse burning process. The collected ash is sieved to the necessary fineness using sieve #300µm, which removes all dirt and bigger particles. This sieved ash can be used in concrete as a cement substitute. (Ref 1)

The sugarcane bagasse contains roughly 50% cellulose, 25% hemicelluloses, and 25% lignin. At a moisture percentage of 50%, each tonne of sugarcane produces around 26 percent bagasse and 0.62 percent residual ash. The chemical makeup of the residue after burning is dominated by silicon dioxide (SiO2). Despite being a material that is difficult to degrade and has few nutrients, ash is utilised as a fertiliser in sugarcane harvests on farms. The ash from sugarcane bagasse was gathered in this container. (ref 2)

Sugar cane varietals, growth, combustion temperature, combustion duration, bagasse purity, bagasse ash collection site, cooling type, boiler equipment, bagasse ash collecting methods, and ash fineness all affect the physical qualities and compositions of SCBA [1]. Bagasse ash collected at the bottom of the boiler, for example, is likely to be coarser and contain irregular particles, but bagasse ash collected through a filtration system contains less carbon [2]. (Ref 3)

WORKABILITY

The workability of fresh concrete in terms of slump reduction was measured using the frustum slump cone. The maximum slump value was 54mm in concrete with 0% SCBA and the lowest slump value was 26mm in concrete with 20% SCBA as cementitious material. Workability declines as the fraction of SCBA increases, as illustrated in Fig. Because SCBA has a larger surface area than cement, it absorbs some water and has a lower drop-in workability.

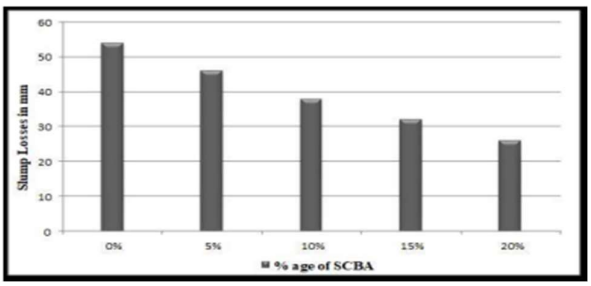

FIG: Workability of Fresh Concrete (ref 1)

Fresh concrete tests are used to determine the workability of a concrete mix. The slump cone test is not performed on pervious concrete because it is also known as zero slump concrete. As a result, the slump cone test is used to measure workability. Slump value was used to assess the workability of freshly mixed concrete. In this study, M25 mix concrete is used to complete the test on a weight basis by partially replacing 5%, 10%, 15%, and 20% of the cement weight with M25 mix concrete. (Ref 2)

Increase with SCBA replacement level increase (ref 3-5)

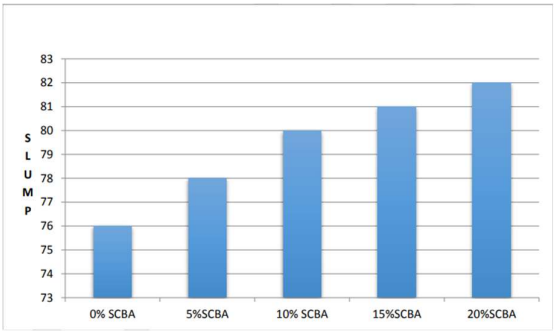

FIG: Workability of Fresh Concrete (ref 2)

COMPRESSIVE STRENGTH

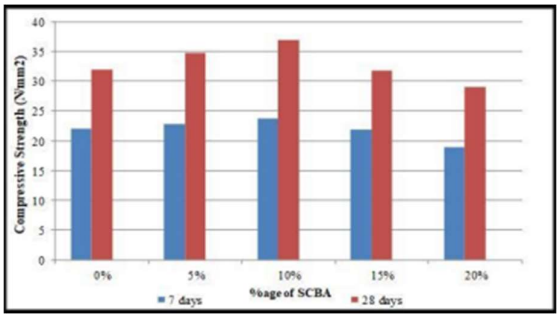

FIG: compressive strength for partial replacement of SCBA as cement (ref 1)

After seven and twenty-eight days, employing 10% SCBA as a cement substitute material in concrete increased compressive strength by 7.95 percent and 15.40 percent, respectively. After 7 and 28 days, compressive strength was reduced by 13.63 percent and 9.38 percent, respectively, when 20 percent SCBA was used as a cement substitute material in concrete.

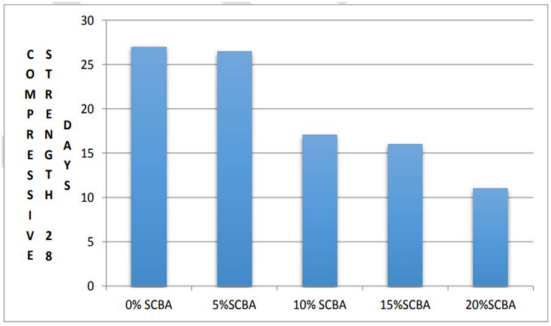

FIG: Compressive Strengths for partial replacement of SCBA as cement (ref 2)

When compared to conventional concrete, rubber-based concretes have a lower strength for partial replacement of coarse and fine material after 28 days.

With an increase in SCBA replacement level, it first rises and subsequently falls [6,7,8]. Reduced with SCBA [9]. (Ref 3)

At 1% bagasse, the compressive strength of grade 30 concrete increases from 28.97 to 48.83. The addition of 3% bagasse reduces the compressive strength of concrete slightly, although this can be explained by the fact that the strength is still high in the controlled sample. (Ref 4)

SPLIT TENSILE STRENGTH

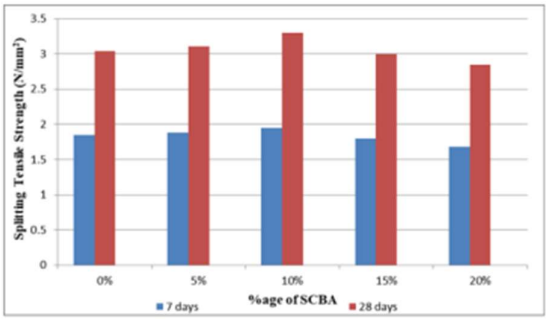

Fig: Tensile strengths for partial replacement of SCBA as cement.

After 7 and 28 days, employing 10% SCBA as a cement substitute material in concrete increased indirect tensile strength by 5.40 percent and 8.55 percent, respectively. After 7 and 28 days, the split tensile strength of concrete using 20% SCBA as a cementitious material was lowered by 9.19 percent and 6.25 percent, respectively. (Ref2)

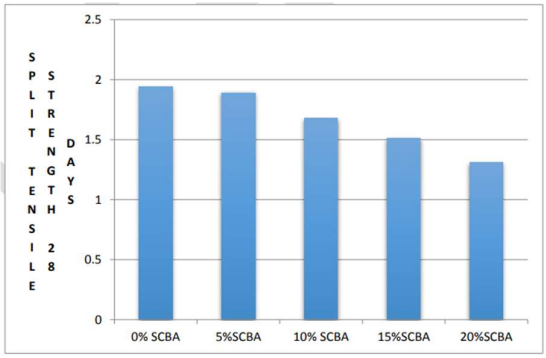

Fig: Tensile strengths for partial replacement of SCBA as cement. (Ref 2)

Split tensile strength Increases first and then decreases with replacement rate increase [6,10]. (Ref 3)

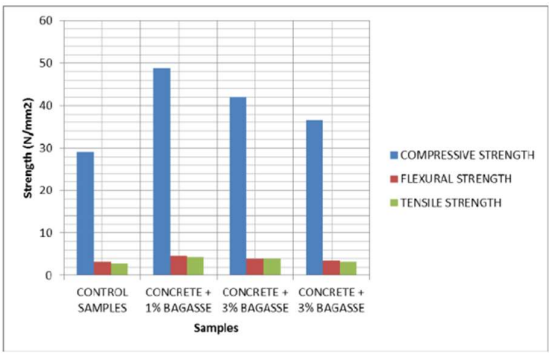

Fig: Tensile strengths for partial replacement of SCBA as cement. (Ref 4)

The presence of sugarcane bagasse in the concrete mix has an effect on the strength of the concrete, as seen in fig. The mechanical properties tests have all yielded positive results. Bagasse, on the other hand, was successful in improving the strength of concrete. It demonstrates that bagasse is akin to a concrete retarder that has no detrimental impact on concrete strength. (Ref 4)

POZZOLONIC ACTIVITY

Supplementary cementitious materials cannot be employed directly as pozzolanic material in the majority of circumstances. Instead, they must be treated to meet specified pozzolanic material criteria. SCBA has been identified as an agricultural-based pozzolanic material, but due to its low pozzolanic activity, it cannot be employed directly in concrete. Crystalline silica and impurities such as unburned carbon are the main causes of SCBA's pozzolanic activity [11]. SCBA is less popular than rice husk ash due to its low amorphous silica content (usually less than 50% silica) [12]. Various processing methods have been employed in past research to increase the pozzolanic activity of SCBA for large-scale SCBA applications. (Ref 3)

ADVANTAGES OF CEMENTITIOUS MATERIAL

Reduces cement contents, increases strength and improves the workability of fresh concrete.

APPLICATION OF CEMENTITIOUS MATERIAL

It is widely used to build commercial buildings as well as related fixtures, Driveways and columns.

PRESENT SCENARIO OF SUGARCANE BAGASSE

lower cost and lower carbon footprint of concrete, higher long-term compressive strength (e.g., at 90 days or more) and durability. Bagasse is a sustainable product because it is sourced with very little impact on the environment.it is easily replenished because the residue can be obtained after every harvest. Bagasse is the essential ingredient for the production of pressed building board, acoustical tile, and other construction materials and can be made into a number of biodegradable plastics.

REPLACEMENT OF SUGARCANE BAGASSE AS CEMENTITIOUS MATERIAL

Replacement of sugarcane bagasse is done to overcome the scarcity of cement.

- **Renewable**
  It is a sustainable product and easily available in the environment but cement is not.it can easily be replenished
  But cement is not.

- **Compostable**
  It never degrades. It can biodegrade normally within 10 days but cement can be renewable.
- **Easily available**
  Bagasse has high bioconversion efficiency and it is readily available and bagasse is obtained easily in larger amounts but cement can't.
- **Environmental aspects**
  Bagasse is free from carbon footprints
  Cement is harmful to the environment
- **Cost aspects**
  bagasse is waste material so it is available in cheaper but cement is more expensive.

GRAPH SHOWING THE COMPRESSIVE STRENGTH OF M30 GRADE OF CONCRETE MIXED WITH SCBA

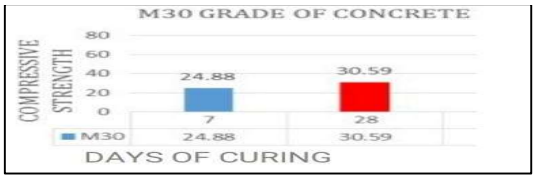

LITERATURE REVIEW

- **Use of Sugarcane Bagasse Ash as Cement Replacement Materials in Concrete Narain Das Bheel, Santosh Kumar Meghwar, Rameez Ali Abbasi, Israr Ahmed Ghunio, Zubair Hussain Shaikh 2019**
- As a cementitious material in concrete, 54mm inclusion with 0% SCBA produced the highest slump value, while 26mm inclusion with 20% SCBA produced the lowest slump value. When the amount of SCBA in the concrete grows, the workability of the concrete gradually declines. After seven and twenty-eight days, employing 10% SCBA as a cement substitute material in concrete increased compressive strength by 7.95 percent and 15.40 percent, respectively. After 7 and 28 days, compressive strength was reduced by 13.63 percent and 9.38 percent, respectively, when 20 percent SCBA was used as a cement substitute material in concrete. Using 10% SCBA as a cement increased indirect tensile strength by 5.40 percent and 8.55 percent, respectively. After 7 and 28 days, use a different material in the concrete. After 7 and 28 days, the split tensile strength of concrete using 20% SCBA as a cementitious material was lowered by 9.19 percent and 6.25 percent, respectively.

- **Usage of sugarcane bagasse ash in concrete b. Mahesh, t. Mahesh Kumar, u. Nikhil& a. Yaka swamy 2017**
  The following conclusions are formed based on the experimental data and their graphs, as well as subsequent discussion of the results. By increasing the percentage of SCBA replacement in concrete, the workability of the concrete improves. Concrete's compressive strength rose by 5% when SCBA was used instead of cement. As the percentage of SCBA increases, the compressive strength decreases. With the addition of SCBA, the tensile strength of concrete decreases.

- **Characteristics and Applications of Sugar Cane Bagasse Ash Waste in Cementitious Materials Qing Xu, Tao Ji, San-Ji Gao, Zhengxian Yang and Nengsen Wu 2018**

  SCBA is typically used as fertiliser or disposed of in landfills, both of which are unsustainable in terms of the environment and human health. The use of SCBA in construction materials offers a promising approach for better SCBA waste recycling and management. By synthesising the results of previous studies, many research have shown that using SCBA in cementitious materials enhanced the short-term mechanical qualities as well as the long-term durability of mortar, concrete, and other building materials. In-depth studies on the endurance of concrete containing SCBA in harsh conditions are lacking. SCBA's impact on reinforced concrete (RC) has been rarely documented.

- **Usage of sugarcane bagasse as concrete retarder Mohamad Azania Yahya, Mohammed alias Yusof, zulkifli abu hassan, Nasrin daud 2013**
  The goal of the study is to see if sugarcane bagasse can be utilised as a concrete additive and retarder. The reaction between sugarcane bagasse and cement lengthens the time it takes for the cement to set. Sugarcane bagasse has a possible application in concrete, and a research of sugarcane bagasse mixed with fresh concrete as a retarder has been completed.

CONCLUSION

(1) Several studies have shown that using SCBA in cementitious materials improves the short-term mechanical qualities as well as the long-term durability of mortar, concrete, and other construction materials. In-depth studies on the endurance of concrete containing SCBA in harsh conditions are lacking. SCBA's impact on reinforced concrete (RC) has been rarely documented.

(2) The heterogeneity of SCBA limits its use in cementitious materials on a broad scale. One of the most major influencing elements on SCBA composition is calcination.

To achieve desirable SCBA pozzolanic activity, more attention should be paid to congenator design, calculation control, bagasse drying process, and so on.

(3) Comparative investigations revealed that different processing methods had both advantages and limits in terms of SCBA pozzolanic activity. For a specific purpose, exploring suitable SCBA processing methods for greatest SCBA pozzolanic activity, simplest processing, and lowest energy usage should be done with caution.

(4) Various processing methods have been employed in past research to increase the pozzolanic activity of SCBA for large-scale SCBA applications.

(5) More study on technical and environmental concerns, as well as standardisation and government policy guidance, is required for the large-scale use of SCBA.

ACKNOWLEDGEMENT

It is our immense pleasure to thank our beloved HOD Dr R. Rajeshwari mam civil engineering department, Dr. H Ramakrishna Sir the Principal of Sapthagiri college of engineering Bangalore, for their comments and suggestions in preparing the manuscript.

REFERENCE

[1] Katare, V.D.; Madurwar, M.V. Experimental characterization of sugarcane biomass ash—A review. Constr. Build. Mater. 2017, 152, 1–15.

[2] Frias, M.; Villar, E.; Savastano, H. Brazilian sugar cane bagasse ashes from the cogeneration industry as active pozzolans for cement manufacture. Cem. Concr. Compos. 2011, 33, 490–496.

[3] Hussein, A.A.E.; Shafiq, N.; Nuruddin, M.F.; Memon, F.A. Compressive strength and microstructure of sugar cane bagasse ash concrete. Res. J. Appl. Sci. Eng. Technol. 2014, 7, 2569–2577.

[4] Srinivasan, R.; Sathya, K. Experimental study on bagasse ash in concrete. Int. J. Serv. Learn. Eng. 2010, 5

[5] Patel, J.A.; Raijiwala, D. Experimental study on compressive strength of concrete by partially replacement of cement with sugar cane bagasse ash. Int. J. Eng. Res. Appl. 2015, 5, 117–120

[6] Ganesan, K.; Rajagopal, K.; Than gavel, K. Evaluation of bagasse ash as supplementary cementitious material. Cem. Concr. Compos. 2007, 29, 515–524

[7] Bahurudeen, A.; Kanraj, D.; Dev, V.G.; Santhanam, M. Performance evaluation of sugarcane bagasse ash blended cement in concrete. Cem. Concr. Compos. 2015, 59, 77–88.

[8] Montakarntiwong, K.; Chusilp, N.; Tangchirapat, W.; Jaturapitakkul, C. Strength and heat evolution of concretes containing bagasse ash from thermal power plants in sugar industry. Mater. Des. 2013, 49, 414–420.

[9] Tantawy, M.A.; El-Roudi, A.M.; Salem, A.A. Immobilization of Cr (VI) in bagasse ash blended cement pastes. Constr. Build. Mater. 2012, 30, 218–223.

[10] Amin, N. Use of bagasse ash in cement and its Impact on the mechanical behaviour and chloride resistivity of mortar. Adv. Cem. Res. 2011, 23, 75–80.

[11] Hernández, J.F.M.; Middendorf, B.; Gehrke, M.; Budelmann, H. Use of wastes of the sugar industry as pozzolana in lime-pozzolana binders: Study of the reaction. Cem. Concr. Res. 1998, 28, 1525–1536.

[12] Frias, M.; Villar, E.; Savastano, H. Brazilian sugar cane bagasse ashes from the cogeneration industry as active pozzolans for cement manufacture. Cem. Concr. Compos. 2011, 33, 490–496

COVID-19 PANDEMIC AND DIGITAL REVOLUTION IN IMPROVING THE QUALITY OF TEACHING AND LEARNING

Bhavya.N.P, Nandini.B.J², Parshwanath.P

Department of Mathematics, Sapthagiri College of engineering#14/5 Chikkasandra, Hesaraghatta main road, Bangalore- 57 India

¹bhavyanp@sapthagiri.edu.com. ²nandinibj@sapthagiri.edu.com, hodmaths@sapthagiri.edu.in

Abstract *- The World Health Organization has declared Covid-19 as a pandemic that has posed a contemporary threat to humanity. This pandemic has successfully forced global shutdown of several activities, including educational activities, and this has resulted in tremendous crisis-response migration of universities with online learning serving as the educational platform. The crisis-response migration methods of universities, faculty and students, challenges and opportunities were discussed and it is evident that online learning is different from emergency remote teaching, online learning will be more sustainable while instructional activities will become more hybrid provided the challenges experienced during this pandemic are well explored and transformed to opportunities. The outbreak of COVID-19 has reminded us that the complexity of education needs responsive practices to facilitate effective teaching and learning across all levels of schooling globally. All over the world, the normative ways of teaching and learning evolved drastically in the first quarter of the 2020 academic year when teachers and students found online offerings to be the dominant option available as a sequel to the pandemic conditions. We argue that teaching the topic on an online platform constrain student teachers' procedural thinking, conceptual development, and demonstration of their thought processes during mathematics learning and assessment.*

I. INTRODUCTION

The outbreak of the novel coronavirus disease (COVID-19) began in the Wuhan region of China in December 2019. By February 2020, cases of COVID-19 had been detected on every continent. Governments are advising citizens to be prepared for an outbreak in their community. Today, we are globally experiencing closures in schools and universities, postponements or even cancellations of conferences and other organized events, and social distancing. In addition, we have also seen the promotion of flexible ways of studying and working to hinder the rapid spread of the virus. The respiratory failure and unwavering deaths caused by COVID-19 continue to cause sparked anxiety worldwide. In South Africa, the Minister of Health Dr. Zweli Mkhize reported the first case of the pandemic on 5 March 2020, when a male citizen in KwaZulu-Natal tested positive upon his return from Italy. It was in this context that the government configured strategies to fight against the virus on March 2020. As cases continued to be reported daily, the South African Government imposed a hard lockdown on the population on March 23 for 21 days effective on March 26 2020. The officially confirmed cases had increased to 554 with zero deaths nationally. The lockdown continued to be extended and adjusted based on recommendations made by South Africa's Ministerial Advisory Committee on COVID-19, with the primary aim being to flatten the curve by reducing daily reported cases and ensuring speedy recovery on infected people. In view of this, universities, colleges, clubs and religious houses, and economic activities involving face-to-face interactions to name but a few were restricted. Accordingly, given the mandate to save the academic year, representatives of both public and private higher educational institutions resorted to putting alternative strategies in place for students and lecturers to continue with their lessons when physical attendance is not feasible.

One of the strategies was a transition from physical attendance of classes to online education, to ensure the limited level of contact with and amongst students while attempting to promote students' learning continuation and growth. It appears that nowadays, we are entering into the new phase of the evolution in academia and higher education that is going to create the 4th generation of universities which can be named "online and digital universities" (Figure 1). Much of that is because of the COVID-19 pandemic that launched a digital revolution in academia and higher education.

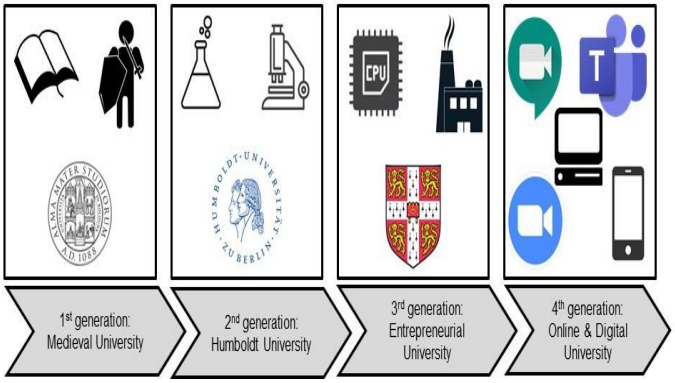

Figure 1. Evolution of academia and higher education

Keywords: academia; higher education; coronavirus pandemic; online tuition; social distancing; COVID-19; digital revolution.

II. Digital revolution

The coronavirus pandemic of 2020 became a push factor that can help everyone to better understand that all the attributes of higher education such as online defences, online entrance and final exams, as well as online academic jobs are as good as those conducted "in real life. Here are some recent examples:

- On the 18th and 20th of March 2020, Imperial College London conducted the world's first online exams for its 280 six-year medical students. The digital "open book" exam was successfully delivered remotely, and many universities in the United Kingdom and worldwide are now likely to follow the Imperial's strategy as a solution for examining students during the COVID-19 pandemic shutdown. According to one of the students who took the exam, this was a good experience because medical school finals measure a higher level of learning then just remembering information. The tests focused on the student's ability to synthesize information to come up with a management, or interpret complex data are skills.
- In addition, it also turns out that if the exams and defenses can be done online, so can be the graduations. In Japan, despite the fact that spring graduation ceremonies were cancelled because of the coronavirus pandemic, the students at the Business Breakthrough University in Tokyo attended remotely (Figure) by controlling avatar robots from their homes.

Figure 2. Online graduation in Japan Source The Guardian (2020)

Digitalization in higher education allows streaming lectures online or enables professors and students to interact in the virtual environments but not everyone is ready for this. Even those young people who do not spend much time in the "real life" and rather prefer playing video games or interacting with others on social network platforms confess that they would have preferred being lectured in real classrooms and in real universities. Sometimes this is just a feature of habit but quite often this can be attributed to the difficulties with personal time management and procrastination when students are left studying online from the comforts of their homes.

III. Academic types

In general, there are three main types of people in today's academia and higher education.

- Lecturers: typically engaged in delivering lectures to students (several lectures a week, several days a week). Some lecturers are good public speakers, are popular among their students, and enjoy their work. However, most lecturers lack time for writing and publishing research papers and many of them loath this activity. Most (but not all) lecturers often use the same (often outdated) material (Power Point slides) for many consecutive lecture courses and years.

- Researchers: writing and publishing many research papers and monographs. Researchers know all about the publishing process, bibliometrics and how this system works. Many researchers are terrible public speakers and prefer not to lecture wherever possible (quite often they "buy out" their lecture time with the research papers or grant projects).

- Businessmen: the rarest type of academics. Businessmen are the directors of research centres, professors, deans, and chancellors. They used to be lecturers or researchers before but discovered their leadership skills. Many businessmen are proficient in writing and securing grant proposals and obtaining funding for their

ISBN: 979-88-35073-61-0

institutions.

IV. Challenges, Compatibility and Opportunities

With Covid-19 pandemic, it has become clearer that education system is susceptible to external dangers rightly noted that this digital transformation of instructional delivery came with several logistical challenges and attitudinal modifications. Feldman (n.d.) while addressing student assessment during this pandemic on how districts can Legislate unbiased and evenhanded grading policies based on these recommendations; (i) pandemic- related anxiety will have negative effects on student academic performance, (ii) academic performance of students might be affect by racial, economic and resource differences, and (iii) the larger parts of instructors were not effectively ready to deliver high-quality instruction remotely. The challenges discussed here are limited to digital transformation of instructional operations during the period of Covid-19 pandemic.

The compatibility of online learning with social science and humanities has been proved effective while researchers have also contested its compatibility with sports sciences, engineering and medical sciences where hands-on practical experiences are required as part of instructional activities . Remote laboratories are used as alternative laboratories in online learning and such virtual laboratories offered by online learning can only fill the theory-to-practice hole. Online learning cannot be effectively and efficiently applied in some disciplines and this compatibility gap is yet to be filled. According to Murphy (2020), based onthe Association of American Medical Colleges (AAMC) recommendations, medical students were directed to abstain from having direct contact with patient in the middle of March 2020, medical-trainees of Brown University were in clerkships and the school were able to "augment" medical students training by migrating some aspects of clinical education to online platform. However, those students are to go back to the wards to complete the direct-patient interaction that is required in clerkship as soon as the suspension due to the Covid-19 has been lifted. This implies that online learning is not compatible with clinical but can only be used to augment face-to-face training method pending the time there will be chance to go back to the normal traditional setting.

Online learning on its own has advantages, such as flexibility ,interactivity, self-pacing and opportunities, the current increase in its adoption by universities is born of their desire to direct their actions toward alignment with both local and global practices and policies to overcome the spread of Covid-19 pandemic and maintenance of academic calendar. Universities and other educational platforms have responded to the pandemic with quick digital transformation of their educational activities. According to Manfuso (2020), Greg Flanik, Chief Information Officer of Baldwin Wallace University in Ohio, stated that when they were informed of the digital transformation of instructional activities, he told his team to make the best use of the opportunity offered by the crisis since they have always said that to get everybody to make use of online learning tools would be an ultimate accomplishment. Greg Flanik continued by adding that online learning has provided a clear roadmap that educators need to take advantage and engage major stakeholders in education to create novel market for instructional delivery and the longer the pandemic lasts, the more likely online learning becomes a general acceptable mode of teaching and learning.

V. Concluding remarks

It is visible that instructional technology, as a research field with several sub-divisions, has played a major role in cushioning the effect of this pandemic on educational activities by serving as the only platform for instructional design, delivery and assessment platforms.
Nowadays, online tuition is often viewed as "incomplete" and "supplementary". It might be that the coronavirus pandemic will change this perception. The major and the most ubiquitous impact of the COVID-19 pandemic on the academia and higher education is that innovations leading to their digitalization that would have taken months or perhaps years under the normal circumstances due to the red tape and the administrative and legal regulations were promptly introduced in a matter of weeks or even days. It turned out that academia and higher education already had all the tools necessary for the online lectures, teleconferencing, or digital open books exams, but were reluctant to unleash their full potential, perhaps waiting for some better days to come.

VI. REFERENCES

- Adedoyin, Olasile Babatunde and Emrah Soykan. 2020. "Covid-19 pandemic and online learning: The challenges and opportunities." *Interactive Learning Environments*: 1–13. https://doi.org/ 10.1080/10494820.2020.1813180.
- Strielkowski, W. (2020). COVID-19 pandemic and the digital revolution in academia and higher education. *Preprints*,2020040290. http://doi.org/10.20944/preprints202004.0290.v1
- Vlachopoulos, D. (2020). COVID-19: Threat or opportunity for online education? *Higher Learning ResearchCommunications*, *10*(1), 2. https://doi.org/10.18870/hlrc.v10i1.1179
- H. Mbhiza , D. Muthelo (2022)."COVID-19 and the quality of mathematics education teaching and learning ina first-year course" *in* South African Journal of Higher Education · May 2022.

DELTA 3D PRINTING ROBOT WITH COST EFFECTIVE INNOVATIONS

AAKASH P*[1], AJEETH N[2], DEEKSHITH GOWDA B M[3], TULSIDAS D[4]

Department of Mechanical Engineering, Sapthagiri College of engineering
#14/5 Chikkasandra, Hesaraghatta main road, Bangalore- 57, India
[1]erucaeutstellae@gmail.com
[2]goodboyajeethlego@gmail.com
[3]deekshithgowdabm@gmail.com
[4]tulsidasd@sapthagiri.edu.in

Abstract **– The project we are working on is a "Delta Style 3D Printer" with certain cost-effective modifications. In today's world 3D Printers are revolutionizing the prototyping industry. They are used almost everywhere. The biggest drawback is the huge upfront costs. Hence, we have decided to tap the technology in a much cheaper way and at the same time not to sacrifice the quality. The printing technology works on the principle of stacking individual 2 Dimensional layers of predefined thickness one upon the other to create a true 3 Dimensioned object. This method is known as additive manufacturing as the process involves addition of raw material rather than removal of material. The biggest pro of this method is its high accuracy. Specifically, for this build we are adopting a method called "software tuning". That is, since most of the build is by hand, there would be higher inaccuracies that could severely affect the output. By compensating for the mechanical errors through software, we were able to get micrometer accuracies in a much efficient and cost-effective manner.**

Keywords – Additive Manufacturing.

I. INTRODUCTION

People, since ancient times, wanted an efficient medium for materializing their ideas and sharing it with others. A traditional printer, also known as the Gutenberg printing press, sparked a revolution since important documents and ideas could be conceptualized and spread to the masses. For Ex. The first document to be printed was the Bible which led to worldwide popularization of Christianity. Also, ideas such as democracy, equality, and communism became popular due to printing. Coming to the 20th century, printing in the form of typewriting had shown its powers. Information of top confidential nature could be easily typed and shared through fax instead of a hand-written letter riding on a horseback. In the late decades of the last century, a printer was used as a peripheral device, which made a persistent human readable representation of the graphics a text in paper. But people of this generation have different needs which is realized again by the revolutionary concept of printing. This time in Three Dimensions. It provides a way through which people materialize their ideas into a tangible product under an unimaginably short period of time. Nowadays 3D printers available are of higher costs that is due to the printing technology used and the material used in the fabrication of a 3D printer, so this project sparks upon the idea of making a 3D printer under reasonable costs by using the scrap materials and a few 3D Printed parts.. The main aim of this project is to make the 3D printer available to a common man and to operate and automate working once the command and specific design is given to this machine. So operating time will automatically decrease as it can handle the task without any human intervention. This also makes this device reasonable and approachable to everyone in this project. This project deals or in other words targets the people who have cost as a main constraint and thus making a 3D printer useful in school laboratories, automobile industries, making a prototype material in industries etc.

II. MATERIALS & METHODOLOGY

Aluminum Composite Sheet: We have found that these low-cost Aluminum composite sheets are the most cost-effective solution for the overall frame due to the following reasons. i) Being widely used building construction material, it is easily available in many hardware stores. ii) Compared with wood, it is extremely light in weight. iii) It is also very easy to work with

considering the fact that the frame was entirely constructed with hand tools. iv) It requires very little post processing compared with wood or sheet metal which requires to be painted hence prolonging production time. v) Their internal rubber core makes it extremely easier to drill holes and tap screws.

Chlorinated Polyvinyl Chloride Hollow Shaft (21" ID): Also known as CPVC pipes, they are mainly used for plumbing and also find its application in our design as vertical support shafts due to the following reasons. i) It's cheaper and readily available as it is also a widely used product. ii) Unlike metallic shafts, it can be drilled laterally and tapped for mounting L Joints. iii) Since the height of the frame the CPVC supports isn't comparatively much, the rigidity of the shaft material takes over its flexibility and hence we get a strong standing structure.

Polished Steel Hollow Shaft (16mm ID): These steel shafts were only meant to replace the Open Beam Extrusions and the main sliding joint for the belt slider. i) The L shaped joints were directly welded to the shaft as it provided a much stronger joint than drilling and using fasteners. ii) Although it's impossible to state the frame is completely stiff with only the CPVC shafts, as a secondary objective, these steel shafts do support the overall structure to some extent.

Untempered Plain Glass (5mm thick): The print surface upon which the final product was to be printed had the following recommendations. i) It must be strong enough such that the force exerted by the nozzle cannot deform it. ii) It must not have any surface indentations that can cause issues while printing. iii) It must have a perfectly flat surface with zero angular imperfections that can cause severe issues including print failure if not accounted for. iv) It must be resilient to temperature changes without deforming or cracking. Confirming with the above recommendations, the material we selected was tempered plain glass, since we were unable to find a producer that can fabricate custom sized tempered glass, we had to defy the last recommendation and go with untempered glass as we were sure that the machine won't be subjected to huge temperature changes.

Miscellaneous 3D Printed Parts: In accordance with the RepRap Philosophy, who believes that self-replicating and self-healing machines are the future, some of our materials were custom or previously designed 3D models that were printed on another 3D Printer at a reasonable price by a being who was happy to support our venture.

The materials discussed previously were used for the mechanical build of the machine in which certain compromises were made. The following the electronic parts that were used in the build:

1. *Arduino Mega*: An open source community driven prototyping board.
2. *RAMPS 1.6*: A shield that interfaces motors, motor drivers and other sensors with the Mega.
3. *NEMA-17 Stepper Motor*: Compared to a traditional brushless DC Motor, this motor divides the entire series of steps that could be individually controlled.

Software tools used:

1. *Marlin Firmware*: It's an open source firmware whose primary function is to convert the G-Code commands into mechanical movements in the machine.
2. *Ultimaker Cura:* Although proprietary in nature, it's a free software used in the slicing of 3D Models into appropriate G-code commands.

Methodology:

1. A study was conducted into the parts and mechanisms of various 3D Printers in the market ranging from low end to high end devices.
2. After a brainstorming session, we developed some alternatives for the mechanisms using cheap and standardized parts.
3. We then used a suitable CAD software to develop a basic prototype whose part drawings are given below.
4. The composite sheets were cut to the required dimensions (by hand) and the basic frame assembly was undertaken.
5. For the 3D Printed parts we outsourced them as they were non standard and 3D Printing was the cheapest solution available.
6. The electronics were then added to the frame with proper cable management techniques.
7. For the power supply, we went with the commonly available LED power supply that provided 12V 20 Amps from the 220V AC mains.

ISBN: 979-88-35073-61-0

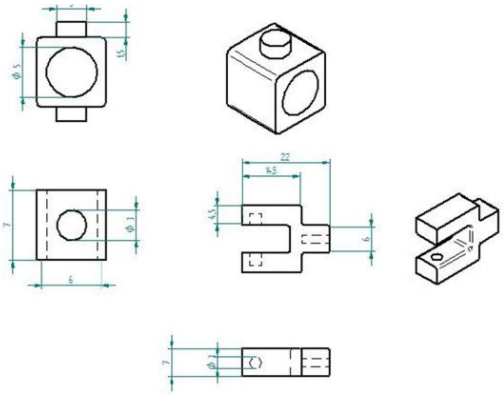

Figure 1: Universal Joint designed in-house

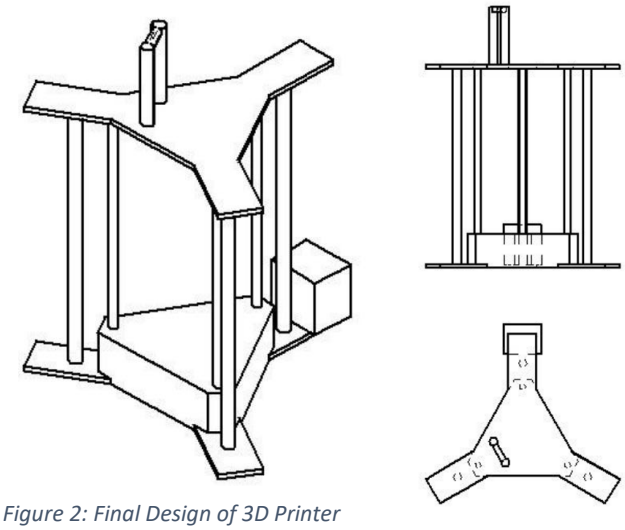

Figure 2: Final Design of 3D Printer

Figure 3: Universal Joint, 3D Printed

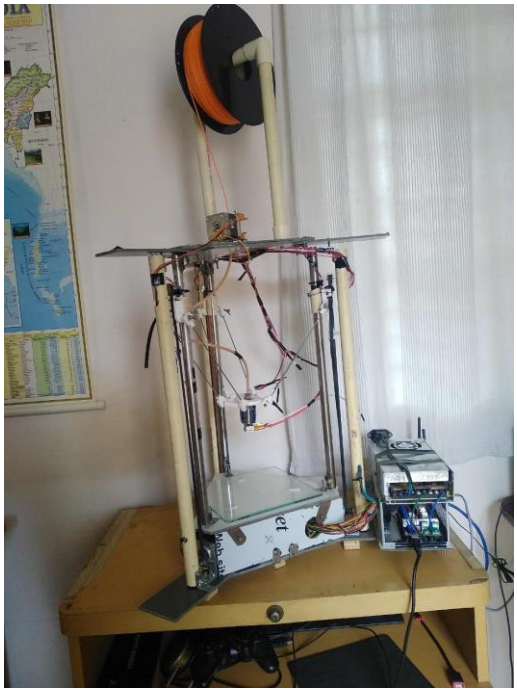

Figure 4: Fully Assembled 3D Printer, Front View

Figure 5: Fully Assembled 3D Printer

ISBN: 979-88-35073-61-0

Figure 6: Fully Assembled Push Rods, 215mm each

Figure 8: End Effector, designed in-house

Figure 7: CoC caricature, printed in-house

Figure 9: A test part showing the dimensional accuracy of the machine

III. RESULTS & DISCUSSIONS

Once the build of the 3D Printer was completed, basic calibration checkouts of the machine were completed and we began our first test prints. The output we received was disappointing at first. We discovered multiple faults that all linked to the inaccurate build of the machine. Usage of hand tools had taken its toll. But it was a blessing in disguise. The firmware we used did have a feature where we could compensate for the inaccuracies of the build. By painstakingly adjusting the myriad of parameters, we were enthralled by the output. As shown in fig the output provided was on par with that of professional machines but at almost 1/10th of the cost. Hence, we had succeeded in our initial objectives.

IV. CONCLUSIONS

1.It is possible to develop an affordable, reliable and an outperforming 3D Printer at minimal costs.
2.A modular, compact and affordable machine can be easily adopted in places such as schools and universities.
3.The use of 3D printed parts calls for the need of a pre-existing 3D Printer as it is the cheapest possible solution. Other methods are also feasible.
4.Further upgrades in terms of design and fabrication methods can also be improvised upon as the design files and the methods are open source in nature.

IV. ACKNOWLEDGMENT

We would like to express our sincere gratitude to the Management, Principal Sapthagiri College of Engineering Bengaluru for the facilities provided and their support. Also we would like to thank the Head of department Mechanical Engineering and faculties, Dr. Tulsidas and Dr. Deshpande for their encouragement and support.

VI. REFERENCES

[1] Deshpande Sharanya Suresh: *Design And Development Of Low Cost 3-D Printer*. Marwadi Education Foundation's Group Of Institutions.

[2] Stefan (CNC Kitchen): *Stefan, from CNC Kitchen has conducted an extensive research into 3D printing materials by assessing various mechanical properties such as strength, working temperatures, fatigue cycles and cost effective alternatives too*. https://www.youtube.com/c/CNCKitchen/

[3] Massimo Banzi: *Make: Getting Started with Arduino*. ASEE 2016.

[4] Johann, *Design of Kossel format of 3D Printers*, Reprap, 2012.

DESIGN AND FABRICATION OF PNEUMATIC BUMPER AND INTELLIGENT BRAKING SYSTEM

SRIKANTH.S*[1], MALIKARJUNA PATIL G*[2], ASHIK K H*[3], SURYA SHUBHAM*[4], THEJAS M S*[5]

Department of Mechanical Engineering, Sapthagiri college of Engineering

#14/5 chikkasandra, Hesaraghatta main road, Bangalore-57 India

[1]srikanths14081999@gmail.com

[2]mallikarjunapatil.1998@gmail.com

[3]gowdaashik192@gmail.com

[4]surya.shubham112@gmail.com

[5]thejasms@sapthagiri.edu.in

(Assistant professor, Department of Mechanical Engineering)

Abstract-Now a day's accident of the vehicles are common and big issue. Our project Pneumatic bumper and intelligent braking system is used to overcome this problem of accident in uncertain road conditions. Proximity sensor plays a major role in Pneumatic bumper and intelligent system. This system will be assembled in a modern day cars. In these system, there are 2 mechanisms they are pneumatic bumper and braking system. Here the infrared sensors senses the obstacles in front of the vehicle. Then the sensor gives feedback to the solenoid valve through the relays. So that the compressed air enters in the direction required. As the compressed air enters the double acting cylinder to which bumper is fixed gets activated and the bumper is pushed forward and the air in the Single acting cylinder pushes the piston forward to which the brake are connected and the brakes are applied and the vehicle is stopped.

KEYWORDS: Pneumatic bumper, IR sensor, car, Safety

I INTRODUCTION

Improving the automobiles safety and conducting researches on it is never an old thing and the interest in this topic grows more and more day by day for the car industry. They will be trying to discover new technologies everyday to improve the safety of the vehicle and passengers inside the vehicle during accidents. Globally around 1.2 million die every year in road accidents.

In modern day technologies there are various safety instruments which are fixed inside the cars like rear view camera, air bags, seat belt etc. to improve the safety during accidents. Road accidents are increasing year by year due to increase in the production of cars, so protection of people from accident who are inside and outside the vehicle is very much important.

The sensor systems used in our project is used to detect the obstacles in front-end of the vehicle and to prevent the accidents. Development of such automatic systems in vehicles will be increased by car manufacturing companies to ensure the safety.

In present day vehicles the brakes are manually operated and during the accident when the driver encounters the obstacles usually he gets confused and nervous and sometimes it fails to apply the break or it does not applies the brake in right time. So to overcome this situation we use the automatic braking system this system. This system helps more the driver who is driving the vehicle during the night time, if the driver has fallen asleep the chances of accident is more.

The bumpers used in current vehicles are not movable it's rigid and fixed, so during the accidents these forces are transferred directly to the passengers inside the vehicle hence it does not ensure safety of the passengers. Sitting inside the vehicle and it cannot reduce the external damage to vehicle, In order to overcome this we have designed pneumatic bumper and intelligent braking systems.

II MATERIAL & METHODS

Initially mildsteel is used to make the frame. The frame is Arc welded. Typically the material is used to construct vehicle chassis and frame is carbon steel. The electrical part consists of IR sensors, IR transmitter, Relays, Limit switches which are connected. The Single acting cylinder and Double acting cylinder are connected to the solenoid valve. The compressed air is of 4 to 5 bar is pressed to the solenoid valve, later passed to the pneumatic cylinders.

III METHODOLOGY

- At first we started this project by gathering the information from various site on internet and learnt how this works by seeing many videos and collected more journal papers which are similar to our topic.
- Then we listed out the required components for our project.
- Then we started 3D modeling of our project by the help of CATIA software
- Started assembling the electrical and mechanical parts

- Observation were made by conducting the experiment repeatedly.
- After we get the desired observation or exact working as we need, the result of the project and conclusion of the project were drawn.

IV WORKING

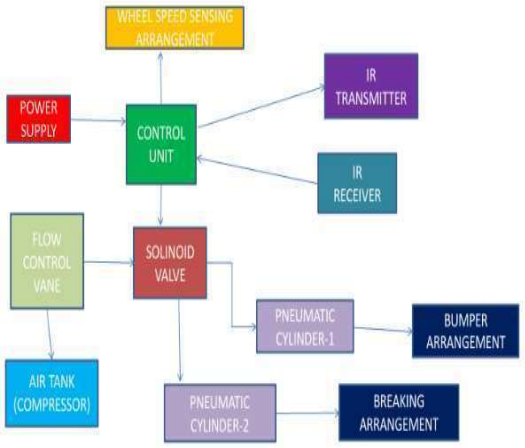

Fig1: Block diagram of working principle

In this system IR sensor plays a major role in detecting the obstacles. As the IR transmitter transmits the infrared rays if there are any obstacles in front of the vehicle the IR rays are bounces back and is received by the IR receiver, then the signal receive is transmitted to the control unit.

Then the relay is operated by the control unit according to signal of the input provided by the control unit. Then the control unit sends the signals to solenoid valve, which controls the direction of compressed air then the compressed air enters both single acting and double acting cylinder. The single cylinder is connected to braking system and double acting cylinder is connected to bumper system. When the compressed air enters the single acting cylinder it applies the brake and makes the vehicle to stop. During the return stroke of the piston the brake is released. When the compressed air enters the double acting cylinder the piston moves forward and the bumper moves forward and avoids the maximum force travelling inside the vehicle and minimize the vehicle's external damage and damage to human.

V COMPONENTS

1. LIMIT SWITCH

It is used to interlock a mechanical position or motion with an electrical circuit. In this system limit switch sends an electrical pulse to electronic relay switch. It is used to ON/OFF the aurdino board by using power from battery.

Fig2: Limit switch

2. SOLENOID VALVE

Solenoid valve is used to control the direction of compressed air from

compressor to pneumatic cylinder and cylinder to exhaust. In our system we have used 5/2 and 2/2 solenoid valves.

Fig3: 2/2 Solenoid valve

3. BASIC FRAME

The basic frame in our project model is made up of mild steel and it consist of 4 wheels, control units and electric motor are fixed to this basic frame.

Fig4: Frame

4. ELECTRONIC RELAY CIRCUIT

The electronic relay circuits used in our project has 2 output which are connected basically to 2 solenoid valves. The electric current is supplied to solenoid valves by these Electronic relay circuit.

Fig5: Relay circuit

5. IR SENSORS

Basically it consists of 2 parts transmitter and receiver transmitter usually transmits the infrared rays to detect the obstacles and receiver is used to receiver these signals.

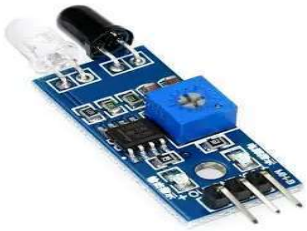

Fig6: IR Sensor

6. CONTROL UNIT

The microcontroller board we have used is aurdino UNO board in which it consists of 14 input for output pins and 6 analog inputs.

Fig7: Aurdino board

7. ELECTRIC MOTOR

The Electric motor we have used in out project is ¼ HP motor, it is used to drive the wheels forward through the belt drive mechanism.

Fig8: Electric motor

8. PNEUMATIC CYLINDERS

Pneumatic cylinder is the main and important component in our project we have used single and double acting cylinder. Single acting cylinder is used to apply the brake and double cylinder is used to push the bumper forward during the accident.

Fig9; Single acting cylinder

VI 3D MODELLING

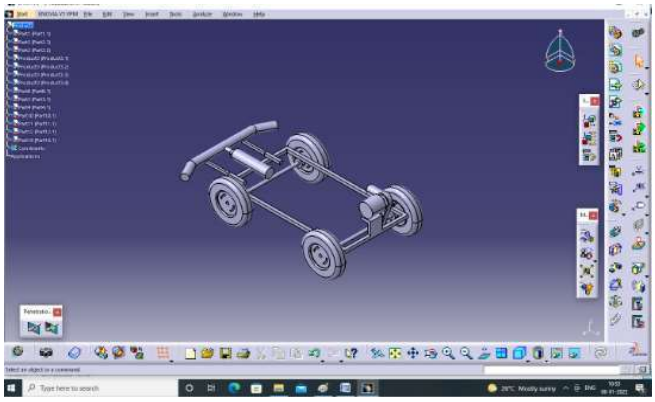

Fig10: Draft image using catia

VII ADVANTAGES

- The prototype vehicle is simple in construction
- It increase the safety of the vehicles and passengers during pre-crash
- It increases the external safety of the vehicle.
- It reduces the risk of accident by applying the brake if the driver fails to do so.
- It reduces the force which transfers to the passengers during the accident and ultimately saves the life of passengers.
- Low cost when compared to other safety instruments like airbags.

VIII LIMITATIONS

- The length of stroke of the system is fixed.

- Since there are more moving parts in the system the maintenance cost will be high.
- In heavy traffic roads it has few limitations. ‘
- It does not any provision to prevent the accidents that occurs from the vehicle’s rear side
- There will be frictional losses because of the linkages.

IX FINAL ASSEMBLY VIEW

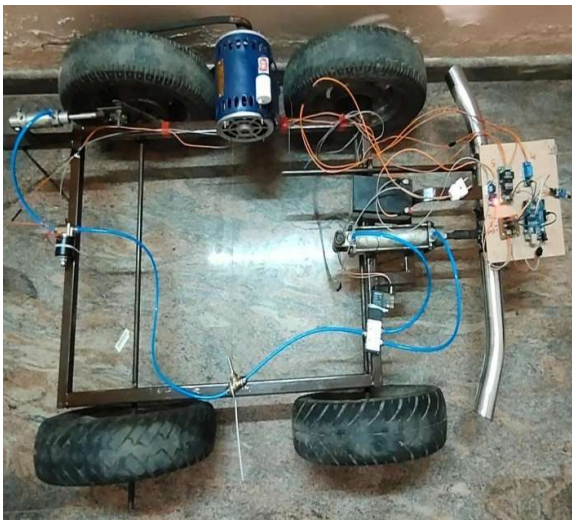

Fig11: Final image

X CONCLUSION

The aim of the project is to reduce the accidents on road and to develop the cost-effective safety instruments. It also minimizes the external vehicle damage during accidents and also reduces the damage and increases the safety to the humans inside and mechanics which is also called as Mechatronics when combined. The prototype developed by our team is working as desired.

The other aim of our project is to provide the same kind of safety as provided by the high end cars, at a low cost.

XI REFERENCES

1. Dr. R. K. Bansal, A textbook of strength of materials, Laxmi publication (P) Ltd.
2. R.S. Khurmi. J.K. Gupta, A textbook of machine design, S. Chand publishing House (P) Ltd.
3. G.B.S. Narang, “AUTOMOBILE ENGINEERING”, Khanna Publishers, Delhi, 1991, pp671.
4. William H. Crowse, “ AUTOMOBILE ENGINEERING”,
5. Pneumatic Control System---Stroll & Bernaud, Tata Mc Graw Hill Publishers, 1991.
6. Pneumatic System--Majumdhar, New Age India International (P) Ltd Publishers, 1997.

Electrodeposition method for the development of a Pt-Rh alloy coating: An Efficient material for the photocatalytic applications

Bharath K. Devendra
Chemistry Department, Srinivas University,
Institute of Engineering and Technology
Managluru, India
bharathkdevenrda@gmail.com

Praveen B.M
Chemistry Department, Srinivas University,
Institute of Engineering and Technology
Managluru, India
bm.praveen@yahoo.co.in

Abstract-A method of electroplating a platinum-rhodium (Pt-Rh) alloy coating with a specified composition on a metal substrate stainless steel (SS304) is presented in this article. The Pt-Rh bath consists of $[Pt(NH_3)_2]HPO_4$, H_2SO_4 and $Rh_2(SO_4)_3$. The Pt-Rh alloy electrodeposition coatings were characterized by different analytical methods such as Scanning Electron Microscopy (SEM) and X-ray diffraction (XRD). SEM images justifies that coating is uniform in 75% duty cycle. XRD confirms that crystalline size was reduced from 75% duty cycle to the rest of the PC's coatings and DC (Direct current). Incorporation of the Pt-Rh metal ions was verified by EDX analyses. A photocatalytic degradation study of Pt-Rh coating was conducted for Methylene Blue (MB) dyes under UV light radiation. PC 75% duty cycles showed an exceptional dye degradation percentage compare to DC coating source. All photocatalytic behaviour was controlled by using UV–Vis spectrophotometer.

Keywords-Platinum-Rhodium, SS304, SEM, XRD, Dye degradation, Corrosion.

1. Introduction

Platinum, palladium, rhodium, ruthenium, iridium, and osmium are members of the platinum group metals (PGM). Only platinum, palladium, and rhodium have previously found significant use in the electrodeposited condition [1]. The main disadvantage of this alloy coating is its high cost; however, its benefits include excellent chemical and oxidation resistance, as well as high strength, mainly resistance to corrosion at high temperatures, are present in different areas such as production of glass [2,3] and nitrogen fertilizers [4,5,6], thermocouples [7], automotive catalysts [9], jewellery [9,10] etc.

Pulse Electrodeposition is considered as more efficient method of Electroplating compare to DC method of Electrodeposition. In PC method, based on the requirement current can be controlled by ON and OFF method. In ON time current is passed into the time it is switched off. During OFF time more time will be given to nucleation and which reduces the nuclei size and give the uniform crystalline size. We value PC over DC in Pt-Rh alloy coating because electroplating of Pt-Rh by DC consumes a major amount of metal ions from the bath solution, resulting in poor coating. The PC plating technique, on the other hand, would be extremely beneficial that have noticeably reduced the amount of Pt-Rh consumed during plating which may find various industrial applications. As a result, production costs will be lower, production time will be shorter, and coating quality will improve [11]. Also, conventionally DC plating only one parameter, namely, current density can be varied. However, PC method three important factors: peak current

density, current ON time and current OFF time can be varied and growth can be controlled [12].

Noble metal coatings were done on stainless steel to control the corrosion in boiler water reactors. Intergranular corrosion is very common in boilers. So development of noble metal coatings on stainless steel with high corrosion resistance is very important in boilers. Noble metal chemical addition is a recent development in this field and it reduces the corrosion abruptly. Many methods are available to coat Noble metal on the steel surface. Electrodeposition is a simple and efficient method for coating Noble metals. In this technique noble metal can be coated uniformly [13].

Roughly 8–20 % of idle dyes and auxiliary chemicals are settled from the textile production into the wastewater stream [14]. Nearly one million tons of dyes are made every year around the biosphere. Furthermore, the majority of these dyes and their components are carcinogenic and mutagenic, posing a threat to all living things on the planet [15, 16, 17]. Even a small amount (less than 1 ppm) of these compounds in water has negative consequences [18]. The excellent corrosion-resistant properties of Pt-Rh catalysts are evaluated for the gradation of dyes. In this work, Pt-Rh coated samples successfully showed positive trends in the degradation of Methylene Blue (MB) dye.

2. Experimental Materials and Methods

2.1 Electrodeposition Development

The solution used in the present study was Pt 5Q electroplating bath [Pt $(NH_3)_2$] HPO_4 and Rhodium Sulphate solution $Rh_2(SO_4)_3$ supplied by Arora Matthey Limited, Kolkata. The electrolyte solution was prepared using 1.5 mL Platinum solution and 0.075 mL Rhodium solution. By adding 5 ml concentrated H_2SO_4 and distilled water, this solution is made to 50 ml. The experiment was carried out in a glass cell Figure 1. Pt-Rh alloy coatings with a 1.7 cm^2 exposed surface area were formed on SS 304. To achieve a smooth finish, abrading 600 grade to 2500 emery paper was used to prepare polished SS304 surfaces and after that, alumina powder is used to polish the surface (1.0, then 0.3 and 0.05 lm grades) on a humid polishing cloth, then thoroughly cleaned with deionized water. Only emery paper abrading ad washing were used to prepare rough surfaces. Freshly machined SS304 discs were used in one set of experiments, and they will had the tool marks from their fabrication on a lathe.

The cathode is made of SS 304 circular discs with a diameter of 15 mm and a thickness of 1 mm and at a distance of 2 mm from the coupon's edge, a 2 mm hole was provided to hold the disc during electrodeposition. While coating process the remaining portion of the backside was masked. The anode was made of platinized titanium. Electrodeposition was carried out for 18 minutes using a current source N6705B Key sight technologies of direct current (DC) and pulse current (PC) for a range of cathodic current densities ranging from 1.0 to 6.0 A/dm^2. pH and temperature are kept at 1.2 and 40 °C, respectively. The coatings were carefully rinsed with distilled water after each deposition and then air-dried.

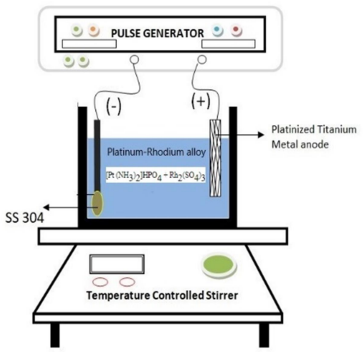

Figure 1. Schematic representation of pulse electrodeposition of platinum on SS304.

Components	Conformation
Platinum solution [Pt $(NH_3)_2$] HPO_4	1.5 ml
Rhodium sulphate solution $Rh_2(SO_4)_3$	0.075 ml
H_2SO_4	5 ml
Electrodeposition Bound	
Heat	40 °C
pH	1.2
Current density	4.0 A/dm^2
Installation time	18 min
PC Duty cycle	25%, 50 % and 75%
DC	Direct current flow

Table 1. Improved component's bath solution

The surface morphology and compositional analysis of the formed coatings were studied using scanning electron microscopy (FESEM Carl ZEISS). The phase structure and crystallite grain size were examined using X-ray diffraction (XRD, RIGAKU).

Electrochemical impedance spectroscopy (EIS) and the Tafel extrapolation technique was used to assess the corrosion behaviour of Pt-Rh alloy Electrodeposition by a three-electrode system, using a CHI608D electrochemical workstation (CH Instruments, Austin, USA) to keep open to air at room temperature. The Ag/AgCl electrode and the platinum electrode, respectively, were used as reference and counter electrodes. The EIS study was conducted on an electrodeposited coated working electrode with an exposed surface area of 1 cm^2 in 0.1M sodium sulphate as corrosive media in neutral pH

Photocatalytic experiments were carried out in the centre of the cylindrical photoreactor, which consists of a light source (here, a UV light lamp, 300 W, absorbance at 664 nm (UV–Vis absorption spectra)) surrounded by eight quartz reactor tubes (each 100 mL in volume), 37 cm in height and 2.3 cm in inner diameter, as well as cooling fans. A reaction mixture consisting of catalytic load of different electrodeposited Pt-Rh alloy coated sample with two different current source, namely DC and PC, with 25%, 50% and 75% respectively, was prepared in 100 ml of 5 ppm MB dye. The suspension was stirred in the dark for 3 hours. The solution was irradiated under UV light at a constant temperature. Samples were also collected every 30 minutes to evaluate the percentage of MB degradation. A visible annular photo reactor (Agilent technology Cary-60) was purchased from the scientific company "HEBER" in Chennai, India for use in photocatalytic studies. The MB solution was prepared in the dark using double distilled water. A central light source powers the cylinder reactor. Surrounded by eight reactor tubing (each with a capacity of 100mL) and cooled by fans in the photo reactor. The Pt-Rh alloy metal coating was done on SS304 using a PC and DC technique with different duty cycles, and the maximum dye degradation was selected from the metal coating and further degradation parameter work was done only for the respective sample. All of these samples were tested for photocatalytic performance.

The percentage of photocatalytic degradation of organic dyes has been determined as follows.

% of degradation = $[(C_a-C_b) / C_a] X 100$ …… equation -1

Where C_a and C_b b is initial and final dye concentration respectively. The research was repeated by a selection of parameters, such as dye concentration, stability, scavengers and pH.

2.3 Results and Discussions

Optimization of Bath Parameters

The electrodeposition method was used to deposit Pt-Rh coatings on mild steel panels using the optimized electrolytic bath listed in Table 1.To obtain a good, desirable coating, pH, temperature,

current density, and composition of the bath plays a crucial role in the evaluation of the coating.

When it comes to achieving the best electrodeposition coating, the current density is crucial. Current density was varied from 1.0 A/dm^2 to 10.0 A/dm^2 to determine the effect of the coating. The formation of a "burnt" black colour deposit occurred at current densities greater than 5 A/dm^2 due to rapid discharge of metal ions from the electrolyte resulting in poor coating and Metal ions deposition is a smaller amount at current densities less than 4.0 A/dm2, uneven and irregular deposition on the substrate occurs and hence in our research, a current density of 4.0 A/cm^2 has been determined to be optimal.

The alloy coating was carried out at the ideal temperature of 40°C by DC and PC method by making the variation in an optimised condition. At 40°C, the electrolyte dissociates, even more, resulting in the highest concentration of metal ions in the bath solution and a uniform coating. In comparison to other temperatures, coating at 40 °C produces a bright and adherent coating. At temperatures of 50°C and higher, we discovered burnt and unusual deposits. The coating obtained below 40 °C provides a seedy appearance due to an uneven coating. As a result, we have decided to test at a temperature of 40 °C.

The pH of the alloy coatings was varied from 0.10 to 3.0, and pH 1.3 was found to be the best, with the majority of the metal ions deposited at this pH. The stability of the bath deteriorated at higher pH values above 2.0, and burnt deposits formed. The coatings were smooth, uniform, and bright at a range from pH 1.0 to 1.5, but the coatings were poor at pH less than 1.0 so more research was done at pH around 1.0 to 2.0.

At 25, 50, and 75 % duty cycles, the deposition was finished by means of both the DC and PC systems. When compared to the PC method with a larger grain size obtained from DC, the coating morphology in the DC method was not uniform. The coating obtained at 75 % in the PC method is more even and regular, with a smaller grain size. In the PC method, fresh nuclei were formed and it produces a uniform and reduced grain coatings during ON and OFF time of the current. The grain size difference is marginal when compared to DC, 25% and 50% duty cycle. In comparison to other methods, the PC-75% method produces bright, uniform, and small grain size.

3. Coating Characterization

3.1 Scanning electron microscope

SEM images were obtained using a 5.00 kV and 15.kV scanning electron microscope (model: FESEM Carl ZEISS) with a mean large gap of 3.7 mm at different magnifications. SEM images of coatings obtained from PCs with various duty cycles and DC plating developed at current density 4.0A/dm^2 as shown in Figure 2**.** When compared to the remaining PCs and DC source in (Figure 2 a)75 % duty cycle coating, the smaller and uniform grains result in a smoother surface of the coatings.. From the Figure 2 b, 2c and 2d, the Pt-Rh alloy was found to be larger and uneven in scale on SS304 and its distribution is not uniform. In DC coating samples, the degree of uniformity decreased as the duty cycle percent decreased from 75 % to 25 % and more. The percent of duty cycle has a significant effect on the surface morphology of Pt-Rh electroplated coatings, as shown in Figure 2 a, 2 b, 2 c, and 2 d. For all the Pt-Rh alloy coating source, strong adhesion and brightness were obtained, but in 75 % duty cycle uniformity was achieved.

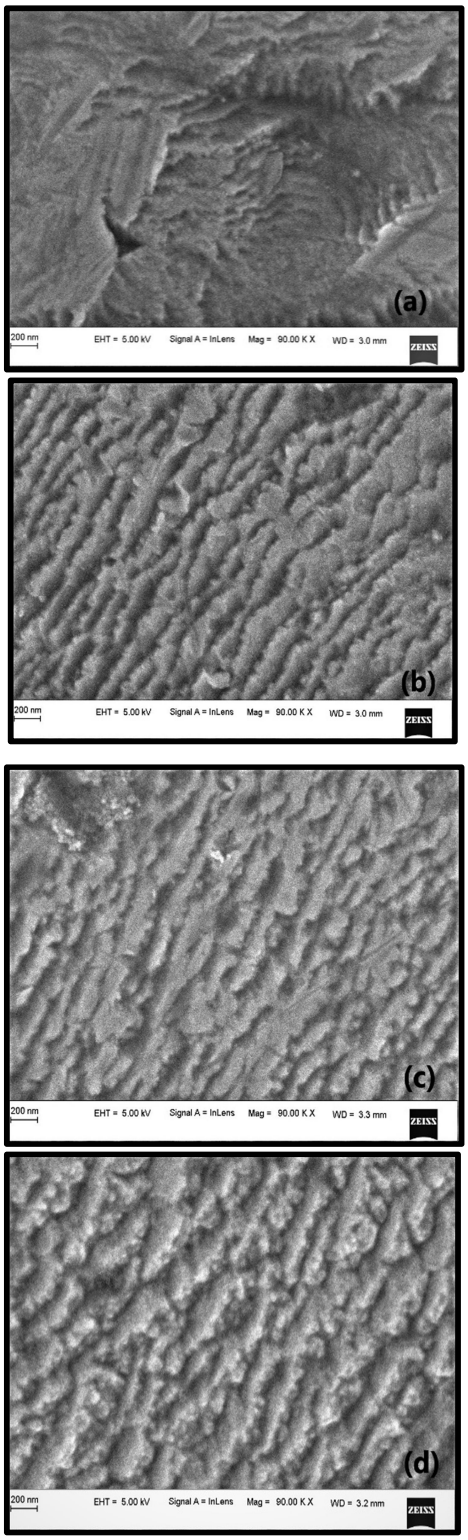

Figure 2 Surface morphology of Pt-Rh deposits produced at PC conditions. (a) 75% (b) 50% (c) 25%, (d) DC.

3.2 X-ray diffraction (XRD)

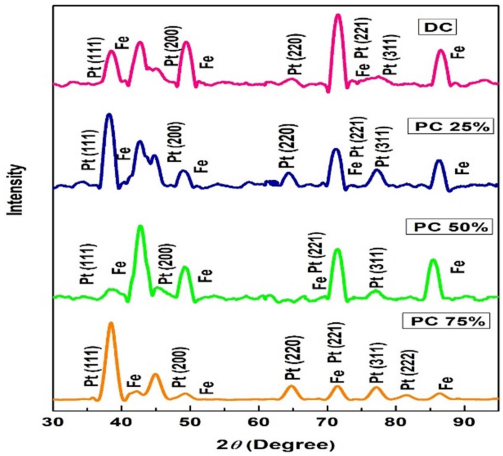

Figure 3. The XDR pattern of Pt-Rh coating obtained at DC and PC (25%, 50% and 75%).

X-ray diffraction (Rigaku Miniflex 600 (5th gen)) was used to obtain patterns of X-ray diffractometers. The XRD pattern of Pt-Rh coating electrodeposited on stainless steel by DC and PC (25%, 50% and 75%) method are as shown in Figure 3. The peaks were analysed by crystallographic search match software using powder diffraction files PDF numbers: 1-1190 Pt, 52-513 Fe and 2-1167 Fe Pt). The diffraction pattern mainly includes of Pt peaks corresponding to planes (111), (200), (220) and (311) and these Pt phases contain a smaller amount of Rh. Further base metal stainless steel (Fe) and Fe-Pt peaks are also observed on XRD pattern. The intensity of Fe peaks reduces in 75% PC coating. The crystallite size purpose was made using the Debye Scherrer method on (111) diffraction peak. In PC (75%) crystallite size was reduced compared to DC plating.

The Scherrer equation can be written as:

$$L = \frac{K\,\lambda}{\beta \cos\theta}$$

Where *L* is the crystallite size (nm), β is the full width half maximum intensity measured in radians, λ is the X-ray wavelength, θ is the diffraction angle and *K* is the Scherrer constant (0.95)

SI No	Source of coating	Average crystalline size in nm
01	PC- 75 %	10
02	PC- 50 %	07
03	PC- 25 %	06
04	DC	05

Table 2. Average crystalline size.

4. Photocatalytic activity

The Pt-Rh coated sample's effect on photocatalytic degradation of MB dye solution was investigated. Methylene blue ($C_{16}H_{18}N_3SCl$) is a cationic heterocyclic aromatic azo-dye whose molecular structure is shown in Figure 4. All trials were carried out in the company of UV light , using a 300W xenon lamp as a light source.

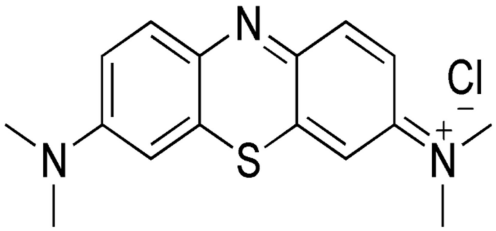

Figure 4. Molecular structure of Methylene Blue

4.1 Probable mechanism of dye degradation

The electrons (e-) in the valence band (VB) excited the conduction band (CB) with the same number of holes (h+) left in the VB when coated metals were irradiated by photons. Photo generated electrons (e-) react with $O2^-$ generating O_2, while photo generated h^+ oxidizes MB on the surface of coated Pt-Rh alloy samples. These powerful oxidants could then substantially degrade MB molecules to H_2O, CO_2, and other molecules of nominal importance. A possible process of photocatalytic degradation of MB over coated metal sample was anticipated as follows:

Pt-Rh + hν → e– (VB) + h+ (CB) ..…... (1)

$O_2 + e– \rightarrow \cdot O_2^-$ ……. (2)

h+ (or $\cdot O_2^-$) + MB → Products ……..... (3)

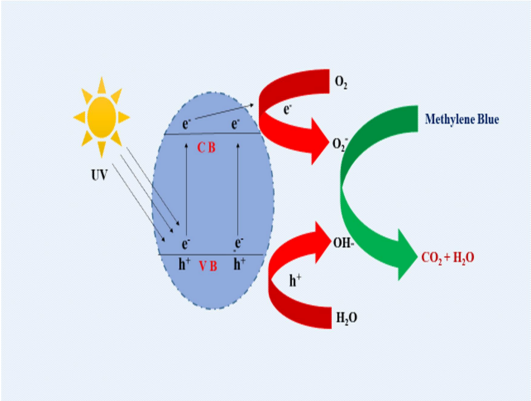

Scheme 1. Proposed mechanism for photocatalytic degradation of MB over Pt-Rh alloy coatings.

4.2 Photocatalytic study

The efficiency of degradation has reached 96 % degradation for Pt-Rh coated alloy sample of PC-75% and subsequent dye degradation of remaining duty cycle and DC samples of Pt-Rh is mentioned in **Table 3.** The dye degradation efficiency of different samples with different concentrations, pH, and scavengers was carried out for 180 minutes with different parameters by selecting the sample with the highest dye degradation from Pt-Rh. We have achieved good degradation for sample coated by PC method in our work, especially at PC-75% duty cycle for Pt-Rh alloy sample compare to DC and other PC samples. This may be due to smaller nanometer grain sizes relative to DC coated samples or other samples. The amount of photons absorbed on its surface is increased by an increase in effluent loading on the catalyst and the OH and e-/h+ pairs are increased. For this purpose, a PC-coated sample with a 75 % duty cycle provides good degradation activities.

Coating source	DC	PC-25%	PC-50%	PC-75%
Degradation %	89	92	94	96

Table 3. Efficiency of Methylene blue dye degradation by different Pt-Rh alloy samples in first trial.

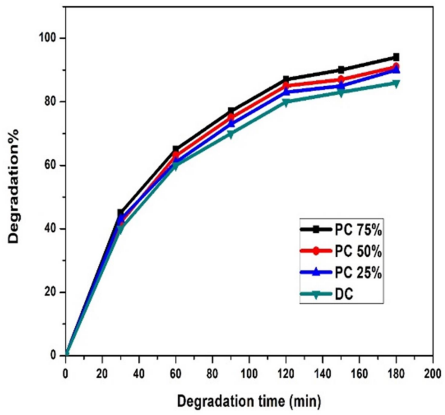

Figure 5. Percentage degradation of MB dye for Pt-Rh coated samples for 5ppm with run time of 180 minutes.

4.3 Effect of dye concentration

Catalyst action reduced with a rise in the concentration of dye. Degradation of the dye below the light source rest on mainly on its concentration. The analysis was carried out in 100 ml over 5 ppm, 10 ppm 15 ppm and 20 ppm dye concentrations to determine the optimum dye concentration as shown in Figure 6. This depends on the concentration of dye molecules on the catalytic surface, which in turn lowers the penetration level of light through the catalyst and thus reduces the degradation of the dye. As a result, the rate of generation of hydroxyl radicals and superoxide radicals was found to be lower. 5 ppm result displays more photocatalytic degradation associated to higher dye concentrations. (10–20 ppm).

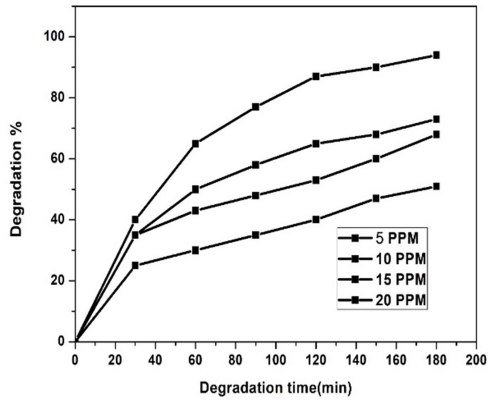

Figure 6. Photocatalytic activities of MB dye at different dye concentrations with respect to Pt-Rh 75% duty cycle.

4.4 Effect of pH on dye degradation

pH stands an important issue that impacts photocatalytic degradation. A 5 ppm MB dye solution was photocatalytically degraded using a Platinum-Rhodium coated sample at 75% duty cycle in pH series extending from 2 to 12. According to Figure 7, photocatalytic activity increases as the pH of the solution increases. In acidic environments, the external surface area of platinum- rhodium covered metal samples is positively charged, while in basic conditions it is negatively charged. Because MB is a cationic dye and Platinum-Rhodium has a negative charge, electrostatic interaction between the negatively charged surface and the cationic MB causes degradation. In the basic medium, the availability of OH^- is higher, which speeds up the photocatalytic degradation process. **Table 4** shows that the Pt-Rh coated sample at 75% duty cycle has higher dye degradation activities than the other coated samples.

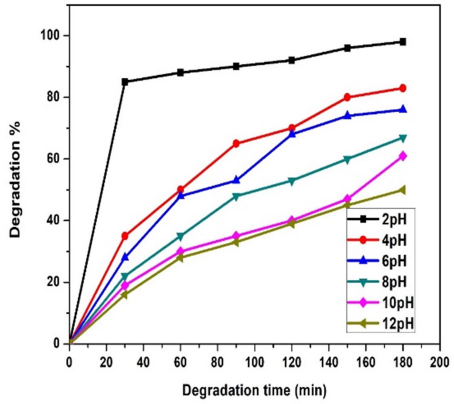

Figure 7. Photocatalytic activities of MB dye at different pH with respect Pt-Rh 75% duty cycle.

Coating Source	2 pH	4 pH	6 pH	8 pH	10 pH	12 pH
Pt-Rh 75%	50	61	67	76	83	96

Table 4. Relative readings of photocatalytic activity of Pt-Rh alloy in terms of different pH.

4.5 Scavenger studies

Scavenger studies looked into the active agents that cause pollutants to degrade. Under UV light, hydroxide anions, hydrogen ions, electrons, and superoxide anions (oxygen species) form during the photocatalytic degradation process. For the scavenger experiment, tertiary butyl alcohol (TBA) was added to separate dyes for hydroxide anions (OH-), EDTA (Ethylene diamine tetra acetic acid) for hydrogen ion (H+), K2Cr2O7 for electrons, and Ascorbic Acid (AA) for oxygen species such as anion scavengers. The photo degradation of MB dyes catalysed by platinum coated with a 75 percent duty cycle under UV light in the presence and absence of scavengers is shown in Figure 8. The most reactive species, hydroxide anion, is found to be the most responsible for MB dye degradation.

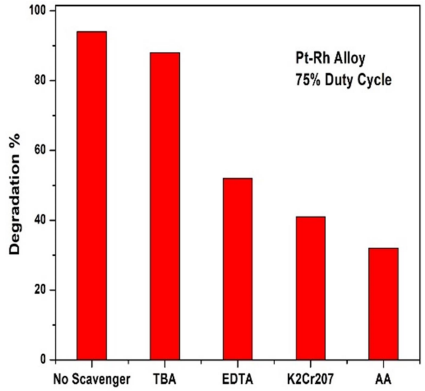

Figure 8. Effect of scavengers for Pt-Rh 75% duty cycle on UV light degradation of MB dye at 5ppm.

4.6 Reusability and stability

Stability and regaining are the foremost worries concerning photocatalytic degradation in Platinum-Rhodium electrodeposition. After degradation (cycle 1) Platinum-rhodium-coated samples were washed with distilled water to remove adsorbed dye molecules on the surface of the photocatalyst, trailed by drying in the oven to remove water molecules. The recovery and stability testing was accompanied using dried samples over four consecutive cycles of degradation. Subsequently four cycles, the reusability efficiency of the photocatalyst decreased from 97 % (1st cycle) to 85 % (4th cycle) as shown in Figure 9. Photocatalyst activity decreased efficiency by 12 %% even after the 4th cycle of degradation. Recycled catalyst can be used for further degradation of dye under visible light source [19].

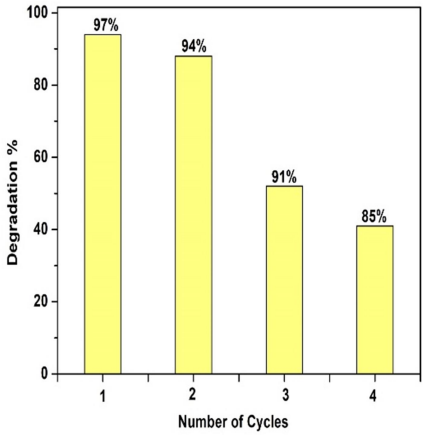

Figure 9. Stability of the Platinum-Rhodium coated sample with different cycles

5. Conclusion

This invention involves the field of electrodeposition of metals. More precisely, it relates to the process of obtaining platinum-rhodium alloy coating by both DC and PC methods and it is distinguished by SEM and XRD. From data of XRD we came up with the conclusion that 75% PC samples reduced the crystalline size more compare to remaining PCs and DC samples. Finest corrosion resistance coating was developed for PC-75% duty cycle. For Methylene blue dye, which is present in the textile industries, Pt-Rh exhibits higher photo degradation and has a great potential application in wastewater treatment**.** All in all, one day electrodeposited Pt-Rh alloy-coated samples will replace the existing methods which is suitable for waste management, water disinfection.

Funds and Acknowledgment

With approval of Project No. 37(2)/14/18/2018, dated 11/07/2018, instrumental and financial funding from the Department of Atomic Energy (DAE) Board of Research in Nuclear Sciences (BRNS), Mumbai, and Government of India. Srinivas University, College of Engineering & Technology, Srinivas Nagar, Mangaluru, Karnataka, has provided laboratory support.

References

1. E. Laister, Metal Ind., 1954;85:427-469.

2. E. Preston, Platinum in the glass industry. Platinum Met. Rev., 1960;4:48-55.

3. B. Fischer, Reduction of platinum corrosion in molten glass. Platinum Metals Rev., 1992;36:14-25.

4. Y. Ning, Z. Yang, H.Zhao, Platinum recovery by palladium alloy catchment gauzes in nitric acid plants. Platinum Met. Rev., 1996;4:80-87.

5. N. Yuantao, Y. Zhengfen, Platinum loss from alloy catalyst gauzes in nitric acid plants. Platinum Met. Rev., 1999;43:62-69.

6. B.Trumić, D. Stanković, V. Trujić, Examining the surfaces in used platinum catalysts. Journal of Mining and Metallurgy, 2009;45:79-87.

7. B. Wu, G. Liu, Platinum: Platinum-rhodium thermocouple wire. Platinum Met. Rev., 1997;41:81-85.

8. M. Funabikia, T. Yamadaa, K. Kayanoa, Auto exhaust catalysts. Catal. Today, 1991;10:33-43.

9. T. Biggs, S. Taylor, E. Van der Lingen, The hardening of platinum alloys for potential jewellery application. Platinum Met. Rev., 2005;49:2-15.

10. J. Wright, Jewellery-related properties of platinum: Low thermal diffusivity permits use of laser welding for jewellery manufacture. Platinum Metals Rev., 2002;46:66-72.

11. W. Canning, The canning Handbook of Surface Finishing Technology (CBS publishers and Distributors, New Delhi), 2005.

12. K. Nasser, Electroplating-Basic Principles, Processes and Practice (Elsevier Ltd., Berlin, Germany), 2004.

13. Jean-Claude P, Frank L (1986) Theory and practice of pulse plating, (American electroplaters and surface finishers Society, Orlando,Florida) 159-171.

14. U. Uday, T. Bandyopadhyay, B. Bhunia, Bioremediation and detoxification technology for treatment of dye(s) from textile effluent. In Textile Wastewater Treatment; Intech Open: London, UK, 2016;75–92.

15. R. Chander, S. Naveen, K. Arora, Environmental Biotechnology: For Sustainable Future; Springer: Singapore, 2019, ISBN 9789811072833.

16. Bharagava R, Emerging and Eco-Friendly Approaches for Waste Management; Springer: Singapore, 2019, ISBN 9789811086687.

17. A. Jorge, M. Rosa, Garcia, **B.** Nathalia, M. Camila, C. Maria , B. Sueli B, Oxicity and environmental impacts approached in the dyeing of polyamide, polyester and cotton knits. J. Environ. Chem. Eng., 2019;7:102973.

18. S. Mahalingam, Ramasamy, Enhanced photocatalytic degradation of synthetic dyes and industrial dye wastewater by hydrothermally synthesized G–CuO–Co3O4 hybrid nanocomposites under visible light irradiation. J. Clust. Sci., 2018;29:235–250.

19. D. Suresh, P. Nethravathi, H. Rajanaika, Udayabhanu, H. Nagabhushana, S.Sharma, Green synthesis of multifunctional zinc oxide nanoparticles using Cassia fistula plant extract and their photodegradative, antioxidant and antibacterial activities, Mater. Sci. Semicond. Process, 2015;31:446–454.

FABRICATION AND ANALYSIS OF ROCKET STOVE FOR RURAL COOKING APPLICATION

Ramkumar M[1], Abhishek N[2], Hemanth Gowda V[3], Hemanth Kumar R K[4], Hemanth B V[5]

[2]*Assistant Professor, Sapthagiri College of Engineering, Bangalore*

[2345]*UG Students, Sapthagiri College of Engineering, Bangalore*

[1]*ramkumarm@sapthagiri.edu.in,* [2]*anilrampr@gmail.com*

ABSTRACT: *In everyday life fuel plays a very prominent role. it has been a common need for human beings for their daily activities. As an example, we can see cooking in essential needs. The exhaustable natural resources such as fossil fuels are widely used to meet people demand as it is an exhaustable resources it should be limitedly used using biomass energy the one of the groundbreakinginnovation is the space rocket stove. Biomass is the one of the natural main energy sources for running biomass rocket stove it is been designed to increase the efficiency of the fuel with efficiency of thermal with combination of heat transfer and an increased combustion efficiency with boiling lump fuel. This approach to this examines is that the plan of the manufacturing space rocket stove burnt through the coconut shell and the bamboo biomass for its essential needs. The boiling of water trial using three forms of solid gasses by the cold start state which has the maximum thermal effiency is coconut leaves of 38% value then the coconut shell combustion which has found lowest thermal effiency with a value of 22%. When hot test starts the coconut fronds firing is gained a highest thermal effiency value is 41%. Similarly simmer water boiling test the coconut fronds firing in a rocket stove has a highest thermal effiencyvalue is 37%. The novel rocket stove is designed to enlarge fuel efficiency and its thermal efficiency and also extent to reduce indoor pollution in cooking applications. The stove improves an environmentally sound and economically cost effective.*

Keywords: space Rocket stoves, Thermal efficiency coconut branches and shells, water hot trials, bamboo.

INTRODUCTION

A mixture of different gases energy is single of the many other energies they are used continuously to decrease the use of energy from petroleum products, gasses and others.

Firewood is One of the biomass energies is having a 4320 Kcal per kg of calorific value.

The use of three stone stove is which measured less efficiency because of uses of firewood fuel that causes forest deforestation.

Traditional stove which has many problems which occurs due to igniting the stove, and to become stable of the size of furnace flame is not easy, particularly from the commencement phase of ignition thus it takes some time to become constant the fire and we also require an additional energy like kerosine which ignition to get the flame and also flame extinguish is very difficult.

The working principle of rocket novel stove is built of single horizontal blocks in which wood fuel can be placed at the bottom it has air pocket that is connected to a heat sink. When the stove is ON, because of air pocket fire gets more oxygen the heat will be passed through the vertical blocks till the top end.

The rocket stove produced a more efficient combustion in which all the wood burns completely comparing to other conventional stove it produces a less smoke.

According to World Health organization (WHO), burning biomass is the most serious consequences in the home which causes respiratory and lung diseases due to indoor smoke inhalation.

1.6 million premature death occurs in each year among them half of the death occurs on the children under five years of age.

MATERIALS AND METHODS

MATERIALS:

Red dust powder and MS sheet metals used for manufacturing a novel rocket heater and the measurement of the heater is sized for a standard family size.

The fuel resources used for performance valuation of locally made-up novel rocket heater are bark free eucalyptus wood a fuel firewood is prepared which has dried out in oven at 105 c then it is stored in an air tight box. A local dominant firewood species which is used for catering as well as heating in all the seasons.

The indoor air pollution monitoring devices which are used to measuring the carbon monoxide and a particulate matter such as crimson laser and electrochemical cell spreading photometer. Particulate matter emission characteristics of fabricating wood stove and the three-pebble wood stove below water boiling trial. According to this test internal air quality stand of world health organization were recorded and compared of the emission concentration of the rocket novel stove.

K type thermocouples are used for monitoring the temperature of water during the WBT process. During the test remaining charcoal and firewood fuel utilization of the wood stove were measured by a appropriate weight gauge of +_ 0.01kg accuracy.

Design principle of novel rocket stove

Inter mitten feed wood burning stove can be off any type it was first designed by local peoples to achieve their needs and then finished by obtaining, according to the principle:

1. Fire using light weight, heat resistant material insulation were made around them
2. As they enter into the fire heating burning of the stick's tips are used.
3. Through the burning fuel maintained of good fast draft was used.
4. Tool less sketch being pulled into the flames which results in overload charcoal and smoke.
5. Creation of low heat sticks and high heat sticks are pulled into the fire.
6. During the heat flow path insulation is maintained.
7. Usage of grate in the fire.
8. Regular cross-sectional region is maintained. This was achieved via similar volume of the opening into the flames, spaces within the wood stove throughout which warm air flows and the chimney.
9. Maximizing the heat transfer of the pot with proper size gaps.

Increase in transfer efficiency by outlet gaps establish the equal cross-sectional region improves sufficient draft for good combustion. This is means that opening into the

burning chamber, the air space beneath the grill and chimney are must be in the similar dimensions.

METHODS:

The waste of biomass is utilized for experimenting sky rocket furnace is planned in such a way that the initial stage is to prepare the biomass desecrate raw objects parameter purpose to make the biomass calculating the biomass stove testing of biomass stove and performance testing.

The thermal energy is produced through burning the sky rocket furnance be able to used for water heating combustion as well as thermal efficiency which particulate matter and then the exhaust emissions will be calculated and it is designed with Indonesian national standards.

Sky rocket furnace equipment, testing materials and waste biomass materials, Oven, Coconut midrib, Bamboo, Analytical Scales, Aluminium Pans, Water and Coconut shells are used as a tools and equipment are used in this study.

The water boiling test (WBT) method is carried out for testing of a biomass rocket stove. WBT technique have three stages of testing, specifically cold and hot start as well as simmer.

The testing takes place until the water reaches its boiling temperature initially from the oven and water in extent temperature and this process is said as Cold start.

Warm start, At Room Temperature the testing starts immediately after a primary stage through a warm stove which is filled among water awaiting the water boils.

Simmer is testing after the secondary stage in the boiler and water is in boiling state.

The initial stage is to set up a vessel containing a litre of water in it and subsequently load the biomass gas in type of coconut plants into the novel rocket heater to the extent that of 1 kg. Arrange a portion of paper to be twisted on as an activate initially in commence and near to analyse the entire operational point stop watch is required. If all the apparatus required to support the explore process is available, if it is perfect after that pace is to switch on the heater, monitor the commence procedure.

Subsequently in the water boiling test (WBT) process, at room temperature, cold start test is started through heating water to boil initially from the saucepan followed by the warm start test is started instantaneously follow the frozen start stage by a warm furnace which is filled with water towards ambitious temperature and followed through the simmer test is started with putting it in the warm water pot follow the warm start segment in which furnace is also warm. Next on the top of stages are frequently repeated through other forms of biomass fuels, specifically bamboo and coconut shield.

WATER BOILING TEST

The WBT process provides the wood stove designer by dependable data regarding the performance of firewood burning novel rocket heater models.

This trial can be made by three stages that regulate the wood stoves capability they are:

1. To bring water to boil from a cold start.
2. To bring water to boil when the stove is hot.
3. At simmering temperature water is maintained.

This test is used to estimate a sequence of wood stoves as they are being urbanized, this analysis cannot be used for comparing the heater commencing dissimilar places because of the dissimilar sizes of pot and firewood used this changes the results.

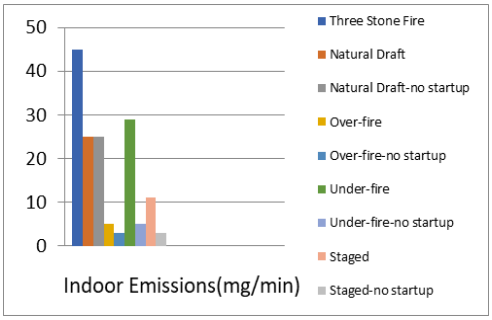

Figure 1. Comparison Graph of Thermal Efficiency

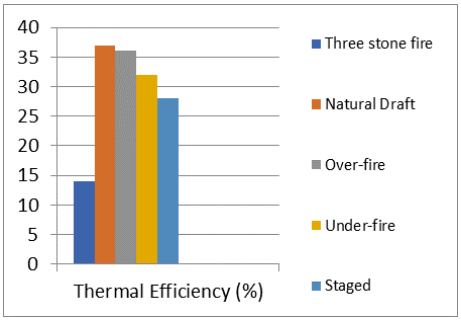

Figure 2. Comparison of Indoor Emissions

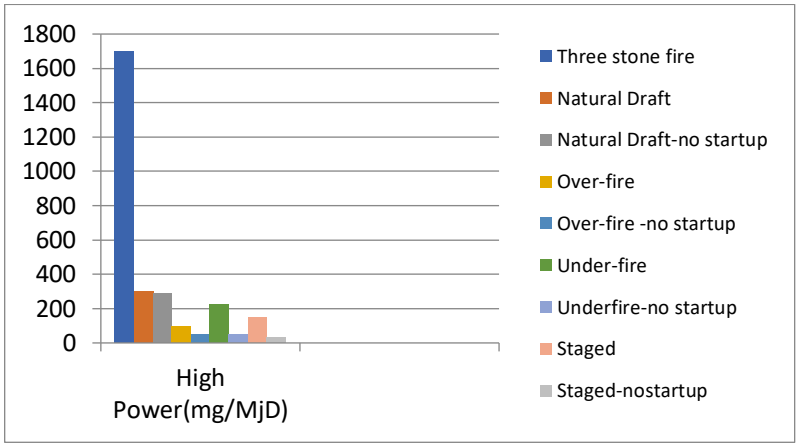

Figure 3. Comparison of High Power

Figure-1. Thermal efficiency (panel A), Figure-2. Indoor emissions (panel B) andFigure-3, high power PM25(panel C) for the TSF, the natural draft stove, and the three forced draft stoves.

Equipment used for water boiling test are:

1. Testing pots.
2. Timer.
3. Digital thermometer.
4. To protect scale heat resistant pad is used.
5. Scale of at least 6kg capacity and one gram accuracy.
6. For holding thermometer probe in water wood fixtures are used.
7. Small spatula is used to remove excess charcoal from heater.
8. For handling charcoal Tongs are used.
9. For transferring charcoal Dust pan is required.
10. For weighing charcoal Metal tray to hold is used.
11. Heat resistant gloves.
12. Three bundles of air dried out fuel wood.

By the commencement for this analysis the process must be followed

1. Air high temperature have to be recorded.
2. load of normally used pot have to be recorded.
3. Charcoal container weight should be recorded.
4. Fuel wood approximate dimensions are calculated.

DESIGN BASIS:

Major parameter is the quantity of water to be vaporized at a sure gap of period is depending to design the novel rocket stove. Lower heat loss and environmental force have to be considered while designing the novel rocket stove.

NOVEL SKY ROCKET STOVE CONSTRUCTION:

Height. length, width of rocket stove parameters was concerned while manufacturing the novel rocket stove.

COMBUSTION CHAMBER HEIGHT:

The combustion chamber height is, T=H+C+L [4]

Were,

H is air pocket hole height in cm.

C is the air pocket hole to pot base height.

L is the distance between the pot mouth and pot bottom.

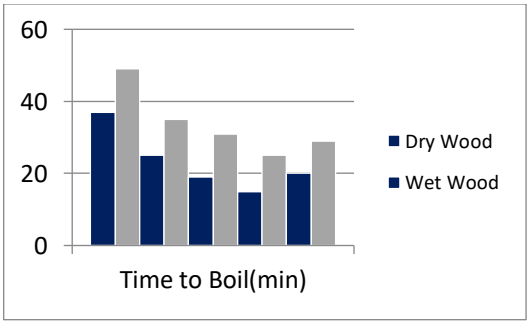

Figure 4. Time to Boil Graph

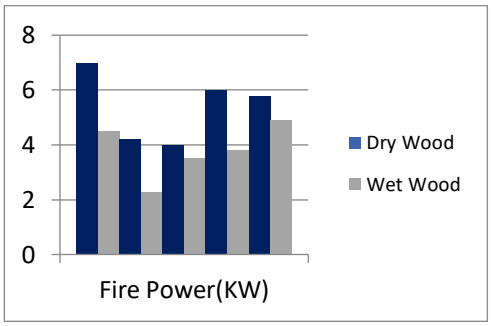

Figure 5. Fire Power Graph

Figure-4. Time to Boil (panel A) and Figure-5. Fire power (panel B) for both Dry Wood and Wet Wood for the Three stone fire, the natural draft stove, and the three forced draft systems.

DESIGN OF NOVEL ROCKET STOVE

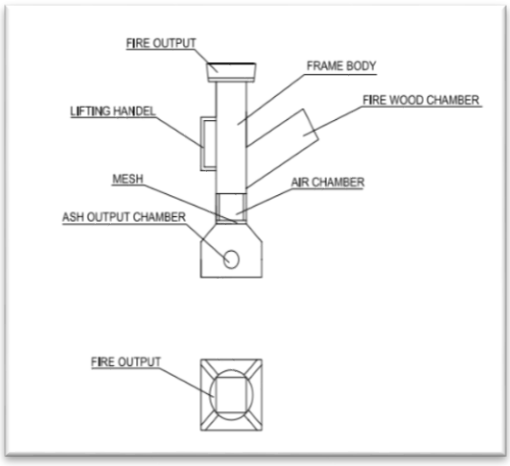

Figure 6. Design of Novel Rocket Stove

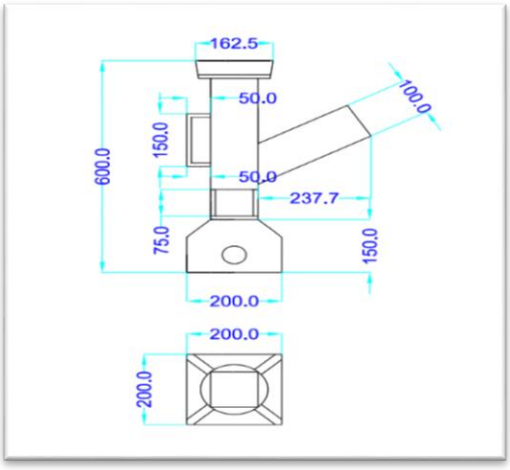

Figure 7. Dimensions of Novel Rocket Stove

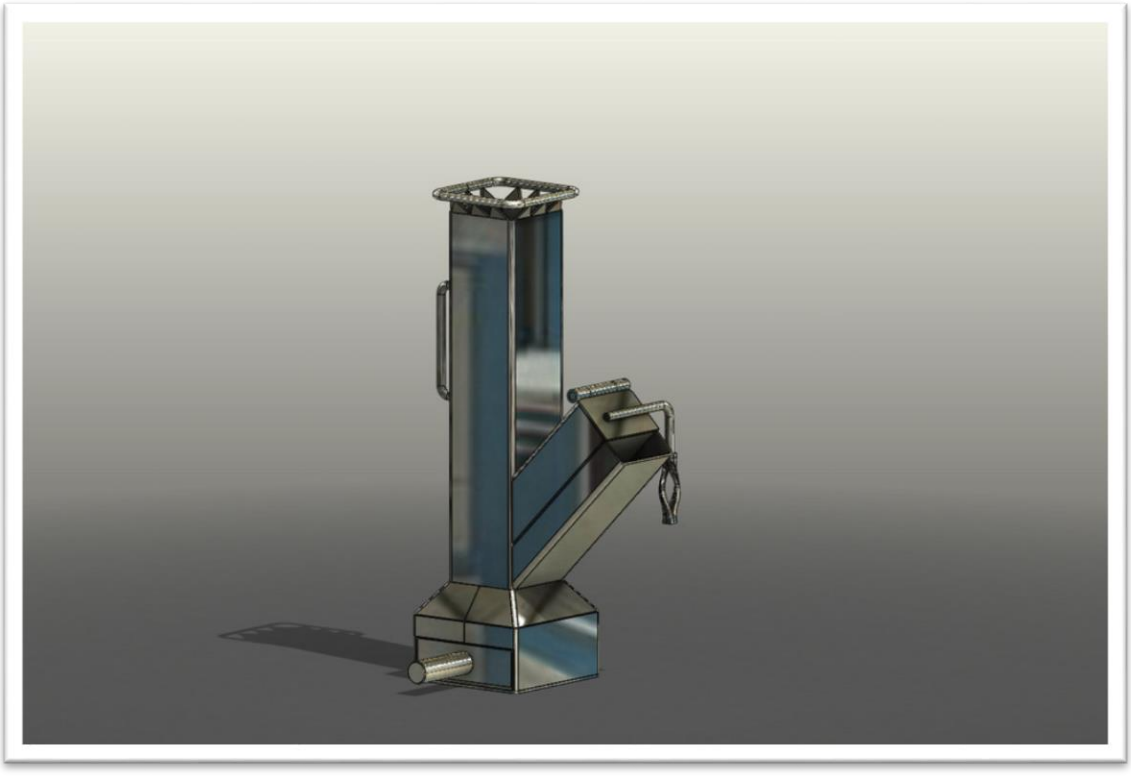

Figure 8. 3D CAD Model of Novel Rocket Stove

Results and discussion:

From this novel rocket stove study. Many stages are carried out first rocket stove design, selecting a biomass firewood is also determining the requirement of a sky rocket heater. for Design of sky rocket furnace, a mild steel by a tallness of 600cm and breadth of 200.0cm.

A furnace whole volume is 0.115x0.115. one kg of teak wood wood twings and plywood waste are used as raw material the furnance is made by arranging mild steel plates into a rocket furnace the selection of biomass fuel uses coconut fronds, coconut shell and bamboo. Every biomass fuel used as different heating vale and variation in rate of burning for each type of firewood.

Based on environmental side selection of biomass fuel will reduce the biomass waste through the atmosphere, as a result it is able to reduce damage to the environment. Novel rocket stove is designed according to Indonesian national standard as been designed which have specification by way of a large fuel supply, thus produced flames will also survive large. The holes are used for intake air due to oxygen in stove maintain the fire flaming. And chimneys been used for transmit smoke to discharge check. The novel rocket heater is also equipped through the collected works of ash dust from burning firewood.

According to Indonesian national standard in furnace is passed that the exact fuel burning up test with a limit of 1kg per hour of a furnance be also approved the combustion efficiency trial and have passed the thermal efficiency test with the minimum value of 20%. the novel rocket stove is passed the carbon monoxide emission test if the carbon monoxide emission test that doesn't exceed 67gm/kg of consumed fuel.

Burning time is used for amount of rate of fuel consumption to boil the water. Then the standard burning rate intended for cold start is 22g/min, hot start is 24g/min, and simmering is found to be 18 g/min.

A firepower is the relative amount of a fuel energy spent through the hob for each unit time. It was initiated through 6.5KW for cold start, 7.1KWfor hot start and 5.4 KW for, simmering correspondingly.

Table-1 Calculated results for all cold start and Hot Start

	Units	Cold start				Hot start			
		Trial -1	Trial -2	Trial -3	Average	Trial -1	Trial -2	Trial-3	Average
Time to heat vessel 1	seconds	1800	2160	2400	2120	1560	1860	2280	1900
Burning time	g/sec	0.45	0.3667	0.3	0.372	0.4333	0.4333	0.33	0.38
Thermal efficiency	%	20	37	31	29.33	28	32	29	29.667
Consumption of fuel	g/liter	90	81	70	80.33	70	90	81	80.33
Firepower	Kilo watts	0.0080	0.0064	0.0052	0.00656	0.0076	0.0076	0.0060	0.0071

Table-2 CO concentration

CO	Unit	Higher value	Lower value
Cold start	mg/m3	5.95	4.35
Hot start	mg/m3	6.90	5.00
Simmering	mg/m3	15.01	13.54

CONCLUSION:

The novel rocket stove is fabricated and designed for nearby accessible equipment such as red dust, coconut fronds, shells and mild steel. from this study the obtained results shows the minor pollutant emissions and enhanced fuel efficiency of the novel rocket stove based on WB test excellent fuel reduction rate.

The performance of novel sky rocket stove have been performed by using WB trial , by a cold start state which has its maximum thermal efficiency is found since the coconut leaves the value of 38% firing, in the coconut shell it has the lowest thermal efficiency during the hot start condition from the coconut fronds obtained a high thermal efficiency of 41% value the coconut shell has the lowest thermal efficiency was found 18% value in next at simmer test the coconut fronds has a highest thermal efficiency of 37% value the coconut shell has the lowest thermal efficiency of 25%

REFRENCES:

1. *Performance Test of a Household Rocket Stoves Fired with Coconut Frond, Coconut Shell and Bamboo Almuzakkir1 , Muhammad2 , Adi Setiawan3 International Journal of Research and Review Vol.8; Issue: 1; January 2021 Website: www.ijrrjournal.com Research Paper E-ISSN: 2349-9788; P-ISSN: 2454-2237*
2. *E. Widawati, S. Octaviani, L. Lauwrence, L.R. P. Sudharma. (2019). Kompor Roket Berbahan Bakar Briket Biomassa. Seminar Nasional AVoER XI 2019 Fakultas Teknik Universitas Sriwijaya.*
3. *Alvenher, E. (2012). Pengaruh Lebar Celah dan Tinggi Selimut Panci Terhadap Kinerja Tungku Rumahan. (Skripsi). Jurusan Teknik Pertanian. Fakultas Pertanian. Universitas Lampung. Bandar Lampung.*
4. *Andi Taufan, Novrinaldi, Umi Hanifah. 2013. Rancangbangun dan Pengujian Tungku Berbahan Bakar Gas Untuk Industri Tahu Tradisional Berbasis Produksi Bersih. AGRITECH. Vol 33. Balai Besar Pengembangan Teknologi Tepat Guna (BBPTTG) - Lembaga Ilmu Pengetahuan Indonesia (LIPI).*

5. *Anonim. SNI 7926:2013. (2013). Kinerja Tungku Biomassa. BSN. 4. Ayo, S. A. (2009). Design, Construction and Testing of an Improved Wood Stove. Journal Mechanical Engineering. Federal University of Technology Minna. Nigeria. Volume 13.*
6. *Bhattacharya, S. C. (2012). A Study on Improved Institutional Biomass Stove. Journal Energy Program. Asian Institute of Technology. Klong Luang. Pathumthani. Thailand.*
7. *Khan, Sabrina., et al. (2016). Development of Portable Rocket Stove and Performance Evaluation. Journal of Enginnering and Techonolgy. 03(12):3644.*
8. *Riseanggara, Rayadeyaka Raditya. (2011). Optimasi Kadar Perekat Pada Briket Biomassa. Skripsi. Fakultas Teknologi Pertanian, Institut Pertanian Bogor. Bogor.*
9. *Bangladesh Bureau of Statistics (BBS), Fifth Population and Housing Census, Government of People's Republic of Bangladesh, 2012.*
10. *Bangladesh Country Environmental Analysis, Volume I: Main Report, Social Development Unit, South Asia Region, World Bank, 2015.*
11. *Indoor Air Pollution and Health: Scopeof the Problem, WHO Fact Sheet No. 292, Geneva: WHO, 2017.*
12. Samuel F. Baldwin, Biomass Stoves: Engineering Design, Development and Dissemination, Princeton University, 2017.
13. Balis, B., D. Ogle, et al., Eds., The Water Boiling Test (WBT), Household Energy and Health Programme, Shell Foundation, 2018.
14. Howell, J.R., "A catalog of radiation conFigureuration factors", McGraw-Hill, 2017.
15. Siegel, R., Howell, J.R., Thermal Radiation Heat Transfer, Taylor & Francis, 2016.

Humidity sensing behavior of rare earth doped Cobalt chromate for sensor applications

N. Ramprasad[1], G.V. Jagadeesha Gowda[2]*, K.V. Arjuna Gowda[3], K.S. Kantharaj[4], Jagadeesha Angadi V[5*]

[1]*Department of Physics, Government First Grade College, Mulbagal, Karnataka, 563131, India*

[2]*Department of Physics, Sapthagiri College of Engineering, Bengaluru-560057, India*

[3]*Department of Physics, Government First Grade College, Hoskote, Karnataka, India-562114*

[4]*Department of Physics, Government First Grade College, Malur, Karnataka, 563130, India*

[5]*Department of Physics, P.C. Jabin Science College, Hubballi-580031, India*

**Corresponding authors:* jagadeeshagowdagv@gmail.com, *jagdeeshbub@gmail.com*

Abstract:

In the present work role of Cerium (Ce^{3+}) on the structural, microstructural, Fourier infrared spectroscopic, electrical and humidity sensing behaviour $CoCr_{2-x}Ce_xO_4$ (CoCrCe) under frequency & humidity conditions are reported. The CoCrCe samples were prepared by solution combustion method. All the samples were sintered for 3 hours for 600°C to get a pure crystalline nature without impurity phase. X-ray diffraction confirms the formation of cubic spinel structures with typical crystallite sizes less than 16 nm. When Ce^{3+} ions are replaced by Cr^{3+} ions, compressive lattice strain is produced, hence we found lowering the lattice parameter. Further samples were analysed by using FTIR technique to know the information about octahedral and tetrahedral stretching band and it is confirming the ferrite structure without impurity. Microstructural studies of the samples were studied by using Scanning Electron microscopy. All the samples were confirmed samples are highly porous in nature. High porosity will help to humidity sensing behaviour. Elemental analysis was done using Energy dissipative spectra and it confirms all the elements is present in the samples. Humidity improves the conduction mechanism in ferrite pellets. With increasing relative humidity, resistivity drops considerably. Further we investigated the relevant conductivity of the samples, the reaction time of the capacitive sensor, and the humidity influence on the relative permittivity characteristics at a constant frequency range of f = 1 kHz. Among all the Ce concentration Ce^{3+} 2 mole % possess superior humidity sensing properties. Our findings indicate that $CoCr_{1.98}Ce_{0.02}O_4$ could be exploited as an active material in humidity sensor applications.

Key words: Chromate, solution combustion method; humidity; permittivity; electrical conductivity.

1. Introduction:

Spinel ferrites are the most studied ceramic materials in recent years due to their unusual mix of structural, magnetic, and dielectric properties [1-5]. These features encourage the use of ferrites in a variety of sectors such as high-frequency applications, electronic devices, and biological devices as catalysts, inductors, sensors, transformer cores, choke coils, filters, drug delivery and nonreciprocal devices, and so on[5-10]. Because of rising environmental concerns, sensors are receiving a lot of attention these days [10-15]. Precise humidity monitoring is critical in domains such as agriculture, manufacturing industries, food storage applications, and indoor and outdoor air quality. In enterprises, optimal humidity levels are critical for enhancing production efficiency [16- 19]. Reduced SARS-CoV-2 transmission is associated with increasing relative humidity, the first pandemic of the twenty-first century [20–23]. Plant growth is negatively impacted by unbalanced humidity levels [24–26]. A excellent humidity sensor has various properties, including high sensitivity, chemical and thermal stability, reversibility, and a quick response time. Because of their porous structure, wide surface-to-volume ratio, humidity variable resistivity, low cost, ease of synthesis, and

adaptability in a variety of operating environments, spinel magnetic oxides have a significant advantage for prospective usage in humidity sensors. Ferrites having a spinel cubic structure with general formula $(A)(B_2)O_4$. The octahedral and tetrahedral are denoted by "B" and "A" respectively. In spinal cations A^{2+} occupy tetrahedral positions, while cations B^{3+} occupy octahedral sites. Due to its chemical stability ferrites are used in the field of sensing and electronic industries [27]. To achieve the highest possible performance, numerous modifications or substitutions with metal ions are performed to the spinel's typical stoichiometric

2. $CoCr_{2-x}Ce_xO_4$ (x=0 to 0.02) synthesis procedure

2.1 Materials used for synthesis

In the present work, we have used cobaltous nitrate (Co^{2+}), chromium nitrate (Cr^{3+}), and Cerium nitrate (Ce^{3+}) as oxidizers. Further we have taken urea and glucose as fuels. Pictorial representation of above said chemicals and synthesis procedure as shown in fig 1.

2.2 Method of preparation

A stoichiometric technique is used to weigh oxidizers and fuel. All of the weighted chemicals are combined in a 500ml glass jar with purified water. After it has been dissolved, all of the compounds in the water jar are found to have a clear and homogeneous solution. The jar with the homogeneous solution is kept in the furnace. We must start the furnace and set the temperature to 400 degrees Celsius. Due to the high temperature maintained in the furnace, all water molecules get evaporated and it will start burning immediately. This process will take around 20 to 30 minutes to get powder. Further powder was used for further studies for XRD, SEM and FTIR studies. The powder samples were uniaxially pressed, using a hydraulic press, into a cylindrical mould, which developed a down force of 10 tonnes, yielding disk-shaped samples for electrical investigations with a diameter of 6mm and a thickness of approximately 1mm.

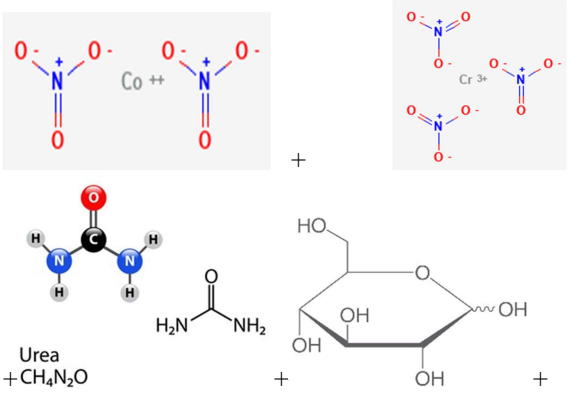

structure. CoCrCe materials have better thermal and chemical stability due to this we intended to chosen rare earth (Ce) doped $CoCr_2O_4$ to understand humidity study.

In the present investigation structural, microstructural, Fourier infrared, electrical and humidity sensing behaviour $CoCr_{2-x}Ce_xO_4$ (x=0 to 0.02) were prepared by solution combustion method were investigated. The effect of relative humidity on the electrical response of the rare earth doped samples were investigated for potential application in humidity sensors applications.

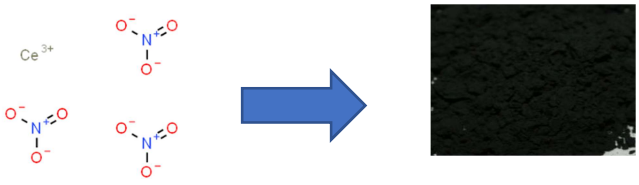

(Ce doped $CoCr_2O_4$ powder)

Fig 1. Molecular structure of oxidizers and fuel use of synthesised element

3. Results and discussions structure, Microstructure Infrared and humidity sensing properties

3.1 Analysis of structure

The phase purity and crystal structure of the sinter CoCrCe ceramics were determined using XRD patterns, as shown in Fig. 2. The data is collected using the Rigaku Miniflex diffractometer (Rigaku Corporation, Tokyo, Japan) with CuK- radiation (λ = 1.5418 Å) is used to collect the data. To analysis the data Full Prof programme and the Rietveld refinement is approached. In good agreement with earlier investigations, the XRD patterns of COCrCe shows diffraction peaks that were indexed to a cubic spinel structure of AB_2O_4. The difference in the intensity of the diffraction peaks could indicate morphology and particle size variations. The crystallite size (from XRD patterns) EDX measurements were performed to gain a better understanding of the crystallite size and morphology of the samples. The crystallite size were calculated through the Debye–Scherrer formula is as shown in in equation 1[28]

$$D = \frac{K\lambda}{\beta \cos\theta} \quad \text{--------(1)}$$

where D is the size of the crystallite, β is the line broadening at full width half maximum (FWHM), θ is the Bragg angle, λ is the X-ray wavelength, and K is a dimensionless form factor with a value near to unity. The size of the crystal is decreases with increasing Ce concentration.

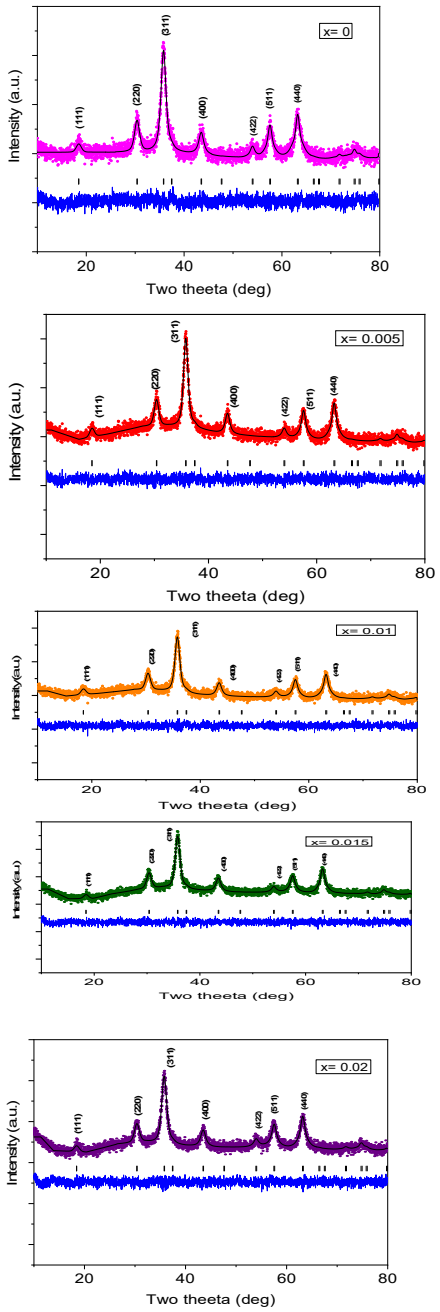

Fig 2 XRD data of $CoCr_{2-x}Ce_xO_4$[x= 0 to 0.02]

Lattice parameter were calculated through the following formula [29]

$$d = a_0\sqrt{h^2 + k^2 + l^2} \quad (2)$$

$n\,\lambda = 2d\,\sin\theta$

where a_0 is the lattice constant, d is the distance between crystal atomic layers, and (hkl) is the plane indexing. The computed lattice parameters for CoCrCe were 8.3289 to 8.3163, respectively, which correspond with previous studies.

Table.1 Data obtained from XRD such as Crystallite size, unit cell volume, lattice parameter

Ce^{3+} content x	lattice parameter (Å)	Crystallite Size D in (nm)	Volume ($Å^3$)	Strain Є (%)	Hoping length (Å)	
					L_A	L_B
0	8.3289	10	577.781	1.4317	3.6065	2.9447
0.005	8.3260	9	577.189	1.3063	3.6052	2.9437
0.01	8.3194	8	575.8144	1.3724	3.6024	2.9413
0.015	8.3180	8	575.5152	1.3823	3.6018	2.9408
0.02	8.3163	7	575.1686	1.541	3.6010	2.9402

3.2 Microstructural Elementary analysis.

Figure 3. SEM micrographs and EDS pattern of $CoCr_{2-x}Ce_xO_4$[x= 0.02]

The fracture surface SEM micrographs (Figure 3) also demonstrated that the structure is composition dependant [30]. Each composition has a typical

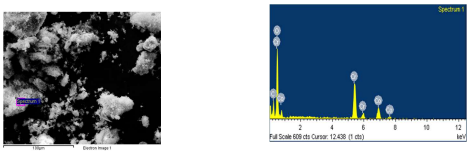

porous structure and tiny crystallites with no interior pores but numerous intergrain holes. In the Ce ions-containing sample created by self combustion, the finest granulation and a tendency to agglomerated particles were found. Furthermore, the intergranular pores are connected via the big pores. The pore structure should be viewed as a network of interconnected voids that create capillary tubes [31]. Dispersive Energy. The amount of Co, Cr, Ce, and O present in the compositions was carefully measured using Energy Dispersive spectroscopy. The graphs are shown in Figure 3. This examination shows that the components are present in almost the same stoichiometric amount as was kept in distilled water according to the chemical composition, with no substantial impurities.

3.3. Fourier infrared Spectroscopy analysis.

Figure 4 depicts the FTIR spectra of the samples. As can be seen, all samples display nearly identical IR absorption behaviour. The absorption peak locations

in the 400–800 cm^{-1} range are attributed to asymmetric stretching and out of plane bending vibrations of the cubic structure's octahedral and tetrahedral sites. The graph exhibit 2 absorption bands between 609 to 380cm^{-1}, which are typical of ferrites. The high frequency band has a frequency range of 450–500 cm^{-1}, whereas the low frequency band has a frequency range of 550–609 cm^{-1}. These two bands correspond to metal ion-oxygen complex vibrations at the A and B sites of the ferrite structure [8, 25]. It has been discovered that as Ce^{3+} substitution increases, the high frequency band expands and the low frequency band contracts. This affects the Ce^{3+}- O vibration, lowering the octahedral vibrational frequency. This could be one of the reasons for the increase in octahedral peak intensity. As the concentration of Ce^{3+} ions with smaller ionic radius and atomic weight increases in the tetrahedral site, the tetrahedral frequency vibration increases. Our samples are all separated into octahedral frequency bands [32-34].

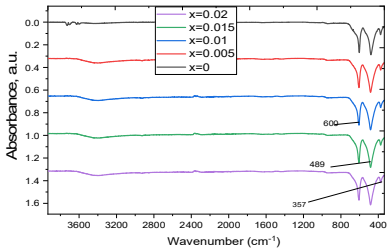

Fig 4. FTIR spectra of the $CoCr_{2-x}Ce_xO_4$[x= 0 to 0.02]

3.4 variation of the relative permittivity against relative humidity

The humidity is the most crucial parameter, which shows its effect on the operation of electronic devices. Hence its very important to record the humidity level of the environment and to note its effects on measured parameters. In this paper for the first time, the variation of the electrical conductivity with the relative humidity was recorded for the (CoCrCe) samples. The conductivity behaviour of these samples was tested at ambient room temperature with in the relative humidity ranging from 0% to 98%. For the measurement the saturated salts solutions which gives definite relative humidity are used [35].

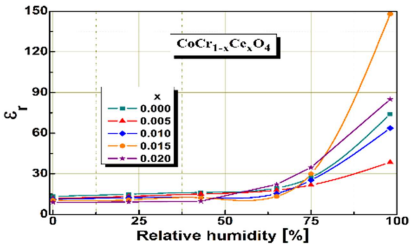

Figure-5: The variation of the relative permittivity against relative humidity at the constant frequency of 1 kHz.

The Fig.5 depicts the variation of the electrical permittivity with the relative humidity of the (CoCrCe) samples for different compositions (x = 0.0, 0.005, 0.010, 0.015 and 0.020). The plots clearly depict that, as the relative humidity increases the relative permittivity also increases and it is maximum for the $CoCr_{2-x}Ce_xO_4$ (x = 0.015) sample. Also, at higher humidity level more enhancement in the permittivity of the samples is observed.

3.5 conductivity against relative humidity

The change in the electrical conductivity with relative humidity was shown in Fig. 6. The electrical resistance of the $CoCr_{2-x}Ce_xO_4$ (x = 0.0, 0.005, 0.010, 0.015 and 0.020) samples shows that, as the relative humidity increases the conductivity decreases. At lower humidity the conductivity is high [36].

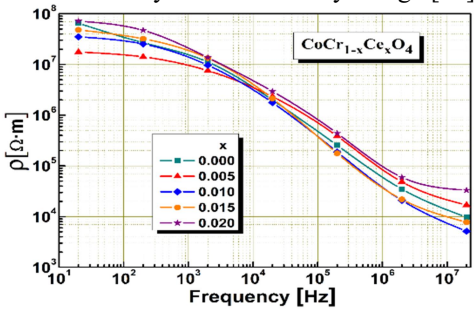

Figure 6. The variation of the conductivity against relative humidity at the constant frequency of 1 kHz.

3.6 Electrical capacity and Electrical resistance in normalised form at the constant frequency of 1 kHz.

The variation of the normalised electrical capacitance and normalised electrical resistance with the relative humidity at room temperature from 0% to 98% relative humidity were recorded and plotted in Fig. 7 and Fig. 8 respectively.

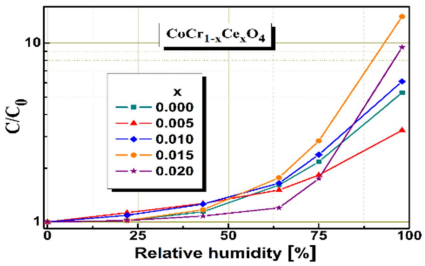

Fig 7 The variation of the electrical capacity in normalised form for the CoCr2-xCexO4 (x = 0.005, 0.010, 0.015 and 0.020) samples at the constant frequency of 1 kHz.

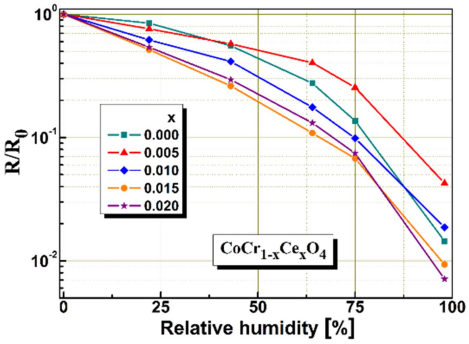

Figure 8. The variation of the electrical resistance in normalised form for the CoCr2-xCexO4 (x = 0.005, 0.010, 0.015 and 0.020) samples at the constant frequency of 1 kHz.

The Fig.7 clearly depicts that below 40% relative humidity the co-efficient of C/C_0 indicates less sensitivity but as the relative humidity more that 40%, the samples show good sensitivity. This good sensitivity for $CoCr_{2-x}Ce_xO_4$ (x = 0.015) sample may be due to the more porous structure of the sample and decreased crystallite size. The Fig. 8 show that, as the relative humidity increases the co-efficient of resistance R/R_o decrease, which intern represents that at lower humidity the sensitivity of the sample's is good but at higher humidity the sensitivity is poor.

3.7. Response time of capacitive sensor and resistive sensor.

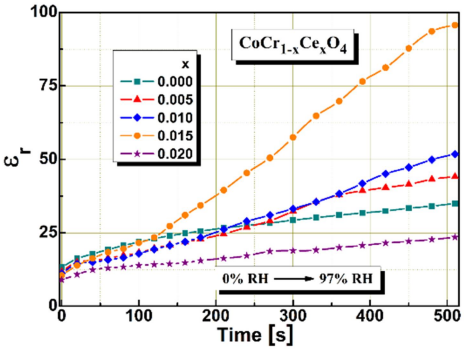

Figure-9: The Response time of capacitive sensor for CoCr2-xCexO4 samples.

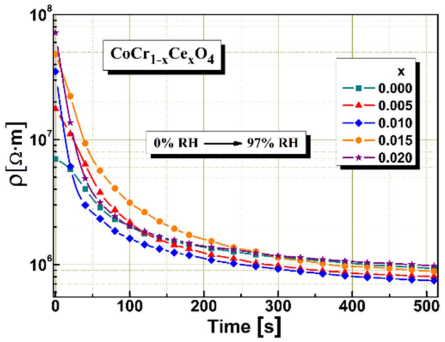

Figure-10: The Response time of resistive sensor for CoCr2-xCexO4 samples.

The timing behaviour is one of the important parameters to judge the potentiality of the sensor. In the present study response time was examined for the $CoCr_{2-x}Ce_xO_4$ samples over a humidity range of 0% to 98% at room temperature. The response time was measure for the variation in resistive (electrical conductivity) and capacitance (electrical permittivity). The Fig. 9 depicts that drastic variation on the response time for electrical permittivity was observed by changing the relative humidity from lower to higher humidity. More variation the permittivity was observed for all the samples, but the $CoCr_{2-x}Ce_xO_4$ (x = 0.015) sample showed a drastic variation of the response time, this may be due to the synergistic effects and porous nature of the sample.

The Fig. 10 clearly gives the response timing behaviour of the electrical conductivity of the samples. The response time for electrical conductivity varies more significantly. The magnitude of two order change in the electrical conductivity was observed for $CoCr_{2-x}Ce_xO_4$ samples. Among these samples the $CoCr_{2-x}Ce_xO_4$ (x = 0.015) has shown a drastic variation. This may be due to the enlarged surface area and maximum porous nature of the sample.

This study gives a new way to the research about the electrical conductivity study with the variation in the humidity. There are fever literatures are available related to this work. The $CoCr_{2-x}Ce_xO_4$ samples has shown better variation in the conductivity as the humidity changes from 0% to 98% at ambient temperature. Among the prepared samples $CoCr_{2-x}Ce_xO_4$ (x = 0.015) sample has shown good sensitivity and better response to the change in the humidity

8. Conclusion

In the present work Ce^{3+} doped and undoped $CoCr_2O_4$ powder were prepared successfully by solution combustion method using glucose and urea as fuels for the first of its kind. The impact of the Ce^{3+} on the structural, Spectroscopic and humidity sensing properties of $CoCr_2O_4$ studied in the present

investigation. Further resistivity decreases with decreasing crystallite size, the highest resistivity achieved in the case of the lower concentration of dopant i.e samples having the highest granulation. The Ce^{3+} substitution adds to a decrease in electrical resistivity, putting the material's resistivity into the measurable zone, which is beneficial for sensor applications. It was discovered that the Ce doped $CoCr_2O_4$ sample is the most susceptible to humidity. The representation from Figure 6 shows acceptable response times of about 150 seconds for electrical resistivity and about 200 seconds for electrical permittivity.

References

1. N. Yamazoe, Y. Shimizu, Humidity sensors: principles and applications, Sens. Actuat., 10 (1986) 379–398.
2. H. Farahani, R. Wagiran, M.N. Hamidon, Humidity sensors principle, mechanism, and fabrication technologies: a comprehensive review, *Sensors,* 14 (2014) 7881-7939.
3. M. Pelino, C. Cantalini, M. Faccio, Principles and applications of ceramic humidity sensors, Act. Passiv. Electron Compon., 16 (1994) 69–87
4. A.Tripathy, S. Pramanik, J. Cho, J. Santhosh, N.A.A. Osman, Role of morphological structure,
5. K. Manjunatha, V. Jagadeesha Angadi, M.C. Oliveira, S.R. de Lazaro, E. Longo, R.A.P. Ribeiro, S.O. Manjunatha, N.H. Ayachit, Towards shape-oriented Bi-doped $CoCr_2O_4$ nanoparticles from theoretical and experimental perspective: Structural, Morphological, Optical, Electrical and Magnetic properties, J. Mater. Chem. C, 9 (2021) 6452-6469.
6. K. Manjunatha, V. Jagadeesha Angadi, R. Rajaramakrishna, U. Mahaboob Pasha, Role of 5 mol% Mg-Ni on the Structural and Magnetic Properties of Cobalt Chromates Crystallites Prepared by Solution Combustion Technique, J. Supercond. Nov. Magn., 33 (2020) 2861-2866.
7. K. Manjunatha, V. Jagadeesha Angadi, K. M. Srinivasamurthy, Shidaling Matteppanavar, Vinayak K. Pattar and U. Mahaboob Pasha, Exploring the Structural, Dielectric and Magnetic Properties of 5 Mol% Bi^{3+}-Substituted $CoCr_2O_4$ Nanoparticles, J. Supercond. Nov. Magn., 33 (2020) 1747–1757.
   Petrila, F. Tudorache, S. Tascu, Micromagnetic investigation of all-optical switching, Phys. Lett. A, 377 (2013) 1495–1498.
   Petrila, V. Manta, Metropolis Monte Carlo analysis of all-optical switching, Comput. Phys. Commun., 185 (2014) 2874–2878.
   Petrila, F. Ungureanu, V. Manta, Effects of laser beam modulation on all-optical switching phase diagrams in magneto-optical ultrafast storage device, J. Comput. Electron., 14 (2015) 627–633.
8. K.K. Bharathi, J.A. Chelvane, G. Markandeyulu, Magnetoelectric properties of Gd and Nd-doped nickel ferrite, J. Magn. Magn. Mater., 321 (2009) 3677–3680.
9. S. Chikazumi, Physics of ferromagnetism, 2nd edition (Oxford University Press Inc., New York, 1997).
10. 15 F. Tudorache, I. Petrila, Effects of partial replacement of Iron with Tungsten on microstructure, electrical, magnetic and humidity properties of Copper-Zinc ferrite material, J. Electron. Mater., 43 (2014) 3522–3526.
11. K. Wu, Y. Lu, Y. Liu, Y. Liu, M. Shen, M. Debliquy, C. Zhang, Synthesis and acetone sensing properties of copper (Cu^{2+}) substituted zinc ferrite hollow micro-nanospheres, Ceram. Int., 46 (18) (2020) 28835–28843.
    Petrila, F. Tudorache, Influence of partial substitution of Fe^{3+} with W^{3+} on the microstructure, humidity sensitivity, magnetic and electrical properties of barium hexaferrite, Superlattices Microstruct., 70 (2014) 46–53.
12. K. Manjunatha, V. Jagadeesha Angadi, R.A.P. Ribeiro, M.C. Oliveira, S.R. de Lázaro, M.R.D. Bomio, S. Matteppanavar, S. Rayaprol, P. D. Babu, U. Mahaboob Pasha, Structural, Electronic and Magnetic properties of Sc3+ doped CoCr2O4 nanoparticles, New J. Chem., 44 (2020) 14246-14255.
13. P.R. Mandal, R. Singh, A. Das, T. Sarkar, T.K. Nath, Enhanced magnetodielectric response in Dy modified $NiCr_2O_4$, J. Magn. Magn. Mater., 432 (2017) 49-55.
14. D. Kumar, K. Nemkovski, Y. Su, C. Rath, Enhancement of Curie- and spin-spiral temperatures with doping Fe in multiferroic $CoCr_2O_4$ nanoparticles, J. Magn. Magn. Mater., J. Magn. Magn. Mater., 488 (2019) 165378.
15. D.P. Dutta, J. Manjanna, A.K. Tyagi, Magnetic properties of sonochemically

synthesized $CoCr_2O_4$ nanoparticles, J. Appl. Phys., 106 (2009) 043915.
16. Natalia Betancur-Granados, Oscar Jaime Restrepo-Baena, Flame spray pyrolysis synthesis of ceramic nanopigments $CoCr_2O_4$: The effect of key variables, J. Eur. Ceram. Soc., 37 (2017) 5051-5056.
17. K. Manjunatha, V. Jagadeesha Angadi, Renan A.P. Ribeiro, Elson Longo, Marisa C. Oliveira, Mauricio R.D. Bomio, Sergio R. de Lazaro, Shidaling Matteppanavar, S. Rayaprol, P.D. Babu, Mahaboob Pasha, Structural, electronic, vibrational and magnetic properties of Zn^{2+} substituted $MnCr_2O_4$ nanoparticles, J. Magn. Magn. Mater., 502 (2020) 166595.
18. V. Jagadeesha Angadi, K. Manjunatha, K. Praveena, Vinayak K. Pattar, Brian Jeevan Fernandes, S. O. Manjunatha, Jakeer Husain, S.V. Angadi, L.D. Horakeri, K.P. Ramesh, Magnetic properties of larger ionic radii samarium and gadalonium doped manganese zinc ferrite nanoparticles prepared by solution combustion method, J. Magn. Magn. Mater., 529 (2021) 167899.
19. Pankaj Choudhary, P. Saxena, A. Yadav, V. N. Rai, A. Mishra, Dielectric and ferroelectric properties of $CoCr_2O_4$ nanoceramics, J. Adv. Dielectr., 9 (2019) 1950015.
20. K. Manjunatha, V. Jagadeesha Angadi, Brian Jeevan Fernandes, K.P. Ramesh, Synthesis and Study of Structural and Dielectric properties of Dy-Ho doped Mn-Zn Ferrite Nanoparticles, Ferrite, Intech Open publishers, (2021), ISBN: 978-1-83962-887-0. DOI: 10.5772/intechopen.99264
21. V. Jagadeesha Angadi, K. Manjunatha, Mustafa Akyol, Ahmet Ekicibil, Shidaling Matteppanavar, A. V. Pavlenko, S. P. Kubrin, Temperature-Dependent Dielectric and Magnetic Properties of Scandium-Substituted $HoFeO_3$ Nanoparticles, J. Supercond. Nov. Magn., 33 (2020) 3525–3534.
22. S. Pavithradevi, N. Suriyanarayanan, T. Boobalan, Synthesis, structural, dielectric and magnetic properties of polyol assisted copper ferrite nano particles, J. Magn. Magn. Mater., 426 (2017) 137-143.
23. K. Ali, J. Iqbal, T. Jan, I. Ahmad, D. Wan, I. Ahmad, Influence of NiO concentration on structural, dielectric and magnetic properties of core/shell $CuFe_2O_4$/NiO nanocomposites, Mater. Chem. Phys. 195 (2017) 283-294.
24. K. Manjunatha, K.M. Srininivasamurthy, C.S. Naveen, Y.T. Ravikiran, E.I. Sitalo, S.P. Kubrin, Siddaling Matteppanavar, N. Sivasankara Reddy, V. Jagadeesha Angadi, Observation of enhanced humidity sensing performance and structure, dielectric, optical and DC conductivity studies of scandium doped cobalt chromate, J. Mater. Sci. Mater. Electron., 30 (2019) 17202-17217.
25. P. Samoila, T. Slatineanu, P. Postolache, A.R. Iordan, M.N. Palamaru, The effect of chelating/combustion agent on catalytic activity and magnetic properties of Dy doped Ni–Zn ferrite, Mater. Chem. Phys., 136 (2012) 241–246.
26. R. Sharma, S. Singhal, Structural, magnetic and electrical properties of zinc doped nickel ferrite and their application in photo catalytic degradation of methylene blue, Phys. B, 414 (2013) 83–90.
27. M.S.R. Prasad, B. Prasad, B. Rajesh, K.H. Rao, K.V. Ramesh, Magnetic properties and DC electrical resistivity studies on cadmium substituted nickel–zinc ferrite system, J. Magn. Magn. Mater., 323 (2011) 2115–2121.
28. Florin Tudorache, Investigations on microstructure, electrical and magnetic properties of copper spinel ferrite with WO_3 addition for applications in the humidity sensors, Superlattices Microstruct. 116 (2018) 131-140.
29. F. Tudorache, I. Petrila, P.D. Popa, S. Tascu, Influence of thermal treatment on the structure, humidity sensitivity, electrical and magnetic properties of barium–tungsten ferrite, Compos. B Eng., 51 (2013) 106–111.
30. F. Tudorache, I. Petrila, K. Popa, A.M. Catargiu, Electrical properties and humidity sensor characteristics of lead hydroxyapatite material, Appl. Surf. Sci. 303 (2014) 175–179.
31. I.Petrilaa, F. Tudorache, Effects of sintering temperature on the microstructure, electrical and magnetic characteristics of copper-zinc spinel ferrite with possibility use as humidity sensors, Sensors and Actuators: A. Physical 332 (2021) 113060.
32. F. Tudorache, Investigations on microstructure, electrical and magnetic properties of copper spinel ferrite with WO3 addition for applications in the humidity sensors, Superlattices and Microstructures 116 (2018) 131e140.

Study on Mechanical Characteristics of GF65/PA6 Composite Laminate

Ram Kumar. M*[1], A.M.Mahesha[2], Mahesh S[3], Mohan. A.E[4]

Department of Mechanical Engineering, Sapthagiri College of engineering
#14/5 Chikkasandra, Hesaraghatta main road, Bangalore- 57 India

[1]ramkumarm@sapthagiri.edu.in
[2]ammahesha@sapthagiri.edu.in
[3]maheshs@sapthagiri.edu.in
[4]mohanae@sapthagiri.edu.in

Abstract *– In this paper, the mechanical properties of the composite material i.e Glass fiber 65 reinforced in Polyamide (Nylon6) composite material is determined using micromechanical analysis techniques like like rule of mixtures, semi-empirical model, and finite element analysis and validated with the experimental results. From the evaluation and study of PA6 GF65 composite, it can be noticed that the results obtained through experimental results are in excellent agreement with finite element and numerical results. So it can be concluded that finite element method can be used as one of the methods to determine the composite properties. The advantage of finite element method over experimental method is that the specimen model may not be prepared and broken. Hence the cost of manufacturing a specimen can be reduced*

Keywords – Glass fiber Composite, Polyamide Composite, Nylon6, Laminate analysis

I.INTRODUCTION TO MICROMECHANICS

Study of mechanical behaviour of a composite material in terms of its constituent materials is termed as micromechanics. In this approach we find the average properties of composite ply from the individual properties of the constituents. Note that the average properties are derived by considering the ply to be homogeneous. At this level, one can optimize for the stiffness and strength requirements of a lamina.

Given the (linear and/or nonlinear) material properties of the constituents, one important goal of micromechanics of materials consists of predicting the response of the heterogeneous material on the basis of the geometries and properties of the individual phases, a task known as homogenization. The benefit of homogenization is that the behaviour of a heterogeneous material can be determined without resorting to testing it. Such tests may be expensive and involve a large number of permutations Furthermore continuum micromechanics can predict the full multi-axial properties and responses of inhomogeneous materials, which are often anisotropic. Such properties are often difficult to measure experimentally, but knowing what they are, is a requirement, e.g. for structural analysis involving composites. To rely on micromechanics, the particular micromechanics theory must be validated through comparison to experimental data.

The second main task of micromechanics of materials is localization, which aims at evaluating the local (stress and strain) fields in the phases for given macroscopic load states, phase properties, and phase geometries. Such knowledge is especially important in understanding and describing material damage and failure.

Most methods in micromechanics of materials are based on continuum mechanics rather than on atomistic approaches such as molecular dynamics. In addition to the mechanical responses of inhomogeneous materials, their thermal conduction behaviour and related problems can be studied with analytical and numerical continuum methods. All these approaches may be subsumed under the name of "continuum micromechanics".

II. RULE OF MIXTURES

Rule of Mixtures is a method of approach to approximate estimation of composite material properties, based on an assumption that a composite property is the volume weighed average of the phases (matrix and dispersed phase) properties.

A. Strength of Materials Approach

In this approach we consider a representative volume element (RVE) of a unidirectional lamina, which consists of the fiber surrounded by the matrix as seen in Figure 1.

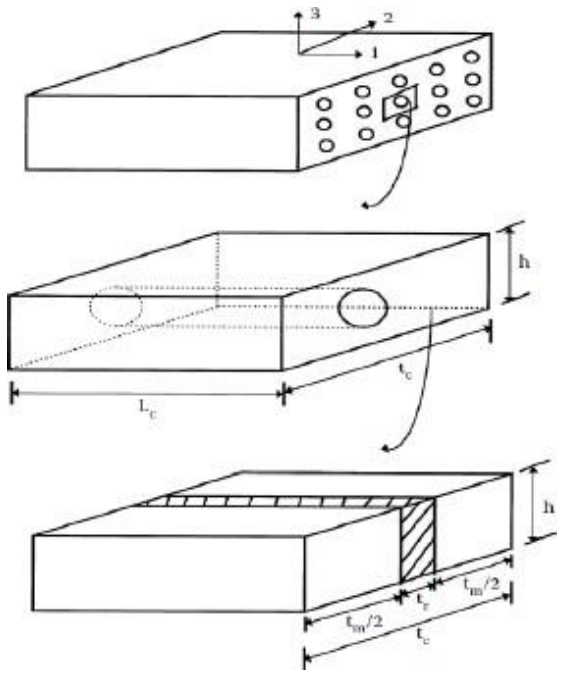

Fig.1 RVE of the composite

Assumptions made in strength of Material approach are
1. The bond between the fibers and matrix is perfect.
2. The elastic moduli, diameters and space between fibers are uniform.
3. The fibers are continuous and parallel.
4. The fibers and matrix follow Hooke's Law i.e. they are linearly elastic
5. The fibers possess uniform strength.
6. The composite is free of voids

In this approach we consider a representative volume element (RVE) of a unidirectional lamina, which consists of the fiber surrounded by the matrix.

The representative volume element can be further represented as rectangular blocks. The fiber, matrix, and the composite are assumed to be of the same width, h, but of thicknesses tf, tm, and tc, and cross-sectional areas Af, Am, Ac respectively

Longitudinal Young's modulus (E_1) which is the modulus of composite along the fiber direction is given by

$E1 = \sigma_1 / \varepsilon_1 = E_f * V_f + E_m * V_m$

$E_f = 85000Mpa$ $E_m = 2400Mpa$ $V_f = 0.65$

$E_1 = 56090Mpa$

Transverse Young's modulus (E_2) which is the modulus of composite along the fiber direction is given by

$E_2 = \sigma_2 / \varepsilon_2 = (V_f * E_m + V_m * E_f) / (E_f * E_m)$

$E_2 = 6515.49$ Mpa

Major Poisson's Ratio is given by

$\nu_{12} = \nu_f * V_F + \nu_m * V_m$; $\nu_{12} = 0.2525$

Minor Poisson's Ratio is given by

$\nu_{21} = \nu_{12} * (E_2/E_1)$; $\nu_{21} = 0.02933$, $\nu_{23} = 0.32789$

In plane Shear Modulus is determined as

$G_{12} = (G_f * G_m) / (V_f * G_m + G_m * E_f)$

$G_{12} = 2426.58$ Mpa

$G_{23} = E_2 / 2 * (1 + \nu_{23})$

$G_{23} = 2453.32$ Mpa

B. Halphin-Tsai Semi Empirical Models

Halphin-Tsai model is a mathematical model for the prediction of elasticity of composite material based on the geometry and orientation of the fiber and the elastic properties of the fiber and matrix. The model is based on the self-consistent field method although often consider to be empirical. The values obtained for transverse Young's modulus and in plane shear modulus through rule of mixture method do not agree well with experimental results. This establishes a need for better modelling techniques.
These techniques include numerical methods such as finite element method, finite difference, and boundary element methods, elasticity solution and variational principal models. Unfortunately, these models are

available as complicated equations or in graphical form. Due to these difficulties, semi empirical models have been developed for design purposes. The most useful of these semi empirical models include those of Halphin and Tsai, since they can be used over a wide range of elastic properties and fiber volume fractions.

Halphin and Tsai developed their models as simple equations by curve fitting to results that are based on elasticity. The equations are semi empirical in nature since involved parameters in the curve fitting carry physical meaning

The Halphin-Tsai equation for the longitudinal Young's modulus is same as that obtained through strength of materials approach, that is,
$E1 = \sigma_1 / \varepsilon_1 = E_f * V_f + E_m * V_m$

$E_f = 85000Mpa$ $E_m = 2400Mpa$ $V_f = 0.65$

$E_1 = 56090Mpa$

Transverse Young's modulus, E_2, is given by
$E_2/E_m = (1+ \xi*\eta *V_f)/ (1-\eta*V_f)$
where $\eta = ((E_f/E_m)-1)/ ((E_f/E_m) +\xi)$

ξ is called reinforcing factor which depends upon fiber geometry, packing geometry and loading conditions
$\eta = 0.91982$, $E_2 = 13105.24$ Mpa

Major Poisson's ratio is given by
$\nu_{12} = \nu_f * V_f + \nu_m * V_m$
$\nu_{12} = 0.2525$

Minor Poisson's Ratio is given by
$\nu_{21} = \nu_{12} * (E_2/E_1)$

$\nu_{21} = 0.05900$

$\nu_{23} = \nu_{12} * (1- \nu_{21}) / (1- \nu_{12})$

$\nu_{23} = 0.31786$

In-plane shear Modulus is G_{12} is $G_{12}/G_m = (1+\xi\eta V_f)/ (1-\eta V_f)$
where $\eta = ((G_f/G_m)-1)/ ((G_f/G_m) +\xi)$

Hewitt and Malherbe suggested choosing a function
$\xi = 1+40 * V_f^{10}$ for $V_f > 50\%$
$\xi = 1.53851$
$\eta = 0.93866$

$G_{12} = 4420.13$ Mpa

$G_{23} = 4972.17$ Mpa

Table 1: Elastic constants of PA6 GF65 by theoretical calculations

Elastic Constants	Strength of Materials Approach	Halphin-Tsai semi empirical method
E_1	56090 Mpa	56090 Mpa
E_2	6515.49 Mpa	13105.24 Mpa
G_{12}	2426.58 Mpa	4420.13 Mpa
ν_{12}	0.2525	0.2525
ν_{21}	0.02933	0.05900

Figures 2, 3 and 4 shows the variation of Stress strain values for Longitudinal Tensile test, Transverse Tensile test and Shear test

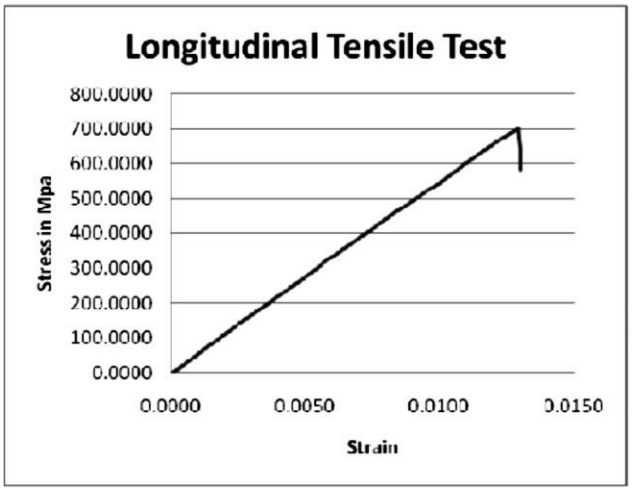

Fig.2 Variation of stress strain values for longitudinal Tensile Test

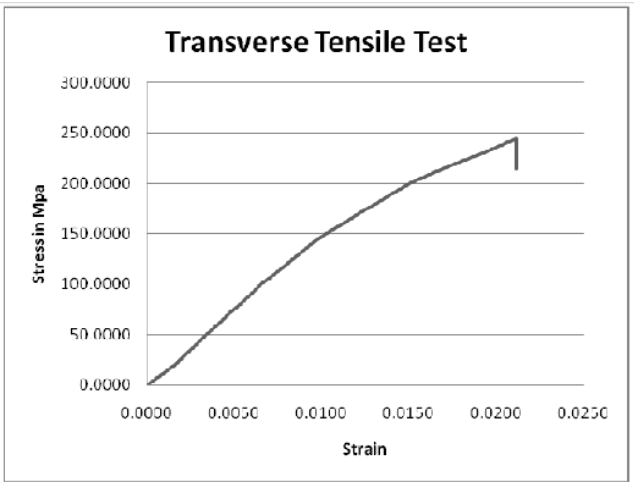

Fig.3 Variation of stress strain values for Transverse Tensile Test

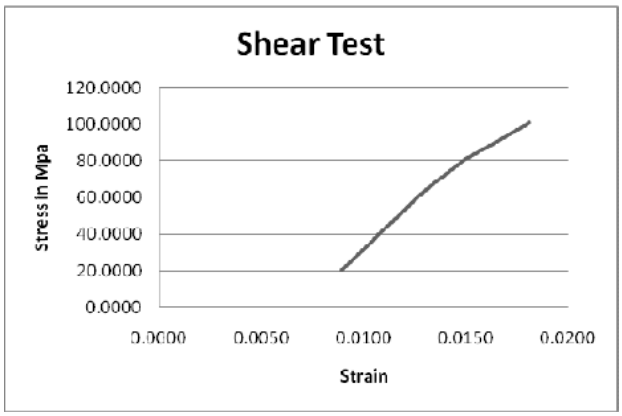

Fig.4 Stress-strain plot for Shear Test

III. LAMINATE ANALYSIS

A. Finite Element Analysis of Laminate Ply

A structure made of composite materials is generally a laminate structure made of various laminas stacked on each other. Knowing the macromechanics of a single lamina, one develops the macromechanics of a laminate. A lamina (also called a ply or layer) is a single flat layer of unidirectional fibers or woven fibers arranged in a matrix. A laminate is constructed by stacking a number of such laminae in the direction of the lamina thickness. Mechanical structures made of these laminates, such as a leaf spring suspension system in an automobile, are subjected to various loads, such as bending and twisting. The design and analysis of such laminated structures demands knowledge of the stresses and strains in the laminate. Also, design tools, such as failure theories, stiffness models, and optimization algorithms, need the values of these laminate stresses and strains.

Here, the finite element analysis of laminate is carried out to determine the stresses and strains induced in the laminate under various loading conditions. Three main types of loading conditions are investigated to determine the mechanical properties. They are

1. Longitudinal loading of composite laminate
2. Lateral Loading of composite laminate
3. Shear loading of composite laminate

Stress- Strain analysis of PA6 GF65 composite is carried out using ANSYS 11.0 software and SHELL99 element is used for the analysis. Fiber orientations are varied considerably for different loading conditions to obtain desirable results

B. SHELL 99 ELEMENT

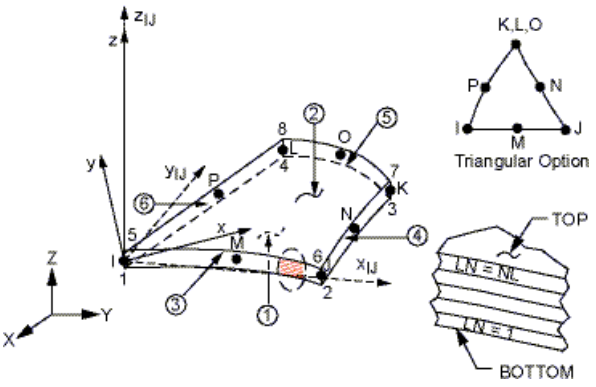

Fig.5 Shell99 Geometry

IV. FINITE ELEMENT ANALYSIS OF COMPOSITE

Following are the steps followed in order to carry out the finite element analysis of
composite:
1. Modeling of the composite model
2. Discretization of continuum.
3. Preprocessing
4. Solution or Processing
5. Post-Processing

Modeling of the composite laminate is done using Ansys preprocessor. Rectangular area of specific dimensions (50mm*10mm) is modeled and real constants like number of layers, layer thickness and orientations are provided for the element. Discretization of the composite shell element is done using Ansys mesh tool and 2D quadrilateral elements are used for meshing. Mesh is refined to obtain the desirable results.
The material properties and the element constants that are provided are written in an input file in the preprocessor of the software. The nodal coordinates and the boundary conditions are read by the preprocessor. Loading conditions are varied for tensile and shear test accordingly. For tensile test, one end of the model is constrained to all degrees of freedom and load applied is applied as pressure (2000N) at the free end of the model. For shear loading the load (1000N) is applied at the both the ends and fibers are oriented in [+45/-45/+45/-45/+45/-45] directions. The required element geometry and the vectors are generated for the chosen element by the preprocessor. Then the assembly module produces

the global matrix equation of the finite element model. The solution for the governing matrix equations is done and recorded in the output file.

The graphical output of the recorded solution can be viewed in this stage. In this stage, displacement, maximum inter-laminar stresses and strains are recorded.

A. LONGITUDINAL TENSILE TEST

Longitudinal tensile test can be simulated using finite element analysis for the composite laminate. A simple rectangular cross-sectional area of required dimensions is created and the real constants like number of layers, layer thickness and fiber orientations are provided for the shell99 element used for the analysis. In this longitudinal tensile test, all fibers are oriented in 0 degrees with respect to the laminar axis. Model is constrained at the fixed end by all degrees of freedom and a tensile load of 2000N is applied at the free end.

Element Chosen: SHELL99
Dimensions of the Laminate ply: 50*10mm
Thickness of each layer =0.6
Number of Layers =6
Thickness=3.6mm

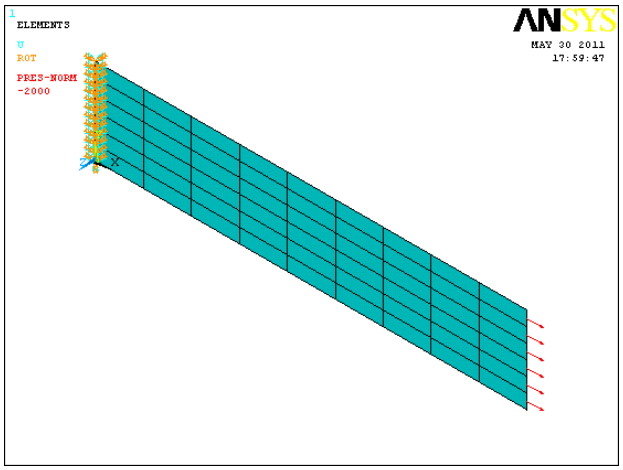

Fig.6 Boundary and loading condition for Tensile Test

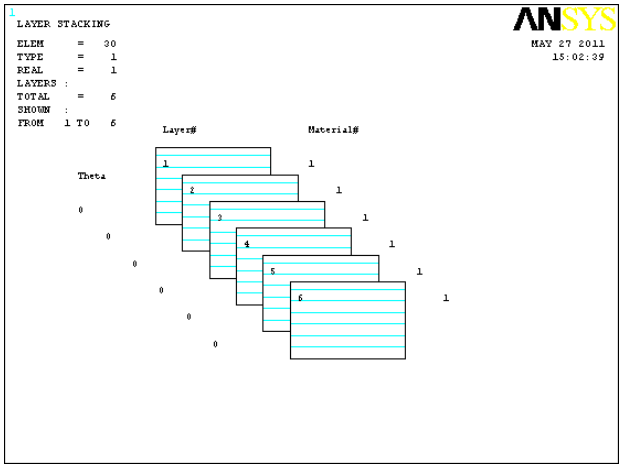

Fig 7: Layer orientation for longitudinal Tensile Test

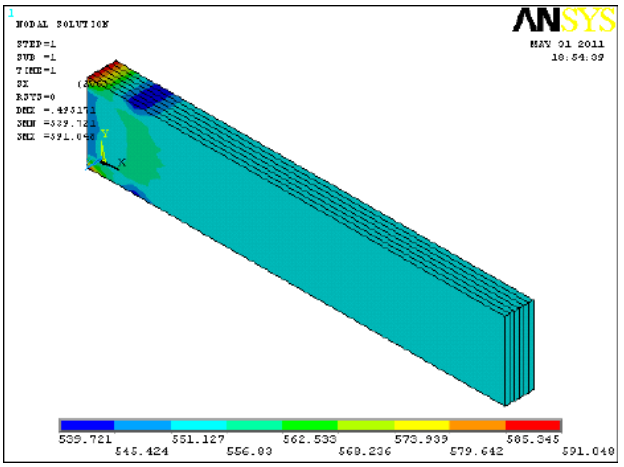

Fig 8: Stress plot for 0 degree laminate subjected to tensile load

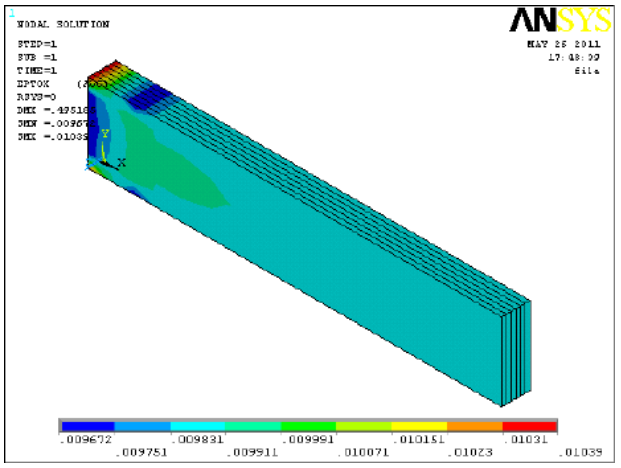

Fig 9: Strain plot for 0 degree laminate subjected to tensile load

B. TRANSVERSE TENSILE TEST

Transverse tensile test can be simulated using finite element analysis for the composite laminate. A simple rectangular cross-sectional area of required dimensions is created and the real constants like number of layers, layer thickness and fiber orientations are provided for the shell99 element used for the analysis. In this transverse tensile test, all fibers are oriented in 90 degrees with respect to the laminar axis. Model is constrained at the fixed end by all degrees of freedom and a tensile load of 2000N is applied at the free end. Results obtained like stresses and strains are studied and compared with the experimental results.

Element Chosen: SHELL99
Dimensions of the Laminate ply: 50*10mm
Thickness of each layer =0.6
Number of Layers =6
Thickness=3.6mm

Boundary and loading conditions for transverse tensile test is same as that for longitudinal tensile test only difference is that for longitudinal tensile test fibers are oriented at 0 degrees i.e. along the direction of loading and for transverse tensile test fibers are oriented at 90 degrees i.e. across the direction of loading

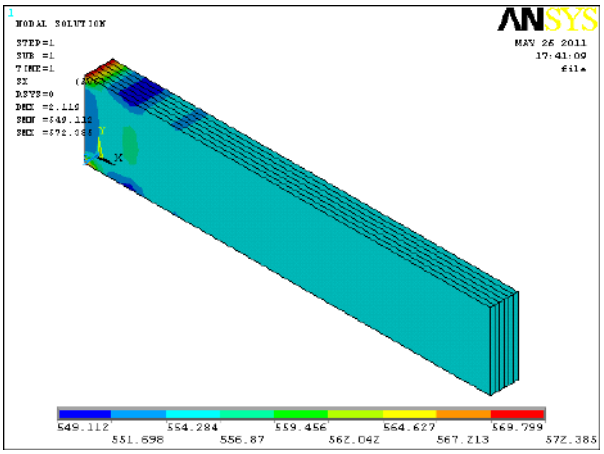

Fig 10: Strain plot for 90 degree laminate subjected to tensile load

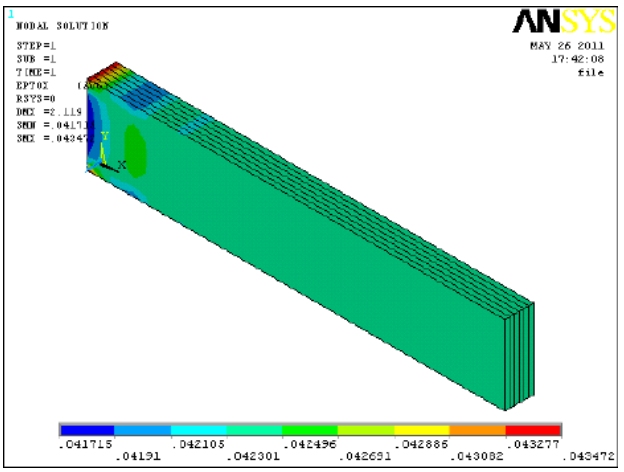

Fig 11: Strain plot for 90 degree laminate subjected to tensile load

C. SHEAR TEST

Shear test can be simulated using finite element analysis for the composite laminate. A simple rectangular cross-sectional area of required dimensions is created and the real constants like number of layers, layer thickness and fiber orientations are provided for the shell99 element used for the analysis. In this shear test, laminate plies with [+45/-45/+45/-45/+45/-45] distribution are loaded on both the free ends with a pressure of 1000N. Results obtained like stresses and strains are studied and compared with the experimental results.

Element Chosen: SHELL99
Dimensions of the Laminate ply: 50*10mm
Thickness of each layer =0.6
Number of Layers =6
Thickness=3.6mm

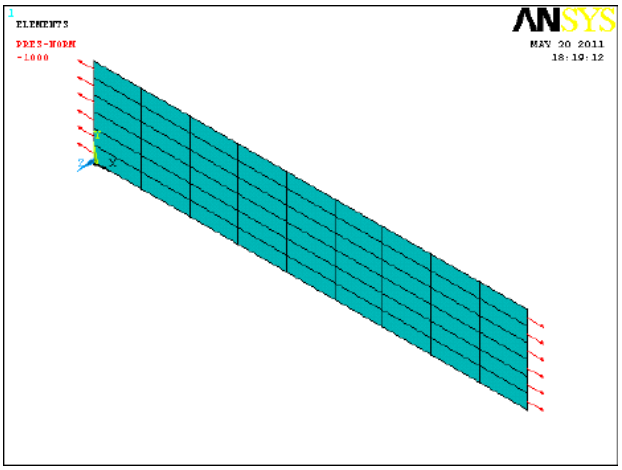

Fig.11 Boundary and loading condition for Shear Test

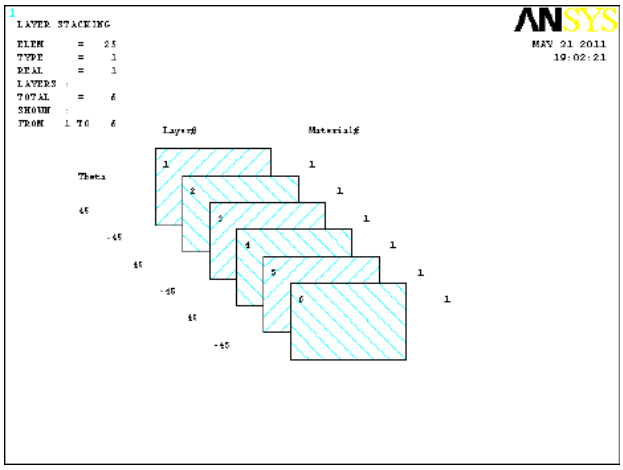

Fig.12 Layer Orientations for laminate subjected to shear load

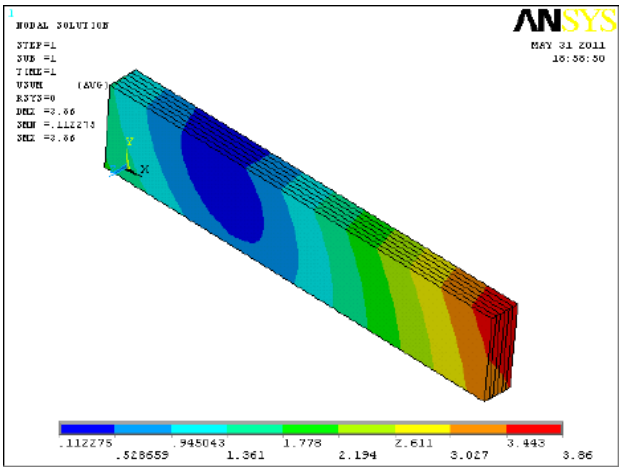

Fig.12 Displacement plot for laminate subjected to shear load

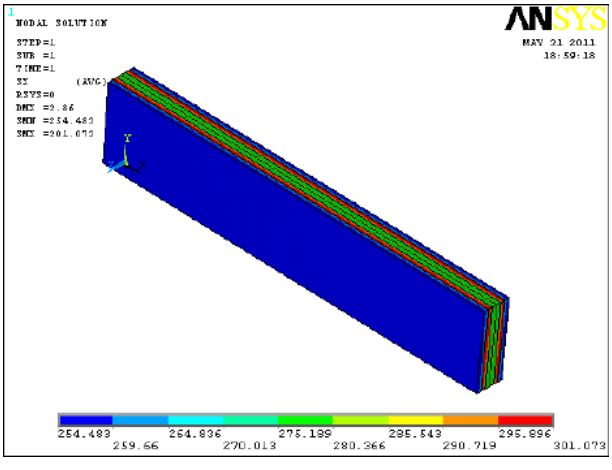

Fig.13 Stress plot in X direction (along the direction of loading) for laminate subjected to shear load

V. RESULTS & DISCUSSION

Elastic properties of GF65/PA6 obtained by experimental testing and finite element analysis are tabulated as shown in the table and graphs are plotted

Table 2: Comparison of elastic constants obtained by finite element and experimental testing

Elastic Constants	Experimental Testing	Finite Element Analysis
Longitudinal Young's Modulus (E_1)	55429.59 MPa	56499.11MPa
Transverse Young's Modulus (E_2)	13854.18 MPa	13170.47 MPa
Shear Modulus (G_{12})	4444.84 MPa	4790.80 MPa

Experimental results and finite element results obtained for Longitudinal (Figure 14), lateral (Figure 15) and transverse tensile tests (Figure 16) are plotted in the following graphs

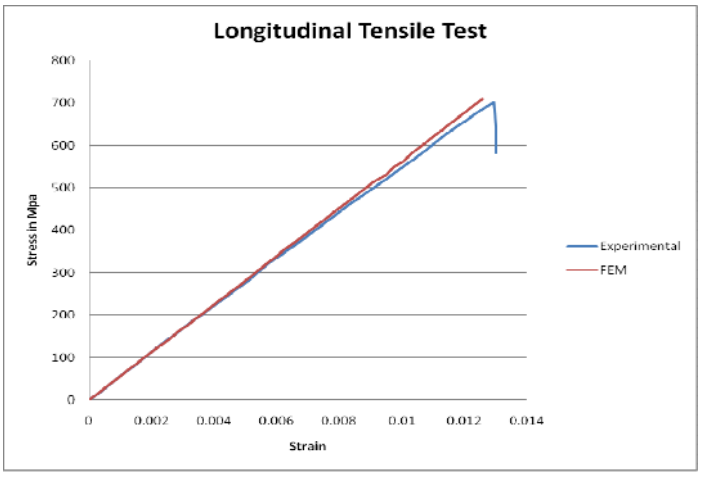

Fig.14 Longitudinal Tensile Test comparison

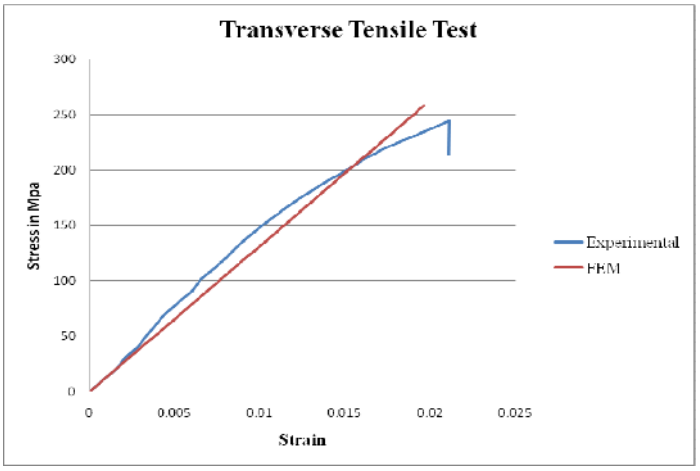

Fig.15 Transverse Tensile Test comparison

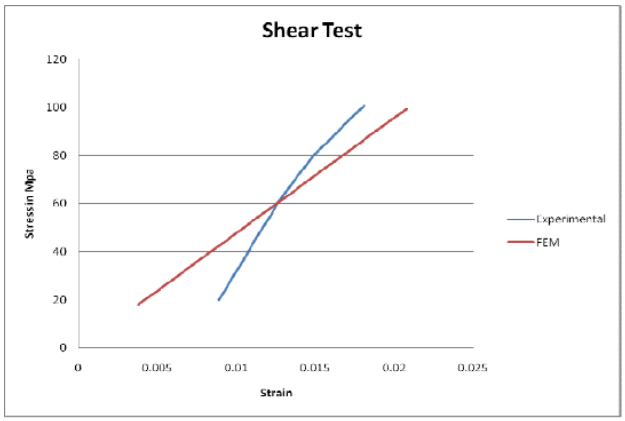

Fig.16 Shear Test Comparison

VI. CONCLUSIONS

From the results compared and the graphs, observation can be made that the finite element analysis coincides with the results obtained using experimental results. So it can be concluded that finite element method can be used as one of the methods to determine the composite properties. The advantage of finite element method over experimental method is that the specimen model may not be prepared and broken. Hence the cost of manufacturing a specimen can be reduced so analysis technique can be used to model the composite for any specific application.

ACKNOWLEDGMENT

We would like to express our sincere gratitude to the Management, Dr. H Ramakrishna, Principal of Sapthagiri College of Engineering, Bengaluru for the facilities provided and their support. Also we would like to thank Dr. P Mahadevaswamy the Head of department, Mechanical Engineering and faculties for their encouragement and support.

REFERENCES

[1]. Du-Xin Li, Xin Deng, Jin Wang, Jun Yang, Xiangxiang Li, Mechanical and tribological properties of polyamide 6–polyurethane block copolymer reinforced with short glass fibers, Wear, Volume 269, Issues 3-4, 18 June 2010, Pages 262-268

[2]. Plamen G. Malchev, Gerard de Vos, Stephen J. Picken, Alexandros D. Gotsis, Mechanical and fracture properties of ternary PE/PA6/GF composites , Composites Science and Technology, Volume 70, Issue 5, May 2010, Pages 734-742

[3]. Izabella Krucinska, Eulalia Gliscinska, E. Mäder, R. Habler, Evaluation of the Influence of Glass Fibre Distribution in Polyamide Matrix During the Consolidation Process on the Mechanical Properties of GF/PA6 Composites, FIBRES & TEXTILES in Eastern Europe, January/March 2009, Vol. 17, No. 1 (72)

[4]. Syed Altaf Hussain, B. Sidda Reddy and V. Nageswara Reddy, Prediction Of Elactic Properties Of FRP Composite Lamina For Longitudinal Loading, ARPN Journal of Engineering and Applied Sciences Vol. 3, No. 6, December 2008

[5]. Thomason, J.L. (2008), The influence of fibre length, diameter and concentration on the strength and strain to failure of glass-fibre reinforced Polyamide 6, 6. Composites Part A: Applied Science and Manufacturing, 39 (10). pp. 1618-1624. ISSN 1359-835X

[6]. Shaocheng Ji, Generalized means as an approach for predicting Young's moduli of multiphase materials, Materials Science and Engineering A366 (2004) 195–201

[7]. Qing-Sheng Yang , Qing-Hua Qin, Modelling the effective elasto-plastic properties of unidirectional composites reinforced by fibre bundles under transverse tension and shear loading, Materials Science and Engineering A344 (2003) 140-1

Mechanical Properties Characterization of Graphene Reinforced Epoxy Polymer Nano Composite

Prashanth B S, Prashanth P, Prathap N, Prithvi K[#1], Ramesh N G[#2]

[#1]*Student, Dept. of Mechanical Engg., Sapthagiri college of Engineering Bangalore-560073, India*

[#2]*Asst. Professor, Dept. of Mechanical Engg., Sapthagiri college of Engineering Bangalore-560064, India*

***Abstract* — Graphene is a novel class of Nano fillers possessing outstanding characteristics including most compatible with most polymers, high absolute strength, high aspect ratio and cost effectiveness. In this study, graphene was used to reinforce epoxy as a matrix, to enhance its mechanical properties. Graphene are reinforced into epoxy matrix to prepare the composites by hand lay-up technique. Four weight percentages were used for these studies which are 0.5 wt%, 1.0 wt% 1.5 wt% and 2 %. . Mechanical properties are investigated in terms of tensile, flexural and Hardness test as per ASTM standards. The results have been shown that mechanical properties are increased with increase the percentage of glass fiber in epoxy matrix.**

***Keywords*- Graphene nano particles, Epoxy, Mechanical properties, ASTM Standards.**

I. INTRODUCTION

Over the last thirty years composite materials, plastics and ceramics have been thedominant emerging materials. The volume and number of applications of compositematerials have grown steadily, penetrating and conquering new markets relentlessly.Modern composite materials constitute a significant proportion of the engineered materials market ranging from everyday products to sophisticated niche applications. While composites have already proven their worth as weight-saving materials, the currentchallenge is to make them cost effective. The efforts to produce economically attractive composite components have resulted in several innovative manufacturing techniques currently being used in the composites industry. It is obvious, especially for composites, that the improvement in manufacturing technology alone is not enough to overcome the cost hurdle. It is essential that there be an integrated effort in design, material, process, tooling, quality assurance, manufacturing, and even program management for composites to become competitive with metals.

Composite materials are engineered materials in which more than one material with significant mechanical properties are combined to form a single structure having unique properties. The superior properties of the composite material depend upon the properties of constituent materials as well as the properties of the interface.

Generally the composites are made of two constituent materials such as matrix and reinforcement. The matrix material surrounds and supports the reinforcement materials by maintaining their relative positions and provides the bulk form of the product. The role of reinforcements provides excellent physical properties to enhance the matrix properties. Composite materials produce considerable enhancement in material properties when compared with the conventional materials.

The reinforcement material is generally stronger and stiffer than the matrix materials, which leads to good physical properties. The matrix holds the reinforcements in a regular pattern. Both matrix and reinforcement materials are combined properly to achieve the required property.

In polymer nanocomposites, polymers are reinforced with small amount of nano sized particles. The dispersed phase can be inorganic particles, clays, minerals etc. The particle filled polymer composites have been extensively studied because of their wide spread applications in the field of automobile, electrical industries, aeronautical and household. Numerous scientists have focused on the interest that nanocomposites offer for applications in high performance coatings, catalysis, magnetic, electronics and biomedical materials.

The primary goal of polymer nanocomposites research is to enhance the strength and toughness of polymeric components using nano particles. Due to the addition of filler materials into matrix materials, the mechanical properties such as modulus, tensile strength, flexural strength, impact strength have been improved and also increased gas barrier, increased heat distortion temperature etc.

II. EXPERIMENTAL PROCEDURE

2.1 MATERIAL

Epoxy resin refers to a type of reactive prepolymer and polymer containing epoxide groups. These resins react either with themselves in the presence of catalysts, or with many co-reactants like amines, phenols etc. it was manufactured by araldite with commercial name Epoxy LY 556 (Epoxy Monomer) and Hardener HY-951.were Supplied by zenith industrial supplier, Bengaluru . Graphene nano particles were supplied by Ultra nanotech Pvt ltd. Bengaluru their purity was higher than by 99%. The average Size of Nano particles is 5nm. The properties are listed in the table 2.1

Table: 2.1

Material -Epoxy LY 556	
Aspect (visual)	Yellow viscous liquid
Viscosity at 25 °C	10000 – 12000 [MPa s]
Density at 25 °C	1.15 – 1.20 [gm/cm3]

Material –Graphene	
Purity	Greater than 99%
Thickness	5–10 nm
Length	5-10 micron
Density	3.1 g/cm3

2.2 FABRICATION

In this study, manual hand layup method is used for preparing composite laminates as shown in Figure 2.21. First of all, a release gel is sprayed on the mould surface to avoid the sticking of epoxy to the surface. Thin plastic sheets are used at the top and bottom of the mould plate to get a good surface finish of the product. Reinforcement in the form of Graphene nano particles .Then epoxy in liquid form is mixed thoroughly in suitable proportion with a prescribed hardener (curing agent) and poured onto the surface of mat already placed in the mould. The epoxy is uniformly spread with the help of the brush and a roller is moved with a mild pressure on the Graphene-epoxy layer to remove any air trapped as well as After placing the plastic sheet, release gel is sprayed on the inner surface of the top mould plate which is then kept on the stacked layers and the pressure is applied. After curing either at room temperature or at some specific temperature at 60˚C - 80˚C, the mould is opened and the developed composite part is taken out and further processed. For epoxy based system, normal curing time at room temperature is 24 - 48 hours.

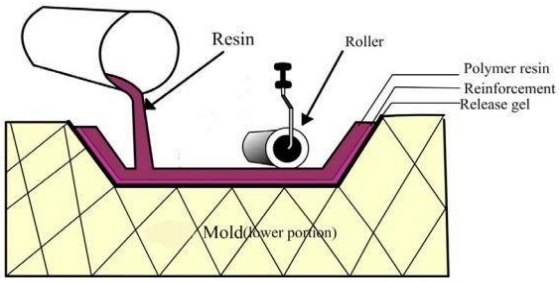

Figure 2.21 hand layup technique

2.3 TESTING OF COMPOSITES

Tensile Test

The tensile test is done by cutting the composite specimen as per ASTM: D638 standard (sample dimension is 216 × 19 × 3 mm^3). A universal testing machine (UTM) (Model: KIC-2-1000-C) is used for testing with a maximum load rating of 100 KN. Composite specimens with different fiber combinations are tested, which are shown in Figure 2.31. In each case, three samples are tested and the average is determined and noted. The specimen is held in the grip and load is applied and the corresponding deflections are noted. The load is applied until the specimen breaks and break load, ultimate tensile strengths are noted. Tensile stress and strain are recorded and load vs length graphs are generated.

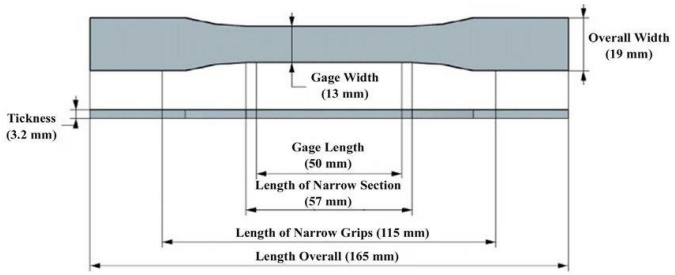

Figure 2.31 ASTM D638 Standard

Flexural Test

The flexural test is done in a three point flexural setup as per ASTM: D790 standard (sample dimension is 150 × 12.7× 10 mm^3). When a load is applied at the middle of the specimen, it becomes bends and fractures as shown in Figure 2.32. This test is carried out in the UTM from which the breaking load is recorded and load vs length graphs are generated.

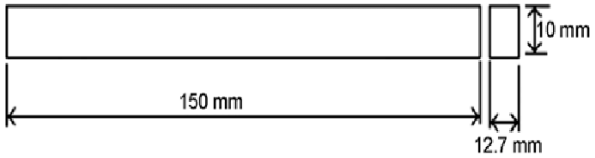

Figure 2.32 ASTM D790 Standard

Hardness test

Hardness is the resistance to permanent indentation or penetration. Hardness of materials like polymer, elastomer and rubbers is measured by Shore D scale. Durometer has an indenter loaded by a calibrated spring. The hardness is determined by the penetration depth of the indenter under the load. Hardness test is done by preparing the specimen as per ASTM: D2240 standard.

3. RESULT and DISCUSSION

Tensile Strength

Tensile properties are studied as per ASTM-D638 using universal testing machine (Model 6025 UK), at 10 mm/minute cross-head speed, using specimen with a width of

19 mm, length of 165 mm and thickness of 3 mm. ASTM standard specimens were prepared for tensile testing and the average values of calculated tensile strength of different samples were tabulated in Table 3.1

Sl.No	Sample	Tensile Strength (N/mm^2)
1	Epoxy	14
2	99.5 % Epoxy +0.5% Graphene	21.80
3	99 % Epoxy + 1% Graphene	18.79
4	98.5 % Epoxy +1.5% Graphene	24.16
5	98 % Epoxy + 2% Graphene	27.82

From the results, it was observed that the Graphene nano particle reinforced with Epoxy specimen possessed higher tensile strength than that of plain Epoxy specimen. it is also concluded that tensile strength of the polymer composite increases with the increase in reinforcement material.

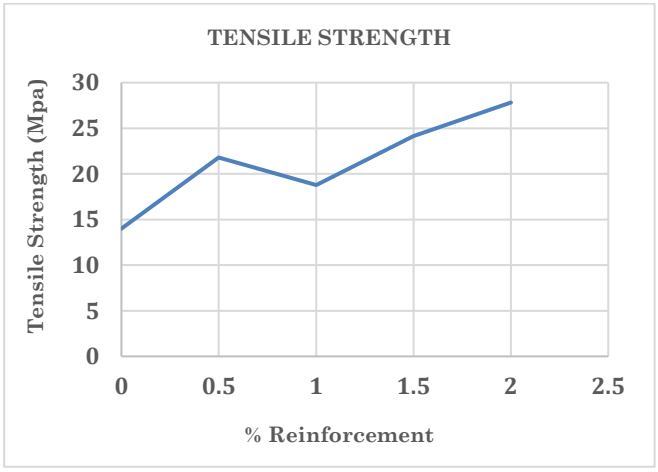

Figure 3.1: Tensile Strength vs Reinforcement

. It was also seen that the specimen had the peak value of tensile strength obtained at 2 wt % of Reinforcement as shown in Figure 3.1.

Flexural Strength

Flexural strength is the ability of composites or materials to resist bending deflection when energy is applied to the structure.

Sl.No	Sample	Flexural Strength (N/mm^2)
1	Epoxy	42
2	99.5 % Epoxy +0.5% Graphene	49.69
3	99 % Epoxy + 1% Graphene	33.86
4	98.5 % Epoxy +1.5% Graphene	46.96
5	98 % Epoxy + 2% Graphene	46.38

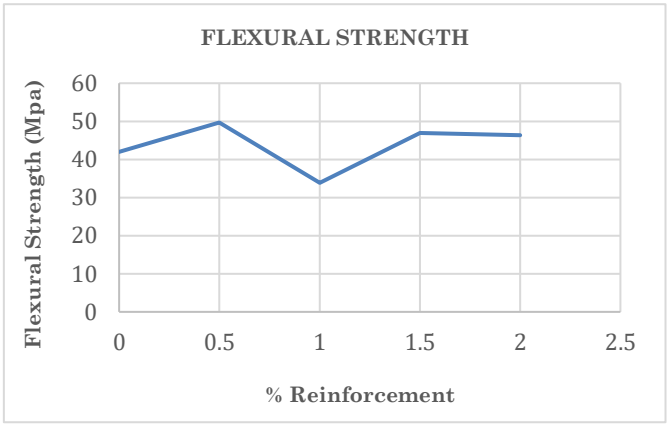

Figure 3.2: Flexural Strength vs Reinforcement

It was seen that Flexure strength did not much increase with increase of graphene content when compared with the plain Epoxy.

Hardness test

Hardness number is resistance to penetration, indentation or abrasion when load is applied on the materials. The increase in the hardness number of the material shows the resistance to penetration.

Sl.No	Sample	Shore Hardness Hs
1	Epoxy	46
2	99.5 % Epoxy +0.5% Graphene	75
3	99 % Epoxy + 1% Graphene	82
4	98.5 % Epoxy +1.5% Graphene	84
5	98 % Epoxy + 2% Graphene	78

.

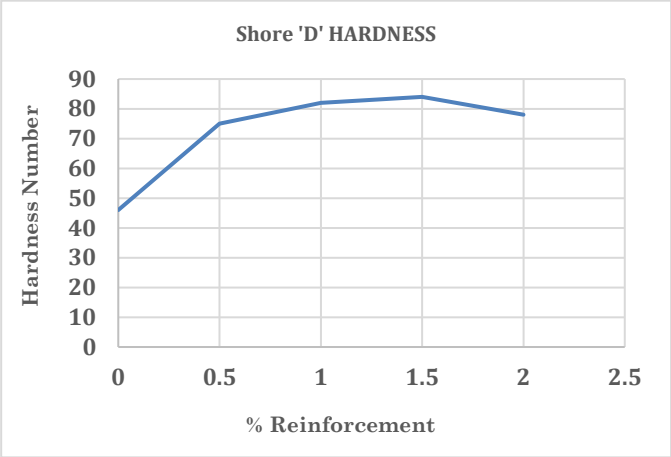

Figure 3.3: Shore D Hardness number vs Reinforcement

From the results, it was observed that the Graphene nano particle reinforced with Epoxy specimen possessed higher Hardness number than that of plain Epoxy specimen. Higher hardness number 84 was obtained at 1.5 wt % of Reinforcement as shown in Figure.

4. CONCLUSIONS

The prepared Graphene reinforced Epoxy composites are tested for mechanical properties and following conclusions are drawn:

1. The mechanical properties such as tensile, found to be maximum for Graphene Reinforced composite with maximum 2% wt of Graphene Nano fillers.
2. The mechanical properties such as flexural strength did not much increase with increase of graphene content when compared with the plain Epoxy.
3. The mechanical properties such as Hardness number did not much increase with increase of Reinforcement content. Higher hardness number 84 was obtained at 1.5 wt % of Reinforcement.

REFERENCES

1. Advances in epoxy/graphene nanoplatelet composite with enhanced physical properties: a review Polym.-Plast. Technol. Eng., 55 (6) (2016), pp. 643-662
2. Surface properties of graphene: relationship to graphene-polymer composites Rev. Adv. Mater. Sci. (40) (2015), pp. 60-71
3. Kesong Hu, Dhaval D, "Graphene-polymer nano composites for structural and functional applications", Progress in Polymer Science 39 (2014)
4. Hurang Hu, "Characterizing and Modeling Mechanical Properties of Nano composites- Review and Evaluation", Journal of Minerals & Materials Characterization & Engineering, Vol. 9, No.4, pp.275-319, 2010.
5. Arunkumar Lagashetty and A Venkataraman, "Polymer Nanocomposites", Advances in Polymer Science, Vol.138, pp.107-148, 1998.
6. Deepak Verma, "Mechanical-Thermal-Electrical and Morphological Properties of Graphene Reinforced Polymer Composites", Trans Indian Inst Met (2014) 67(6):803–816.
7. Gupta M K, Srivastava R K, Kumar Sushil, Gupta Suresh, Nahak Binayak. Mechanical and water absorption properties of hybrid sisal/glass fibre reinforced epoxy composite. American J Polym Sci Eng. 2015, 3: 208-2019
8. Chow W S. Water absorption of epoxy/glass fiber/organo-montmorillonite nanocomposites. eXPRESS Polym Lett. 2007, 2: 104-108
9. Kornmann X, Rees M, Thomann Y, Necola A, Barbezat M, Thomann R. Recent Advances in Polymer Nanocomposites: Synthesis and Characterisation. Compos Sci Technol. 2005, 65: 2259-2268
10. Xie H-Q, Zhang S, Xie D. An efficient way to improve the mechanical properties of polypropylene/short glass fiber composites. J Appl Polym Sci. 2005, 96: 1414-1420.
11. Morye S S, Wool R P. Mechanical properties of glass/flax hybrid composites based on a novel modified soybean oil matrix material. Polym Compos. 2005, 26: 407-416
12. Mishra S, Mohanty A K, Drzal L T, Misra M, Parija S, Nayak S K, Tripathy S S. Studies on mechanical performance of biofibre/glass reinforced polyester hybrid composites. Compos Sci Technol. 2003, 63: 1377-1385

Modification of Agricultural Tiller

Basavaraj Ganiger[1], Varun B K[2], Vasanth G[2], Yogesh Gowda K S [2], Shashidaran R[2]
[1]Assistant Professor, Department of mechanical engineering, Sapthagiri college of engineering, Bangalore.
[2]Undergraduate students, Department of mechanical engineering, Sapthagiri college of engineering, Bangalore.

Abstract:- Agriculture starts from human existence. It is important part in human life as it feed us and thereby it runs the ecosystem though. It is extreme important section for living beings. But modern farming techniques are heavy-coughed and very intensive. Modern tractors which runs by fuel are detrimental to environment and not affordable to farmers. Tilling in farming is main step and traditional techniques were time consuming and very intensive and modern ones are non-affordable and hazardous to environment. Portable Electric power tiller machine uses battery-powered mechanism to serve the tilling purpose at minimum cost, time in tilling and thereby increasing productivity, efficiency to enhance healthy environmental purpose too.

Keywords:- *Electric Tiller machine, motor, portable, mini tractor, frame design, vibration and traction effort.*

I. INTRODUCTION

To enable good soil gripping, the machine uses a wheel with welded angles. The wheel design was created to offer a tight grip on the soil that would allow the cultivator prongs to be dragged during the tilling process. The machine is turned on and off using a switch on the handle. The machine is powered by an electric motor that drives the pulling wheel using a sprocket chain configuration.

The motor is powered by a battery and has enough force to draw the forks through the soil. The three cultivator forks allow for precise and easy tilling, which is ideal for farming. The machine's direction can be easily controlled while in use because to its portable, lightweight construction. For carrying the machine, it can also be simply carried around in vehicles or by hand. As a result, the electric power tiller offers a smart, fuel-free mechanism for farm and garden tilling.

Prashant Rahat et al., [1] studied the portable battery charged electric power tiller machine. Farming practises used in traditional agriculture. To provide maximum soil grip, the machine uses a wheel with welded angles. The wheel design was created to offer a strong grip on the soil that would allow the cultivator prongs to drag during the tilling process. An electric motor drives the pulling wheel through a sprocket chain arrangement. By adopting a motorised tilling system, it minimises human effort at a very low cost. Using a unique portable design, the electric power tiller reduces the time and cost of tilling, enhancing agricultural output and efficiency.

Zakariya et al., [2] after preliminary study, it was found out that power tiller could be adopted for weeding. As a result, the study sought to improve its performance by altering some essential components, such as weeding blades and depth blades. Three sets of four, six, and eight blade gangs were fabricated from 3 mm mild steel sheet metal. There were four levels of blade types 'B' and three levels of weeding depth 'D.' At two (2) weeks, the field was put out in a 43 randomised complete block design.

Shabbir J. Karjatwala et al., [3] studied and concluded that traditional farming methods, which are time-consuming, labour-intensive, and expensive, therefore they introduced new technologies. Machines are commonly employed for farming purposes in India, which is at a higher level. They are creating this model in order to solve this challenge. This document discusses the operating machinery that would be used to till one and a half hectors. With this new technology, the plough will be able to go ahead and the base wheel will rotate with blades that provide traction.

Mahesh Gavali et al., [4] in their study, a comparison of portable welders and power tillers in the Indian market is examined. Various weed-removal procedures for crops are also mentioned. The examination of various equipment used for mechanical weed removal is the main focus of this project.

According to this survey, the majority of Indian farmers, the majority of whom are small-scale farmers, can only afford portable welders. As a result, mechanical weed management is not used by these small-scale farmers. These small-scale farmers primarily utilise chemical and manual weeding methods. Portable welders are less expensive to operate and maintain, according to the literature review, but they are also less adaptable. Power tillers are more expensive, but they are more efficient.

In this current project work the objectives are as follows:

- Design of electrically operated tiller machine for field conditions.
- Conducting standard analysis of different working parameters for same operating conditions.
- Comparison between working model and other active machines in present.

II. EXPERIMENTAL DETAILS

A motorised tiller is operated by walking behind the machine. The machine consists of electric motor, battery, chain sprocket, wheel angles, bearing, electrical & wiring, mounts and joints, supporting frames, screw and fitting, bicycle wheel, the machine is powered by an electric motor that drives the pulling wheel using a sprocket chain configuration. The motor that drives the forks into the soil is powered by a battery. The cultivator forks enable for precise and easy tilling, as required by farming. The machine is light in weight and portable. Due to easy construction of machine the maintenance is very low.

The machine works on motor which gives power to overall system to run the object. The machine is drive by electric motor which is in contact with belt drive which ultimate helps to run the working of wheels of tiller during operation. For tiller machine the neat and accurate modification of supporting frame is provide For tiller machine the neat and accurate modification of supporting frame is provided which gives output voltage of fixed proposition. It is in such way that magnitude remains constant and input voltage doesn't change for conditions of voltage. Regulator connected at main wire which is connected to switch. Regulator and wire are connected to motor to running the operation. Motor is fitted to suitable angle as per stability for a worker during operation. Wheels are provided for ease in working during agriculture. When motor generates power machine runs and thereby teeth run side by side capable of digging in agricultural land with ease. One sensor is provided. The working of sensor is to stop or to cut off the extra or over or the extra energy which not needed battery is placed for energy supply to working of tiller machine.

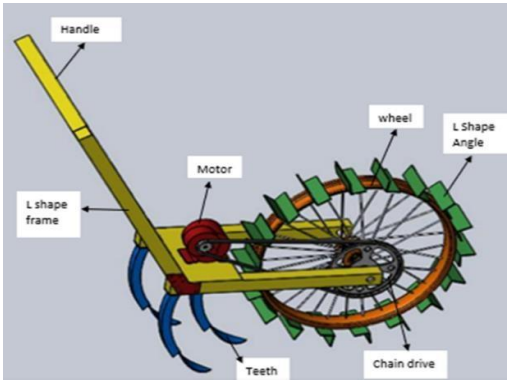

Fig.1 3-D view of conceptual tiller.

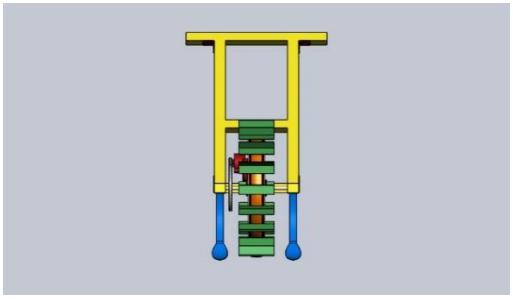

Fig. 2 Conceptual front view of Tiller.

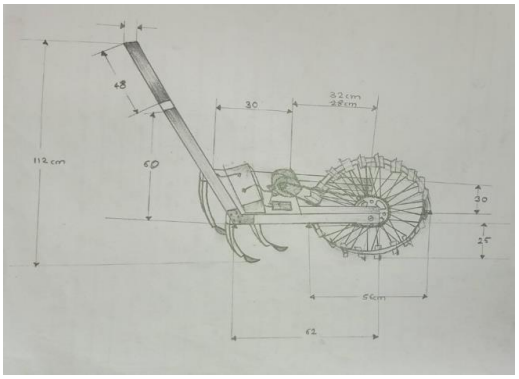

Fig. 3 Conceptual drawing of Tiller.

III. DISCUSSION

The power tiller is most suited for usage in hilly locations, moist conditions, and on small farms because it can do both primary and secondary tillage operations. The power tiller, with the correct set of tools and attachments, can handle most of the field operations in intensive cultivation. The power tiller's small weight makes it ideal for working in both wet and dry situations. Depending on the type of work, external attachments can be added to the tiller. As a result, the tiller can be utilised for a variety of tasks.

ACKNOWLEDGEMENT

The authors are very much thankful to the management of SCE Bangalore for the facility provided to carry out this project.

REFERENCES

[1] Prashant Rahat et al., “Design of portable electric power tiller machine”, International Journal of Advanced Research in Science, communication and technology (IJARSCT), 2021.

[2] Zakariya et al., ‘Modification of Portable Power Tiller for Small Scale Weeding Operation”, Journal of Engineering Research and Reports perform, 2021.

[3] Shabbir J. Karjatwala et al., “Design development and fabrication of mini cultivator and tiller”, international journal of science and engineering, 2018.

[4] Mahesh Gavali et al., “A comparison of portable welders and power tillers”, International Journal of Innovative Research in Science, Engineering and Technology, 2014.

Mossbauer spectroscopy Study of $LuFeO_3$

Kantharaj K.S.[1]
Department of Physics, Government First Grade College, Malur, Karnataka, 563130, India
kantharajksoma@gmail.com

Dr Jagadeesha Gowda G.V [2]
Department of Physics, Sapthagiri College of Engineering, Bengaluru-560057, India
jagadeeshagowdagv@gmail.com.
Ramprasad N [3]
Department of Physics, Government First Grade College, Mulbagal, Karnataka, 563131, India
ramprasadn1981@gmail.com

Dr. Arjuna Gowda KV [4]
Department of Physics, Government First Grade College, Hoskote, Karnataka, India-562114
kvarjunagowda@gmail.com
Jagadeesha Angadi V[5]
Department of Physics, P.C. Jabin Science College, Hubballi-580031, India
jagdeeshbub@gmail.com

***Abstract* —** In the present work we investigate the electronic structural microstructure and spectroscopic characteristics of $LuFeO_3$. Sample is prepared by the solution combustion method. X-ray diffraction patterns of $LuFeO_3$ nanoparticles confirms the *orthorhombic* structure crystallite size were found in nano range. X-ray photoelectron spectra were excited with a monochromatized AlK _-line radiation. Absolute resolved energy interval was 0.6 eV, which was determined with the $Ag3d_{5/2}$ line. The diameter of the X-ray spot on a sample was 500 mkm; it was small enough to study the samples obtained Mossbauer spectra of $LuFeO_3$ were collected in the temperature range of 13K – 700K. At 700K the spectra of both samples are paramagnetic doublets with similar parameters. At the lowest temperature (14K) the spectra of both samples are magnetically split sextets. The isomer shift values of the sextets and doublets are typical for Fe^{3+} ions in oxygen octahedron. .Morphology study and elemental analysis results reveals that the particle morphology and size is highly dependent on the reaction temperature, synthesis method and fuel. Further the active vibrational bands in these spectra correlate to the functional groups found in the examined system.

Keywords— XPS, Powdered XRD, FTIR, SEM, Mössbauer spectroscopy, $LuFeO_3$

1.INTRODUCTION

The most stable orthorhombic structure -$LuFeO_3$ andthe metastable hexagonal structure- $LuFeO_3$ are bothfound in Lu-ferrite [1, 2]. Because of its meta-stability, experimental studies of bulk hexagonal structure- $LuFeO_3$ multiferroicity are difficult and consequently uncommon [3–5]. Further because of hexagonalstructure-$LuFeO_3$ has a greater unit cell capacity than O- $LuFeO_3$. Although hexagonal structure- $LuFeO_3$ films may be stabilized on various substrates, strain effects, interface/surface effects, and widely presentflaws in films can all have a significant impact on their inherent physical characteristics [6]. As a result, it's critical to conduct experiments with high-quality bulk samples. However, unlike $RMnO_3$, where the hexagonal phase takes precedence over the orthorhombic when $R^{3?}$ is low, the orthorhombic phase in $RFeO_3$ is always stable since $Lu^{3?}$is alreadythe smallest rare earth ion. Scandium (Sc)-substituted$LuFeO_3$ has recently been found to have a stable hexagonal structure [6]. Three intriguingquestions have arisen as a result of this research. First, why does the addition of Sc maintain the hexagonal structure, despite the fact that neither$ScFeO_3$ nor $LuFeO_3$ prefers the P63cm hexagonal form? Second, how such a swap affects or does not influence certain physical features, particularly multiferroicity. Third, does the replacement result in a high-temperature magnetic transition? There was no magnetic measurement above ambient temperature in Ref., although a mild ferromagnetic order was identified below TR 162 K. Further, P. V. Coutinho etal. [7] reported structural, vibrational, and magnetic properties of the orthoferrites $LaFeO_3$ and $YFeO_3$: A comparative study. He concentrated specifically distortions induced in the bulk material due to the exchange between elements with different atomic radii in the individual A sites of perovskite. He got single phase with orthorhombic-distorted structure belonging to the space group Pnma.
But we need to understand $RFeO_3$ structure in proper manner. C Sai Vandana et al. [8] reported cobalt-substituted $GdFeO_3$ orthoferrites. These sample orthoferrites disclosed the orthorhombic *Pbnm* structure. It is thus a perfect time to take a step backand recap what we already know about the structure of $RFeO_3$. The main motivation of the work is how functional materials work in order to design the next generation of materials in their domains. We chose LuFeO3 and $Lu(YFe)O_3$ to study the electronic structural and spectroscopic properties using X-ray photoelectron spectroscopy and Mossbauer spectra to accomplish this.
In this work in order to understand the electronic structure of $LuFeO_3$and Yttrium-doped $LuFeO_3$
samples were examining through X-ray photoelectron spectroscopy and Mossbauer Spectra.

2.Experimental

2.1 Method

The $LuFeO_3$ powdered samples are produced by combustion method(CM) using carbamide and glucose. Oxidizers(O) and fuels(F) is taken 1:1 ration. All the O and F i.e $Lu(NO_3)_3.5H_2O$, (NH_2CONH_2) and ($C_6H_{12}O_6$) are mixed in a 500 ml beaker with distilled water. The solution is kept in furnace which is heated at 450 °C. After completion of burning process powdered is heated for 1250 degrees Celsius to get phase.

2.2 Characterizations

XRD is used to characterise the sintered samples, which uses CuK radiation. The data were taken in the detector-angle regime (2θ), with a step of 0.02° per minute, in the range of 20° to 80°. The Bragg reflection peaks identify the crystalline phases of the materials.

Using an X-ray photoelectron microprobe ESCALAB 250, XPS of powdered samples are collected at ambient temperature. A monochromatized AlK-radiation was used to excite the spectra. The Ag3d5/2 line profile provided the absolute energy resolution of 0.6 eV. The X-ray spot on a sample surface had a diameter of 500 um. To compensate for the sample's charge, slow electron flow was utilized. The C1s line was used to monitor the status of the surfaces. Although its intensity was modest, the line was nevertheless discernible against the background, allowing us to use it to calibrate the energy scales for all of the spectra. The binding energy of the C1s line was calculated to be 285 eV.

The MS1104Em spectrometer, created and manufactured by Southern Federal University's Scientific Research Institute of Physics, was used to capture Mössbauer spectra. The geometry of a moving source is used. ^{57}Co in a chromium matrix was used as the source of γ-quanta. The isomer shifts were estimated using the metallic -Fe as a reference. The samples were cooled in the helium cryostat CCS-850 (Janis Res. Inc., USA). The experimental spectra were fitted using

Sample	Lu	Y	Fe	O
$LuFeO_3$;	24.6	-	6.7	68.6

SpectrRelax software (Matsnev & Rusakov, 2012).Morphology of the samples were done by using SEM (S-4800-Hitachi-Japan)Agilent FTIR were were employed to characterizethe nano-sized LaFeO3 powder.

3. Results and discussion.

3.1 XRD Analysis

In Fig. 1 we have presented XRD graphs of $LuFeO_3$ nanoparticles confirms the orthorhombic structure. XRD data is matched to ICDD: 98-002-7285 [9]. All the diffraction peaks can be indexed to the o-LuFeO3 phase, and no traces of second phases are detected in the XRD patterns. The peak position and intensity is confirms no change in orthorhombic structure. The size of the sample are calculated by use of Scherrer formula(1) and found to be 56 nanometer range [10].

$$D = \frac{0.9\lambda}{\beta \cos\theta} \text{ nm ------1}$$

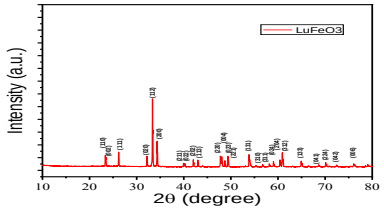

Fig. 1: X-ray diffraction patterns of $LuFeO_3$ nanoparticles

3.2. XPS.

XPS spectra were obtained using X-ray photo-electron microprobe ESCALAB 250. Powder particles are deposited on a conductive carbon double sided adhesive tape secured to the metal sample holder.

Figure 2 shows survey spectra from the surface of $LuFeO_3$ nanoparticles.

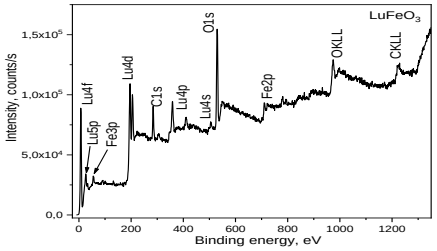

Fig. 2. Survey spectra from the surface of LuFeO3nanoparticles.

The survey spectrum shows that the qualitative elemental composition of the studied sample corresponds to the declared one. To determine the quantitative composition, the standard technique described in [11] was used. In accordance with this technique, Fe2p, Lu4d, and O1s X-ray photoelectron lines were recorded separately.

Elemental composition of the sample was determined via a standard method using the relation: (1):

$$C_i = \frac{I_i / I_i^{\infty}}{\sum_{j=1}^{n} I_j / I_j^{\infty}}$$

Here I_i are the integral intensities of the $Fe2p_{3/2,1/2}$, $Lu4d_{5/2,3/2}$ and O1s XPS lines, and I_i^{∞} are Wagner's empirically derived atomic sensitivity factors for XPS. The background was subtracted using Shirley method. Elemental composition was then determined using the software kit of the spectrometer. Table 1 shows the elemental composition of nanoparticle samples, measured by the above method of X-ray photoelectron spectroscopy.

Table 1. Elemental composition of nanoparticle sample in at.%, measured by X-ray photoelectron spectroscopy

Figure 3 shows the $Fe2p_{3/2,1/2}$, $Lu4d_{5/2,3/2}$ and O1s XPS of nanoparticles of the sample with the formal elemental $LuFeO_3$.

Considering that the surface of nanoparticles is analyzed, the elemental composition presented in Table 1 does not coincide with the formal composition. The reason for this discrepancy is primarily the excess in oxygen. The actual formula of the compound that nanoparticles consist of according to Table 1 can be written $Lu_{1.23}Fe_{0.34}O_{3.43}$. This means that the elemental composition of the nanoparticle surface measured by the XPS method has a lack of iron and an excess of lutetium and oxygen. Table 2 shows the binding energies of $Fe2p_{3/2,1/2}$, $Lu4d_{5/2,3/2}$, and O1s levels determined from X-ray photoelectron spectra in $LuFeO_3$ nanoparticles.

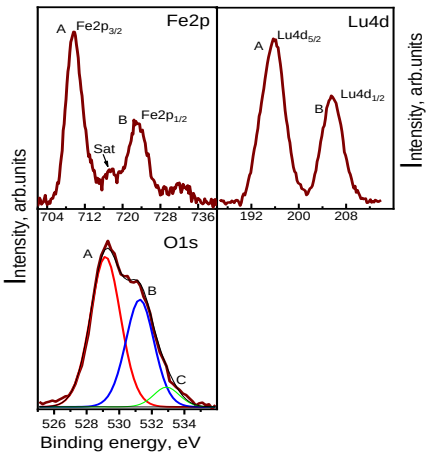

Fig. 3. $Fe2p_{3/2,1/2}$, $Lu4d_{5/2,3/2}$ and O1s XPS X-ray photoelectron spectra of nanoparticles of samples with the formal elemental composition $LuFeO_3$.

Table 2 Binding energies of $Fe2p_{3/2,1/2}$, $Lu4d_{5/2,3/2,}$ 2 and O1s levels in nanoparticles with the formal composition $LuFeO_3$.

In Fig. 3, component B in the O1s spectrum with an energy in the range of 531.4–531.7 eV, according to [12–14], refers to oxygen adsorbed on the surfaces of nanoparticles. The presence of this component increases the integral intensity of the O1s spectrum and changes the elemental composition normalized to 100%. We attribute the other component A with an energy of 529.2 eV in both samples to the oxygen of metal oxides. $Fe2p_{3/2,1/2}$ – X-ray photoelectron spectrum has a charge transfer satellite located at about 718.2 eV between the $Fe2p_{3/2}$ and $Fe2p_{1/2}$ peaks. According to the data [13,14], this makes it possible to unambiguously classify iron in the nanoparticle sample under study as trivalent. Lutetium, according to the binding energies of the Lu4d levels in Table 2, is also trivalent [15,16].

Figure 4 shows the X-ray photoelectron spectrum of the valence band of nanoparticles of the composition $Lu_{1.23}Fe_{0.34}O_{3.43}$.

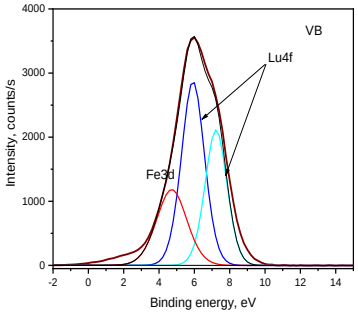

Fig.4 , Valence bands of samples of nanoparticles $Lu_{1.23}Fe_{0.34}O_{3.43}$.

VB $Lu_{1.23}Fe_{0.34}O_{3.43}$ the spectrum is decomposed into components corresponding to the position of the valence Fe3d and Lu 4f states in iron and lutetia, respectively [15,17]. Due to the small amount of lutetium in the Lu 4f sample, the states are less pronounced in the valence band of the $Lu_{1.23}Fe_{0.34}O_{3.43}$ nanoparticles.

3.3 Mössbauer spectra

$LuFeO_3$ Mössbauer spectra were recorded at temperatures ranging from 13K to 700K. The spectrum of $LuFeO_3$ at 700K is composed of paramagnetic doublets with the values indicated in Table. The quadrupole splitting values found are comparable to those obtained by Eibschutz et al. [19]. Zeeman splitting lines emerge in the spectra of both samples at temperatures below 620 K. The sextet is the only component of the spectrum of $LuFeO_3$ samples below 615. We utilize a sextet with the most likely value of the hyperfine magnetic field to match spectra recorded around the magnetic phase transition temperature. The distribution of hyperfine magnetic fields was used to find the most likely value of the hyperfine magnetic field. The spectrum is magnetically split sextet at the lowest temperature (14K).The isomer shift values of the sextets and doublets are typical for Fe^{3+} ions in oxygen octahedron [18].

Sample	Lu4d		Fe2p		O1s		
	A	B	A	B	A	B	C
$LuFeO_3$;	195.7	205.8	709.6	723.2	529.2	531.4	532.9

Table 3 Parameters of $LuFeO_3$ Mössbauer spectra

T, K	Component	δ±0.001, mm/s	Δ/ε±0.001, mm/s	H±0.4, kOe	Γ±0.002, mm/s
14	Sextet	0.464	-0.015	546.2	0.266
100	Sextet	0.460	-0.017	543.1	0.291
200	Sextet	0.417	-0.019	525.6	0.330
300	Sextet	0.354	-0.019	489.0	0.389
400	Sextet	0.289	-0.019	433.7	0.406
500	Sextet	0.223	-0.019	356.5	0.453
600	Sextet	0.151	-0.019	176.9	0.668
607	Sextet	0.137	-0.019	129.7	0.756
615	Doublet	0.141	0.348		0.407
625	Doublet	0.138	0.324		0.368
650	Doublet	0.113	0.330		0.326
700	Doublet	0.075	0.334		0.334

δ - isomer shift, ε - quadrupole shift, Δ -quadrupole splitting for paramagnetic component, H - hyperfine magnetic field on ^{57}Fe nucleus, Γ – linewidth.

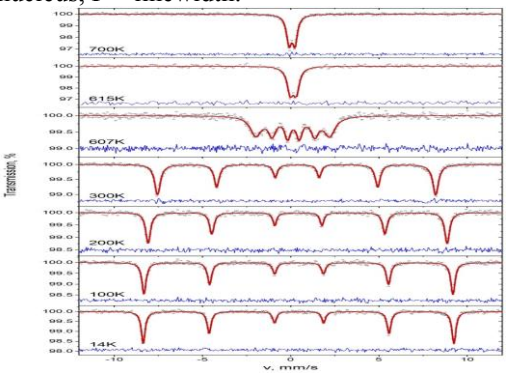

Fig. 5. Mössbauer spectra of $LuFeO_3$.

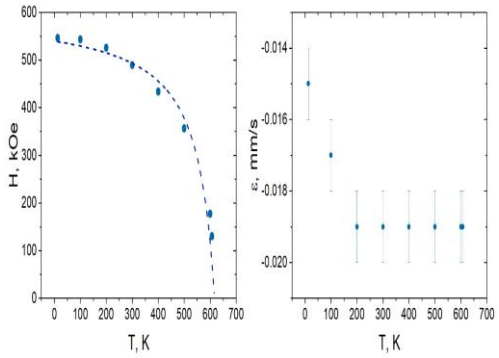

Fig. 6. Temperature dependencies of hyperfine magnetic field $H(T)$ and quadrupole shift $\varepsilon(T)$ for $LuFeO_3$.

The temperature dependence of hyperfine magnetic field values (H(T)) for the LuFeO3 sample is shown in Fig. 6a. Power Law and Brillouin functions were used to fit the H(T) dependencies. The best match was found in the second scenario, as shown by the dashed curve in Fig. 6a. Near 610K, the H(T) of $LuFeO_3$ becomes zero. The Curie (TC) temperature values obtained are lower than those recorded in polycrystal samples [20, 21]. The decrease in TC could be explained by the nanoscale reduction in crystalline size. The temperature dependences of quadrupole shift values ((T)) are shown in Fig. 6b. For $LuFeO_3$, the (T) dependencies change their slopes towards 200K. The following equations can be used to describe the quadrupole shift:

$$\varepsilon = \frac{eQq}{2}\left(\frac{3\cos^2\alpha - 1}{2}\right),$$

where Q is the nuclear quadrupole moment, q is the magnitude of the largest component of the electric field gradient (EFG) and α is angle between hyperfine magnetic field (H) and EFG. If we assume that $\frac{eQq}{2}$ do not change significantly in whole temperature range, then ε value is mainly determined by α. The α could change due to reorientation of H or EFG. The first case means the spin reorientation transition which accompanied by changing of quadrupole shift sign [22]. Since we do not observe the changing of quadrupole shift sign the anomaly on $\varepsilon(T)$ dependencies cannot be associated with reorientation transition. Therefore, the anomaly on $\varepsilon(T)$ can be explained by changing direction of EFG. The reorientation of EFG can occur duo to some rearrangement of electronic structure.

3.4. Microstructural analysis

Rare-earth orthoferrites $LFeO_3$ powders; the SEM morphology of the powder calcined at 1250 °C is illustrated in Fig 7. . It is seen that the particle morphology and size is highly dependent on the reaction temperature, synthesis method and fuel. In general, fuels like citric acid, amino acid, carbamide, and hydrazine compound are used in solution combustion. The cost of amino acids and hydrazine compounds is high, and car-capacity bamide's to chelate and complex metallic cations is limited. Furthermore, carbamide's combustion temperature might reach 1,600°C, making it difficult to generate ultrafine powder with good dispersion. Surprisingly, urea and glucose are a type of polycarboxylic acid with a low price, strong chelation ability, and mild combustion temperature, making them an excellent choice as a fuel for $LuFeO_3$ preparation. Solution combustion is a complex technique that necessitates strict drying conditions and costly alkoxide precursors [17]. What's more, because the phase of $LuFeO_3$ may be directly generated in the as-burnt powder, the calcination temperature for $LuFeO_3$ is relatively low using this solution combustion approach. To generate the required $LueFeO_3$ phase, other procedures in related sources typically require calcination temperatures of up to 1250°C. Citric acid functions as a fuel for the combustion process and is oxidized by the nitrates, resulting in a considerable volume of brown smoke developing during the self-propagating combustion process.

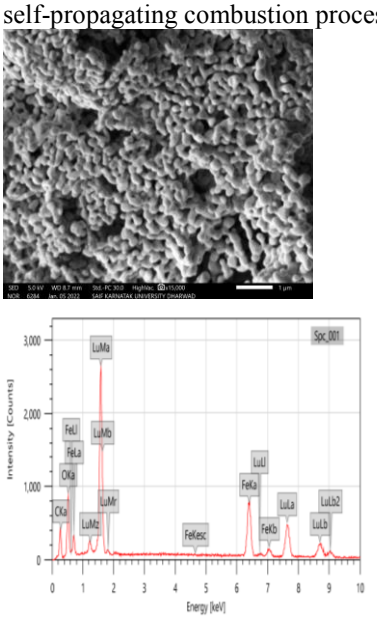

Fig 7. SEM micrograph and EDAX pattern of $LuFeO_3$

To further examine the presence and the atomic percentage of Lu, Fe, and oxygen in the prepared samples, dispersive analysis of X-rays (EDAX) was employed. Figure 7 shows the EDAX spectra of $LuFeO_3$ in which presence of Lu, Fe ions are clearly seen. The percentage composition of given elements for all prepared composition as obtained by EDAX.

3.5 FTIR analysis

The synthesised samples' Fourier Transform Infrared (FTIR) spectra are recorded in the 400–4000 cm^{-1} range, as shown in Fig 8. The active vibrational bands in these spectra correlate to the functional groups found in the examined system. The development of $LuFeO_3$ phase corresponds to the active vibrational bands at 402 and 554 cm1 [20-21]. Fe–O bending vibrations of FeO6 are identified in the band at 402 cm^{-1}, and it is sensitive to the Fe–O–Fe bond angle. Due to the technological constraints of the apparatus, this band does not appear in the case study. The two observed peaks are thought to reflect the primary characteristics of perovskite oxides [22].

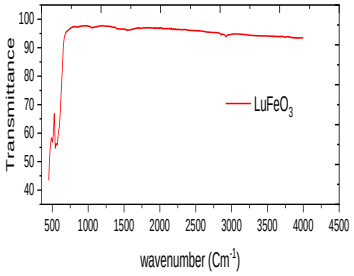

Fig. 8 FTIR Spectra $LuFeO_3$

4. Conclusion

X-ray diffraction patterns of $LuFeO_3$ nanoparticles confirms the *orthorhombic* structure. crystallite size of $LuFeO_3$ found in nano range. The XPS data confirmed that all lutetium and iron in the samples are trivalent. The $Fe2p_{3/2,1/2}$, $Lu4d_{5/2,3/2}$ and O1s XPS X-ray photoelectron spectra of nanoparticles of the sample with the formal elemental composition $LuFeO_3$. The presence of this component increases the integral intensity of the O1s spectrum and changes the elemental composition normalized to 100. Mössbauer spectra of $LuFeO_3$ were collected in the temperature range of 13K – 700K. At 700K the spectra of the samples are paramagnetic doublets with similar parameters. At the lowest temperature (14K) the spectra of both samples are magnetically

split sextets. The $H(T)$ for $LuFeO_3$ become zero near 610K, The obtained values of the Curie temperature are lower than those of the observed in polycrystal samples. The temperature dependencies of quadrupole shift change their slopes near 200K for $LuFeO_3$. These anomalies correspond to the spin reorientation transitions. SEM confirms the morphology of the samples in porous nature. Stretching vibration band were studied by FTIR.

References:

[1] Xiong Zhang, Hongjia Song, Congbing Tan, Shengsheng Yang, Yuxiong Xue, Jinbin Wang, Xiangli Zhong, Epitaxial growth and magnetic properties of h-LuFeO3 thin films, J. Mater. Sci., 52 (2017) 13879-13885. DOI: 10.1007/s10853-017-1469-8

[2] Jarrett A. Moyer, Rajiv Misra, Julia A. Mundy, Charles M. Brooks, John T. Heron, David A. Muller, Darrell G. Schlom, Peter Schiffer, Intrinsic magnetic properties of hexagonal LuFeO3 and the effects of nonstoichiometry, APL Mater., 2 (2014) 012106. DOI: https://doi.org/10.1063/1.4861795

[3] B.S. Holinsworth, D. Mazumdar, C.M. Brooks, J.A. Mundy, H. Das, J.G. Cherian, S.A. McGill, C.J. Fennie, D.G. Schlom, J.L. Musfeldt, Direct band gaps in multiferroic h-LuFeO3. J. Appl. Phys., 111(2012) 056105. DOI: 10.1063/1.3693588

[4] W. Wang, J. Zhao, W. Wang et al., Room-temperature multiferroic hexagonal LuFeO3 films. Phys. Rev. Lett., 110(23) (2013) 237601. DOI: https://doi.org/10.1103/PhysRevLett.110.237601

[5] K. Sinha, Y. Zhang, X. Jiang et al., Effects of biaxial strain on the improper multiferroicity in h-LuFeO3 films studied using the restrained thermal expansion method, Phys. Rev. B, 95(9) (2017) 094110.DOI: https://doi.org/10.1103/PhysRevB.95.094110.

[6] L. Lin, H.M. Zhang, M.F. Liu, Shoudong Shen, S. Zhou, D. Li, X. Wang, Z.B. Yan, Z.D. Zhang, Jun Zhao, Shuai Dong, J.M. Liu, Hexagonal phase stabilization and magnetic orders of multiferroic Lu1-xScxFeO3, Phys. Rev. B 93 (2016) 075146. DOI: https://doi.org/10.1103/PhysRevB.93.075146

[7] P.V. Coutinho, F. Cunha, Petrucio Barrozo, Structural, vibrational and magnetic properties of the orthoferrites LaFeO3 and YFeO3: A comparative study, Solid State Commun., 252 (2017) 59-63. DOI: https://doi.org/10.1016/j.ssc.2017.01.019

[8] C. Sai Vandana, B Hemalatha Rudramadevi, Structural, magnetic and dielectric properties of cobalt doped GdFeO3 orthoferrites, Mater. Res. Express 6 (2019) 126126. DOI: https://doi.org/10.1088/2053-1591/ab768f

[9] Chandra Bhal Singh, Dinesh Kumar, Narendra Kumar Verma, and Akhilesh Kumar Singh, Structural, dielectric, semiconducting and optical properties of high-energy ball milled $YFeO_3$ nano-particles, AIP Conf. Proc., 2115 (2019) 030619. DOI: https://doi.org/10.1063/1.5113458

[10] Zubida Habib, M. Ikram, Kowsar Majid, K. Asokan, Structural, dielectric and ac conductivity properties of Ni-doped HoFeO3 before and after gamma irradiation, Appl. Phy. A, 116 (2014) 1327-1335. DOI: https://doi.org/10.1007/s00339-014-8228-3

[11] Practical Surface Analysis by Auger and X-ray Photoelectron Spectroscopy, ed. by D. Briggs and M. P. Seach, John Wiley & Sons, Chichester, (1983), p. 533.

[12] Yamashita, P. Hayes, Analysis of XPS Spectra of Fe2+and Fe3+Ions in Oxide Materials, Appl. Surf. Sci., 254 (2008) 2441–2449. DOI: https://doi.org/10.1016/j. apsusc.2007.09.063.

[13] A.T. Kozakov, A.G. Kochur, A.V. Nikolsky, K.A. Googlev, V.G. Smotrakov, V. V. Eremkin, X-Ray Photoelectron Study of the Valence State of Iron in Iron-Containing Single Crystal (BiFeO3, PbFe1/2Nb1/2O3), and Ceramic (BaFe1/2Nb1/ 2O3) Multiferroics, J. Electron Spectrosc. Relat. Phenom., 184 (2011) 508–516. https://doi.org/10.1016/J.ELSPEC.2010.10.004.

[14] A.T. Kozakov, A.G. Kochur, A.V. Nikolskii, I.P. Raevski, S.P. Kubrin, S.I. Raevskaya, V.V. Titov, A.A. Gusev, V.P. Isupov, G. Li, I.N. Zakharchenko, Valence State of B and Ta Cations in the AB1/2Ta1/2O3 Ceramics (A =Ca, Sr, Ba, Pb; B =Fe, Sc) from X-Ray photoelectron and M¨ossbauer Spectroscopy Data, J. Electron Spectrosc. Relat. Phenom., 239 (2020) 146918(14). DOI: 10.1016/j. elspec.2019.146918.

[15] J.F. Moulder, W.F. Stickle, P.E. Sobol, K.D. Bomben Handbook of X-ray Photoelectron Spectroscopy ULVAC-PHI/Physical Electronics USA, Chigasaki, Japan/Minnesota, USA (1995), p. 107.

[16] Yu A Teterin, A Yu Teterin, Structure of X-ray otoelectron spectra of lanthanide compounds, Russ. Chem. Rev., 71 (5) (2002) 347-381. DOI 10.1070/RC2002v071n05ABEH000717

[17] K. Siegban, C. Nordling, A. Fahlman, R. Nordling, K. Hamrin, J. Hedman, G. Johanson, T. Berggmark, S.-E. Karlsson, I. Lindgren, B. Lindberg. ESCA, Atomic, Molecular and Solid State Structure Studied By Means of Electron Spectroscopy, Uppsala.1967. in Nova Acta Regiae Societatis cientiarum Upsaliensis, Ser.IV. Vol.20.

[18] M. E. Matsnev and V. S. Rusakov. SpectrRelax: An application for Mössbauer spectra modeling and fitting., AIP Conf. Proc., 1489 (2012) 178. DOI: 10.1063/1.4759488.

[19] M. Eibschütz, S. Shtrikman, D. Trevest. Mössbauer Studies of ^{57}Fe in Orthoferrites. Phys. Rev., 156 (1967) 562-577.

[20] X. Yuan, Y. Tang, Y. Sun, M. Xu. Structure and magnetic properties of $Y_{1-x}Lu_xFeO_3$ ($0 \le x \le 1$) ceramics. J. Appl. Phys., 111 (2012) 053911. DOI: 10.1063/1.3691243.

[21] N.N. Greenwood, T.C. Gibb, Mossbauer Spectroscopy, Chapman and Hall, London, (1971).

[22] J. Ramesh, N. Raju, S. Shravan Kumar Reddy, M. Sreenath Reddy, Ch. Gopal Reddy, P. Yadagiri Reddy, K. Rama Reddy, V. Raghavendra Reddy, ^{57}Fe Mössbauer study of spin reorientation transition in polycrystalline $NdFeO_3$, J. Alloys Compd., 711 (2017) 300-304; DOI: 10.1016/j.jallcom.2017.03.353.

MOTORIZED SCISSOR JACK

DEEKSHITH K N[1], GAGAN G[2], PAVAN KUMAR B[3], PRADEEP R[4], MOHAN. A. E[5]

Department of Mechanical Engineering, Sapthagiri College of engineering
#14/5 Chikkasandra, Hesaraghatta main road, Bangalore- 57 India

[1]ddeekshith753@gmaicom
[2]gagang6025@gmail.com
[3]pavankalyan9742@gmail.com
[4]Pradeepjackson743@gmail.com
[5]mohan@sapthagiri.edu.in

ABSTRACT: **This paper illustrates the description about the complete design and working of a motorized scissor jack. A Scissor jack is mechanical equipment used to lift up heavy loads. The power screw mechanism included in a scissor jack is design to lower the amount of force needed to lift the heavy loads. The operation of a scissor jack starts by using a z shaped crank that is mounted to a small hole on the mechanism. After rotating the crank, the screw jack rotates and acts like a gear mechanism. The lifting section consists of arms. The turning of screw operates the arms in such a way that it lifts up very gently. Now the arm rotates very gently and force needed to lift the vehicle is divided into parts and user can lift very heavy objects with comparatively very less force. Also the weight of the load is not enough to push the scissor down, since it would require very large force. Thus it allows us to life heavy loads like cars by just using human strength, also the system is further improved by making it motorized so user does not need to operate it manually but just press a button for lifting and lowering it.**

Keywords – scissor jack, light source, motorized scissor jack

I. INTRODUCTION

With the increasing levels of technology, the efforts being put to produce any kind of work has been continuously decreasing. The efforts required in achieving the desired output can be effectively and economically be decreased by the implementation of better designs.

Scissor Jack are used to convert rotary motion into translatory motion. A Scissor Jack is an example of a power screw in which a small force applied in a horizontal plane is used to raise or lower a large load. The principle on which it works is similar to that of an inclined plane. The mechanical advantage of a Scissor Jack is the ratio of the load applied to the effort applied. The Scissor Jack is operated by turning a lead screw. The height of the jack is adjusted by turning a lead screw and this adjustment can be done either manually or by integrating an electric motor.

In this project, an electric motor will be integrated with the Scissor Jack and the electricity needed for the operation and there by the mechanical advantage will be increased.

II. PROBLEM STATEMENT

Available jacks present difficulties for the elderly people and women and are especially disadvantageous under adverse weather conditions. Presently available jacks further require the operator to remain in prolonged bent or squatting position to operate the jack which is notergonomic to human body. It will give physical problems in course of time. Moreover, the safety features are also not enough for operator to operate the present jack.

Furthermore, available jacks are typically large, heavy and also difficult to store,transport. Carry or move into the proper position under an automobile. The purpose of this project is to overcome the Problems. An automatic car jack which has a frame type of design by using electricity from the car will be developed. Operator only need. to press the button from the controller without working in a bent or squatting position for a long period of time to change the tire.

ISBN: 979-88-35073-61-0

III. OBJECTIVES

Main objectives of project are:

1. To design a power scissor jack which is safe and reliable to raise and lower the load easily.
2. To develop a car jack that is power car and fully automated with a button System.
3. To reduce the time consumption
4. Easy to operate
5. Easy maintenance

IV. METHODOLOGY

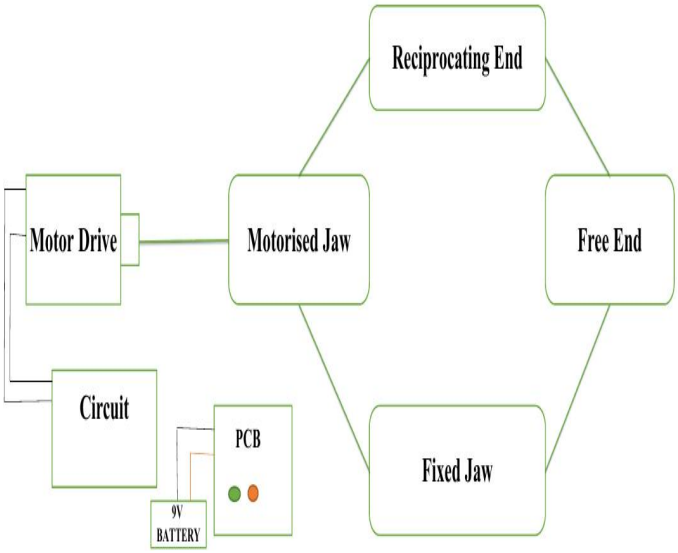

Fig 1: block diagram of motorized scissor jack

3D DESIGN OF MOTORIZED SCISSOR JACK

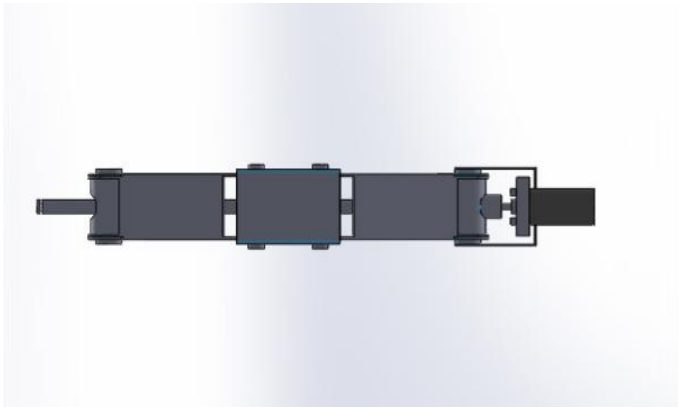

Figure: Top view

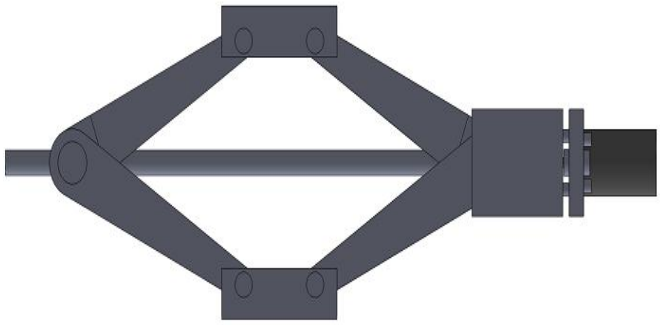

Figure: Front view

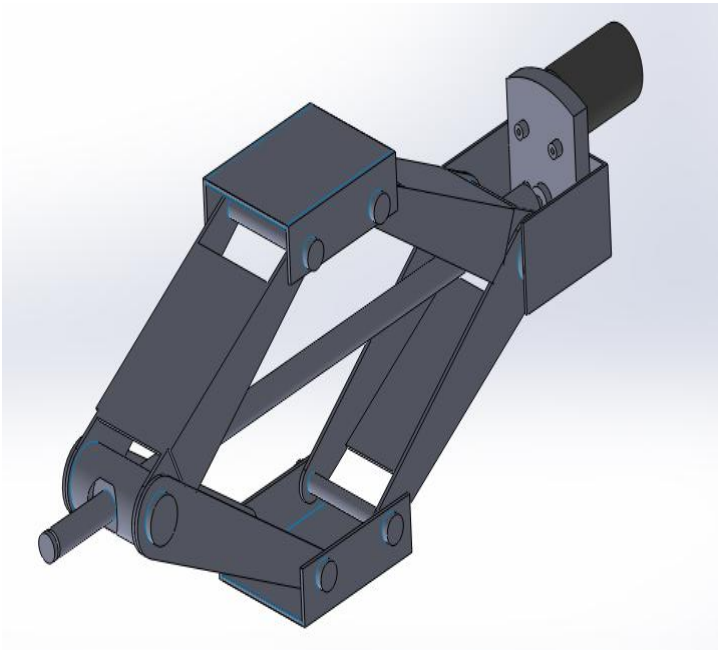

Figure: Isometric view

COMPONENTS

1. Scissor jack

A scissor jack is operated simply by turning a small crank that is inserted into one end of the scissor jack. This crank is usually "Z" shaped. The end fits into a ring hole mounted on the end of the screw, which is the object of force on the scissor jack. When this crank is turned, the screw turns, and this raises the jack. The screw acts like a gear mechanism. It has teeth (the screw thread), which turn and move the two arms, producing work. Just by turning this screw thread, the

ISBN: 979-88-35073-61-0

scissor jack can lift a vehicle that is several thousand pounds.

Fig 2: Scissor jack

2. 12V DC Geared motor

- Geared motors are a very high torque motors.
- Gear box is built to handle the stall torque produced by the motor.
- Uniformity of part

Specifications:

- Motor type selected: 12V DC Geared motor
- Operating voltage: 12V DC
- Rated current: ≤4800ma
- Shaft length: 27mm
- Shaft diameter: 8mm

Fig 3: 12V DC geared motor

3. Nut and bolt

Fig 3: Nut and bolt

A nut is a type of fastener with a threaded hole. Nuts are almost always used in conjunction with a mating bolt to fasten two or more parts together. The two partners are kept together by a combination of their threads friction (with slight elastic deformation), a slight stretching of the bolt, and compression of the parts to be held together.

4. Motor controller

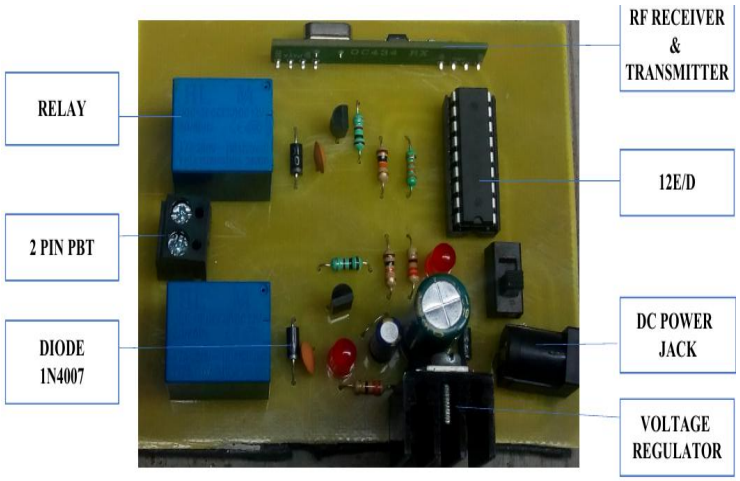

Fig 4: Motor controller

5. Remote

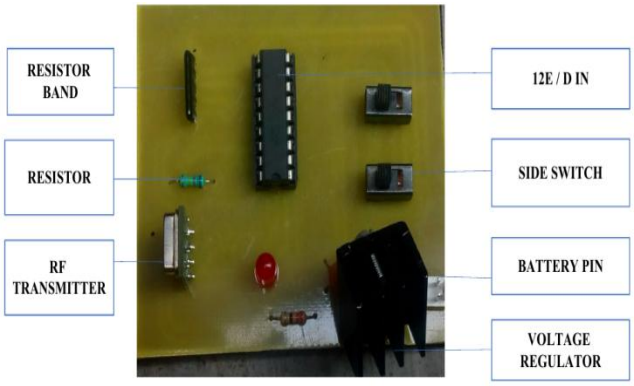

Fig 5 remote control

ISBN: 979-88-35073-61-0

6. Assembly of Motorized scissor jack

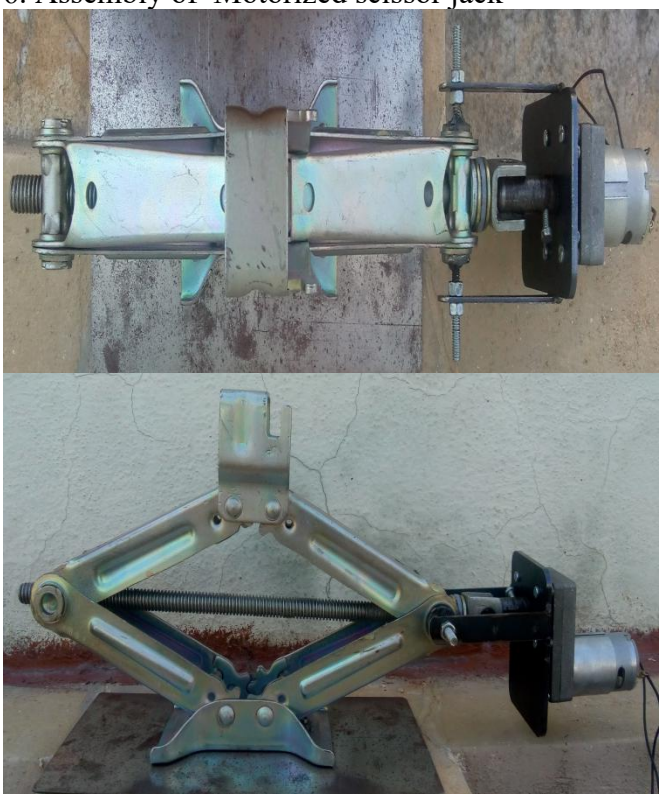

Fig 6: Assembly

7. Construction & working:

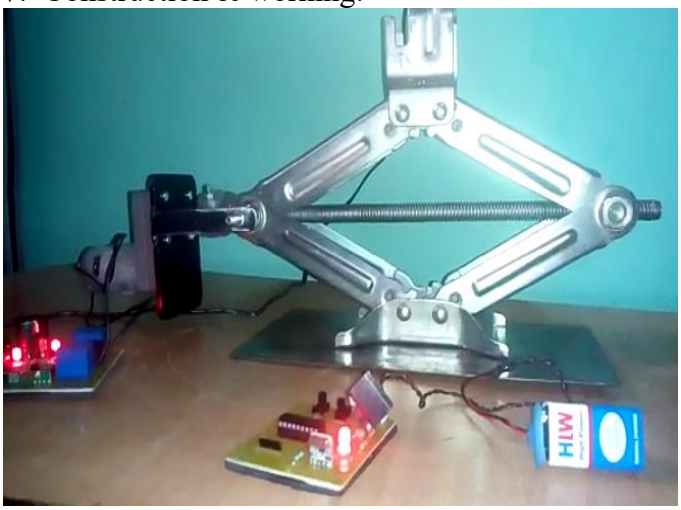

Fig 7: Construction of motorized scissor jack

STEP 1: The 12V Adopter is used to drive the D.C motor. The D.C motor shaft is connected to the screw through coupling. If power is driven to the D.C motor, it will run so that the screw also runs and converts rotary to translatory motion. The arms of jack move upwards, so that the vehicle lifts from the ground. The vehicle is lifted by using the lifting platform at the top of the jack. The motor draws power supply from the electricity. The lifting and uplifting is done by changing the supply to the motor controller.

STEP 2: After pressing the switch, power from motor controller is transferred to the motor that is connected to the screw. Now the screw starts moving. Now controlling the switch in remote.

STEP 3: Now pressing the switch, the circuit is completed and voltage from the adapter is pass to the motor controller. When tapping the switch to the positive pole, positive voltage is supplied to the DC motor moves in clockwise direction and lead screw moves in downward direction.

STEP 4: When tapping the switch to the negative pole, negative voltage is supplied to the DC motor moves in anticlockwise direction and lead screw moves in upward direction. In this way the directions of motor can be controlled which in turns regulate the lift load direction either upward or downward as per the requirements.

V. CONCLUSION

Our proposed design is similar to common SCISSOR designs in some aspects, but also advantageous in others. It can safely raise a load of 800kg to the required heights with relative ease on the user. The features of our design are lifting the required load without human effort by using 12V DC supply, to lift the heavy vehicles and making easy manufacturing. Unique to our design, however, is the manufacturability of our design, which is much simpler.

Since only z-shapes are utilized, bulk material can be more efficiently purchased and used. Also, less machining is required since there are no complex sleeves for the power screw. Only simple attachments which can be welded on are proposed. Therefore, when compared to similar scissor jack designs that perform equally as well, our proposed design is recommended for its easy handling, manufacturability and lower cost. We recommend that this design will very useful at the time of tyre puncture and absence of cleaner without any human effort. It can be easily operated by ladies and handicapped. If this project is developed to high load carrying capacity, the heavy vehicles can be lift with less effort.

ISBN: 979-88-35073-61-0

VI. SCOPE OF FUTURE WORK

In this section, further areas of improvement and enhancement points that can be looked upon to make the product more attractive in the market were suggested.

- ✓ As a development the web part of the arms can be replaced by stiffening ribs to reduce the overall weight .
- ✓ The top and base plates can be made fold able to make the unit more compact.
- ✓ Permanently mounted jacks on the vehicle can be developed so that tire change can be completely automated.

ACKNOWLEDGMENT

We would like to express our sincere gratitude to the Management, Dr. H Ramakrishna, Principal of Sapthagiri College of Engineering, Bengaluru for the facilities provided and their support. Also we would like to thank Dr. P Mahadevaswamy the Head of department, Mechanical Engineering and faculties for their encouragement and support. We would also like to thank our guide Mr. Mohan A. E, Assistant Professor, Mechanical Engineering, for his support and coordination in completing this project.

REFERENCE

- ✓ http://powerjacks.com/about-us/powerjacks-what-we-do.php
- ✓ Powerjack.com/downloads/Design%20 Guides/PJLMPT-02/S1-Screw-Jacks PJLNIPIDG-02.pdf
- ✓ Rajput, R.K, (2007), ―A Textbook of Manufacturing Technology‖,
- ✓ Laxmi Publications,1st Edition, 899pp. ISBN: 978 –81 – 318 – 244 – http://en.wikipedia.org/wiki/Jackscrew
- ✓ Academia...u/6167889/Modification_of_the_ Existing_Design_of_a_Car_ jack.
- ✓ http://ww.ijceronline.com/papers/Vol 14_issue07/Version-1/A0470101011.pdf
- ✓ Design and fabrication of motorized automated object lifting jack; IOSRJEN.ISSN(e):2250-3021.
- ✓ IOSR Journal of Engineering (IOSRJEN) www.iosrjen.org, ISSN (e): 2250-3021, ISSN(p): 2278-8719, VoL 04, Issue 07 (July. 2014), and IIVI II PP 15 28

ISBN: 979-88-35073-61-0

MULTIPURPOSE VEHICLE USING COMPUTER VISION

Mr. Mohan AE
Asst. Professor
Dept. of Mechanical engineering
Sapthagiri college of engineering
Bangalore, India
mohan@sapthagiri.edu.in

Mr. Rahul K R
student
Dept. of Mechanical engineering
Sapthagiri college of engineering
Bangalore, India
rahulkr2606@gmail.com

Mr. Sandeep Gowda BS
Student
Dept. of Mechanical engineering
Sapthagiri college of engineering
Bangalore, India
sandeepgowda9742@gmail.com

Mr. Bharath kumar S R
Student
Dept. of Mechanical engineering
Sapthagiri college of engineering
Bangalore, India

Mr. Rajath Gowda HR
Student
Dept. of Mechanical engineering
Sapthagiri college of engineering
Bangalore, India
rajathgowda467@gmail.com

***Abstract* — This paper illustrates the description about the complete design and working of a multipurpose vehicle which is used to detect landmines using a metal detector and computer vision. The lifecycle of landmines are forever. Unless and until someone finds out where these dangerous mines have been planted rest of the society is in danger.**

Landmines are the most used common traps that are setup to mainly harm the enemy, but innocent individuals fall into this trap and suffer casualties. Many individuals get in danger of working on the front lines to detect such mines .So in order to ensure the safety of the personal this vehicle has been designed. This system can be implemented at any location at any time since it works wirelessly and is battery powered. The techniques described in this paper are having their own merits and demerits, but all of these are discussed below.

Keywords—Arduino Uno, handheld metal detector, L298 motor driver module, Lithium polymer battery, HC-05 Bluetooth module, camera module .

I. INTRODUCTION

Many countries in the deepest parts of Africa suffer from the problem of landmines. During the current war between Ukraine and Russia landmines have been planted by both parties to which the innocent public gets affected. In the early and current days landmines are setup and covered in such a way that the enemy would not be able to spot it. This is a problem that a lot of local people are currently facing. The guardian news agency estimates that an average of five – six people die due to landmines in Nigeria.

Keeping the cost point of view and the technology basics used, the locals do not have to depend upon the government to develop and provide these technologies. Rather they can use the same materials described in the paper which is available on the market to assemble it by themselves. Currently metal detectors are available but neither of them are wireless. These systems have been developed also to avoid the casualties of landmine personal and ensure their safety too.

II. PROBLEM STATEMENT

Detection of landmines can be made using a metal detector, but the problem of these machines are that none of them are portable rather they are handheld where in which the person who is operating these machines comes in close contact with these landmines and can fall prey. A mistake can also be made by the operator may ultimately lead to injuries or death.

The United Nations claims that there were around 7000 casualties who suffered major injuries because of landmines and 2800 victims died. This data is usually made from the areas monitored nearly highly conflictive and dangerous war zones But if we consider the local people who have suffered the number is estimated to grow even more even though more donation has been received. This clearly states that basic technology use and locals volunteering are the best way to eradicate this problem, so that their communities and societies can be safe and protected.

III. OBJECTIVES

The main objective of this paper is to develop technologies in making the metal detection more cost effective, affordable and safe as possible. Keeping the safety factor in mind the following vehicle has been designed to work wirelessly and provide the accurate reading output as possible.

To make this project fully functional and encourage researchers to develop new solutions using these technologies certain goals has to be met:-

1. Ideally the built metal detection vehicle must have a very low ground pressure so that it will not be able to trigger the landmine.
2. Maneuverability is also a technical programmable challenge. The robot has to designed and programmed in such a way that it can rotate left and right by its own axis.
3. Use technologies like Arduino, computer vision etc. which already has a major source or community of developers who may volunteer to openly help so that they can make the model more efficient.
4. Must be able to detect mechanically pressure sensitive landmines which are usually made up of metal casing.
5. Make the technology hardware and software open-source so that the community can actively decide and update the software including hardware as well.
6. To make use of CPVC pipes as they are much cheaper and cost effective rather compared to traditional materials such as aluminium or iron.

IV. LITERATURE SURVEY

1. Wouter van Verre et al. stated in his article about defining ways in which metallic objects can be found out in the soil with a method called magnetic induction spectroscopy.
2. Ross N. Gillanders et al. implemented a new way of searching landmines. He defined that a honeybee based bio hybrid system is the best approach for splitting up the land area. This means that the landmines will be assessed based on breaking down the given landmark

into a honey bee based hexagonal structure and covering these areas proportionately.

3. Hany kasban et al. has introduced a system where in which he has outlined the different types of landmines that are in use. He also discusses about the different methods that are used to detect landmines such as ground penetrating radar, microwave radar, millimeter wave radar, LIDAR, optical detection, nuclear quadrupole resonance radar.
4. L.Silberbauer et al. defined in his article upon detecting landmines in different geographical conditions. This was achieved by designing a 6 wheel rover which had the ability to operate on steep hills as well.

V. METHODOLOGY

To drive the multipurpose vehicle we will be using direct current motor. The motor will be powered by a lithium polymer based battery. This metal detection vehicle will be controlled using Bluetooth through our smartphone.

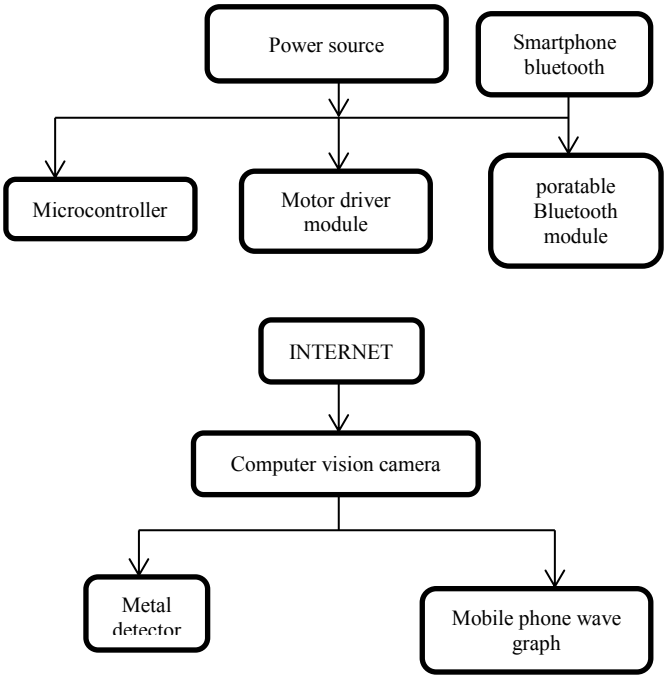

Fig 1 : Flowchart diagram of the multipurpose vehicle

VI. COMPONENTS

1. Smartphone controller :

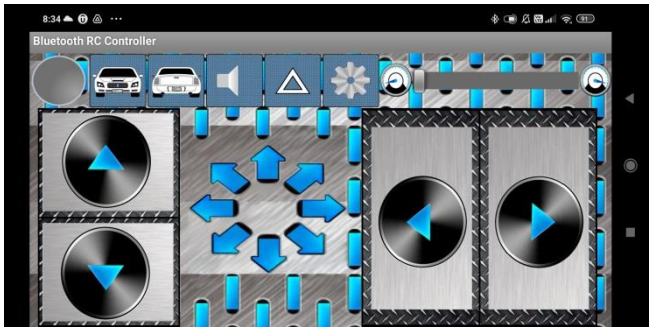

Fig 2 : Pic of the controller available on the smartphone app

The smartphone app send the signals to the Arduino via a Bluetooth module. The variable stored in each button is as shown :

DIRECTION	VARIABLE STORED
Forward	F
Reverse	B
Left	L
Right	R

2. Lithium polymer battery :

Fig 3 : Absd lithium polymer battery

Unlike other radio controlled cars this vehicle needs a power source which is why we are using a lithium polymer battery which is most suitable for these kinds of projects and is also rechargeable, portable and easily available.

We have used a 3 cell lithium polymer battery with an XT-60 connector and a 4 plug connector for recharging.

SPECIFICATIONS	RANGE
Discharge Voltage	11.1 V – 12.2 V
Discharge Current	2.2A
Storage capacity	2200maH
Charging current	3*700ma

3. Lithium polymer battery charger :

Fig 4 : Battery recharger

As the vehicle is being used the power gets discharged from the battery due to which it needs to be recharged. We are using the B3 pro battery recharger which works for both

SPECIFICATION	RANGE
Input voltage	110-240V, 50-60 Hz
Output current	700mA

2 cell and 3 cell batteries.

4. HC-05 Bluetooth module :

Fig 5 : HC-05 Bluetooth module

Vcc : It is mainly used to connect the Bluetooth module to the power source. In this project the power source is being drawn by Arduino 5 volt port.

GND : This is the ground pin of the module which is connected to the ground pin in the Arduino.

TXD : TXD is called as transmit serial data where in which it is used to wirelessly transmit out data serially .

RXD : RXD is called as Receive data serially which is used to receive the data.

5. Arduino Uno R3 :

Fig 6 : Arduino Uno R3

The Arduino is like the brain of this project which is used to direct the vehicle by receiving data from the Bluetooth module. The Arduino is mainly a controller which is open source software which uses the Arduino IDE to input the data. The programming language which is used is C++. The Arduino board receives power from the driver module.

The Arduino is also equipped with a self kill switch which means that any high supply of input energy would make the board to Turn OFF or cutoff automatically.

SPECIFICATIONS	RANGE OR DETAILS
Microcontroller	ATmega328P
Current time voltage	5V
Input operating voltage	7-12V
Direct current per I/O Pin	20mA
Direct current for 3.3V	50mA
In out limiting Voltage	6-20V

6. L298 Driver module :

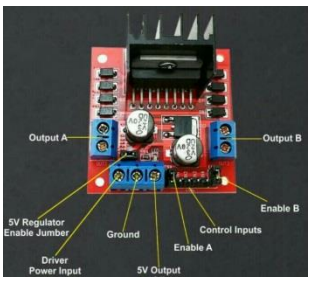

Fig 7 : L298 Driver module

The L298 Driver module is the heart of the vehicle. The main power source is from the lithium polymer battery. Left side motors are connected to output A and the right side motors are connected to output B. Heat sink is available to dissipate heat from the driver module

SPECIFICATIONS	RANGE
DC motor output max. voltage	46V
DC motor output max current	2A
Logical operating voltage	5V
Logical operating current	0-36mA
Driver usage Voltage	5-35V
Driver usage Current	2A
Maximum Power	25W

7. Direct Current Motor :

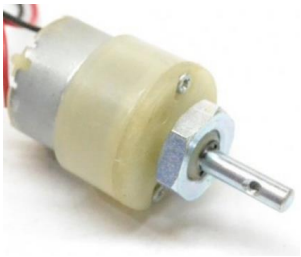

Fig 8 : DC motor

The motor used in this vehicle runs on DC current supplied from the L298 motor driver module. Motor works on the principle related to Electromagnetism where a current is passed through the coil which ultimately leads to the generation of electromagnetic field along the center of the coil which makes the armature to rotate. The RPM of the DC motor can be controlled by regulating the output voltage of the armature.

SPECIFICATIONS	RANGE
Operating input voltage	9V
Operating input current	0.9A
RPM	50

8. Chlorinated polyvinyl chloride :pipes :

Fig 9 : CPVC pipes

The main reason that these pipes are used in this project is because of the fact that a low ground pressure energy had to be applied. If it was rather made from metals like aluminum etc. then there will be a creation of wrong readings during metal detection.

9. Multimeter :

Fig 10 : Mastech multimeter

The multimeter is used for the detection of magnetic landmines. Whenever the magnetic field comes in contact with the copper wire a necessary minimum voltage is recorder and identified by the multimeter.

10. Copper coil :

Fig 11 : winded up copper coil

The copper coil is winded up to have a nominal diameter of 160mm. The diameter of the copper coil used in 27 standard wire gauge which is near to 0.41mm. We have used enameled copper wire which has an extra layer of coating, so before we connect it to the multimeter that extra layer of coating at the end must be scraped.

VII. WORKING

1. Electrical connectivity :

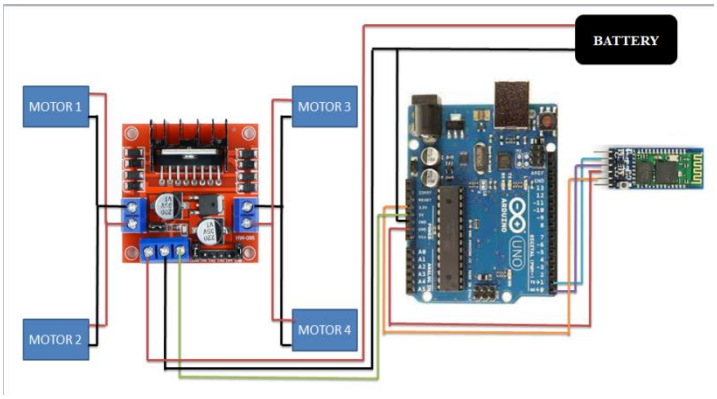

Fig 12 : Electrical connection

The above diagram shows the electrical connectivity between the Arduino, L298 driver module and the HC-05 Bluetooth module.

2. Mechanical structure :

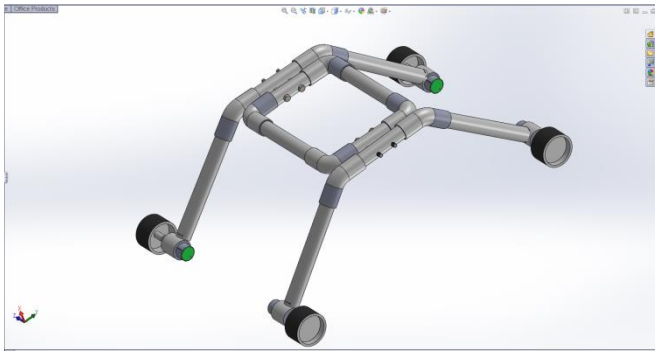

Fig 13 : 3D CAD model of the mechanical structure.

The mechanical structure is mainly made up of CPVC pipes because the entire structure should possess a low ground pressure. Also the detection variation in detecting metals can also be altered if the structure was made up of metal alloys such as aluminium etc.

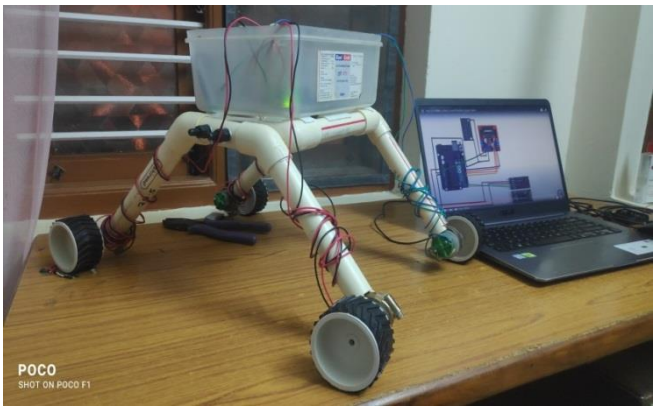

Fig 14 : Actual mechanical structure of the Bluetooth operated vehicle .

3. Detection of magnetic mines :

Anti tank Landmines are usually made up of magnets. They are made up of magnets because whenever a heavy duty vehicle comes near this mine the magnetic pressure plate gets automatically triggered due to the presence of metals.

Fig 15 : The german made Hafthohlladung is a anti tank mine made up of magnetic components

TEST 1: Strong magnet

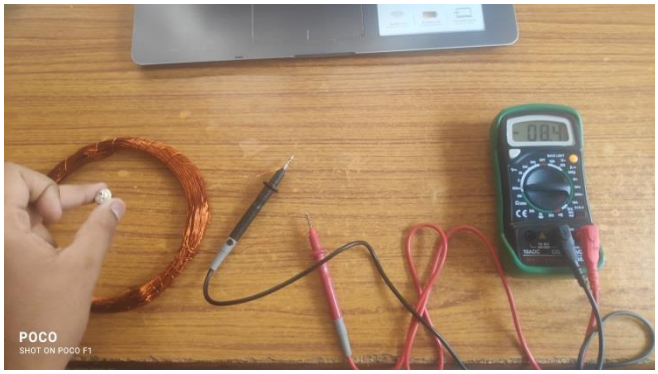

Fig 16: testing a strong magnet

In this test we wanted to know the voltage generated by the strong magnet. The maximum voltage generated was 8.4mV.

TEST 2 : Weak Fridge magnet

Fig 17: Testing a weak magnet

In this test we wanted to know the voltage generated by the weak fridge magnet. The multimeter showed negative reading which means the Voltage generated is less than mV.

Explanation:

Whenever a magnet comes near a circular copper coil the magnetic field of the magnet comes in contact with the copper wire. Due to this fact electrical eddy current gets generated. The generated voltage is measured by the multimeter.

4. Detection of metal mines :

Anti-personnel mines are usually made up of metal box like structure which has a pressure spring type mechanism or a pressure sensor type mechanism . They are mainly used to target individual enemies.

Fig 18 : Yugoslavian made PROM 1 anti personnel mine made out of metallic components

Fig 19 : Soviet made PMN 2 anti-personnel land mine.

TEST 1 : Screw driver

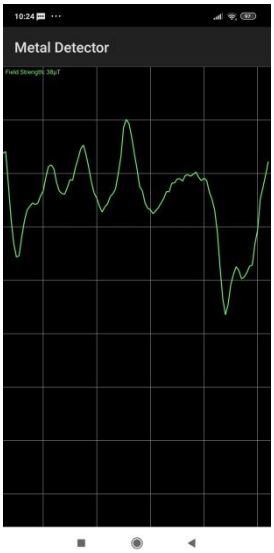

Fig 20 : Screenshot of the variations in the app plotted against field strength vs time

Explanation:

The smartphone application utilizes the built in magnetometer which is mainly used for compass application but it can also cause deflection when it is bought near a metal.

The changes in the initial and the final reading are plotted through a graph with field strength n the Y axis and time on the X axis.

VIII. COMPUTER VISION

The people operating in such dangerous areas must always keep a lookout for the people who are around them. So computer vision helps in detecting people automatically in daylight.

During night since many of these areas are under developed there will not be any streetlight for the camera to see. During these situations computer vision becomes a lot helpful which utilizes minimum light as much as possible. As there will be a change in the pixels gradient it can easily identify such patterns.

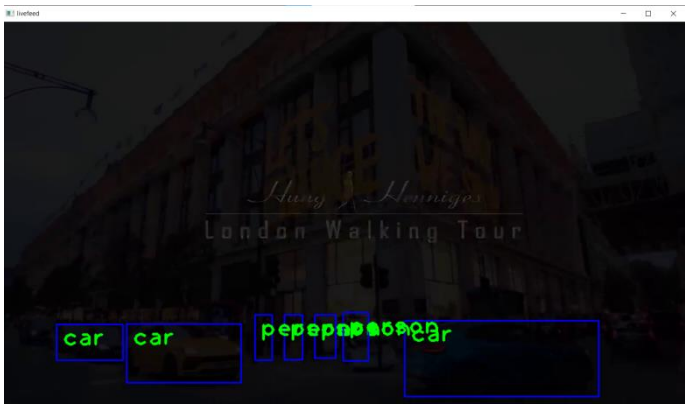

Fig 21 : Computer vision applied to a recorded dark video.

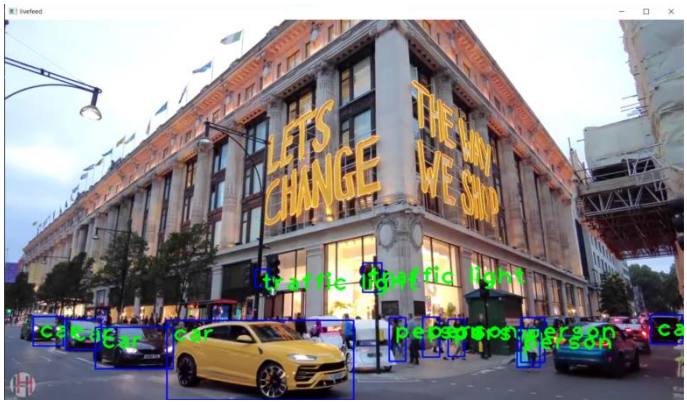

Fig 22 : Computer vision applied to the same recorded bright video.

Programming language used	Python
Libraries	Open CV numpy
Datasets used	Coco names
IDE used	Jet Brains Pycharm

Explanation:

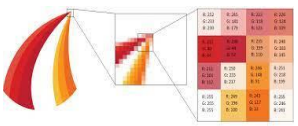

Fig 23 : Pixel breakdown

Computer vision works on the main principle of breaking down the given image into data sets. Each pixel will be assigned an Individual data point where in which the program is specifically built to produce significant output by comparing the input image with these datasets.

Computer Vision is also used in construction sites to monitor the safety of the workers automatically by the computer. So we hope that it can also warn the operator if any person enters the field or area. Computer vision can be compared or trained like a human vision itself, keeping the source as open code would engage the community in developing the software according to their local needs and requirements

Actual Test :

Fig 24 : computer vision applied to the video nearby vivanta taj hotel near yeshwanthpur.

In the Fig 24 we can correctly see the accuracy of using computer vision. The software also detects the person who is peeping out of the KSRTC bus window.

IX. FUTURE WORK

1. Even though this vehicle can detect surface level landmines, there is still needed to a lot of work to be done in order to encourage and promote robotics in demining operations as well.

2. This vehicle is suitable for flat lands and deserted areas, but is not suitable in terrains or hilly regions. So further research must be done in improving the vehicle dynamics so that it can cross through all terrains. A robotic arm can also be developed to carry specific sensors needed to detect such landmines.

3. It is hard to detect mines which are purely made out of plastic. So further development must advance in the field of ground penetrating radar as well as x Ray scanners which might be helpful in such situations.

4. Low cost metal detectors which use RX and TX transmitters must also be developed keeping the cost point of view so that each individual or community who suffer from these problems can actually afford to buy it as well.

ISBN: 979-88-35073-61-0

X. CONCLUSION

It is possible to design and build a low cost multipurpose vehicle using common Internet of things platforms which is helpful in detecting landmines. The built vehicle can be used to detect both metal landmines and anti-tank magnetic mines as well.

XI. ACKNOWLEDGEMENT

We would like to express our sincere gratitude to the Management, Principal of Sapthagiri College of Engineering Bengaluru for the facilities provided and their support. Also, we would like to thank the Head of department Mechanical Engineering and faculties for their encouragement and support.

XII. REFERENCES:

1. Habib, M. K. (2007). Humanitarian Demining: Reality and the Challenge of Technology -The State of the Arts. International Journal of Advanced Robotics Systems (special issue on Robotics and Sensors for Humanitarian Demining), Vol. 4, No. 2, pp. 151-172
2. Kopacek, P. and Silber Bauer, L. (2008). Mechanical Design of a New Locomotion Concept for Humanitarian De-mining, The 7th IARP Workshop, Robotics and Mechanical assistance in Humanitarian De-mining and Similar risky interventions, HUDEM'2008, 28- 30 March, 2008, The American University in Cairo (AUC), Cairo, EGYPT.
3. Magyar, T. (2011). Evaluation and Optimization of an Intelligent Mobile Robot Designed for Landmine Detection. Ph.D. thesis, Vienna University of Technology.
4. Silber Bauer, L. (2008b). A new 6 wheeled robot for humanitarian demining. In: EURON/IARP International Workshop on Robotics for Risky Interventions and Surveillance of the Environment. Spain.
5. Mastny, W. (2010). Improvement of the mechanical construction of advanced mobile robots for Landmine detection. PhD. Thesis, Vienna University of Technology.

RETROFITTING OF ELECTRIC VEHICLE FOR A GEARED BIKE

Mr.Thejas MS
Asst. Professor Dept. of Mechanicalengineering Sapthagiri college of engineering Bangalore, India
Thejas@sapthagiri.edu.in

Mr.Puneeth Gowda S M
Student
Dept. of Mechanical engineering Sapthagiri college ofengineering Bangalore, India
gaudapuneeth@gmail.com

Mr.MD Shahid
Student
Dept. of Mechanical engineering
Sapthagiri college of engineering
Bangalore, India
shahidmukthi23@gmail.com

Mr. Sachin KT
Student
Dept. of Mechanical engineering
Sapthagiri college of engineering
Bangalore, India
Sachinsachi.kt@gmail.com

Mr. Supreeth Kumar K
Student
Dept. of Mechanical engineering
Sapthagiri college of engineering
Bangalore, India
supreethgowda1999@gmail.com

***Abstract* — Nowadays the non renewable energy sources are depleting at a rapid rate.Transportation industry must look at other possible energy sources which are also ecofriendly and as effective as non renewable energy sources. Due to this the world moves towards electric vehicle which are of lesser carbon footprint.Our attempt by taking up this project is to give the people who gave a great deal of a attachment towards traditional bikes the experiences in an electric vehicle.So inorder to deliver this the suitable thing to do is retrofitting an internal combustion engine bike with electric vehicle compnents like, BLDC motor(48V,750W),Controller, battery unit, etc .**

I. INTRODUCTION

Rising problems like pollution global warming enables more and more technological advancements. Depleting energy resources forces human kind move towards other energy resources.It is mainly affecting the modes of transportation so the world move towards electric vehicle.To tackle these problems this project is suitable. Retrofitting of a electric vehicle for geared motorbike means stripping out the mechanical components of an old 100cc motorbike like head, bore, piston,corburator,petrol tank,connecting rod,exhaust andreplacing it with electric vehicle compnents like, BLDC motor (48V,750W),Controller, battery unit, etc.the electric vehicle after being built should not be in anyway less than a traditional motorbike.the overall performance should turnout equal to any present day motorbike.There is no equivalent product available in the market.NO company is manufacturing electric motorbikes in indian market.We have electric scooters only which are not preferred by most of the people. Secondly there is no electric motorbike which as great performance in terms of power,pickup,efficiency, speed and smooth ride.thus it is very suitable for the present conditions .Gearbox is utilized from the orginal motorbike. The electric motor is mounted upon the disassembled engine . A sprocket is welded or mechanicaly fixed to the crankshaft then the electric motor is connected by a chain . Basically gearbox works same as in the orginal motorbike . The gears are utilized for better power and speed .

II. PROBLEM STATEMENT

In the current situations in the world there are 2 major reasons that are causing the problems for the mankind. Firstly, the global warming which is caused by the combustibles used in wide range, and secondly the emission releasing from the automobiles even for the shortest distances. Due to these there is an immense reduction in the fuel quantity great effect on the environment. As the population is been gradually increasing in India, it has become the one of the most pollutant country in the world. In the major areas 72% of the pollution is been observed only from vehicles. And there are many bikes and vehicles are being purchased every day. Energy to drive Electric Bike. This bike can be driven with the help of electricity or also with the help of solar energy. Therefore the manufacturing of the vehicles for human is one of greatest need to survive on earth. As there is increase in the IC engine bikes, due to which there are various problems arises like traffic jam in urban cities where temperature sensibly rises in current situations. The heavy and bulk IC engines take more space which may be difficult to pick and place from one place to another. We are dependent on the conventional engine systems till now, it's time to change to non-conventional energy systems which are un-exhausted and cause no pollution and environment friendly.

III. OBJECTIVES

- To find out the awareness of consumer about the electric bikes.
- To find out the reason why consumer prefers to electric bike.
- To find out the factor influencing the sales of electric bike.
- To know the users perception about electric bikes
- To reduce the manufacturing cost of petrol bike by converting it into an electric one.
- To accelerate the efficiency of the bike and reduction of rate/km.
- To reduce the pollution and global warming.
- To Increase the range per charge of the electrical vehicle.
- To use lower battery capacity and give best range.
- To give the rider the same feeling as driving the IC engine powered vehicle.
- To implement run time charging by using dynamometer
- Nature friendly, cut back expenses, they are the future of transportation.

IV. LITERATURE SURVEY

The main aim of this review paper is to present the idea of harnessing the various energy and use it in today's existence of human life. For human being travelling has become vital. In order to sustain in this fast forward world he must travel from place to place. It is very important that time taking for travelling should be less; also it should be economical and easily available. With the fast depleting resources of petrol and diesel, there is need to find intermittent choice. Taking all this into account, a shift away from conventional based fuels to using renewable sources of energy is a must. Electric bike which will be driven with the help of battery and thus provide required voltage to the motor. The focus of this report is to perform power calculations and system design of this

ISBN: 978-88-35073-51-0

such bike is indispensable. The paper presents a review propelled by double electric motor. This motor was so designed that it was attached with the crank set axle. Later in 1990's torque sensors and power controls were developed including some modified versions of bike with NiMH, NiCd and/or Li-ion batteries which offered lighter, density capacities batteries. But this bikes faced decrease in production when petrol and diesel resources came in existence [3][5][6][7]. Taking considerations of recent events of meager resources and facilities at their disposal, over increasing traffic, snags problem of parking and the need to make automobile a more environmental friendly, designers of vehicles are back with a view to hit upon a novel concept that completely alter the conventional design. The paper presents a review on Portable Electric Bike (PEB). This was first developed in 1890's in US and those were documented within various US patents. On 31st Dec, 1895 Ogden Bolton designed a battery powered cycle. He designed using 6 pole brush and commuter DC hub motor connected to the rear wheel. He was then granted a US patent. Couple of years later, Hosea W. Libbeyss invented electric bike which was propelled by double electric motor

V. Block Diagram

The diagram shows the parts and the connection between them so it can be easily identified. The parts are as follows: • Battery • Motor • Controller • Shaft drive • Throttle • Charger

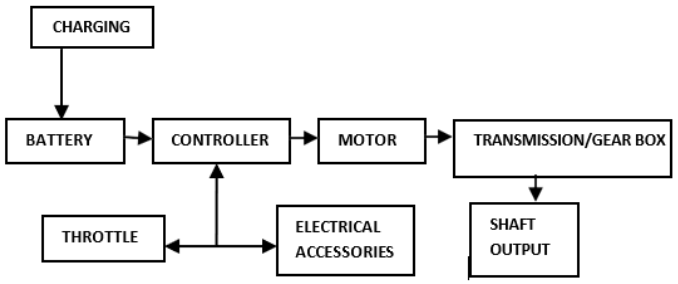

Fig:1 Block diagram

VI. COMPONENTS OF E-BIKE battery

2.1 48V/20 AH Battery A lithium-ion battery, sometimes known as a Li-ion battery, is a rechargeable battery type. Lithium-ion batteries are widely used in portable electronics and electric vehicles, and their use in military and aerospace applications is growing.

1. THE MOTOR

is 750watt having capacity with maximum 3100rpm. Its specifications are as follows Specifications: • Rated Voltage: 48 Volt DC. • Rated Power: 750W. • Base motor RPM: 3100RPM. • No Load Speed: 600 RPM. • Rated Torque: 90Kg-cm. • No load current: 2.8A • Rated Current: 15.6A. • Motor Weight: 7.80 kg. • Gear Ratio: 1:6

2. TRANSMISSION

A transmission is a machine in a power transmission system, which provides controlled application of the power. Often the term transmission refers simply to the gearbox that uses gears and gear trains to provide speed and torque

3. The Controller

Controller which comes in a number of forms, allows you to regulate the electric assistance on your electric bike and is a crucial aspect of how they work. For convenience, the controller is mounted on the handlebar. Throttle-based controllers use a basic throttle mechanism to operate. The throttle will be either a thumb-press or a twist-grip style. To gain electric help with a throttle, simply pull back or press the throttle. Some electric bikes only require you to activate the throttle, allowing you to ride without pedaling. Electric bikes are, for the most part, simple to operate, ride, and maintain. In general, they require less maintenance than a regular bicycle.

4. Chain Drive

is a way of transmitting mechanical power from one place to another. It is often used to convey power to the wheels of a vehicle, particularly bicycles and motorcycles. It is also used in a wide variety of machines besides vehicles. Fig: 4 Chain Drive A chain-drive system uses one or more roller chains to transmit power from a differential to the rear axle. This system allowed for a great deal of vertical axle movement (for example, over bumps), and was simpler to design and build than a rigid driveshaft in a workable suspension. Also, it had less unsprung weight at the rear wheels than the Hotchkiss drive, which would have had half the weight of the driveshaft, and differential to carry as well.

5.Throttle

The throttle mode is similar to how a motorcycle operates. When the throttle is engaged the motor provides power and propels you and the bike forward. The motor power can be increased or decreased by the restriction of current (by use of a throttle), but usually decreased. The term throttle has come to refer, informally, to any mechanism by which the power or speed of an engine or motor is regulated. A few e-bikes have a throttle, which may conjure visions of a motorcycle's twist grip, but in reality is usually just a small electric button. Pressing the throttle works just like depressing the gas pedal on your car no other action is required to accelerate or continue forward

VII. THEORY OF OPERATION

(A) AC Servo motor used for Position Mode mainly, also with Torque Mode & Velocity Mode have magnets on rotor as per designed poles of stator, for example if stator has 8 poles winding, the rotor will have 8 magnets on its rotor. Here high frequency pulse is injected in the stator, i.e. in 2 phases out of 3 phase winding, to from + & - on the stator. This gives magnets fitted on the rotor a starting push, the position of stator winding is achieved by (3 hall sensors) encoder fitted on non drive end of rotor, the servo motor, which is driven by a servo drive detects the positioning of rotor and accordingly gives pulse in all two phases out of three, where 1 phase is floating, i .e. if 'R' & 'Y' are given + & - pulse respectively 'B' is floating, if 'B' & 'Y' are given + & - pulse respectively 'R' is floating. Similarly in case of 'B' & 'R' given + & - pulse respectively 'Y' is floating. See Figure-5. The position of 3 phases is sensed by Hall Effect sensors, which gives position of stator winding excitement with pulse, which is sensed by Hall Effect sensors fitted at 120 degree, i.e. each at 60 degree from another. 8 poles motor will have weight small magnets fitted on dice to pass through (over) these sensors to give signal to panel for injecting pulse, i.e. supply. (B) The above motor is also called BRUSH LESS DC (BLDC) / AC SERVO MOTOR in technical terminology because commutation of this is taken care by encoder as designed in AC Servo motors because 3 phase AC winding given on stator is also called 3 phase AC servo motor & because commutation is achieved by encoder. Therefore it is also called BRUSH LESS DC (BLDC) / AC SERVO MOTORS.

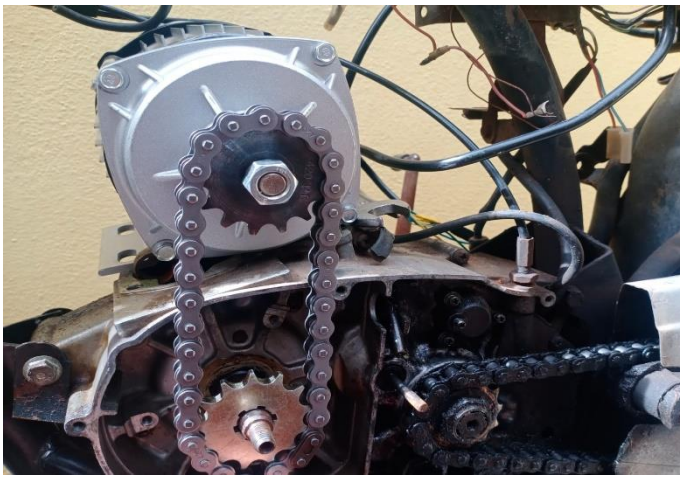

VIII. WORKING

The present study comprised of two separate procedures; firstly, the data for the operating conditions of the electric two-wheelers were collected by conducting primary surveys among the vehicle owners with formatted questionnaires. The daily travel data have been recorded from the available odometers, over a month. The energy consumption data were also provided by the owners and were also estimated from the battery capacity. A daily pattern of utilization of electric two-wheelers was thus obtained. Secondly, the real time performance of an electric two-wheeler was studied as a part of the experiment, for obtaining the energy consumption data and the performance characteristics with the present traffic conditions. The experiment has been conducted based on a low speed electric two-wheeler available in the market. The data from the electric two-wheeler study has been analyzed to obtain its pattern of energy consumption at different loading conditions, its performance in present day traffic and to check the suitability with different traffic conditions. Working

IX. Future Possibilities

This thesis is in a way defining e-bikes, trying to analyze the basic functions of various mechanisms which are available only in such e-bikes. Besides the aim is to highlight its importance in general, to promote the possibility for global Welfare, where Clean Climate plays a role. Having this basic purpose in place, it is also be said that this subject contains simple to advanced features containing all three departments, therefore very useful Thesis for Bachelor level students, just because in e-bikes all three variations of engineering is associated. Such as electronics in controller, mechanical in motor, and electrical in batteries. Therefore it can be a very resourceful work if it is possibly done using equipped labs, and

somehow by using the same level of possibilities in advanced simulation software to analyze e-bike's properties better. The study of ebikes can be done extensively, and it has been left for those interested researchers for exploring in depth of its possibilities in defining it

X. CONCLUSION

With the increasing consumption of nonrenewable resources such as petroleum and diesel, we are moving toward renewable sources such as solar, hydroelectric electricity, and batteries. There are different methods for conserving energy. One such mode of transportation is the electric bike; it is also a new mode of transportation that provides us with a convenient mode of transportation. It is also a new mode of transportation that provides us with a simple mode of transportation for people of all ages. It is a low-cost mode of transportation that everybody may afford. The motor in this bike is highly efficient, and the battery bank is light and fast. The electric bike's most important feature is that it does not use fossil fuels, which saves billions of dollars in foreign currency. The second most important feature is that it produces no pollution, is environmentally friendly, and operates quietly. The most viable solution for reducing environmental pollution is to ride an on-board electric bike. If there is an emergency, it can be charged using an AC converter.

ISBN: 979-88-35073-61-0

SMART LAWN TRIMMER RUN BY USING SOLAR POWER

Basavaraj G
Assistant Professor,
Department of Mechanical Engineering, Sapthagiri College of Engineering, Bangalore, India
ganiger2011@gmail.com

Prajwal S
Student
Department of Mechanical Engineering, Sapthagiri College of Engineering, Bangalore, India
prajwalvkn@gmail.com

Sandesh R
Student
Department of Mechanical Engineering, Sapthagiri College of Engineering, Bangalore, India
sande7h@gmail.com

Sanjayprasad R P
Student
Department of Mechanical Engineering, Sapthagiri College of Engineering, Bangalore, India
rpsanjayprasad@gmail.com

Yashwanth B G
Student
Department of Mechanical Engineering, Sapthagiri College of Engineering, Bangalore, India
yash.bg.496@gmail.com

***Abstract*: The sun is the major source of energy for life on earth used for heat and lighting. Nowadays, solar energy has been known as a renewable energy and an alternative energy to that of fossil fuel. This paper introduces a new development of lawn mower, named as Smart lawn trimmer, by using solar irradiance as a primary energy source with the presence of a solar panel. This grass cutter prototype is developed to reduce air pollutant and improve the current design specifically the blade based on the previous studies. With current technology, this new prototype is designed as remotely controlled grass cutter using Arduino UNO. Smartphone is used as the remote controller. Therefore, it can be concluded that the prototype is reliable and environmentally friendly.**

Keywords: lawn trimmer, Arduino, Bluetooth, solar energy.

I. INTRODUCTION

The conventional grass cutters have been widely used recently by workers in the gardening and agricultural industries. However, the manual handled grass cutters are consuming a lot of energy and producing air pollution which can directly affect the workers' health. The conventional grass cutters are also creating a high level of noise and vibration which can cause serious health issues such as grip strength, decreased hand sensation and dexterity, finger blanching or 'white fingers' and carpal tunnel. In order to address these issues, a new design of a grass cutter machine has been proposed. This device can be fueled by solar energy and smartly controlled, which has been named as a Smart lawn trimmer that has three main systems which are smart control system, solar system, and the grass cutter. According to the national air space association (NASA), there is a 1.361 kW/m² of solar irradiance received at the top of Earth's atmosphere. Approximately 1.8/10MW amount of power from the sun has been interrupted by the planet Earth, which is thousands of times larger than the present global consumption rate of the energy. This has motivated the governments, researchers and power industries to increase their investments in the renewable energy industry aiming to utilize more this clean energy and relief the global warming. Many researchers have proposed new designs of autonomous and non-autonomous solar grass cutters. Moreover, a few fully automated designs using sensors to detect obstacles and avoid any harm or injuries have been also proposed. Patil S.M. et al. proposed a solar grass cutter called Smart Solar Grass Cutter with Lawn Coverage. The proposed design aimed to develop an automatic grass cutting machine that could be remotely controlled, and able to charge the used batteries while the solar powered grass cutter is operating during daytime. Dilip B.P. et al. used several sensors in their prototype design providing the proposed solar grass cutter the capability to avoid the unnecessary objects and/or obstacles in the field during operation. Asha N. et al. proposed a programmable robot that is able to work either autonomously or wirelessly using an Android Smart phone via Bluetooth from a safe distance. The grass cutter can cut the grass according to present shapes while the blade was able to be adjusted to maintain the different length of the grass. The robot is a dual powered with a Hybrid Solar panel and Lithium-Ion rechargeable battery. This programmable robot is used to decorate the lawn and encourage the implementation of the renewable energy resources. Ulhe P.P. et al. fabricated and modified the solar grass cutter that can be used to cut the different grasses with different applications. A remote-control unit was added to help the unskilled persons to operate it. The used battery in the designed grass cutter can be charged by using solar panels regardless of the operating conditions. An AC charging system and spiral cutting blades were used to increase the cutting efficiency. Amrutesh P. et al. designed a solar grass cutter by implementing a linear blade and Scotch Yoke mechanism. The cutter was coupled with PV panels installed at 45 degrees angle and Lithium-ion battery as the power supply. The used solar charger has automatically controlled the charging from the solar panels when it was required. However, the authors found that the Scotch Yoke mechanism did not produced the expected efficiency. Solar based automatic grass cutter was fully automated grass cutting robotic vehicle powered by solar energy introduced by Gaikwad Y.M. et al. The device was capable of fully automated grass cutting without the need of any human interaction.

The main objectives of this project are

i. Fabrication of lawn dresser, powered by solar energy and with the help of Bluetooth application.
ii. To reduce the dependency on conventional electrical energy.
iii. To reduce the cost lawn maintenance.

ISBN: 978-93-25073-61-0

II. EXPERIMENTAL DETAILS

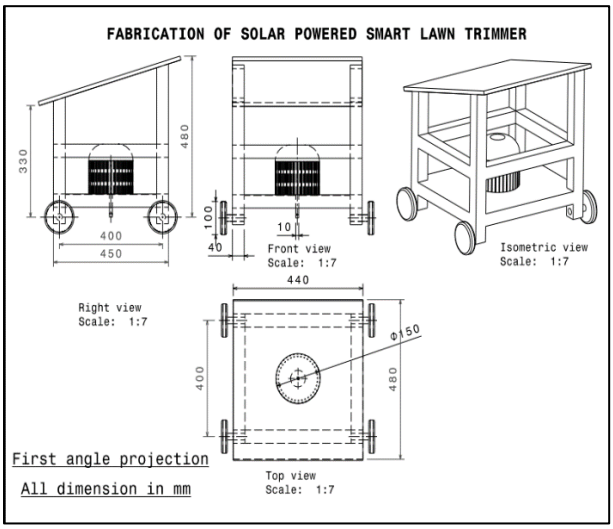

Fig. 1 conceptual design of smart lawn trimmer.

Fig. 2 Nylon wire as grass cutter.

This Smart lawn trimmer is a simple design which is optimizing the usage of materials. The overall dimensions are depending on the size or the dimensions of the solar panel. Three motors are used for rear tires and the blade. The height of the roof is depending on the height of the battery. The rubber rotating wheel is used as the front tires as it will automatically change the direction depending on the rear tires. One motor is implemented for each rear tire. The design is cost effective and compatible to the main objectives. Starting from the hand sketch, the prototype is designed in multidimensional using SolidWorks software. Dimensions of the design are very important and need to be accurate and precise to enhance the safety factor. Arduino microcontroller known as the brain of the prototype and PV panels are the main power supply. The PV panel supplied the absorbed energy to the battery through the solar charge controller. The solar charge controller protected the battery from overcharge as well as to maintain the battery performance. Bluetooth module will be used to connect the Smart Solar Grass Cutter with the smartphone. The grass cutter will be controlled by using the smartphone and the direction is depending on the requirement. The microcontroller will be programmed to ensure both motors at the rear wheels will be having the same speed when it is required. If the grass cutter is needed to move to the right direction, the left motor will be having a higher speed compared to the right motor and vice versa. From the hand sketching and digital design of Smart Solar Grass Cutter was created and shown in Figure 3. The Arduino Board, Bluetooth module and other electrical components are included in circuitry.

Two DC motors were used for rear wheels and the third motor was used for the blades. The front wheels are made of rotating rubber tires located below the main body. The selection of the used materials and components are very important to produce a reliable and effective design of smart solar grass cutter.

Table. 1 Dimensions of the Lawn Trimmer.

Part	Dimension (mm)&specification
Bottom frame	480 X 440
cutter motor	12V , 120W
battery	12V, 7.5AH
Solar panel	12V, 50W
Bluetooth module	HC-05 type

III. DISCUSSIONS

The technology assisted lawn trimmer operation has found satisfactory and effective. The ease of operation has become more, compared to conventional one. The design and fabrication of a solar-powered grass trimmer that is environmentally friendly, produces less noise and affordable was achieved. Also, by the usage of solar energy for this lawn trimmer functioning the dependency on the convention energy has reduced and maintenance cost can also be reduced. By this device the small scale industries and institutions can have lavish green, neat gardens using this smart trimmer. Therefore, it can be concluded that the developed design of the proposed Smart Solar Grass Cutter has achieved the main objectives and it can be further developed by industry

ACKNOWLEDGMENT

The authors would like to express gratitude to the management of Sapthagiri college of engineering, Bangalore for providing facilitation to carry out this work.

REFERENCES

[1]. T. Koppel, P. Tint, G. Karajeva, K. Reinhold, and S. Kalle, "Vibration and noise caused by lawn maintenance machines in association with risk to health," Agronomy Research, vol. 10, pp. 251-260, 01/01 2012.

[2]. R. C. Willson and A. V. Mordvinov, "Secular total solar irradiance trend during solar cycles 21–23," Geophysical Research Letters, vol. 30, no. 5, 2003,

[3]. .

[4]. R. V. Sanjana Arunesh, Shreyas Arunesh, Nivetha N., "Design and Implementation of Automatic Lawn Cutter," IJSTE - International Journal of Science Technology & Engineering, vol. 2, no. 11, 2016,

[5]. N. K. Santosh S.Gudi, P.B.Bhagawati, "Smart Solar Grass Cutter For Lawn Coverage," International Journal of Innovative Science and Research Technology, vol. 2, no. 5, 2017, doi: https://www.scribd.com/document/347922063/Smart-Solar-GrassCutter-for-Lawn-Coverage.

[6]. B. P. Prof. S.M.Patil, Kumbhar Snehal, Patil Dhanashri, "Smart Solar Grass Cutter With Lawn Coverage," International Research Journal of Engineering and Technology (IRJET), vol. 5, no. 3, 2018,

[7]. B. P. Dilip, N. B. P. , V. S. U. , S. W. , and P. S. M. , "Design and Implementation of Automatic Solar Grass Cutter," International Journal of Advanced Research in Electrical, Electronics and Instrumentation Engineering, vol. 6, no. 4, 2017,

[8]. M. J. S. Asha N, Saraswathi R, Rahul R, Ravikiran, "Smart Grass Cutter," Perspectives in Communication, Embedded-Systems and Signal-Processing (PiCES), vol. 1, no. 6, 2017.

[9]. F. D. W. Praful P. Ulhe, Manish D. Inwate, Krushnkumar S. Dhakte, "Modification of Solar Grass Cutting Machine," IJIRST –International Journal for Innovative Research in Science & Technology, vol. 2, no. 11, 2016.

[10]. O. A. Tanimola, Diabana, P. D, Bankole, Y. O., "Design and Development of a Solar Powered Lawn Mower," International Journal of Scientific & Engineering Research, vol. 5, no. 6, 2014.

[11]. H. B. Vuthaluru, V. K. Pareek, and R. Vuthaluru, "Multiphase flow simulation of a simplified coal pulveriser," Fuel Processing Technology, vol. 86, no. 11, pp. 1195-1205, 2005/07/25/ 2005.

ISBN: 979-88-35073-61-0

Smart Umbrella for Car

CHETHAN S[1], HALEMBRE AMBIKA[2], JEEVITH ARVIND[3], MANJUSHREE K[4], Dr. P MAHADEVASWAMY[5]

Student[1234], Professor & HOD[5], Dept. OF Mechanical Engineering, Sapthagiri College of Engineering
#14/5 Chikkasandra, Hesaraghatta main road, Bangalore- 560057 India

[1]chethanshetty2001@gmail.com
[2]ambika.ratnapurkar@gmail.com
[3]jeevitharvind75@gmail.com
[4]manjushreek72@gmail.com
[5]hodmech@sapthagiri.edu.in

***Abstract* – In today's world, cars are playing a vital role in everyone's life. Most of the times, cars are parked in open or unshaded area and due to this, there is a worry about the car getting damaged by the sun rays and rain. Smart car umbrella can be an effective solution for the conventional car covers. It can be carried to any location and thus can provide shelter to the car. This helps in decreasing the temperature inside the car which gets heated up, thus provide comfort to the passengers. For structural parts the materials used are mild steel and cast iron, the mechanism used is scissor mechanism and lead screw mechanism. 3D modelling is created in Creo and Fusion360 software.**

Keywords: Automatic Car Umbrella, Scissor and Leadscrew mechanism, Creo software.

I. INTRODUCTION

Automobiles is a symbol of personal growth and development. They have become essential to the function of people in everyday life by using them for transportation from one point to another on daily basis. Today, there is a huge advancement in the technologies in automobiles.

Our personal vehicle is the major cause for global warming. When the cars are parked in an unshaded area in a hot sunny day, the sunlight penetrates the car in the form of thermal radiation through all the windows heating the car dashboard and seats. These thermal radiations are trapped inside the car cabin causing temperature increase inside the car.

For example, a dark dashboard or seat can easily reach temperature in the range of 180 to more than 200ºF. These objects heat the adjacent air by conduction and convection and also given off long wave radiation which is every efficient at warming the air trapped inside the car. The temperature inside a vehicle rises significantly with the majority of the temperature rise occurring within first 15-30 minutes.

Hence, a smart umbrella for car with an automatic mechanism which opens and closes by itself with a button is an effective solution. This smart umbrella protects the car parked in an unshaded area from harmful effects of sun's radiation, acid rain, bird droppings, dust and dirt.

A. A. Konde(1) et. al. (2020) Design and analysis of the umbrella links was done. The mechanism used was scissor mechanism.

Saad Bin Abul Kashem(2) et. al. (2017) Constructed automatic device on vehicle to prevent heat penetration inside the car body. Their system will prevent any vehicle from getting affected by heat produced by the solar energy.

Issam Mohammed Ali Aljubury(3) et. al. (2015) investigated the effects of solar radiation on car cabin components (dashboard, steering wheel, seat, and inside air). The test vehicle was oriented to face south to ensure maximum (thermal) unload on the front windscreen. Six different parking conditions were investigated. A suggested car cover was examined experimentally.

II. OBJECTIVES

- To select the proper mechanism for satisfactory working of smart umbrella for car.
- To select the good covering sheet material which can resist rainfall and heat.
- To implement an automatic feature that the umbrella will open and close automatically with just a tap.
- To select the material for links and lead screw.
- To carry out 3D modelling in Creo and Fusion 360.

III. METHODOLOGY

- Methodology involves modelling using Creo and Fusion 360 CAD software, design and

fabrication of smart car umbrella has been carried out.

- Reading and analysing the various research papers and journal papers has been done with respect to our work, so as to understand the previous work done.
- Various calculations relating to drag force, pressure of the wind, area of the umbrella links and the total load acting on them was calculated.
- A conceptual design was made using Creo and Fusion360 by considering the dimensions and 2D model was also drafted.
- Components were selected based on the calculations done and also selecting most economical based on the quality of the components.
- Fabrication of the body was done based on conceptual model and considering the preliminary calculation.
- Testing of the functioning of different components present in system was carried out. The functioning of the smart umbrella was checked to meet the objectives of the smart umbrella.

IV. DESIGN CALCULATIONS

The calculations are carried out by considering the dimensions of the link as shown in table 1.

TABLE I. DIMENSIONS OF LINK

Dimensions	
Length	600 mm
Breadth	19mm
Thickness	3mm
Material	Mild steel

1. Area of each link (a)

a = (600)*(3) = 1800
∴ a = 1800 mm2
As there are 32 links used,
∴ Area of 32 links = (1800) * (32)
= 57600 mm^2

2. Drag force (F_D)

It is calculated using the formula,
$F_D=1/2\ \rho CAv^2$
Where,
C is the drag coefficient = 2.1 (for rectangular body)
A is the area of the object facing the wind = 0.595 m^2
ρ is the density of the air = 1.2 kg/m3
v is the velocity of speed = 40mph (assumed)
=17.88 m/s
(∵ 1mph = 0.477m/s)

F_D = (1/ 2) * (1.2) * (2.1) * (0.595) * (17.88^2)
∴ F_D = 239.67 N

3. Wind pressure (P)

It is calculated using the formula,
P = F_D /A
= (239.67) / (0.595) = 402.8
= 402.8 N/m2
∴ P = 402.8 Pa

4. Total load acting on links (F)

It is calculated using the formula,
F = A*P
= (402.8) * (0.0576)
∴ F = 23.20 N
∴ Load acting on each link = (23.20) / (32)
= 0.725 N.

5. Degree of freedom (DOF)

It is calculated using the formula,
DOF = 3(n-1) – 2j – h
where,
n - number of links
j – number of binary joints
h – number of higher pairs

DOF = 3(10 -1) – 2(13) - 0
= 27 – 26
=1

V. 3D MODELS

The models of the umbrella component design are prepared using CREO software. The models of smart car umbrella are shown in below figures.

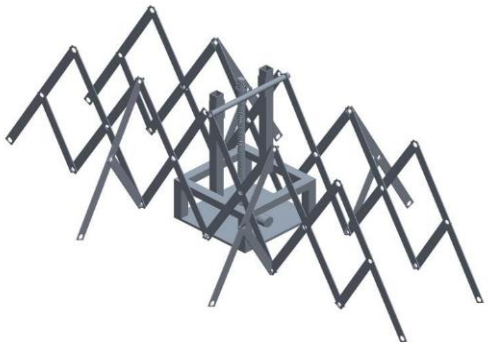

Figure 1. Isometric view

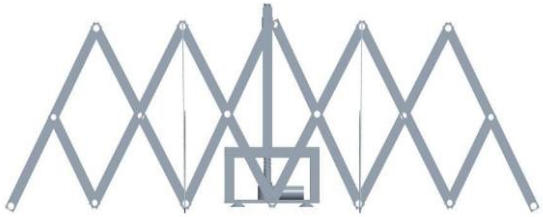

Figure 2. Front View

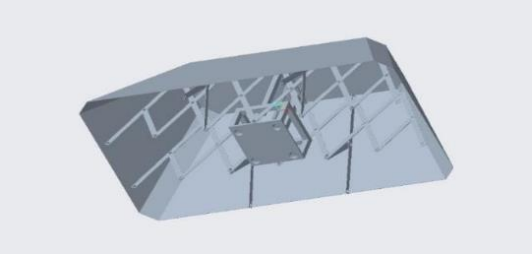

Figure 3. Isometric view with canopy

VI. COMPONENTS USED

1) WORM GEAR MOTORS

Worm Gear Motors are used to generate high torque in a small package size. They are mainly used for applications that require a self- locking or breaking feature since the output shaft can't rotate when there's no power applied. In addition to this, their heads can transfer motion in 90 degrees. They have high reduction ratio and avoids the need for unnecessary gears.

Figure 1. Worm gear motor

2) ESP8266

The ESP8266 Wi-Fi Module is a self-contained system on chip with integrated TCP/IP protocol stack which gives any microcontroller access to Wi-Fi network. It is capable of either hosting an application or offloading all Wi-Fi networking functions from another application processor. It uses the Lua scripting language. It is a 32-bit RISC microprocessor core based on the Tensilica Xtensa Diamond Standard 106Micro running at 80 MHz, with a memory of 32 KiB instruction RAM, 32 KiB instruction cache RAM, 80 KiB user-data RAM and 16 KiB ETS system-data RAM.

Figure 2. ESP8266

3) LEAD SCREW

A lead screw is a screw used as a linkage in a machine to translate turning motion into linear motion. It is also called as translation screw or power screw. It is mainly used in instrument grade applications where smooth, precise, clean, and maintenance free operation is required.

Figure 3. Lead screw

4) LINKS

A stretcher is attached to the ribs of the umbrella. Its function is to stretch out the canopy when the umbrella is being opened.

Figure 4. Links

5) COVERING MATERIAL

Polypropylene non-woven fabric material is used which has high heat reflection capacity. This fabric is breathable and prevents mould or dust from becoming trapped against the surface of your car, while keeping moisture out. This material covers are water-resistant, meaning they will protect your car from rain and other small amounts of moisture like dew. Polypropylene also protects against UV rays, which can degrade the paint on your vehicle over time.

VII. WORKING OF SMART UMBRELLA

In the smart umbrella, scissor mechanism is used where the links are in a Criss cross i.e., X pattern. 8 links are attached in X pattern at one side. Therefore, 32 links are been used in total. Starting end of the links pattern is connected to the shaft. The shaft is connected to one end of the lead screw such that the shaft can make linear motion; and another end is fixed to the worm gear motor which is grounded to the base. As the shaft moves, the assembled links make scissor mechanism. To control the opening and closing of the umbrella, ESP8266 is used. The power supply is provided directly from car. The model for open position is carried out in Fusion 360 for better view as shown in the below figures.Open postion with a maximum angle and closed with minimum angle between the two links.

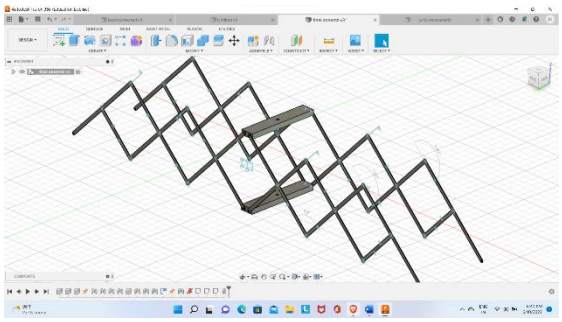

Figure 4. open position of the umbrella

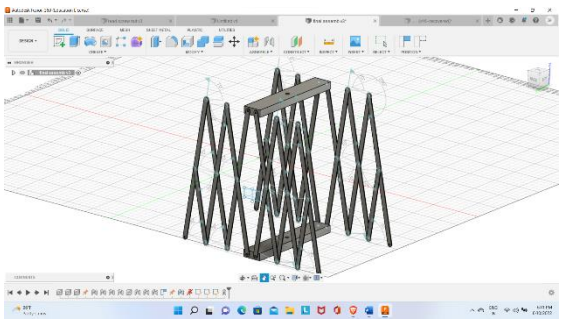

Figure 5. closed position of the umbrella

VIII. CONCLUSION

We have fabricated a smart umbrella for a car at affordable price. A smart umbrella for car with an automatic opening and closing mechanism with just a tap is an effective and alternative solution to conventional car cover. It helps in protecting the environmental effects of sun rays, rain, bird dropping, dirt and dust onto the car by covering it entirely on the top surface. As the technology has advanced, there is a possibility of making varieties of car covering shelters.

IX. ACKNOWLEDGEMENT

We would like to express our sincere gratitude to the Management, Principal of Sapthagiri College of Engineering, Bengaluru for the facilities provided and their support. Also, we would like to thank the Head of the Department of Mechanical Engineering and faculties for their encouragement and support.

X. REFERENCES

1) A. A. Konde, A. B. Bhane, Dr. A. D. Desai “Design and analysis of an innovative umbrella for car”, IJRSET Vol 02, July 2020.
2) Saad Bin Abul Kashem, Aws Dhafir Yasin & Elammaran Jayamani, “Autonomous vehicle sunshade” Vol 5, Issue-4, April-2017.
3) Issam Mohammad Ali Aljubury, Ammar A. Farhan, Muther A. Mussa “Experimental study of interior temperature distribution inside automobile cabin”, ResearchGate, Vol 21, Mar 2015.

Spectroscopic studies of Eu^{3+} doped B_2O_3–PbO–Ag_2O Glasses

Gnanendra D S
Department of Physics
Sapthagiri College of Engineering
Bangalore–560057, India
gnanendrads@sapthagiri.edu.in

Keshavamurthy K *
Department of Physics
Vivekananda Institute of Technology
Bangalore–560074, India
keshav.m85@gmail.com

***Abstract*— Europium (Eu^{3+}) doped lead borate glasses have been successfully prepared by the conventional melt quenching method. Their structural studies and luminescence properties were carried out using transmittance, excitation, and emission spectra. The investigation of FTIR spectra shows the presence of boron atoms in both BO_3 and BO_4 units in the glass network. Also found that the presence of new structural groups such as Boroxyl rings, pyro, and Dipent-Borate. Photoluminescence (PL) spectroscopy was used to examine down-conversion (DC) emission under 394nm excitation exhibits five emission bands centered at 577nm, 590nm, 612nm, 650nm, and 697nm corresponding to $^5D_0$-$^7F_0$, $^5D_0$-$^7F_1$, $^5D_0$-$^7F_2$, $^5D_0$-$^7F_3$ and $^5D_0$-$^7F_4$ transitions of Eu^{3+} ions, respectively and also recorded emission spectra at 306nm and 296nm, both the excitations exhibit two emission bands centered at 590nm and 612nm corresponding to $^5D_0$-$^7F_1$ and $^5D_0$-$^7F_2$ transitions of Eu^{3+} ions.**

Keywords*— Silver Lead borate; FTIR; Photoluminescence.

I. INTRODUCTION

Rare-earth doped glasses are superior materials for solid-state laser, optical amplifiers, display, and photo-electronic devices [1]–[3]. Among the other rare-earth (RE) ions, trivalent europium is due to the narrow emission band, producing almost monochromatic light and a long radiative lifetime [4]. This kind of glass is widely used as efficient red phosphors in mainly designing mercury-fluorescent lamps and plasma displays. Silver-containing glasses have been technologically interesting materials for solid-state batteries and electrochemical devices due to their valuable optical properties and high ionic conductivity value [5], [6]. Lead borate glasses are of research interest due to their structural peculiarities. The addition of PbO into the borate network brings modification of boroxol rings and formation of complex groups with one or two 4 coordinated boron atoms [7]. Lead borate glasses have several applications, including radiation shields and optical and thermal properties [8].

In the present work, we report the structural studies and luminescence properties of europium doped lead borate glasses through Fourier Transformer Infrared (FTIR) spectroscopy and Photoluminescence (PL).

* Corresponding author Tel.:+91 903 530 3005
Email address: keshav.m85@gmail.com

II. EXPERIMENTAL

The raw materials of reagent grade chemicals H_3BO_3, PbO, Ag_2O, and Eu_2O_3 were used to synthesize the samples by the conventional melt quenching method. The glass with the composition of $70B_2O_3$–29PbO–29PbO–(1-x)Ag_2O–xEu_2O_3 (x = 0.5 mol%) was taken in a porcelain crucible and placed in a furnace set temperature at 1100ºC for 2 hrs and stirring several times to ensure complete melting and homogeneity for the prepared glass. The homogeneous molten liquid was cast into a brass mold and quickly pressed with another mold. The prepared sample was immediately transferred to another muffle furnace set at 150ºC for 1hr to remove thermal stress and strain. The prepared sample was cut into appropriate dimensions for the required measurement.

The FTIR spectra of powdered glass were recorded at room temperature by Nicolet spectrometer with a resolution of 0.2 cm^{-1} in the frequency range 400 – 4000 cm^{-1} using the standard KBr pellet method. The excitation and fluorescence spectra were recorded using F-2700 FL Spectrophotometer with a xenon flash lamp as the source.

III. RESULT AND DISSCUSSION

A. FTIR studies

The FTIR spectra of the glass system as depicted in figure 1, and their assignments of the bands are presented in table 1. The broad composite band extending from 3200–3600 cm^{-1} is attributed to the hydroxyl (OH) or water group [9]. The broad water bands have divided into:

- Peak 2700–3000 cm^{-1} — originating from hydrogen bonding;
- Peak 3200–3500 cm^{-1} — originating from molecular water; and
- Peak 3600–3750 cm^{-1} — originating from OH-groups.

In figure 1, it can be seen that robust broadband appeared at 1292 cm^{-1} is attributed to B–O asymmetric stretching of trigonal BO_3 unit, and the shoulder at 1234 cm^{-1} may rise from B–O stretching vibrations of $(BO^3)^{3-}$ units in metaborates, pyroborates and orthoborates [10]. Similarly, the band at 1004 cm^{-1} is due to the vibration of some boron atoms attached to

ISBN: 979-88-35073-61-0

non-bridging oxygen in the form of BO_4 units [11]. The absorption of around 1000 cm^{-1} is attributed to the formation of diborate in the glass system. The band at 993 cm^{-1} in the spectra may be assigned to the stretching vibration of the B–O–Pb linkage. The band at 710 cm^{-1} is assigned to bond bending vibrations of B–O–B linkages of the boron–oxygen network [9]. The absorption band at 692 cm^{-1} is assumed to be due to the combined vibration of BO_4 and PbO_4 groups, and the band around 699 cm-1 indicates that oxygen bridges two trigonal boron atoms. The spectral domain 400-760 cm^{-1} is dominated by the band centered at 670 cm^{-1} and is attributed to Pb–O bond vibrations and O–B–O bond bending vibrations [8]. No characteristic vibration of modes of bonds from Eu_2O_3 and Ag_2O oxides was detected in the FTIR spectra.

TABLE I. WAVE NUMBERS AND THEIR ASSIGNMENTS FOR FTIR SPECTRA OF GLASS.

Wave number (cm^{-1})	*Assignment*
3600–3750	OH–group
3200–3500	Molecular water
2700–3000	Hydrogen bonding
1292	B–O asymmetric stretching of trigonal BO_3 unit
1234	B–O stretching vibrations of $(BO^3)^{3-}$ units in metaborates, pyroborates, and orthoborates
993	Stretching vibration of B–O–Pb linkage
710	Bending vibrations of B–O–B linkages of the boron–oxygen network
670	Pb–O bond vibrations and O–B–O bond bending vibrations

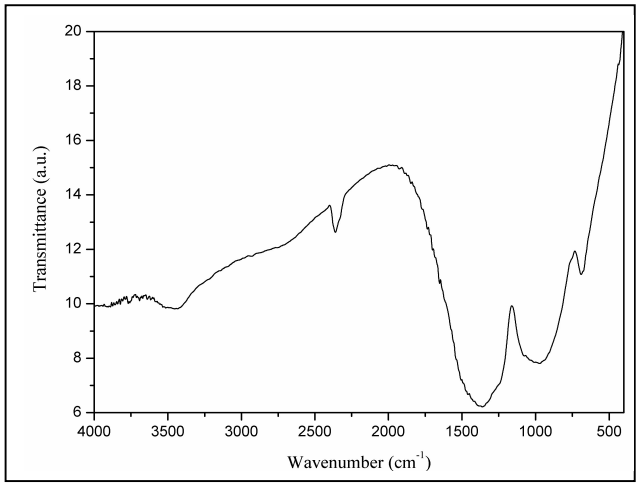

Fig. 1. FTIR spectra of the B_2O_3– PbO–Ag_2O–Eu_2O_3 glass system.

B. Photoluminescence studies

The downconversion (fluorescence) property of Eu^{3+} ions in silver-lead borate glass was examined. The excitation spectra of Eu^{3+} were monitored at λ_{em} = 590, and 612 nm of $^5D_0$-$^7F_1$ and $^5D_0$-$^7F_2$ transitions are depicted in figure 2. The spectral range from 200 to 600nm consists of sharp lines attributed to transitions between the 4f energy levels of Eu^{3+}. The excitation bands can be assigned to 362 nm ($^7F_0$-$^5D_4$), 381nm ($^7F_0$-$^5G_3$), 394 nm ($^7F_0$-$^5L_6$), 414 nm ($^7F_0$-$^5D_3$), 465 nm ($^7F_0$-$^5D_2$) and 533 nm ($^7F_0$-$^5D_1$). All the assigned transition values are in good agreement with excitation values of Eu3+ ions, as reported by many authors [12]–[14]. The excitation spectra show the strongest peak at 394 nm for Eu^{3+} and found peaks at 296 and 306 nm for λ_{em} = 590 nm and λ_{em} = 306 nm, respectively; there is a peak shift observed in the different emission values of Eu^{3+}. Thus, we consider 394, 306, and 206 nm ideal pump wavelengths to generate emissions from the prepared sample.

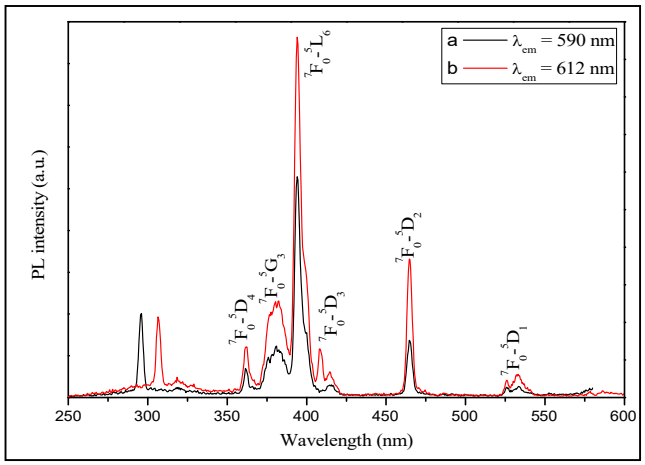

Fig. 2. Excitation spectra of Eu^{3+} glass were monitored at λ_{em} = 590 and 612 nm.

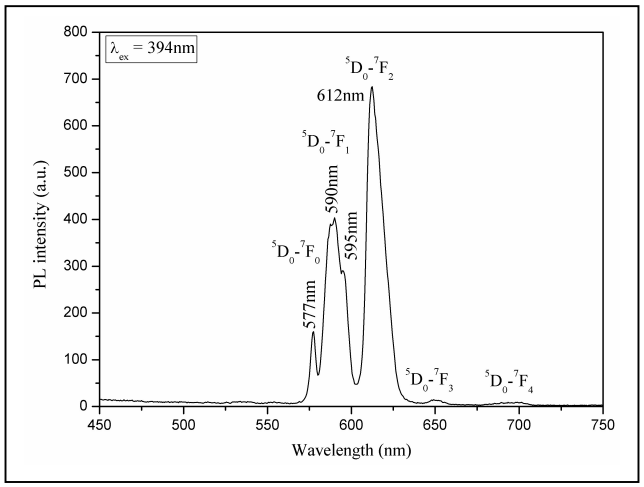

Fig. 3. Emission spectra of Eu^{3+} glass were monitored at λ_{ex} = 394 nm.

Figure 3 shows the emission spectra at λ_{ex} = 394 nm of Eu^{3+} ions in the glass. In glasses, due to the absence of a center of symmetry and long-range periodicity of atoms, an amalgamation of the 4f orbitals with opposite parity orbitals occurs. This rise in the electric dipole (ED) allowed transitions. The crystal field environment forces the $^5D_0$-$^7F_2$ emission transition in the vicinity of the Eu^{3+} ions. It is a hypersensitive (ΔJ=2) transition, and its intensity is very sensitive to the local environment. The $^5D_0$-$^7F_1$ emission

ISBN: 979-88-35073-61-0

transition (magnetic dipole, ΔJ=1) of Eu^{3+} ions is forbidden under selection rules and has intensity independent of the host environment. It is found that in figure 3, small, stark splitting (590 and 595 nm) depending upon the ligand fields being experienced by them and other emissions $^5D_0$-^7F_J (J=0, 3, and 4) are strictly forbidden and appear with low intensities [15]–[19]. The emission spectra at λ_{ex} = 394 for Eu^{3+} ions show a brightly red luminescent optical material.

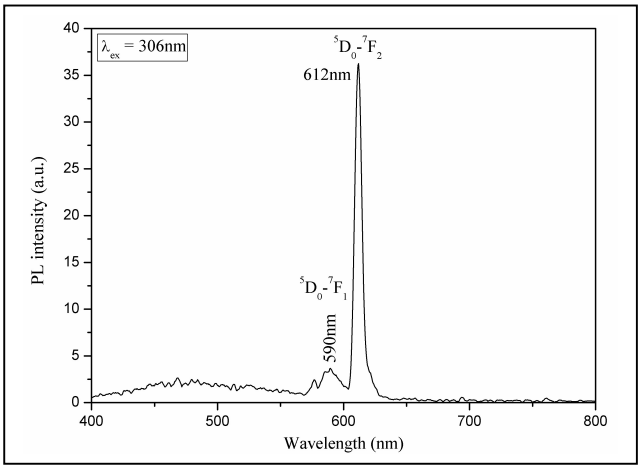

Fig. 4. Emission spectra of Eu3+ glass were monitored at λ_{ex} = 306 nm.

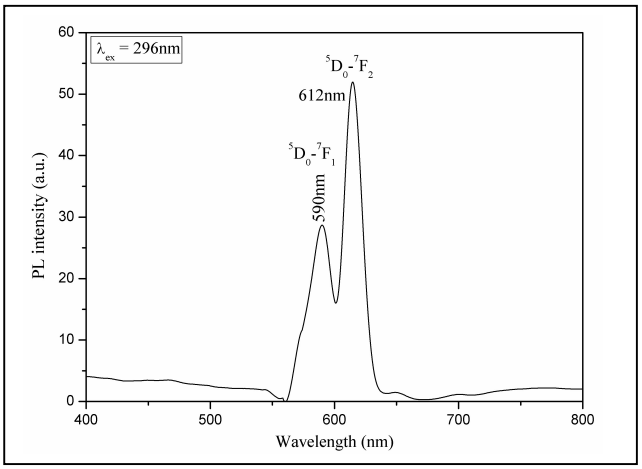

Fig. 5. Emission spectra of Eu3+ glass were monitored at λ_{ex} = 296 nm.

Figure 4 and 5 shows emission spectra at λ_{ex} = 306 and 305 nm of Eu^{3+} doped glass due to $^5D_0$-$^7F_1$ and $^5D_0$-$^7F_2$ transitions, respectively. In figure 4, it can be seen that intense emission is attributed to the $^5D_0$-$^7F_2$ transition (electric dipole) and observed that a shallow intense peak at 590 nm corresponds to the $^5D_0$-$^7F_1$ transition (magnetic dipole). Similarly, figure 5 shows the same trend but a slight increase in the intensity of the 590 nm peak. From the above discussion, we concluded that the excitation beam at 306 and 296 nm has also been suggested to be an ideal one to demonstrate europium glass as highly monochromatic light.

IV. Conclusions

The glasses of composition $70B_2O_3$–29PbO–29PbO–(1-x)Ag_2O–xEu_2O_3 (x = 0.5 mol%) have been prepared by conventional melt quenching method. The investigation of FTIR spectra revealed that in the glass matrix, various borate groups are randomly interconnected. The presence of boron atoms in both BO_3 trigonal units and BO_4 tetrahedral units with new structural groups like boroxol rings, pyro, and dipent-borate. The fluorescence spectrum of the glass system is found to be a brightly red luminescence peak. These glasses are widely used as efficient red phosphors and have several potential applications in photonic devices.

Acknowledgements

The authors would like to express their gratitude to the Management of Janatha Educational Society, Bengaluru–560055, Karnataka, India, for their unwavering support.

References

[1] Y. Z. Li, Q. Y. Zhang, D. M. Shi, Q. Qian, and S. H. Xu, "gallate – lead – bismuth – germanium glass by rare-earth co-doping," *Opt. Mater. (Amst).*, vol. 32, no. 2, pp. 334–338, 2009.

[2] G. N. Conti, "Rare-earth doped tungsten tellurite glasses and waveguides : fabrication and characterization," vol. 346, pp. 343–348, 2004.

[3] C. Bensalem, M. Mortier, D. Vivien, P. Gredin, G. Patriarche, and M. Diaf, "Thermal and Structural Characterization of Transparent Rare-Earth Doped Lead Fluoride Glass-Ceramics," vol. 2012, no. April, pp. 65–74, 2012.

[4] Y. Hatefi, N. Shahtahmasebi, A. Moghimi, and E. Attaran, "Frequency-conversion properties of Eu 3 + doped chlorophosphate glass ceramics containing CaCl 2 nanocrystals," *J. Lumin.*, vol. 131, no. 1, pp. 114–118, 2010.

[5] J. a. Jiménez, S. Lysenko, H. Liu, E. Fachini, and C. R. Cabrera, "Investigation of the influence of silver and tin on the luminescence of trivalent europium ions in glass," *J. Lumin.*, vol. 130, no. 1, pp. 163–167, Jan. 2010.

[6] V. Sharma, S. P. Singh, G. S. Mudahar, and K. S. Thind, "Synthesis and Optical Characterization of Silver Doped Sodium Borate Glasses," vol. 2012, no. October, pp. 133–137, 2012.

[7] S. Faculty, "Synthesis and characterization of cadmium doped lead – borate glasses," no. February 2006, pp. 55–58.

[8] L. Balachander, G. Ramadevudu, M. Shareefuddin, R. Sayanna, and Y. C. Venudhar, "IR analysis of borate glasses containing three alkali oxides," *ScienceAsia*, vol. 39, no. 3, p. 278, 2013.

[9] D. Singh, K. Singh, G. Singh, S. Mohan, M. Arora, and G. Sharma, "Optical and structural properties of ZnO–PbO–B 2 O 3 and ZnO–PbO–B 2 O 3 –SiO 2 glasses," *J. Phys. Condens. Matter*, vol. 20, no. 7, p. 075228, Feb. 2008.

[10] E. I. Kamitsos, G. D. Chryssikos, and M. A. Karakassides, "Investigation of the Cation-Site Interactions," no. 19, pp. 1067–1073, 1987.

[11] G. V. Mahavidyalaya, "Infrared spectra of zinc doped lead borate glasses," vol. 100, no. February 2002, pp. 75–78.

ISBN: 979-88-35073-61-0

[12] A. Kumar, D. K. Rai, and S. B. Rai, "Optical studies of Eu 3 + ions doped in tellurite glass," vol. 58, pp. 2115–2125, 2002.

[13] D. Hreniak, M. Jasiorski, K. Maruszewski, L. Kepinski, L. Krajczyk, J. Misiewicz, and W. Strek, "Nature and optical behaviour of heavily europium-doped silica glasses obtained by the sol–gel method," *J. Non. Cryst. Solids*, vol. 298, no. 2–3, pp. 146–152, Mar. 2002.

[14] Y. Hatefi, N. Shahtahmasebi, A. Moghimi, and E. Attaran, "Ultraviolet to visible frequency-conversion properties of rare earths doped glass ceramics," *J. Rare Earths*, vol. 29, no. 5, pp. 484–488.

[15] M. Dejneka, E. Snitzer, and R. E. Riman, "of Eu3 + in fluoride glasses," vol. 65, pp. 227–245, 1995.

[16] S. Arunkumar, K. Venkata Krishnaiah, and K. Marimuthu, "Structural and luminescence behavior of lead fluoroborate glasses containing Eu3+ ions," *Phys. B Condens. Matter*, vol. 416, pp. 88–100, May 2013.

[17] V. Venkatramu, D. Navarro-Urrios, P. Babu, C. K. Jayasankar, and V. Lavín, "Fluorescence line narrowing spectral studies of Eu3+-doped lead borate glass," *J. Non. Cryst. Solids*, vol. 351, no. 10–11, pp. 929–935, Apr. 2005.

[18] P. Babu, R. Vijaya, K. H. Jang, and H. Y. O. J. I. N. Seo, "Local structure of Eu 3 + ions in fluorophosphate laser glass," pp. 1005–1010.

[19] P. Babu, K. H. Jang, E. S. Kim, R. Vijaya, C. K. Jayasankar, V. Lavín, and H. J. Seo, "Local field dependent fluorescence properties of Eu3+ ions in a fluorometaphosphate laser glass," *J. Non. Cryst. Solids*, vol. 357, no. 10, pp. 2139–2147, May 2011.

ISBN: 979-88-35073-61-0

Structural, Physical and Optical Properties of Alkali Lead Boro Tellurite Glasses: Role of Eu^{3+} Ions on

C. Devaraja,
[1]Department of Physics, Sapthagiri College of Engineering, Bengaluru-560057, India
deva.drr@gmail.com

G.V. Jagadeesha Gowda[1],
Department of Physics, Sapthagiri College of Engineering, Bengaluru-560057, India.
Corresponding author:
jagadeeshagowdagv@gmail.com

Abstract

In this work, the consequences of doping europium ions in to alkali lead boro-tellurite glasses on physical, structural and optical properties are explored. By conventional melt quenching method the new set of glass were prepared. Structural properties were studied by XRD and Raman spectrometer. Variations in density were estimated by Archimedes principal and other physical properties such as molar volume, oxygen packing density, interionic distance, field strength, were estimated by applying suitable formulae. To analyse the optical properties of all prepared glass samples the absorption spectra were taken in UV-visible region in the wave length region 200-1100 nm. Optical properties like optical energy band gap and Urbach energy were determined by means of Davis-Mott method. By using estimated refractive index values, the corresponding molar refraction, molar polarizability, dielectric constant, reflection loss and metallization criterion of all prepared glass samples were measured by applying appropriate formulae.

1 Introduction

In recent research, the preparation and studies on structural, optical and physical properties of metal oxide glasses doped with rare earth ions have attracted attention of researchers due to their huge applications in the fields such as optical amplifiers, optical fibers, optical materials, waveguide lasers, sensors, displays, and optical data storage devices[1][2][3][4]. Tellurium dioxide is a better conditional glass former and tellurium based borate glasses have unique properties such as , low phonon energy and relatively high thermal stability, ease of production and high chemical durability, high thermal and chemical stability, reasonably low phonon energies, and excellent nonlinear-optical properties [5]–[8]. These remarkable features made tellurite glasses as potential materials for developing of photonic devices [9]. Over the decades researchers were using B_2O_3 due its excellent glass forming ability and remarkable structural variations when it is inserted in to alkali and alkaline earth cations and optical properties[10]–[14]. Lead oxide (PbO), if it is added to boro-tellurite network improves ability of glass forming property and decreases the crystallization rates [7], [15], [16]. Among the few lanthanide oxides, europium oxide is popularized as a explorer of the optical behaviour of the boro-tellurite glasses due to a very good fact that Eu^{3+} ions contains narrow band emission(4f6), high lifetime of optically active state and almost monochromatic nature [17]–[19]. Though some works have been done already, but not many details reported about effect of Eu^{3+} and PbO on optical and structural and physical properties of boro tellurite glasses[15], [17], [20].

In the current work authors reported synthesis of lead boro-tellurite glasses undoped and doped with Eu^{3+} ions and study of their optical, physical and structural properties.

2 Experimental details

Analytical grade chemicals such as H_2BO_3, TeO_2, PbO, Na_2CO_3 and Eu_2O_3 from sigma –Aldrich 99.9% purity have been used for the preparation of glass. Eu^{3+} ions undoped and doped alkali lead boro tellurite glasses with chemical composition 70-y (B_2O_3)-15TeO_2-5PbO-10Na_2O-yEu_2O_3 (where y=0, 0.1, 0.2, 0.3, 0.4, and 0.5 mol %) here onwards named as E0LBT, E1LBT, E2LBT, E3LBT, E4LBT and E5LBT, respectively, were prepared by following conventional melt quenching method. Investigated ELBT glasses are polished for characterizations. To know noncrystalline nature of prepared EBTE glass X-ray diffraction measurements were carried out with the help of Bruker D8 Focus X-ray diffractometer instrument which is having Cu Kα radiations of wavelength 1.54Å and operated at 40 kV. These measurements were carried out at room temperature in 2θ range of 10° - 80° and the diffracted X- rays intensities were recorded by a scintillation detector. Raman spectra of all prepared glass samples were carried in unpolarized mode with Peak Seekar Pro Raman spectrometer though exciting the samples with the laser source of wavelength 758 nm operated at 5-300 mW at room temperature by keeping laser spot as 100 micron and data was collected in RSIQ software with accumulation time as 5 seconds. Archimedes principle was involved to determine the density of the glass. For all polished glass pellets having thickness around 1.2 mm optical absorption spectra were recorded at room temperature with the aid of Perkin-Elmer Lambda-30 absorption spectrophotometer in the wave length region 200 nm to 1100 nm. With the help of absorption edge studies the optical properties were evaluated by using relent formulae.

3 Results and discussion

3.1 XRD and physical properties

The XRD patterns of Eu^{3+} ions doped alkali lead boro tellurite glasses shown in Fig. 1. From the diffraction patterns it is noticed that the presence of a broad diffused peaks scattering at lower angles and absence of Bragg peaks which greatly indicates the noncrystalline nature. The broad hump between 25°-30° of 2θ readings in figure 1 was observed for the ELBT glass, which is attributing of the glass structure. Density(ρ) of glasses was calculated by Archimedes principle (1) by taking toluene as an immersion liquid where ρ_t is refers density of toluene, w_a and w_t weight of the glass in air and in immersion liquid

$$\frac{\rho}{\rho_t} = \frac{w_a}{w_a - w_t} \quad (1)$$

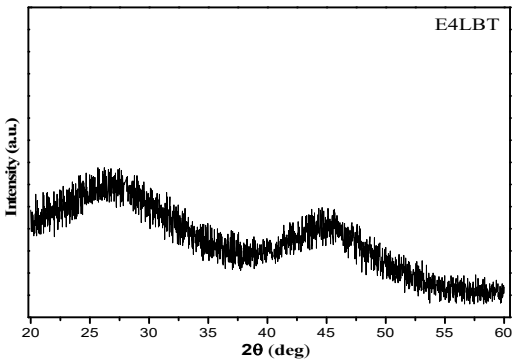

Fig. 1 Typical XRD pattern of E4LBT glass

Further, the corresponding molar volume (V_m) of all glasses was calculated by a mathematical relation $V_m = M_w / \rho$, where M_w indicates the molecular weight of glass.

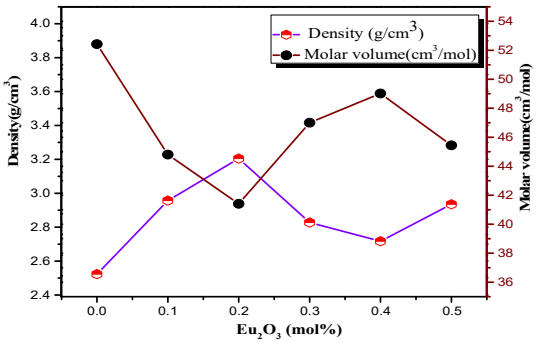

Fig. 2 Variation of density and molar volume with Eu_2O_3 concentration

With the addition of Eu_2O_3 in to glass network the structure of glass expected to modify and it can be analysed through mathematical equation i.e., average borate-borate distance. The highest value of d_{B-B} found as 5.242 Å for E0LBT glass due to less density and similarly lowest value found as 4.846 Å for E2LBT glass due to more density.

$$< d_{B-B} >= \left(\frac{V_m}{2N_A(1-X_B)}\right)^{1/3} \quad (2)$$

Where N_A indicates Avogadro's number and X_b is molar fraction of B_2O_3 in each glass.

Density is one of the useful constraints to investigate the structural modification in glass materials. Density and molar volume shows opposite nature. Density of the ELBT glass showed in Fig. 2 and it clearly shows that the ρ increased up to 0.2 mol% and shows considerable fall at 0.4 mol% and again increased at 0.5 mol%. This kind of trend is reported in previous work and there it is said that, the variations in the density are may be due to formation of non-bridging oxygen (NBOs) bonds. More is the formation NBOs less is the density and vice versa.

The oxygen packing density (OPD), rare earth (Eu^{3+}) ion concentration, field strength, polaron radius, and interionic concentration were calculated by using appropriate formulae[21][22]. It is noticed that, both interionic distance and polaron radius are decreases as Eu^{3+} ion concentration increase which indicates the improvement in Eu-O bond strength and this results as strong field strength around Eu^{3+} ions.

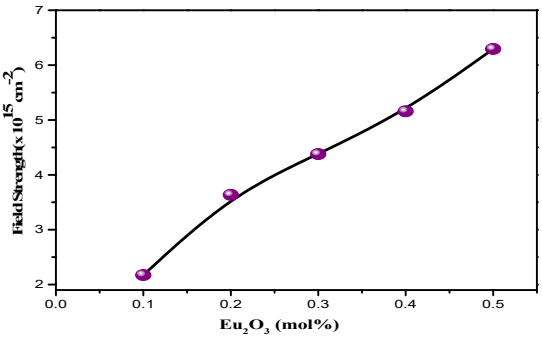

Fig. 3 Plot of field strength versus Eu_2O_3 concentration

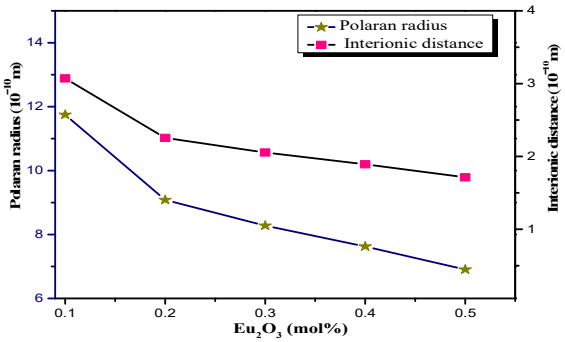

Fig. 4 Variation of polaron radius and interionic distance with Eu_2O_3 concentration

Fig. 4 shows variation of polaron radius and interionic distance with respect to Eu^{3+} ion concentration. OPD gives the idea about the organisation of oxygen atoms in the glasses. The highest OPD recorded for 0.2 mol% due to more density and less formation of NBOs. Determined all physical properties of ELBT glasses were tabulated in Table 1.

3.2 Raman spectra analysis

The Fig. 5 indicates the Raman spectra of ELBT glasses and it is noticed that spectra having considerable broadbands which are obtained may be due to overlie of one or more peaks. At ~431 cm^{-1} broad band represents the Te-O-Te bonds in stretching vibrations. Intensities of the peaks were observed as varying for glasses having Eu^{3+} ions concentrations more than 0.1 mol%. A tiny band at ~579 cm^{-1} of E2LBT glass implies the asymmetric vibrations of Te-O-Te bonds and a diffused a band at ~761 cm^{-1} is identified and it is ascribed as stretching vibrations of Te-O in TeO_3 triangular pyramid group as well as TeO_{3+1} polyhedra and this band is also attributed to symmetrical breathing vibrations in borate rings consists of six members of boron consists of one or more tetrahedra of BO_4 with one or more BO_4 tetrahedra. A more intensive band is recognised

exactly at ~681 cm^{-1} of a E4LBT glass which is attributed to antisymmetric vibrations in the linkages of Te-O-Te bonds originated by two dissimilar Te-O bonds and also it then leads to the little deformation in the TeO_4 trigonal bipyramid groups. The other small peak near ~921 cm^{-1} reveals the existence of ortho-borate in glass structure. The shoulders between 1250-1350 cm^{-1} was found in all prepared glasses which implies the presence of symmetric stretching vibrations of BO_3 triangular units in meta-borate, ortho-borate and pyro-borate units.

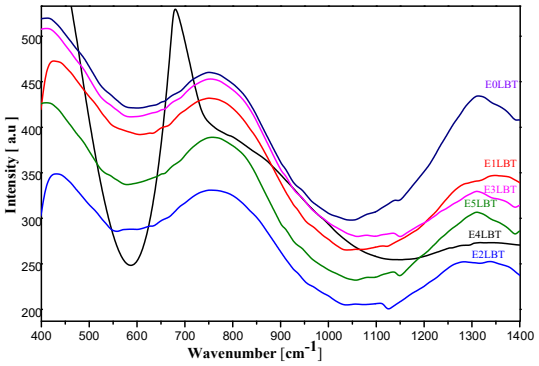

Fig. 5 Raman spectra of undoped and doped ELBT glasses.

Table 1 Average molecular weight (M_w), density (ρ) , molar volume (V_m), Borate – Borate separation (< d_{B-B}>), rare earth ion concentration (N_i), Inter ionic distance (R_i), Polaron radius (R_p), Field Strength (S) and Oxygen Packing Density (OPD) .

x mol%	M_w (g/mol)	ρ (g/cm^3)	V_m (cm^3)	$d_{<B-B>}$ (Å)	N_i x10^{19} (ions/cm^3)	R_i (nm)	R_p (Å)	S x$10^{14}cm^{-2}$	OPD (g-atom/l)
	± 0.01	± 0.001	± 0.001	± 0.001	± 0.001	± 0.001	± 0.001	± 0.001	±0.01
0	131.71	2.522	52.424	5.254	-	-	-	-	46.162
0.1	131.93	2.957	44.803	4.980	4.033	3.072	11.749	2.173	54.014
0.2	132.16	3.205	41.406	4.846	8.727	2.254	9.083	3.635	58.445
0.3	132.39	2.828	47.000	5.049	11.533	2.054	8.277	4.378	51.489
0.4	132.62	2.717	49.013	5.104	14.746	1.892	7.626	5.157	49.374
0.5	132.85	2.935	45.441	4.982	19.881	1.713	6.903	6.294	53.255

3.3 Optical properties

Absorption spectra of all Eu^{3+} ions doped ELBT glasses were showed in the Fig. 6. For better understanding, absorption spectra of E4LBT glass showed in the inset of Fig. 6. It consists of seven prominent and sharp peaks situated at 393,415,465,524,579, and 586 nm which are due to the electronic transitions of $^7F_0$-$^5L_6$, $^7F_1$-$^5D_3$, $^7F_0$-$^5D_2$, $^7F_0$-$^5D_1$, $^7F_1$-$^5D_1$, $^7F_0$-$^5D_0$ and $^7F_1$-$^5D_0$, respectively. For all glass samples, the absorption co-efficient i.e. α(ν) were measured near absorption edge at photon energies. It has been reported that, for direct and indirect band gap data well fits to an equation (3) proposed by Davis and Mott.

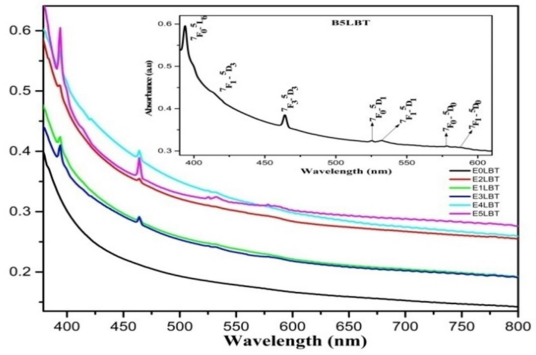

Fig.6 UV-visible absorption spectra of ELBT glasses and E5LBT glass (inset)

$$\alpha(h\vartheta) = \left(\frac{B}{h\vartheta}\right)\left(h\vartheta - E_{opt}\right)^m \qquad (3)$$

$$\alpha(\lambda) = 2.303\left[\frac{A}{d}\right] \quad (4)$$

Where A is the absorbance, d is the thickness of the ELBT glass samples and where m indicates an index that have values such as 2, ½, 3/2 and 3 corresponds to indirect allowed, direct allowed, direct forbidden and indirect forbidden respectively, B is a constant which indicates the band tailing parameter and hν is photon energy and E_{opt} is the optical energy band gap. The direct and indirect band gap energy values were found by the Tauc's plots and showed in the Figs. 7 and 8. Obtained direct and indirect band gap values were lies between 3.367 to 3.653 eV and 2.019 to 3.021 eV, respectively. The significant variations in the band gap values with the addition of Eu^{3+} ions into glass were noticed which mainly because of formation of NBOs. Urbach energy is the parameter which measures the disorderness in the both crystalline and noncrystalline materials. It can be measured by a relation (5) and by taking the reciprocal of the slope at linear region of curves in plot of ln(α) versus hν and it shown in Fig. 9.

Table 2. Optical direct band gap - $E_{g(d)}$(eV), Indirect bad gap - $E_{g(ind)}$(eV), Urbach energy - ΔE (eV), Steepness parameter - (S), Molar refraction - R_m(cm^3/mol), Refractive index - (n), Dielectric constant - (ε), Electronic molar polarizability - α_m (10^{-29}), reflection loss R_L(%) and metallization criterion (M)

x (mol%)	$E_{g(d)}$ ± 0.001	$E_{g(ind)}$ ± 0.001	ΔE ± 0.001	S ± 0.0001	R_m ± 0.001	n ± 0.001	$\mathscr{E}$ ± 0.001	R_L ± 0.001	α_m ± 0.001	M ± 0.001
0	3.597	2.863	0.464	0.0556	35.257	2.260	5.107	0.672	1.399	0.327
0.1	3.418	2.531	0.590	0.0438	31.143	2.358	5.5601	0.695	1.235	0.304
0.2	3.520	2.548	0.621	0.0416	27.925	2.268	5.143	0.674	1.108	0.325
0.3	3.653	3.021	0.600	0.0431	31.390	2.241	5.022	0.667	1.245	0.332
0.4	3.367	2.019	0.564	0.0458	33.434	2.301	5.294	0.682	1.326	0.317
0.5	3.477	2.720	0.471	0.0548	30.768	2.279	5.193	0.677	1.220	0.323

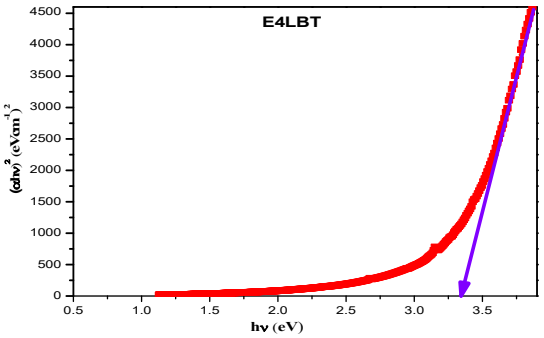

Fig. 7 Plot of $(\alpha h\nu)^2$ versus hν for E4LBT glass

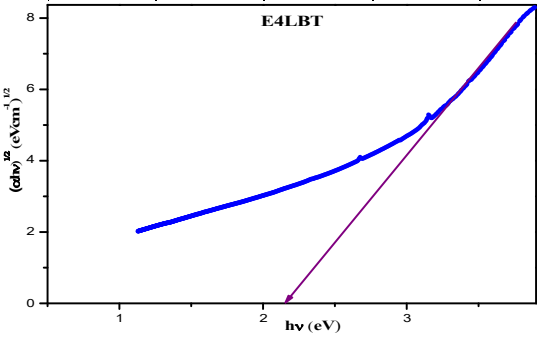

Fig. 8 Plot of $(\alpha h\nu)^{1/2}$ versus hν for E4LBT glass

$$ln\alpha = ln\alpha_o + \frac{h\vartheta}{\Delta E} \quad (5)$$

The obtained results tells the fact that considerable variations originated by the addition of Eu_2O_3 in to the glass network. The highest disorderness obtained for the E2LBT glass.

An important and more useful parameter i.e. refractive index was evaluated by a Lorentz- Lorentz equation (6) here Eg refers the energy gap.

$$\frac{n^2-1}{n^2-2} = 1 - \sqrt{\frac{E_g}{20}} \quad (6)$$

Further, with knowledge of refractive index the dielectric constant, molar refraction, molar polarizability, reflection loss and metallization criterion were determined with precise mathematical formulae[20]–[23] and obtained are tabulated in the Table 2.

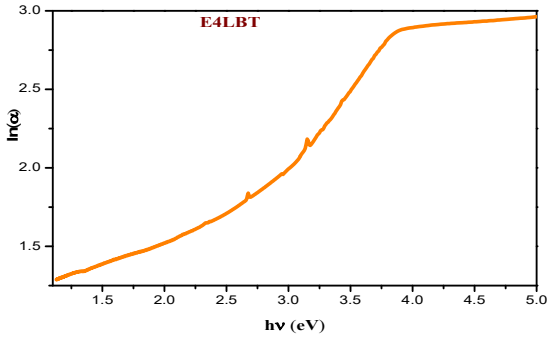

Fig. 9 Plot of ln(α) versus hν for E4LBT glass

The highest refractive index was found for the E1LBT glass and lowest one found for E3LBT glass. The obtained values were relatively compared to other reported data. Molar refraction and molar polarizability are directly proportional and same we can observe in the Fig. 10.

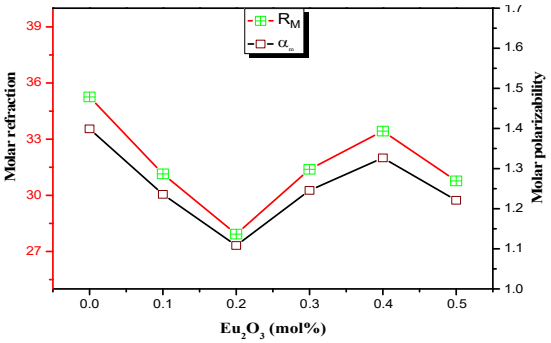

Fig.10 Variation of molar refraction and molar polarizability with Eu_2O_3 concentration

The accountable and significant variations were observed in all parameters with addition of Eu_2O_3 into glass network was mainly due to production of additional NBOs. Metallization criterion value are depends on the reflection loss values i.e., if $R_M / V_M > 1$ then it is metal and $R_M / V_M < 1$ then it is non metal. The values obtained for ELBT glass are in the range 0.304 to 0.332 and this range is well fit with the nonlinear optical values having rage 0.3 to 0.4. Due to this reason these LBTE glasses can be used in the manufacture of optical switching, optical computing and optical data storage devices.

4. Conclusion

Eu_2O_3 doped lead boro tellurite glass samples were synthesised by conservative melt quenching technique. Non-crystalline nature of the glasses was declared by XRD patterns. On increasing europium ion concentration the significant variations in both density and molar volume were observed which are mainly due to the formation of nonbridging oxygen and changes in OPD. By Raman studies , the Te-O-Te bonds in stretching vibrations, asymmetric vibrations of Te-O-Te bonds, stretching vibrations of Te-O in TeO_3 triangular pyramid group, symmetrical breathing vibrations in borate rings consists of tetrahedra of BO_4, symmetric stretching vibrations of BO3 triangular units in meta-borate, ortho-borate and pyro-borate units were explored. The optical energy band gap found to be having variations with raising concentration of Eu_2O_3 which is due to shifting of absorption edge. Optical properties were found to be undergoing significant variations by increasing Eu_2O_3 concentration, the highest refractive index is found as 2.358 for glass E1LBT and the lowest one found as 2.241 for E3LBT glass which is because of NBOs. The overall obtained results and studies leads to a conclusion that the prepared glasses find potential applications in developing optical fibers and optical devices.

References

1. Zhou, Tunable colors and applications of Dy^{3+}/Eu^{3+} co-doped CaO-B_2O_3-SiO_2 glasses. J. Am. Ceram. Soc. **102**, 5890–5898 (2019)
2. Elazoumi, Effect of PbO on optical properties of

tellurite glass. Results Phys. **8**, 16–25 (2018)

3. M.Haouari, F. Ben Slimen, A. Maaoui, Gaumer, Structural and spectroscopic properties of Eu^{3+} doped tellurite glass containing silver nanoparticles. J. Alloys Compd. **743**, 586–596 (2018)
4. Reza Dousti, Ghassemi, Sahar, Mahraz, Chemical durability and thermal stability of Er^{3+}doped zinc tellurite glass containing silver nanoparticles. J. Lumin. **11**, 111–119 (2014)
5. S. Rada, M. Culea, E. Culea, Structure of TeO_2 ÁB_2O_3 glasses inferred from infrared spectroscopy and DFT calculations. J. Non. Cryst. Solids **354**, 5491–5495 (2008)
6. M. N. Ami Hazlin, M. K. Halimah, F. D. Muhammad, Optical properties of zinc borotellurite glass doped with trivalent dysprosium ion. Phys. B Condens. Matter **510**, 38–42 (2017)
7. S. Selvi, K. Marimuthu, G. Muralidharan, Effect of PbO on the B_2O_3–TeO_2–P_2O_5–BaO–CdO–Sm_2O_3 glasses: Structural and optical investigations. J. Non. Cryst. Solids **461**, 35–46 (2017)
8. S. Bale, S. Rahman, Electrical conductivity studies of Bi_2O_3–Li_2O–ZnO–B_2O_3 glasses. Mater. Res. Bull. **47**, 1153–1157 (2012)
9. N. Kaur, A. Khanna, P. Krishna, F. González, Optical properties of borotellurite glasses containing metal oxides. AIP Conf. Proc. **1665**, 070029 (2015)
10. R Cao, Spectroscopy of thulium and holmium co-doped silicate glasses. Opt. Mater. Express **6**, 2252 (2016)
11. T. Hasegawa, Optical properties of Bi_2O_3-TeO_2-B_2O_3 glasses. J. Non. Cryst. Solids **357**, 2857–2862 (2011)
12. K. Maheshvaran, K. Linganna, K Marimuthu, Composition dependent structural and optical properties of Sm^{3+} doped boro-tellurite glasses. J. Lumin. **131**, 2746–2753 (2011)
13. M. Rajesh, M. R. Babu, N. J. Sushma,B. D. Raju, Influence of Er^{3+} ions on structural and fluorescence properties of SiO_2-B_2O_3- Na_2CO_3-NaF-CaF_2 glasses for broadband 1.53 µm optical amplifier applications. J. Non. Cryst. Solids **471**, 1-12 (2019)
14. H. S. Yoo, W. Bin, S. W. Kim, B. H. Kwon, D. Y. Jeon, Continuous nano-coating of Y_2O_3:Eu^{3+} phosphor shell on SiO_2 core particles and its photoluminescence properties. J. Lumin. **130**, 153–156 (2010)
15. A. Madhu, B.Eraiah, P. Manasa, N.Srinatha, Nd^{3+}-doped lanthanum lead boro-tellurite glass for lasing and amplification applications. Opt. Mater. (Amst). **75**, 357–366 (2018)
16. A. Madhu, B. Eraiah, Lanthanum lead boro-tellurite glasses doped with samarium trioxide for luminescent devices application. AIP Conf. Proc. **1942**, 3–7 (2018)
17. S. Selvi, K. Marimuthu, N. Suriya Murthy, G. Muralidharan, Red light generation through the lead boro-telluro-phosphate glasses activated by Eu^{3+} ions. J. Mol. Struct. **1119**, 276–285 (2016)
18. A.N.Yerpude, S. J. Dhoble, N. S. Kokode, Photoluminescence properties of $Ca_3B_2O_6$:RE^{3+} (RE = Dy and Eu) phosphors for ecofrindly solid state lighting. Optik (Stuttg). **179**, 774–779 (2019)
19. K. Maheshvaran, K.Marimuthu, Concentration dependent Eu $^{3+}$ doped boro-tellurite glasses - Structural and optical investigations. J. Lumin. **132**, 2259–2267 (2012)
20. B. Srinivas, A. Hameed, M. N. Chary, M. Shareefuddin, Physical, Optical and FT-IR studies of Bismuth-Boro-tellurite Glasses containing BaO as modifier. IOP Conf. Ser. Mater. Sci. Eng. **360**, 012022 (2018)
21. P.Ramesh, G. Jagannath, B.Eraiah, M. K. Kokila, Optical and Physical Investigations of Lanthanum Bismuth Borate glasses doped with Ho_2O_3. IOP Conf. Ser. Mater. Sci. Eng. **310**, 012032 (2018)
22. F. Zaman, Physical, structural and luminescence investigation of Eu^{3+}-doped lithium-gadolinium bismuth-borate glasses for LEDs. Solid State Sci. **80**, 161–169 (2018)

Structural studies of Cobalt and Tin Embedded Calcium Nano-Ferrites: Effect of SiO_2

G. Harisha[1], C Devaraja[2*], G V Jagadeesha Gowda[2], K M Rajashekara[1,*]

1Department of Physics, S J C Institute of Technology, Chickballapur-562101, Karnataka, India.
2Department of Physics, Sapthagiri College of Engineering, Bengaluru-560057, Karnataka, India

[*]***Corresponding author e-mail:*** *km_rajashekar@yahoo.co.in, & deva.drr@gmail.com,*

Abstract: **By using the sol-gel microwave auto combustion technology, a set of cobalt and tin substituted calcium nano-ferrite samples of chemical composition Ca(Co-Sn)Fe2-xO3+SiO2x (x = wt percent) have been created with varied SiO2 ratios. An X-ray diffractometer confirms the structural representation of prepared samples (XRD). XRD tests validated the samples' Z-type tetragonal crystal structure and crystal planes. Scanning Electron Microscope was used to examine the morphological features of ready samples (SEM). The existence of nano ferrites with a particle size of 33 to 74 nm is indicated by the SEM examination. The EDS tests confirm that there are no impurity elements present. The fundamental composition of materials was identified by "Energy Dispersive X-Ray analysis technique (EDS). The average particle size in powder samples was found in the range of 41 -57 nm.**

Keywords: Calcium nano-ferrite; Aloe Vera; Agglomeration; Z-type tetragonal crystal.

1. INTRODUCTION

The new ferrites are ferromagnetic materials made up of massive iron oxides as well as additional oxides such as barium, cadmium, strontium, nickel, manganese, zinc, cobalt, lithium, tin, and calcium [1-8]. Because of their distinctive magnetic, electrical, mechanical, and optical properties, ferrites with the chemical formula MFe2O4 (where M is a divalent metal ion) showed promise in technological applications [1,4]. As a result, ferrites have been identified for a variety of applications such as magnetic recording medium, MRI augmentation, catalysis, magnetic fluids in the storage or retrieval of data sensors, and pigment [1,2,7,8]. The structure of spinal-type ferrites consists of a densely packed oxygen array with 32 oxygen ions forming a single cell. For the production of ferrite nanoparticles, a variety of processes are available, including hydrothermal [9], chemical co-precipitation[10], combustion[11], sol-gel [12,13], traditional ceramic process[14-18], and RF-sputtering [9,10,18]. Among all acknowledged technologies, simple and cost-effective approaches for preparing nano-ferrites with the lowest cost for use, nontoxic and ecologically friendly precursors are extremely relevant. The sol-gel microwave auto combustion method was employed to manufacture calcium nano-ferrites in the current study. The use of diverse plant extracts for the manufacture of nanoparticles with particle sizes ranging from 5 to 50 nm has been documented in recent research [19,20].

Aloe Vera is one of the boons to researchers because i) It contains 99.5% of water in its leaves and the rest is solid content, ii) The solid material of Aloe Vera possesses over 75 diverse ingredients, namely salicylic acid, sugars, minerals, enzymes, sterols, vitamins, amino acids, saponins, etc., iii) It is a natural plant and easily available in India and many other countries, iv) Aloe Vera gel is mainly used in cosmetics products such as sun lotions, lip balm, face creams, healing ointments, hydrating elements in liquids. v) Further, it is also used in pharmacology for anti-inflammatory, and burn treatment[21]. Aloe Vera is a good reducing agent and it can reduce the particle size to nanometers [22,23]. The effect of various diamagnetic-paramagnetic cations on the nanostructure and magnetic properties of M-type hexaferrite has been reported to be important for use in technical applications [24-31]. It is stated by Preksha N, et al [32] that, the $Sr_3Co_{2-x}Ga_xFe_{24}O_{41}$ hexaferrite materials can be used for microwave absorbers applications. The replacement of Nd^{3+} ions in nickel ferrites can improve the magnetic parameters [33,34]. E. Ahilandeshwari et al showed that the nano ferrite materials with the chemical formula $BaNd_xFe_{2-x}O_4$ are potential candidates for the reduction of EMI with the least reflection loss over a broad frequency range [8]. It is stated that [35-37], the simultaneous inclusion of SiO_2 and CaO is well-matched to stimulate the densification of hard ferrite magnets without letting in large amounts of grain growth.

The present investigations are mainly focused on synthesis, structural, morphological, and elemental analysis of calcium nano ferrites, doped with cobalt and tin. The result of SiO_2 on crystalline size, structural, microstructure, and elemental analysis of calcium nano ferrites was analyzed with XRD, SEM, and EDS.

2. EXPERIMENTAL METHOD

Calcium ferrites doped with cobalt and tin ions having chemical composition $\mathbf{SiO_{2x}Ca(Co\text{-}Sn)Fe_{2-x}O_3}$ have been synthesized by sol-gel microwave auto combustion method. The ferrite samples were prepared by taking analytical reagent grade (AR) chemicals such as calcium nitrate $Ca(No_3)_24H_2O$, cobalt nitrate $Co(No)_3$, tin oxide (SnO_2), ferric nitrate $Fe(No_3)_29H_2O$ having 99% purity procured by Sigma Aldrich as starting materials. Here $Co(No)_3$ and SnO_2 were taken as substituting material, urea (NH_2-Co-NH_2), and Aloe Vera plant extract were used as fuel with suitable ratios. Further, the sol-gel combustion is one of the best approaches for the synthesis of nano-materials due to the following factors, i) it gives ultrafine powder nanoparticles, ii) better particle size distribution, iii) high probability of forming a single structure, and iv) excellent chemical homogeneity. The calcium nano ferrites were prepared by microwave-induced sol-gel combustion method [29,35]. Here, instead of a conventional furnace, the microwave oven was used for combustion, because it gives uniform heating during the sample combustion process.

For preparation, the quantified amount of metal nitrates was dissolved into distilled water and heated at a temperature of 353.15 K for 3 hours by taking urea as fuel, which gives the necessary energy to start an exothermic

reaction. The gel formed was burnt in a digitally controlled microwave oven, yielding powder (ash). The resulting powder was followed by grinding for 5 hours in pestle motor to get ultrafine homogeneous crystallized nanoparticle powder of samples and then heated in an electric furnace at up to 1073.15 K and then cooled at the same rate. The obtained powder is then taken for XRD, SEM, and EDS analysis. The crystal structure, phases or planes, and lattice parameters were calculated by Bruker AXS D8 Advance X-ray diffractometer, containing Cu Kα, λ = 1.54 Å. The morphology, elemental analysis, and particle size of the ready samples were performed by JEOL 6390 scanning electron microscope.

3. RESULTS AND DISCUSSION

3.1. Analysis of X-Ray Diffraction

The XRD graph of synthesized nano-ferrites is depicted in **Fig. 1** and it is observed that the samples reveal the tetragonal structure. The Debye Scherer equation (1) is taken to find the particle size of the powder samples of nano-ferrites.

$$D = \frac{k\lambda}{\beta cos\theta} \quad (1)$$

Where, λ is the wavelength of X-rays i.e. 1.54 Å, k referred to Scherer constant (for hexaferrite K=0.89), β denotes the full width at half maxima (FWHM) and θ is the Bragg's angle [8-17]. The average particle size in powder samples was found in the range of 41 -57 nm. The crystal parameters such as lattice constants a, c, and volume of the unit cell V_{cell}, were determined by using mathematical equations (2), (3) [8-11,24-30] and obtained Miller indices (h k l) values, inter planner distanced recorded in **Table 1**.

$$\frac{1}{d^2} = \left[\frac{h^2+k^2+l^2}{3a^2}\left(\frac{a^2}{c^2}\right)\right]\left(\frac{1}{a^2}\right) \quad (2)$$

$$V_{cell} = a^2c \quad (3)$$

Table 1. Lattice parameters, average crystallite size, d-spacing, and unit cell Volume of prepared calcium nano ferrites.

Composition SiO_2(x) Ca(Co-Sn)$Fe_{2-x}O_3$	Sample Name	Lattice parameters		Average particle size (nm)	d-Spacing (Å)	Volume of unit cell (Å)
		a (Å)	c (Å)			
0	CCTF-1	5.325	7.579	57.61	2.43	214.90
0.02	CCTF-2	5.224	7.351	55.12	2.32	200.61
0.04	CCTF-3	5.072	7.179	46.65	2.27	184.68
0.06	CCTF-4	4.791	7.012	41.48	2.17	160.95

The XRD patterns of Calcium –Cobalt-Tin Ferrites (CCTF) nano ferrites are depicted in **Fig. 1**. From **Fig. 1,** it is observed that the prepared nano-ferrites are exhibiting a Z-type tetragonal structure. The obtained Braggs diffraction planes are closely matched with the JCPDS no. 41-753. The crystallite size of prepared samples is appearing in nanometers, also recorded in Table 1. Few noisy peaks were noticed in pattern in all CCTF nano ferrites might be owing to i) the crystallite size being relatively small ii) the instrumental error. The crystallite size of undoped CCTF-1 nano ferrite is 57.61 nm and it is relatively more than that of the SiO_2 doped nano ferrites (i.e.41-55nm). This may be due to the replacement of Si^{4+} with Fe^{4+} in calcium nano ferrites reducing the crystallite size in the presence of Aloe Vera fuel. The trend of lessening in the crystallite size concerning an increase in silicon dioxide was also described by researchers in their work [35-37]. It is also observed in **Table 1** that, the values of lattice parameters SiO_2 doped CCTF nano ferrites are decreasing with an increase in the concentration of SiO_2 owing to the higher difference in the ionic radii of the element ions [35-37]. The decrease in unit cell volume in samples with an increase in SiO_2 might be due to the blocking of grain growth.

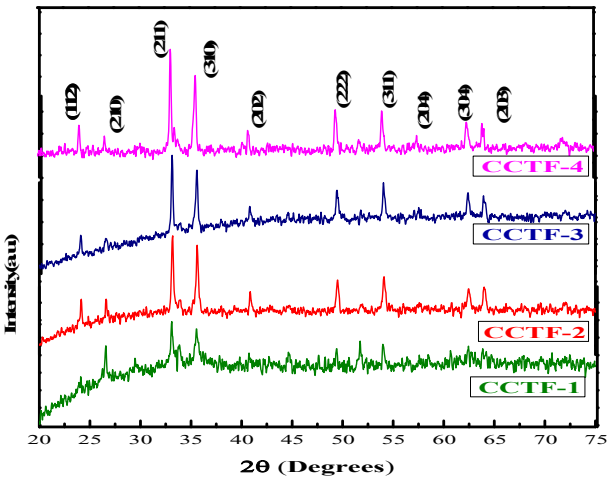

Fig.1. XRD pattern of SiO_2(x) Ca(Co-Sn)$Fe_{2-x}O_3$

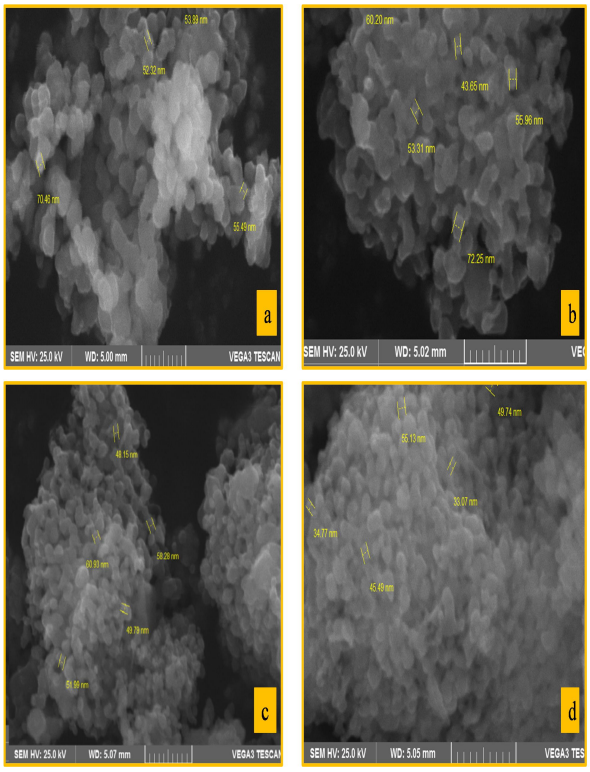

Fig. 2. SEM micrographs of CCTF nano ferrites.

3.2. Morphological and Elemental Analysis

The Scanning Electron Microscopy (SEM) of the undoped and doped CCTF nano ferrites was depicted and the SEM micrographs are used to analyze the morphology of prepared CCTF nano ferrites as shown in **Fig.2**. The prepared ferrites are not spherical but lightly agglomerated. The presence of small agglomeration at the nano-scale is because of the high surface and dangling bonds of nano ferrites [38-40].

The particles are in nano-scale and the distribution is weakly irregular, due to low sintering temperatures and ultra-short intervals involved in the process of sample synthesis. This may reduce the increase in aggregation and may not disturb the re-crystallization of the lattice [41-45]. The morphological structures are depicted in fig. 2 (a), fig. 2(b), fig 2(c), and fig. 2(d), are being influenced by Si_2O_2 content and the average particle size of nano ferrites decreasing [35-37].

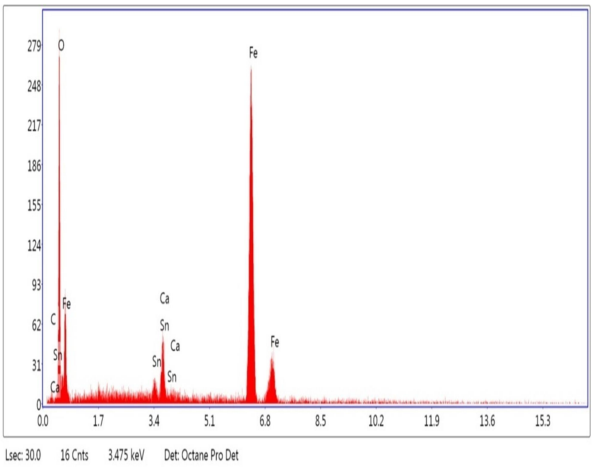

3a) EDS spectrum of CCTF-1 nano ferrite.

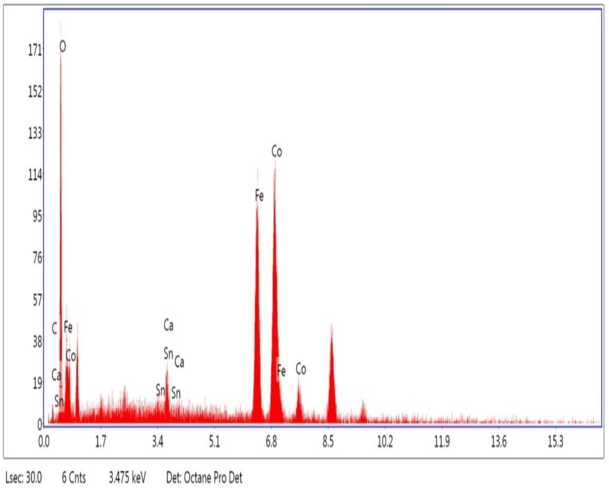

3b) EDS spectrum of CCTF-4 nano ferrite.

Fig. 3. a) EDS spectrum of CCTF1 nano ferrite and 3b) EDS spectrum of CCTF-4 nano ferrite.

The energy-dispersive X-ray spectroscopy of CCTF nano ferrites are depicted in **Fig. 3(a)** and **3(b)**. The energy peaks of elements O, Fe, Ca, Sn and Co, which are used for synthesis, are identified in **Fig. 3(a).** Therefore, samples of nano-ferrite are synthesized with the correct stoichiometric ratio to ensure that they are homogeneous and that there is no excess material and impurity from the calcium ferrites prepared by the sol-gel microwave auto combustion method with Aloe Vera as fuel give nano ferrites. The particle size of the prepared CCTF nano ferrites is in the range of 33 to 74 nm. In **Fig. 3(b)** the energy peaks for the dopant SiO_2 were not recorded, probably due to less molar concentration. But the impact of SiO_2 on structural and morphology properties was noticed in their crystallite size, lattice parameters, unit cell volume, and particle size in SEM micrographs.

4. CONCLUSIONS

The $SiO_{2x}Ca(Co\text{-}Sn)Fe_{2-X}O_3$ single-phase tetragonal calcium nano ferrites were prepared by the sol-gel microwave auto combustion technique. The crystallite size of calcium nano ferrites was determined by the Debye Scherer equation and it comes in the range of 41-57 nm. The decrease in particle size, lattice parameters, and unit cell volume with increasing SiO_2 concentration has been studied, and this may be due to greater variation in the ionic radius of the Si^{4+} component with Fe^{4+}. The SEM analysis of calcium nano ferrites reveals that the particle size is in the nano-scale (33 to 74 nm) and contains less agglomeration. The distribution of nanoparticles is faintly irregular, due to high sintering temperatures. The EDS analysis confirms the presence of energy peaks corresponding to elements used for preparation and it also confirms the homogeneous nature of CCTF nano ferrites and the absence of impurities.

ACKNOWLEDGMENTS

The authors thank the Department of Physics, BMS Institute of Technology and Management for providing the necessary experimental setup for the preparation of samples.

REFERENCES

[1] M. Sugimoto, “The past, present, and future of ferrites” *Journal of American ceramic Society*, vol. 82, p. 269, 1999.

[2] I. Safarik, M. Safarikova, H. Hofmann, Z. Rahman, U. Schubert, “Magnetic nano particles and biosciences in nanostructured materials’’, *Springer, Wien*, pp. 1-23, 2002.

[3] F. Li, J.J. Liu, D.G. Evans, X. Duan, “Stoichiometric Synthesis of Pure MFe_2O_4 (M = Mg, Co, and Ni) Spinel Ferrites from Tailored Layered Double Hydroxide (Hydrotalcite-Like) Precursors”, *Chemistry of materials,* vol.16, p.1597, 2004.

[4] D. Caruntu, Y. Remond, N. H. Chou, M.J. Jun, G. Caruntu, G. Goloverda, C.O. Connor, V. Kolesnichenko, “Synthesis of transition metal ferrites with the structure of discrete nanoparticles complexed with long-chain carboxylate anions, *Inorganic chemistry*, vol. 41, p.6137, 2002.

[5] M. Yokoyama, T. Sato, E. Ohta, T. Sato, “Magnetization of cadmium ferrite prepared by co-precipitation” *Journal of Applied Physics*, vol. 80, p.1015, 1996.

[6] Y.I. Kim, D. Kim, C.S. Lee, “Synthesis and characterization of $CoFe_2O_4$ magnetic nano particles prepared by temperature-controlled co precipitation method”, *Physica B: Condensed Matter*, vol. 337, p. 42, 2003.

[7] X. M. Liu, S. Y. Fu, J. Huang, “Synthesis and magnetic characterization of novel $CoFe_2O_4$–$BiFeO_3$ nano-composites”, *Materials Science and Engineering: B*, vol. 121 (15), pp. 255-260, 2005.

[8] E. Ahilandeswari, R. Rajesh Kanna, K. Sakthipandi, "Synthesis of neodymium-doped barium nano ferrite: Analysis of structural, optical, morphological and magnetic properties" *Physica B: Condensed Matter,* vol. 599, pp. 412425, 2020.

[9] T. Koutzarova, S. Kolev, C. Ghelev, K. Grigorov, I. Nedkov, "Structural and magnetic properties and preparation techniques of nano-sized M-type hexaferrite powders", *Advances in Nano scale Magnetism*, vol. 1, (122), pp. 183-203, 2007.

[10] S. S. Khot, N. S. Shinde, B.P. Ladgaonkar, B.B. Kale, S.C. Watawe, "Magnetic and structural properties of magnesium zinc ferrites synthesized at different temperature" *Advances in Applied Science Research*, vol. 2(4), pp. 460-471, 2011.

[11] D. Mishra, S. Anand, R. K. Panda, R. P. Das, "Studies on characterization, micro-structures and magnetic properties of nano-size barium hexa-ferrite prepared through a hydrothermal precipitation–calcination route," *Material chemistry and physics*, vol. 86, p. 132, 2004.

[12] V. Pillai, P. Kumar, M.S. Multani, D.O. Shah, "Structure and magnetic properties of nanoparticles barium ferrite synthesized using micro emulsion processing," *Colloids and Surfaces A: Physicochemical and Engineering Aspects*, vol. 80, pp. 69-75, 1993.

[13] L. Lechevallier, J. M. Le Breton, J. F. Wang, I. R. Harris, "Structural analysis of hydrothermally synthesized $Sr_{(1-x)}Sm_xFe_{12}O_{19}$ hexagonal ferrites", *Journal of Magnetism and Magnetic Materials,* vol. 269 (2), pp. 192-196, 2004.

[14] C. O. Augustin, R. KalaiSelvan, R. Nagaraj, L. John Berchmans, "Effect of La^{3+} substitution on the structural, electrical and electrochemical properties of strontium ferrite by citrate combustion method," *Materials Chemistry and Physics*, vol. 89, pp. 406-411, 2005.

[15] Kashinath C. Patil, Singanahally T. Aruna, Sambandan, Ekambaram, "Combustion synthesis," *Current Opinion in Solid State and Materials Science,* vol. 2, (2), pp. 158-165, 1997.

[16] E.Wu. S. J. Campbell, W. A. Kaczmarek, "Mossbauer effect study of ball-milled strontium ferrite", *Journal of Magnetism and Magnetic Materials*, vol. 177, pp. 255-256, 1998.

[17] W.A. Kaczmarek, B. Idzikowski, K.H. Muller, "XRD and VSM study of ball-milled $SrFe_{12}O_{19}$ powder, "*Journal of Magnetism and Magnetic Materials*", vol. 177, pp. 921-922, 1998.

[18] A. Sharma, O. Modi, G. Gupta, "Effect of fuel to oxidizer ratio on synthesis of alumina powder using solution combustion technique-aluminum nitrate and glycine combination," *Advances in Applied Science Research*, vol. 3 (4), pp. 2151-2158, 2012.

[19] Santi Phumying, Sarawuth Labuayai, Chunpen Thomas, Vittaya Amornkitbamrung,
Ekaphan Swatsitang, Santi Maensiri, "Aloevera plant-extracted solution hydrothermal synthesis and magnetic properties of magnetite (Fe_3O_4) nanoparticles" *Applied Physics A,* vol. 111, pp. 1187-1193, 2013.

[20] SantiPhumying, SarawuthLabuayai, EkaphanSwatsitang, VittayAmornkitbamrung, SantiMaensiri, S. Phumying, "Nanocrystalline spinel ferrite (MFe_2O_4, M= Ni, Co, Mn, Mg, Zn) powders prepared by a simple Aloevera plant-extracted solution hydrothermal route", *Materials Research Bulletin*, vol. 48, pp. 2060-2065, 2013.

[21] http://www.internethealthlibrary.com/PlantRemedies/AloeVera.html, (2006).

[22] S.P. Chandran, M. Chaudhary, R. Pasricha, A. Ahmad, M. Sastry, "Synthesis of gold nano triangles and silver nanoparticles using Aloevera plant extract", *Biotechnology Progress,* vol. 22, pp. 577-583, 2006.

[23] S. Maensiri, P. Laokul, J. Klinkaewnarong, S. Phokha, V. Promarak, S. Seraphin, "Indium oxide (In_2O_3) nanoparticles using Aloevera plant extract: Synthesis and optical properties," *Optoelectronics and advanced materials*, vol. 2 (3), pp. 161 – 165, 2008.

[24] J. Klinkaewnarong, E. Swatsitang, C. Masingboon, S. Seraphin, S. Maensiri, "Synthesis and characterization of nano crystalline HAp powders prepared by using aloe vera plant extracted solution" *Current Applied Physics*, vol. 10, pp. 2010, 521-525.

[25] M. A. Ali1, M. M. Uddin, M. N. I. Khan, F. U. Z. Chowdhury, D. K. Saha, S. M. Hoque, S I. Liba, and S. Akhter, "Effect of sintering temperature on structural and magnetic properties of $Ni0.6Zn0.4Fe_2O_4$ ferrite: synthesized from nano crystalline powders", *Journal of Physics: Conference Series*, vol. 1718, p. 012013, 2021.

[26] J. Singh, C. Singh, D. Kaur, H. Zaki, I.A. Abdel-Latif, S. BindraNarang, R. Jotania, S.R. Mishra, R. Joshi, P. Dhruv, M. Ghimire, S.E. Shirsath, S.S. Meena, "Elucidation of phase evolution, microstructural, Mossbauer and magnetic properties of Co^{2+} Al^{3+} doped M-type BaSr hexaferrites synthesized by a ceramic method", *Journal of Alloys and Compounds,* vol. 695, pp. 1112-1121 (2017).

[27] Robert C. Pullar, "Hexagonal Ferrites: A Review of the synthesis, properties, and applications of hexaferrite ceramics," *Progress in material science,* vol. 57, pp. 1191-1334, 2012.

[28] G. Asti, M. Carbucicchio, A. Deriu, E. Lucchini, G. Slokar, "Magnetic characterization of Ca substituted Ba and Sr hexaferrites," *Journal of Magnetism and Magnetic Materials,* vol. 20, pp. 44-46, 1980.

[29] S.K. Chawla, R.K. Mudsainiyan, S.S. Meena, S.M. Yusuf, "Sol–gel synthesis, structural and magnetic properties of nano scale M-type barium hexaferrites $BaCo_xZr_xFe_{(12-2x)}O_{19}$", *Journal of Magnetism and Magnetic Materials*, vol. 350, pp. 23-29, 2014.

[30] M. Hashim, S.E. Shirsath, S.S. Meena, M.L. Mane, S. Kumar, P. Bhatt, R. Kumar, N.K. Prasad, S.K. Alla, J. Shah, R.K. Kotnala, K.A. Mohammed, E. Senturk, Alimuddin, "Manganese ferrite prepared using reverse micelle process: Structural and magnetic properties characterization", *Journal of Alloys and Compounds*, vol.642, pp. 70-77, 2015.

[31] S. Singhal, A.N. Garg, K. Chandra, "Evolution of the magnetic properties during the thermal treatment of nanosize $BaMFe_{11}O_{19}$ (M=Fe, Co, Ni and Al) obtained through aerosol route, *Journal of Magnetism and Magnetic Materials*, vol. 285, pp.193-198, 2005.

[32] Preksha N. Dhruv, Sher Singh Meena, Robert C. Pullar, Francisco E. Carvalho, T.V. Chandrasekhar Rao, C.B. Basak, "Investigation of structural, magnetic and dielectric properties of gallium substituted Z-type $Sr_3Co_{2-x}Ga_xFe_{24}O_{41}$ hexaferrites for microwave absorbers", *Journal of Alloys and Compounds*, vol. 822, p.153470, 2020.

[33] Israfil S ¸abikoglua, OndrejMalina, LeventParal, Petr Novak, Josef Kaslik, Jiri Tucek, Jiri Pechousek, JakubNavarik, OldrichSchneeweiss, "The effect of neodymium substitution on the structural and magnetic properties of nickel ferrite", *Progress in Natural Science: Materials International*, vol. 25, pp. 215-221, 2015.

[34] K. Kamala Bharathi, J. Arout Chelvane, G. Markandeyulu, "Magnetoelectric properties of Gd and Nd-doped nickel ferrite", *Journal of Magnetism and Magnetic Materials,* vol. 321, pp.3677-3680, 2009.

[35] Thomas Dippong, OanaCadar, ErikaAndrea Levei, Iosif Grigore Deac, "Microstructure, porosity and magnetic properties of $Zn_{0.5}Co_{0.5}Fe_2O_4/SiO_2$ nano composites prepared by sol-gel method using different polyols," *Journal of Magnetism and Magnetic Materials,* vol. 498, p. 66168, 2020.

[36] Xiang Ding & Xing-Min Guo, "The Formation Process of Silico-Ferrite of Calcium (SFC) from binary calcium ferrite, *Metallurgical and Materials Transactions* B, vol. 45, pp.1221–1231, 2014.

[37] Xiang Ding, Xing-Min Guo, "The Sintering Characteristics of Mixing SiO_2 with Calcium Ferrite at 1473 K (1200 °C)", *Metallurgical and Materials Transactions B*, vol. 46, pp.1742–1750, 2015.

[32] Gill, Neeraj, SmithaPuthucheri, Dharmendra Singh, Vijaya Agarwala, "Critical analysis of frequency selective surfaces embedded composite microwave absorber for frequency range 2–8 GHz", *Journal of Materials Science: Materials in Electronics,* vol. 28(2), pp. 1259-1270, 2017.

[41] Li, Honglin, Zhong Zhang, Jinzhao Huang, "Optical and structural analysis of rare earth and Li co-doped ZnO nanoparticles", *Journal of Alloys and Compounds,* vol. 550, pp. 526-530, 2013.

[42] JijingXu, GuijuanJi, HaifengZou, Yuan Zhou, ShucaiGan, "Structural, dielectric and magnetic properties of Nd-doped Co_2 Z-type hexaferrites" *Journal of Alloys and Compounds,* vol.509, pp. 4290–4294, 2011.

[43] Thakur, Ankush, R. R. Singh, P. B. Barman, "Synthesis and characterizations of Nd^{3+} doped $SrFe_{12}O_{19}$ nanoparticles", *Materials Chemistry and Physics*, vol. 141 pp. 562-569, 2013.

[44] B. Poornaprakash, D.Amaranatha Reddy, G. Murali, N. Madhusudhana Rao, R. P. Vijayalakshmi, B. K. Reddy, "Composition dependent room temperature ferromagnetism and PL intensity of cobalt doped ZnS nanoparticles", J*ournal of Alloys and Compounds,* vol. 577, pp. 79-85, 2013.

[45] R. Rajesh Kanna, K. Sakthipandi, S. M. Seeni Mohamed AliarMaraikkayar, M. Sivabharathy, "Doping effect of rare-earth (lanthanum, neodymium and gadolinium) ions on structural, optical, dielectric and magnetic properties of copper nanoferrites", *Journal of Rare Earths,* vol. 36, pp. 1299-1309, 2018.

STUDIES ON THERMAL BARRIER COATING INFLUENCE ON C I ENGINE PERFORMANCE FUELLED WITH BIODIESEL

BASAVARAJ GANIGER[1], T B PRASAD[2], H M SANJAY[3]

[1]Sapthagiri College of Engineering Bangalore, *Karnataka,India.*
[2]Sri Siddhartha Institute of Technology, Tumkur,Karnataka,India.
[3]Sai Vidya Institute of Technology Bangalore, Karnataka,India.
ganiger2011@gmail.com

Abstract— The combustion chamber surfaces (piston crown face, cylinder head & valves) were coated with ceramic material. Ceramic layers of ZrO_2-Y_2O_3 were coated by using plasma spray method onto the base of NiCrAlY bond coat to thicknesses of 0.28mm & 0.07mm respectively. The engine was tested at different load conditions like 20%, 40%, 60% and 80% of rated load without coating. The engine with coated piston crown, cylinder head and valves was tested at the same conditions as of standard (without coating) engine. The results showed a reduction in brake specific fuel consumption and an increase in brake thermal efficiency.

Keywords: ZrO2-Y2O3, plasma spray, piston crown, specific fuel consumption and brake thermal efficiency.

1. INTRODUCTION

Thermal barrier coatings (TBCs) because of their ability to provide thermal insulation have generally been accepted to improve brake thermal efficiency for diesel engines. So reduction of heat transfer from the combustion chamber reduces the energy loss to the coolant during the power stroke of the cycle thus increases the operating temperatures to improve efficiency [1]. The thermal efficiency of most commercially available diesel engines ranges from 38% to 42%. Therefore 58% to 62% of the energy content of the fuel is lost in the form of waste heat. Approximately 30% is retained in the exhaust gas and the remainder is removed by cooling water/air. In order to save energy, it is an advantage to protect the hot parts by thermal insulating layer [1 & 2].

One of the development trends for heat engines is improvement of their thermal efficiency. In case of internal combustion engines, one of the ways to achieve improved thermal efficiency is by engine adiabatization. One of the possible methods to adiabatize an engine is to cover the surface of the combustion chamber with a Thermal Barrier Coating (TBC) of low thermal conductivity. The thermal insulation thus obtained is supposed to lead to an improvement in the engine's heat efficiency and a reduction in consumption according to the second law of thermodynamics. Higher temperatures in the combustion chamber can have a positive effect in diesel engines, due to the reduction in delay and hardness of engine operation [3, 4 & 5]. A two layer TBC system consists of a ZrO_2-Y_2O_3 ceramic top coating and an oxidation resistant metallic bond coat of NiCrAlY to thicknesses of 0.28mm and 0.07mm respectively. These thermal barrier coating systems are applied to the metal substrate by plasma spray technique [1, 5, 7, 8 &10]. Experiments were conducted with single cylinder, directly injected, diesel/biodiesel fuelled C I engine with and without thermal barrier coating at different loads ranging from 20%, 40%, 60% and 80% of rated load [6 &9]. The main objectives of present investigation is to evaluate the effect of thermal barrier coating on engine performance parameters like brake specific fuel consumption (BSFC) and Brake thermal efficiency (BTE) and

exhaust gas temperature (EGT) for neat diesel and honge blend B20.

Table 1
Properties of ZrO_2-Y_2O_3

Materials	Coefficient of thermal Expansion	Thermal Conductivity (at 100°C) W/m-°C
ZrO_2	9-10	0.0047
Y_2O_3	9	0.0690

Table 2
Properties of Diesel and Honge oil

Characteristics	Diesel	Honge oil
Calorific Value (KJ/kg)	42500	35800
Viscosity at 40°C (mm^2/s)	2-5	56
Cetane number	45-55	40
Density ($kg/m^{3)}$	820	927

Table 3
Engine Specifications

Engine type	TV1 (Kirloskar)
Cylinder number	Single Cylinder
Stroke number	Four Stroke
Bore (mm)	87.5mm
Stroke (mm)	110mm
Compression ratio	17.5:1
Rated power	5.2 KW (7 HP) @1500RPM
Dynamometer	Eddy Current dynamometer
Load measurement	Strain gauge load cell
Speed measurement	Rotary encoder
Temperature indicator	Digital, K- type temperature sensor
Cylinder pressure measurement	Peizosensor, range 2000psi
Water flow measurement	Rota meter

2. *EXPERIMENTAL WORK*

Fig.1 shows the piston, cylinder head and valves coated with thin thermal barrier coating. The piston, cylinder head and valves coated with partially stabilized Zirconia to the thickness 350µm (0.35mm). A 70µm (0.07mm) super alloy bond coating (NiCrAlY) is first applied on to these engine components and then coated with ZrO_2-Y_2O_3 to a thickness of 280µm (0.28mm) using robotized plasma spray technique. The performance of ceramic coated engine is compared with standard engine.

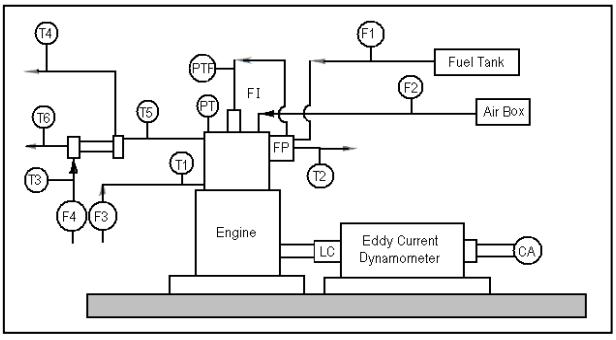

Fig.1: Piston, Cylinder head and Valves coated with ZrO_2-Y_2O_3.

Fig.2: Schematic Diagram of the Experimental Set-up.

PT Combustion Chamber Pressure Sensor
F1 Liquid fuel flow rate
PTF Fuel Injection Pressure Sensor
F2 Air Flow Rate
T1 Jacket Water Inlet Temperature
F3 Jacket water flow rate.
T2 Jacket Water Outlet Temperature
F4 Calorimeter water flow rate.
T3 Inlet Water Temperature at Calorimeter
EGC Exhaust Gas Calorimeter.

T4 Outlet Water Temperature at Calorimeter
LC Load Cell
T5 Exhaust Gas Temperature before Calorimeter
CA Crank Angle Encoder
T6 Exhaust Gas Temperature after Calorimeter.
FP Fuel Pump
FI Fuel Injector

Fig.2 shows the schematic diagram of the complete experimental setup. The specification of the engine is given in Table-3. It is provided with temperature sensors for the measurement of jacket water, calorimeter water, and calorimeter exhaust gas inlet and outlet temperatures. It is also provided with pressure sensors for the measurement of combustion gas pressure and fuel injection pressure. An encoder is fixed for crank angle record. The signals from these sensors are interfaced with a computer to an engine indicator to display P-Θ, P-V and fuel injection pressure versus crank angle plots. Provision is also made for the measurement of volumetric fuel flow. The built-in program in the system calculates indicated power, brake power, thermal efficiency, volumetric efficiency and heat balance. The software package is fully configurable and averaged P-Θ diagram, P-V plot and liquid fuel injection pressure diagram can be obtained for various operating conditions. Standard engine (without coating) is fully instrumented and connected to the dynamometer. The experiments are conducted at constant speed at four different load levels ranging from 20%, 40%, 60% and 80% of rated load. The engine is loaded by using eddy current dynamometer. The same procedure is repeated for coated engine. Engine has a compression ratio of 17.5 and a normal speed of 1500 RPM controlled by the governor. An injection pressure of 210 bar is used for the best performance. The engine is tested with neat diesel at loading conditions of 20%, 40%, 60% and 80% of rated load. At each loading conditions, performance parameters like speed, exhaust gas temperature, brake power, peak pressure are measured under steady state conditions. The experiment was repeated for diesel and 20% honge oil blend. Table - 2 shows the properties of diesel and honge oil.

3. RESULTS AND DISCUSSIONS

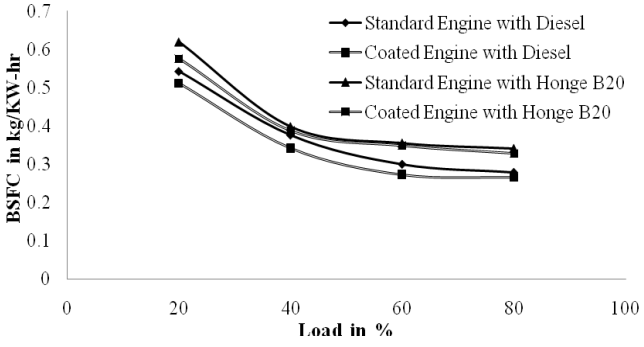

Fig.3: Variation of BSFC with Load for Neat Diesel and Honge B20.

Fig.3 shows the variation of the brake specific fuel consumption (BSFC) in standard and coated engines for neat diesel & Honge B20 at different loads. It can be observed that with neat diesel there is 5% decrease in BSFC at lower loads and about 9% decrease in BSFC at higher loads for ceramic coated engine when compared to standard engine. This can be attributed to the high temperature reached in the combustion chamber which results in better combustion efficiency. It is

also observed from Figure 3 that with Honge B20 blend there is 0.5% decrease in BSFC at lower loads and about 2.5% decrease in BSFC at higher loads for ceramic coated engine compared to standard engine. It can be observed that the BSFC is high for Honge B20 blend for both coated engine and standard engine which can be attributed to lower calorific value of biodiesel compared to that of unblended diesel.

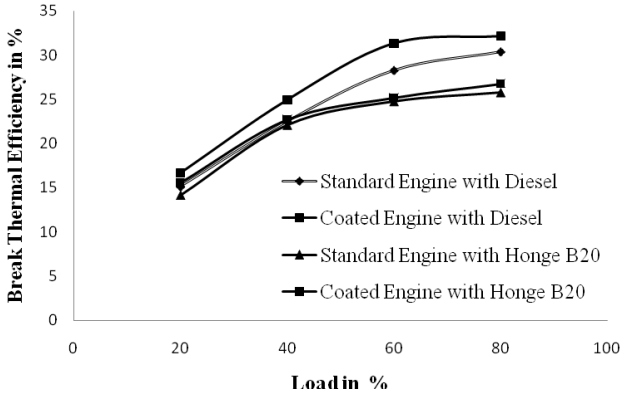

Fig.4: Variation of BTE with Load for neat Diesel and Honge B20.

Fig. 4 shows the variation of the brake thermal efficiency (BTE) for standard and coated engines with neat diesel & Honge B20 at different loads. It can be observed that with neat diesel there is maximum increase in brake thermal efficiency of about 8.5% at 60% load and minimum increase of 2.0% at 20% load in coated engine compared to standard engine. This can be attributed to increase in combustion temperature due to TBC which acts as insulator.

It can also be observed that with biodiesel blend a maximum increase of brake thermal efficiency is 1.78% at 60% load in coated engine when compared to standard engine. It can be observed that increase in brake thermal efficiency with biodiesel is less in both coated and standard engines compared to neat diesel. This is due to the lower calorific value of biodiesel compared to that of standard diesel.

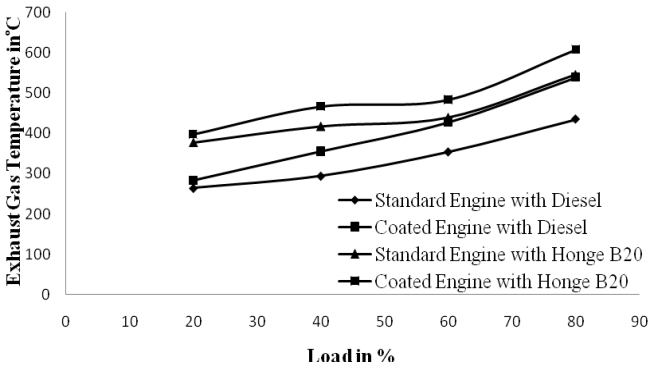

Fig.5: Variation of EGT with Load for neat diesel and Honge B20.

Fig.5 shows the variation of exhaust gas temperature (EGT) in standard and coated engines for neat diesel & Honge B20 at different loads. It can be observed that with neat diesel for coated engine there is an increase in temperature of exhaust gas by about 20°C when compared with standard engine. Similar trend has been observed by Ekrem Buvukkaya et.al (5). This increase in exhaust gas temperature in coated engine is attributed to the fact that the insulated combustion chamber retains the heat released. From Figure 5 it can also be observed that with biodiesel blend there is an increase of exhaust gas temperature in coated engine to an extent of 15°C to 50°C. It can be observed that exhaust gas temperature with biodiesel in both coated and standard engine is less compared to neat diesel. This is can be attributed to the fact that biodiesel is an oxygenated fuel.

4. CONCLUSIONS

The following conclusions are drawn from the above experimentation.

1. Coated engine shows a maximum decrease of 2.5% and 9% in Specific fuel consumption with neat diesel and Honge B20 respectively.

2. Coated engine shows a maximum increase of 8.75% and 1.78% in Brake thermal efficiency with neat diesel and Honge B20 respectively.
3. In Coated engine it is found that there is maximum 75°C and 55°C rise in exhaust gas temperatures with diesel and biodiesel blend respectively.

ACKNOWLEDGMENT

The authors are very much grateful to the Sri Siddhartha Institute of Technology Tumkur, Karntaka, India for providing requisite faculities to successfully carry out this research work.

REFERENCES

[1] Garud Vikrant, Bhoite Sanjiwan, Patil Sagar, Ghadage Suraj, Gaikwad Nilesh, Kute Devesh, Sivakumar G., "Performance and Combustion Characteristics of Thermal Barrier Coated (YSZ) Low Heat Rejection Diesel Engine", Materials Today: Proceedings 4 (2017) pp.188–194.

[2] Sharma K.T., "Performance and emission characteristics of the thermal barrier coated SI engine by adding argon inert gas to intake mixture", Journal of Advanced Research 6, 2015, pp, 819–826.

[3] Jalaludin Helmisyah Ahmad, Abdullah Shahrir, Ghazali Mariyam Jameelah, Abdullah Bulan, Abdullah Nik Rosli, "Experimental Study of Ceramic Coated Piston Crown for Compressed Natural Gas Direct Injection Engines", Procedia Engineering 68, 2013, pp, 505 – 511.

[4] Devan P.K. , Mahalakshmi N.V., Performance, emission and combustion characteristics of poon oil and its diesel blends in a DI diesel engine", Fuel 88, 2009, pp, 861–867.

[5] Imdat Taymaz, "The effect of Thermal barrier coating on diesel engine performance", Surface and Coatings Technology, Vol. 201, pp. 5249-5252, 2007

[6] Labeckas Gvidonas, Slavinskas Stasys, "Performance of direct-injection off-road dieselengine on rapeseed oil", Renewable Energy 31, 2006, pp, 849–863.

[7] Buyukkaya, Tahsin Engin and Muhammet Cerit "Effects of thermal barrier coatings on gas emissions and performance of a LHR engine with different injection timings and valve adjustments", Energy conversion and management, pp. 1298-1310, 2006.

[8]I.Taymaz, K.Cakir and A.Mimaroglu, "Experimental study of effective efficiency in a eramic coated diesel engine" Surface and Coatings Technology, pp. 1182-1185, 2005

[9] Raadnui Surapol, Meenak Anant, "Effects of refined palm oil (RPO) fuel onwear of diesel engine components", Wear 254 :-Elsevier, 2003, 22, pp. 1281–1288.

[10] Abdullah Uzun, Ismet Cevik, and Mustafa Akcil, "Effect of Thermal barrier coating on a turbocharged diesel engine performance," Surface and Coatings Technology, pp. 116-119, 1999.

Ultrasonication Assisted Synthesis of Dy^{3+} Activated $CaAl_2O_4$ nanophosphor: Photoluminescent and Photometric Properties Prompted WLED's and Latent Fingerprints Development Applications

B. S. Shashikala[1, 2], H. B. Premkumar[3*], G. P. Darshan[3], H. Nagabhushana[4]

[1]Department of Physics, Sapthagiri College of Engineering, Bangalore -560 057, India

[2]Visvesvaraya Technological University, Regional Center Bangalore -560 091, India

[1 3]Department of Physics, M. S. Ramaiah University of applied Sciences, Bangalore -560 054, India

[4]Prof. C.N.R. Rao Centre for Advanced Materials, Tumakuru University, Tumakuru–572103, India

Abstract: Systematic study of lanthanide based calcium aluminate nanophosphor was considered to be eventual building blocks for multifunctional applications. In this work, Dy^{3+} activated $CaAl_2O_4$ (1-11 mol %) nanophosphor was explored via sonication method using fresh lemon juice as a bio surfactant. The cause of sonication time, pH value, sonication power and temperature on the framework of the prepared nanophosphor were studied and discussed. The powdered x-ray diffraction results of prepared nanophosphor consist of monoclinic phase. The morphological and elemental analysis was studied through SEM and EDAX. The PL emission spectra of $CaAl_2O_4$:Dy^{3+}(1-11mol %) nanophosphor show intensive and sharp peaks centered at ~ 483, 574 and 636 nm, mature to $^4F_{9/2}\rightarrow{}^6H_{15/2}$, $^4F_{9/2}\rightarrow{}^6H_{13/2}$ and $^4F_{9/2}\rightarrow{}^6H_{11/2}$ transitions of Dy^{3+} ions, respectively. The dipole-dipole interaction between the activator ions leads to concentration quenching transpire at 9 mol %. The optimized sample was utilized for visualization and revelation of authenticated ridge details present in latent fingerprints (LFPs). The CIE and CCT results affirm the present NPs intensify white light emission eminently useful for the fabrication of white light emitting diodes.

Keywords: Sonochemical route; Photoluminescence; forensic; WLED

INTRODUCTION

Fingerprints (FPs) are commonly employed in advanced forensic investigations since they provide unique evidence on people. The ridge and furrow characteristics of FPs provide proof on the donors because they are precise and unmistakable for each individual [1-2]. Identification of fingerprints helps investigators to track a criminal's record and the FPs detectable in crime scene investigation was latent and therefore the visualization has created new possibility in various fields, like medical diagnostics, forensic investigation etc [3-4].Till date, many chemical, physical, and biological methods are rapidly emerged for visualization of latent fingerprints (LFPs). However, most of these conventional methods consist of drawbacks such as low sensitivity, selectivity, background hindrance as well as high toxicity [5-6]. Among these, the powder dusting method has been most widely utilized approach in crime investigation due to its convenience and broad applicability [7]. Regular and metallic powders are the two types of fingerprint powders available. However, the presence of resinous polymers (starch, rosin, silica gel, etc.) in normal powders, as well as hazardous components such as lead, gold, and silver in metallic powders, made identifying the latent fingerprint of surface contamination problematic [8]. On the other hand, luminescent nanomaterials give high sensitivity, low background hindrance, spatial resolution and hence provide noticeable applications in forensic science. LFPs universal recognition is mostly based on the level II structures (such as ridge termination, bifurcation, and crossover). Sometimes, the collected LFPs may be incomplete, and even don't have enough characteristics features. Therefore, more characteristics excluding level II of fingerprints are required for better recognition. In addition to level II details, the level III characteristics (sweat pore) on fingertips are also permanent, indisputable and unique to visualize the fingerprint more effectively [9]. Various fluorescent materials have been used in the past to visualize LFPs, followed by a powder dusting method capable of revealing clear friction ridge features such as level I to III primarily with UV stimulation [10]. To avoid the damaging effects of UV radiation, $CaAl_2O_4$:Dy^{3+} NPs were utilized as a fluorescent marker for the imaging of level I to level III ridge patterns under normal light.

Nowadays, the advancement of luminous resources is gaining ubiquity in nanotechnology owing to their numerous applications in a variety of fields, such as plasma displays, field emission displays, latent finger prints (LFP), opto-electronic devices, cathode ray tubes, solid state lasers,

ISBN: 979-88-35073-61-0

fluorescent paints, jackets, light emitting diodes(LED's) [11]. Material scientists have focused their attention in recent years on trivalent rare-earth metal doped inorganic host lattices, resulting in phosphors with brilliant luminescence, superior color rendering index, excellent chemical, physical and structural properties, such as larger surface area, smaller particle size, higher quantum efficiency with better colour purity, and tremendous thermal stability [12]. Among different kinds of host materials, aluminates have received a kind of interest due to its easy preparation, wide bandgap, low cost, and excellent physical and chemical stability [13]. Dysprosium doped luminescence materials are at the top of research due to possible applications like WLEDs devices and visible lasers. The two noticeable transitions, such as $^4F_{9/2}\rightarrow{}^6H_{13/2}$ and $^4F_{9/2}\rightarrow{}^6H_{15/2}$ levels in the blue (483 nm) and yellow (574 nm) region is useful for white light phosphor applications [14].

In this work, white light emitting $CaAl_2O_4:Dy^{3+}$ (1-11 mol %) NPs were synthesized by ultrasonication method using fresh lemon juice as a bio-surfactant. To know the phase structure and find the mean size of the NPs, X-ray diffraction (XRD) analysis carried out. The morphological investigations, Photoluminescence (PL) and photometric properties of the prepared NPs are studied in detail. Also, the synthesized NPs were employing for visualization of latent fingerprints on different surfaces. The present work has an objective of providing eco-friendly way of fabricating NPs for display and forensic applications.

MATERIALS & METHODS

The ensuing chemicals are used for the preparation of $CaAl_2O_4:Dy^{3+}$ (1-11mol%) NPs by ultrasound-assisted sonochemical route. Calcium nitrate hydrate [$Ca(NO_3)_2{\cdot}xH_2O$; 99.99 %], aluminum nitrate nonahydrate [$Al(NO_3)_3.9H_2O$;99.97 %], dysprosium (III) nitrate hydrate [$Dy(NO_3)_3.xH_2O$;99.9 %], aqueous NH_4OH solution are procured from Merck Ltd. and used without further purification. The fresh lemon juice was used as a bio-template and its extraction was made as per previous literature. The stoichiometric amount of precursors and bio-surfactant lemon juice (~ 30 ml) were well dissolved in double distilled water using a magnetic stirrer for 30 min. Later, aqueous NH_4OH solution was added drop wise into the already prepared solution with regular stirring so that the pH level (8) was maintained properly. Then, the resultant solution was kept for ultrasonication by inserting titanium probe sonicator maintained at 20 kHz frequency and 300 W of power for ~ 1 h. The white precipitate was obtained at the end of the reaction was collected, washed thoroughly with deionised water, and then dried in a hot air oven at 70 °C for ~ 3 h. At last, the obtained product was subjected to calcination for ~900 °C for 3 h. The experimental procedure was repeated with different concentrations of Dy^{3+} ions.

RESULTS& DISCUSSIONS

Figure.1 (a) shows XRD profiles of $CaAl_2O_4:Dy^{3+}$ (1-11 mol %) NPs synthesized via ultra- sonication method. It was observed that, sharp and intense diffraction peaks analogous to monoclinic phase of $CaAl_2O_4$ lattice and are good in agreement with standard JCPDS No: 88-2477. No presence of impurity peaks in the profiles with increase of the Dy^{3+}concentration, which implies that the product was good purity and hints that the dopant Dy^{3+} ions were successively substituted in the Ca^{2+} sites of the $CaAl_2O_4$ system. To empower this, acceptable percentage difference (Δ_r) between dopant Dy^{3+} ions and substituted sites was calculated using the following relation;

$$\Delta_r = \frac{R_m - R_d}{R_m} x100 \quad \text{---------- (1)}$$

where R_m; the ionic radius of hostCa^{2+}site (1Å) and R_d; the ionic radius of the Dy^{3+}ions (0.912 Å).The $\Delta_r$value between Dy^{3+} and Ca^{2+}in 6-coordinated sites was estimated and found to be 8.8%.The estimated Δ_r value was within the standard value of 15 %, which surely indicates that the Dy^{3+} ions preferentially substituted in 6-coordinated Ca^{2+} sites in the $CaAl_2O_4$ lattice. The crystallite size and micro-strain of the prepared NPS was calculated using Scherrer's relation and W-H approach using fallowing relations;

$$D = \frac{0.9\,\lambda}{\beta\cos\theta} \quad \text{---------- (2)}$$

$$\frac{\beta\cos\theta}{\lambda} = \frac{0.9}{D} = \frac{\varepsilon\sin\theta}{\lambda} \quad \text{---------- (3)}$$

where, λ; wavelength of the X-rays (0.15406 Å), β; full width at half maximum (FWHM in radian),ϵ; microstrain, θ; Bragg's angle. The W-H plot of the prepared NPs was depicted in Fig .1(b). The estimated average crystallite size and microstrain were tabulated in Table 1.

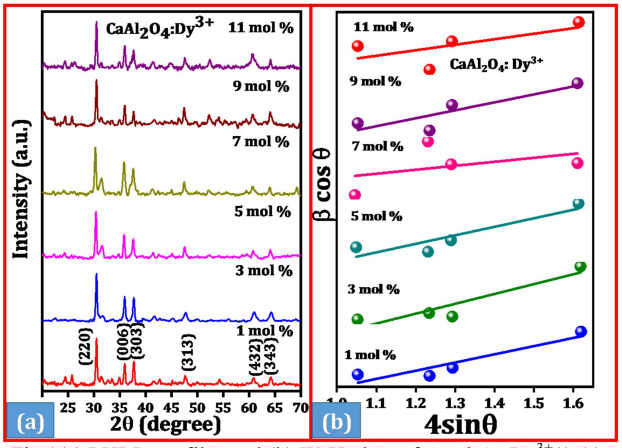

Fig.1(a) PXRD profiles and (b) W-H plots of $CaAl_2O_4:Dy^{3+}$(1-11 mol %) NPs

Table 1: Estimated crystallite size and micro-strain, of $CaAl_2O_4:Dy^{3+}$ (1-11 mol %) NPs.

Dy^{3+} conc. (mol %)	Average crystallite size (nm)		Micro-strain x10^{-3}
	Scherrer's method	W-H plots	
1	23	28	4.85
3	22	37	5.23
5	24	38	4.52
7	22	25	5.03
9	25	38	4.35
11	23	38	4.73

Fig.2 (a) depicts the PL excitation spectrum of $CaAl_2O_4$:Dy^{3+} (3 mol %) monitored at ~572 nm emission wavelength. The spectra include intensified several peaks at ~ 322, 346,361,386,418,450 and 479 nm, which are attributed to $^6H_{15/2}\rightarrow {}^4M_{17/2}$, $^6H_{15/2}\rightarrow {}^4M_{15/2}$, $^6H_{15/2} \rightarrow {}^4I_{11/2}$, $^6H_{15/2} \rightarrow {}^4I_{13/2}$, $^6H_{15/2} \rightarrow {}^4G_{11/2}$, $^6H_{15/2} \rightarrow {}^4I_{15/2}$ and $^6H_{15/2} \rightarrow {}^4F_{9/2}$transitions of the Dy^{3+} ions, respectively [15]. The PL emission spectra of $CaAl_2O_4$:Dy^{3+} (1-11 mol %) NPs recorded upon ~386 nm excitation wavelength were displayed in Fig.7 (b). The spectra show intensive and sharp peaks at ~ 483, 572,and 635 nm, owing to $^4F_{9/2}\rightarrow {}^6H_{15/2}$, $^4F_{9/2}\rightarrow {}^6H_{13/2}$,and $^4F_{9/2}\rightarrow {}^6H_{11/2}$ transitions of Dy^{3+}ions, correspondingly(Fig.2(b)). An intense peak at ~572 nm was mainly ascribed to hypersensitive electric dipole transition ($^4F_{9/2}\rightarrow {}^6H_{13/2}$) of Dy^{3+} ions, which was powerfully checked by the chemical surrounding of the Dy^{3+}ions in the host lattice. Similarly, a peak at ~ 635 nm ($^4F_{9/2}\rightarrow {}^6H_{15/2}$) was magnetically allowed and hardly varies with the crystal field strength and coordination environment around the Dy^{3+} ions. The intensity of the electric dipole transition ($^4F_{9/2}\rightarrow {}^6H_{13/2}$) is more dominating than the magnetic dipole transition ($^4F_{9/2}\rightarrow {}^6H_{15/2}$), which provides evidence that Dy^{3+} ions occupy the lattice site without inversion symmetry. The degree of distortion from inversion symmetry of the local environment surrounding the Dy^{3+} ions in the lattice site is estimated by an asymmetric ratio as follows;

$$A21 = \frac{\oint I_2(^4F_{9/2}\rightarrow {}^6H_{13/2})}{\oint I_1(^4F_{9/2}\rightarrow {}^6H_{15/2})} \quad \text{----------(4)}$$

where I_2;the intensity of the electric dipole transition and I_1;the intensity of the magnetic dipole transition.

The variation of the PL intensity with Dy^{3+}concentration was studied and shown in Fig.2(c). As evident that, a remarkable improvement of the PL intensity NPs up to 9 mol % was noticed and then shows decreasing tendency with further increase of Dy^{3+} concentration. The declining nature of the PL intensity was mainly attributed to familiar concentration quenching phenomena [16]. The observed concentration quenching arises through non-radiative energy transfer between dopant Dy^{3+} ions. Hence the critical distance between Dy^{3+} ions for energy transfer was calculated using the Dexter's relation;

$$R_c = 2\left(3V/4\pi NX_c\right)^{1/3} \quad \text{----------} (5)$$

where,V; unit cell volume, N; the number of crystallographic sites per unit cell, and X_c; critical concentration of the Dy^{3+} ions. By substituting V =97.435 Å^3, N=4, X_c = 0.09 in above equation, the R_c value was calculated and estimated to be ~8.02 Å> 5 Å, demonstrating multipolar interaction among nearest Dy^{3+} ions. The type of multipolar interactions concerned in the non-radiative energy transfer was determined by using the VanUitert equation;

$$\frac{I}{x} = \frac{K}{\beta(x)^{\frac{Q}{3}}} \quad \text{----------} (6)$$

where, x; Dy^{3+}concentration, K and β; constants for a given excitation, and Q; multipolar interaction, which is 6 for dipole-dipole, 8 for dipole-quadrupole and 10 for quadrupole-quadrupole respectively. The 'Q' value was estimated by plotting log (I/x) vs. log x (Fig. 2 (d)).The value Q was found to be 3.45, indicating that the *dipole–dipole* interaction is solely responsible for observed concentration quenching.

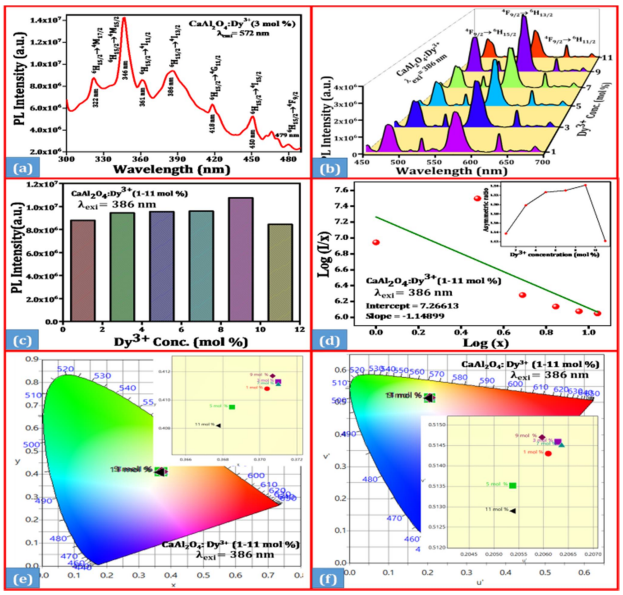

Fig.2 (a) PL excitation spectrum, (b) Emission spectra, (c) Variation of PL intensity with Dy^{3+} concentration, (d) Logarithmic plot of x and (I/x) (Inset asymmetric ratio Vs Dy^{3+} concentration), (e) CIE diagram and (f) CCT diagram of $CaAl_2O_4$:Dy^{3+}(1-11 mol %) NPs.

Fig.2 (e) illustrates the Commission International 1931 De I-Eclairage (CIE) chromaticity diagram of $CaAl_2O_4$: Dy^{3+} (1-11 mol %) NPs under 386 nm excitation. The estimated CIE coordinates are tabulated in Table 2. It was evident that the obtained CIE values were close to the standard white light chromaticity coordinates (x=0.333 and y=0.333), signifying

the higher white-light-emitting excellence of the prepared NPs.CIE diagram shows thecolor co-ordinate values of $CaAl_2O_4$: Dy^{3+} NPs fall on white light section. Further, correlated color temperature (CCT) values were calculated by relating the (x, y) values of the light source to (U', V') by using subsequent relations;

$$U' = \frac{4x}{-2x+12y+3} \text{ ---------- (7)}$$

$$V' = \frac{9y}{-2x+12y+3} \text{ -------- (8)}$$

The CCT diagram of $CaAl_2O_4$: Dy^{3+} (1-11 mol %) NPs were shown in Fig. 2 (f).The CCT value was obtained in the range 4000–5500 K. The subsequent CCT values for $CaAl_2O_4$: Dy^{3+} (1-11 mol %) NPs were listed in Table 2. The obtained CCT values were lesser than 5000 K, representing the warm white light source and used for display applications [17].
Further, the color purity of the prepared NPs was calculated using the following relation;

$$Colopurity = \frac{\sqrt{(x_s - x_i)^2 + (y_s - y_i)^2}}{\sqrt{(x_d - x_i)^2 + (y_d - y_i)^2}} \times 100\% \text{ --------(9)}$$

where (x_d, y_d); chromaticity coordinates of the dominant wavelength, (x_s, y_s); co-ordinates of the sample point and (x_i, y_i); white illuminate co-ordinates (x_i=0.33, y_i=0.33). The color purity of prepared NPs was estimated and found to be ~ 34.26%. The results largely point out that the optimized NPs find potential applications in display devices and WLEDs.

Table 2: Photometric characteristics of $CaAl_2O_4$:Dy^{3+} (1-11 mol %) NPs.

Dy^{3+} conc. (mol %)	CIE co-ordinates		CCT co-ordinates		CCT (K)	CP (%)
	x	y	U'	V'		
1	0.37039	0.41079	0.2061	0.5143	4468	34.5
3	0.37104	0.41123	0.2063	0.5146	4454	34.8
5	0.36854	0.40955	0.2054	0.5135	4510	33.6
7	0.37104	0.41105	0.2064	0.5145	4453	34.8
9	0.37074	0.41163	0.2060	0.5147	4463	34.9
11	0.36779	0.40831	0.2054	0.5129	4524	33.0

The prepared NPs are used for visualization of LFPs onvarious porous and non-porous surfaces under normal light Well defined ridge characteristics, which includes level II ridge details, which are useful for fingerprint classification and indexing but not enough for precise person identification hence level II ridge details like a lake, ridge end, short ridge, scar, loop, bifurcation, trifurcation, and sweat pores are studied (Fig.3), which demonstrates that the sensitivity of the prepared NPs helping in the visualization of LFPs on various substrates.

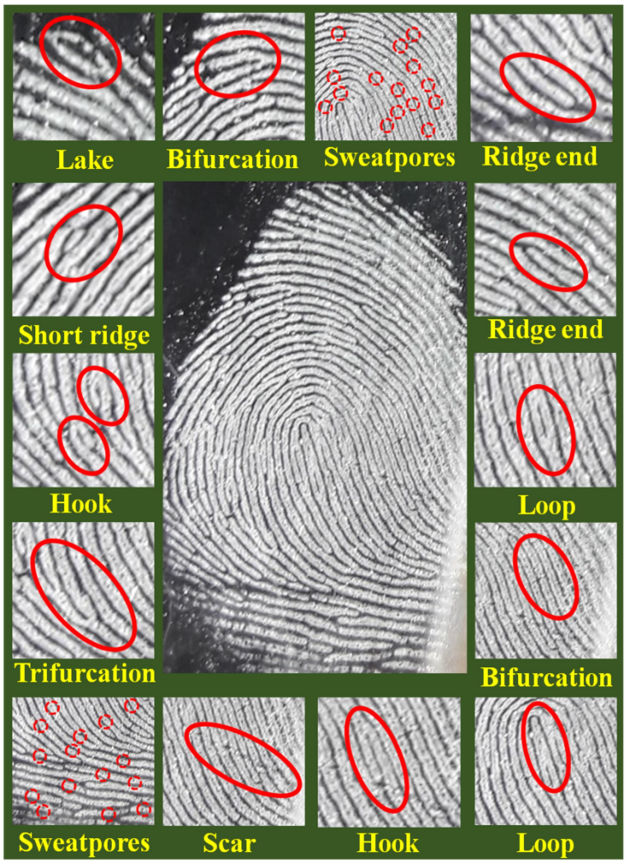

Fig.3. Magnified images of high-resolution FPs developed using $CaAl_2O_4$:Dy^{3+} (9 mol %) NPs under normal light show various ridge details, including a lake, bifurcation, sweat pores, ridge end, loop, hook, scar, and trifurcation.

CONCLUSIONS

In summary, $CaAl_2O_4$:Dy^{3+} (1-11mol %) NPs were prepared by eco-friendly ultrasound-assisted sonochemical route using lemon juice as a bio-surfactant. The average crystallite size of the prepared samples was estimated and found to be ~ 20-40 nm. The noticeable increment in the PL intensity up to 9 mol % and later it diminishes with further increase of Dy^{3+}concentration, which ascribed to concentration quenching. The *dipole–dipole* interaction among Dy^{3+} ions was mainly responsible for the observed concentration quenching. The estimated CIE coordinates fall on the white region of the chromaticity diagram and its average CCT value was found to be ~ 4464 K with 34.26 % of color purity. Prepared NPs are effectively used to visualize of

LFPs on various substrates under normal light, which enables level I-III ridge characteristics identification with outstanding sensitivity, selectivity, and low background hindrance.

ACKNOWLEDGMENT

We would like to express our sincere gratitude to the Management, Principal Sapthagiri College of Engineering Bengaluru for the facilities provided and their support. Also we would like to thank the Head of department Engineering Physics and faculties for their encouragement and support.

REFERENCES

[1]. Jingwei Wan, Lei Chen, Wei Li, Shengfeng Cui, Binfang Yuan, Preparation of Novel Magnetic Nanomaterials Based on "Facile Coprecipitation" for Developing Latent Fingerprints (LFP) in Crime Scenes, *ACS omega.,*7 (2022) 1712-1722.

[2]. Hamdi Trabelsi, Marx Akl, Samer Hassan Akl, Ultrasound assisted Eu^{3+}– doped strontium titanate nanophosphors: Labeling agent useful for visualization of latent fingerprints, *Powder Technol*., 384 (2021) 70–81.

[3]. Vishal Sharma, Sonal Choudhary, Priyanka Mankotia, Amrita Kumari, Kashma Sharma, Rakesh Sehgal, Vijay Kumar, Nanoparticles as fingermark sensors, *Trends Anal.Chem*., 143 (2021) 114.

[4]. Hak-Sung Jung, Junsang Cho, Keir C. Neuman, Highly stable cesium lead bromide perovskite nanocrystals for ultrasensitive and selective latent fingerprint detection, *Anal. Chim. Acta*., 1181 (2021) 338850.

[5]. Sudipta Som, Che-Yuan Yang, Chung-Hsin Lu, Subrata Das, Synthesis of Li+-ion activated $NaYF_4$: Er^{3+}/Yb^{3+} phosphors via a modified solid-state process for latent fingerprint detection, *Ceramics International*., 45 (2019) 5703-5709.

[6]. Eluri Pavitra, Ganji Seeta Rama Raju, Jin Young Park, Sk Khaja Hussain, Gattupalli Manikya Rao, An efficient far-red emitting Ba_2LaNbO_6:Mn^{4+} nanophosphor for forensic latent fingerprint detection and horticulture lighting applications, *Ceramics International.,* 46 (2020) 9802-9809.

[7]. Antika Das, Subhajit Saha, Karamjyoti Panigrahi, Uttam Kumar Ghorai, Kalyan Kumar Chattopadhyay , Enhanced Photoluminescence Properties of Low-Dimensional Eu^{3+} Activated $Y_4Al_2O_9$ Phosphor Compared to Bulk for Solid-State Lighting Applications and Latent Fingerprint Detection-Based Forensic Applications, *Microsc Microanal..,*25 (2019) 1422 – 1430.

[8]. C. Suresh , G.P. Darshan c , S.C. Sharma, M. Venkataravanappa f , H.B. Premkumar g , S. Shanthi h , K.N. Venkatachalaiah i , H. Nagabhushana , Imaging sweat pore structures in latent fingerprints and unclonable anti-counterfeiting patterns by sensitizers blended LaOF: Pr^{3+} nanophosphors, *optic material.,* 100 (2020) 109625.

[9]. Samvit G. Menon, Arup Kumar Kunti, David E. Motaung, Hendrik C. Swart, A new recipe for the rapid microwave synthesis of high quantum yield Mn^{2+}-doped $ZnGa_2O_4$ phosphors for potential forensic applications, *New J. Chem.,* 43 (2019)17446.

[10]. Santosh K. Gupta, Jose P. Zuniga, Maya Abdou, Melonie P. Thomas, Manisha De Alwis Goonatilleke, Beth S. Guiton, Yuanbing Mao, Lanthanide-doped lanthanum hafnate nanoparticles as multicolor phosphors for warm white lighting and scintillators, *Chemical Engineering Journal.,* 379 (2020) 122314.

[11]. S. Yang *et al.*, Solid-phase combustion synthesis of calcium aluminate with $CaAl_2O_4$ nanofiber structures, *Ceram. Int.*, 44 (2018) 6186–6191.

[12]. H. Liu, Y. Hao, C. Pan, H. Wang, and B. Xu, Luminescent properties of Eu^{2+}-activated $(Sr_{1-z}, Caz)(Al_{1-y}, By)_2O_4$ phosphors for UV LEDs, *Mater. Sci. Eng. B Solid-State Mater. Adv. Technol.*, 178 (2013) 719–724.

[13]. I. Omkaram and S. Buddhudu, Photoluminescence properties of $MgAl_2O_4$:Dy^{3+} powder phosphor, *Opt. Mater. (Amst).*, 32 (2009) 8–11.

[14]. F. Femila Komahal, H. Nagabhushana, G. P. Darshan, and B. Daruka Prasad, Hierarchical zinc aluminate 3D nanostructures, synthesized by bio-inspired ultrasound assisted sonochemical route: Display and dosimetry applications, *Arab. J. Chem.*, 13 (2020) 580–594.

[15]. C. Suresh, H. Nagabhushana, G. P. Darshan, R. B. Basavaraj, B. Daruka Prasad, S. C. Sharma, M. K. Sateesh, J. P. Shabaaz Begum, Lanthanum oxyfluoride nanostructures prepared by modified sonochemical method and their use in the fields of optoelectronics and biotechnology, *Arab. J. Chem.*, 11 (2018) 196–213.

[16]. H. Jamil, I. M. Dildar, Usman Ilyas, J. Z. Hashmi, Saima Shaukat, M. N. Sarwar, M. Khaleeq-ur-Rahman, Microstructural and Optical study of polycrystalline manganese oxide films using Kubelka-Munk function, *Thin Solid Films*, 732 (2021) 138796.

[17]. M. Chaitra, R. Anandakumari, G. Nagaraju, Dysprosium Activated $Sr_3Al_2O_6$ Nanophosphor for Display Device Applications, *J. Sci. Res.*, 64 (2020) 261–266.